Imperial College London

Faculty of Medicine

National Heart and Lung Institute

Mitochondrial transfer as a cell-cell communication mechanism between airway smooth muscle cells in COPD

Júlia Frankenberg Garcia

Supervisors: Dr Pankaj K Bhavsar and Dr Charalambos Michaeloudes

Secondary supervisor: Dr Tristan Rodriguez

Submitted in part fulfilment of the requirements for the degree of

Doctor of Philosophy at Imperial College London

March 2022, London, United Kingdom

Copyright Declaration

Declaration of Originality

I hereby declare that all the content presented in this thesis is original and represents work of my own, unless otherwise stated, with reference to the published or unpublished work of others. The content of this thesis has not been previously submitted in any type of report for other academic qualifications.

Acknowledgements

Here's my favourite part

Because a PhD is a solitary journey

Yet, as I found, impossible to achieve on your own

First things first, thank you to my supervisors

Charis, for the all the advice and teachings throughout these four years, for the WhatsApp troubleshooting on western blots and other unloved experiments, for the passionate rants about work and life

Pank, for trusting me, for the patience, for the tips on good restaurants, for teaching me "A PhD is a degree in thinking" - and for guiding me in getting there

Thank you to Tristan Rodriguez, Katie Raby, Ana Lima and everyone in the academic world who gave me feedback, help and inspiration

Thank you to all who crossed my path in Guy Scadding Building, for gladly sharing the ups and downs of the day-to-day in the lab, for commiserating in failed experiments, and for celebrating in making them work, for invigorating chit-chat breaks and cake

And of course,

Thanks to everyone in the very important "life" side of work-life balance,

Mãe, Pai, Marta and Chico, and everyone in my family, thank you for bringing joy in all our moments together

My housemates, Claire, Laura and Subhro, for putting up with me every single day, for making lockdowns bearable, for making our house a home

Everyone at Regional do Grafton and friends, for sharing this passion for music (and

dance) that never failed to transport me to a land far far away from PhDs

My girlfriends, Kayley, Andreea, Clara, for the dinners, trips, parties and countless moments alike, for being there for me; special thanks to Clara for sharing so much of this journey with me

I am also grateful for many other people with whom I have spent cherished moments throughout these years.

So thank you - really really thank you - to everyone that has been by my side during this time. You made it happen.

Abstract

Chronic obstructive pulmonary disease (COPD) is an inflammatory lung disease characterised by a progressive airflow limitation. Airway smooth muscle (ASM) dysfunction, such as cell hyperproliferation and increased extracellular matrix deposition, contributes to airway remodelling, an important pathological feature of COPD. There is also evidence of defective mitochondria in the lungs and in cultured ASM cells (ASMCs) from patients with COPD. Cigarette smoke (CS), the main cause of COPD, induces cellular and mitochondrial dysfunction, but only a proportion of smokers develop COPD. Homeostatic mechanisms that prevent sustained damage in response to CS may be impaired in COPD. Transfer of mitochondria from stem cells to structural cells in the lung protects the latter from stress-induced mitochondrial dysfunction. In this study, I hypothesised that mitochondrial transfer between ASMCs is a homeostatic mechanism that preserves mitochondrial function, and that it is impaired in COPD leading to sustained mitochondrial dysfunction in response to stress. I show that CS leads to persistent mitochondrial damage in ASMCs, an effect that is more pronounced in cells from COPD patients. However, it remains unclear whether this drives pathogenic ASM phenotypes. I demonstrate that ASMCs, from both healthy and COPD patients, are capable of exchanging mitochondria, a process that occurs, at least partly, via extracellular vesicles. Mitochondrial transfer is induced by exposure to CS, suggesting it is a stress response mechanism. Contrary to my hypothesis, the results of this study indicate that mitochondrial transfer may not be impaired in COPD. However, irrespective of disease status, this process is associated with an up-regulation of mitochondrial respiration and a reduction in cell proliferation. Therefore, mitochondrial transfer between ASMCs may be exploited as an endogenous protective mechanism to reverse mitochondrial and cellular dysfunction in the lungs.

Table of Contents

List of Figures

List of Tables

List of Abbreviations

Δψm Mitochondrial membrane potential

AAT Alpha-1 antitrypsin

ALIX ALG-2-interacting protein X

ARMS-qPCR Amplification refractory mutation system-qPCR

ASM Airway smooth muscle

ASMC Airway smooth muscle cell

BALF Bronchoalveolar lavage fluid

CCCP Carbonyl cyanide m-chlorophenylhydrazone

CdM Conditioned media

COL Collagen

COPD Chronic obstructive pulmonary disease

COX8 Cytochrome c oxidase subunit VIII

CS Cigarette smoke

CSM Cigarette smoke medium

CXCL-1, -10 C-X-C motif chemokine ligand 1, 10

DAMPs Damage-associated molecular patterns

DMEM Dulbecco's modified eagle medium

DRP1 Dynamin-related protein 1

DYNC1H1 Dynein cytoplasmic 1 heavy chain 1

ECAR Extracellular acidification rate

ECM Extracellular matrix

ELISA Enzyme-linked immunosorbent assay

ELN Elastin

ETC Electron transport chain

EVs Extracellular vesicles

FACS Fluorescence-activated cell sorting

FBS Foetal bovine serum

FCCP Carbonyl cyanide-p-trifluoromethoxyphenylhydrazone

FEV Forced expiratory volume

FITC Fluorescein isothiocyanate

FSC Forward scatter

FVC Forced vital capacity

GM-CSF Granulocyte-macrophage colony-stimulating factor

GOLD Global initiative for chronic obstructive lung disease

HAPLN3 Hyaluronan and proteoglycan link protein 3

HBSS Hank's balanced salt solution

HRP Horseradish peroxidase

IL-6, -8 Interleukin-6, -8

IMM Inner mitochondrial membrane

KIF5B Kinesin family member 5B

LAMC2 Laminin subunit gamma 2

LPS Lipopolysaccharide

MMP Matrix metalloprotease

MFI Median fluorescence intensity

MFN-1, -2 Mitofusin-1, -2

MIRO-1, -2 Mitochondrial Rho GTPase-1, -2

mn-SOD Manganese superoxide dismutase

MSCs Mesenchymal stem cells

MT-CO2 Mitochondrially encoded cytochrome C oxidase II

mtDAMPs Mitochondrial damage-associated molecular patterns

mtDNA Mitochondrial DNA

mtROS Mitochondrial reactive oxygen species

MYO19 Myosin XIX

NMOC Non-mitochondrial oxygen consumption

NOX NADPH oxidase

OCR Oxygen consumption rate

OMM Outer mitochondrial membrane

OPA1 Optic atrophy protein 1

OXPHOS Oxidative phosphorylation

PBS Phosphate-buffered saline

PCNA Proliferating cell nuclear antigen

PGC1-α, -β Peroxisome proliferator-activated receptor gamma coactivator 1-alpha, -beta

PINK1 PTEN-induced kinase 1

PPC Particles per cell

PI Propidium iodide

RIPA Radioimmunoprecipitation assay

ROS Reactive oxygen species

SEM Standard error of the mean

siRNA Small interfering RNA

SSC Side scatter

TGF-β Transforming growth factor-beta

TMRM Tetramethylrhodamine methyl ester

TNF-α Tumour necrosis factor-alpha

TNTs Tunnelling nanotubes

TOM20 Translocase of outer membrane 20

TRAK-1, -2 Trafficking kinesin protein-1, -2

TSG101 Tumor susceptibility gene 101

Chapter 1

Introduction

1.1 Introduction to COPD

Chronic obstructive pulmonary disease (COPD) is a inflammatory lung disease characterised by a progressive airflow limitation that is poorly reversible [1, 2]. It is a heterogenous disease that encompasses chronic respiratory symptoms, structural pulmonary abnormalities and lung function impairment [1]. In 2019, COPD was the third leading cause of death, accounting for 3.23 million deaths worldwide [3]. In the United Kingdom, an estimated 1.2 million people live with diagnosed COPD [4]. COPD has a significant economic burden, accounting for 3% of the total annual healthcare budget in the European Union [5]. In the USA, COPD costs $4000 per patient per year [6]. The annual economic burden of COPD in the United Kingdom is of £1.9 billion [4]. It is predicted that the burden of COPD will increase over the years, and that by 2060 there may be over 5.6 million deaths annually from COPD [7, 8]. Despite these alarming statistics, there are no available therapies to reverse disease progression.

Patients with COPD present symptoms such as dyspnoea, chronic cough and/or sputum production. The clinical diagnosis of COPD is confirmed by evaluating lung function with a spirometry test, which allows for the assessment of airflow limitation. The test consists in measuring the volume of air forcibly exhaled from the point of maximal inspiration (forced vital capacity, FVC) and the volume that has been exhaled at the end of the first second of forced expiration (FEV_1), after administration of a bronchodilator. COPD

is diagnosed when the ratio between these two measurements (FEV_1/FVC) is below 0.7 [1, 2]. The Global Initiative for Chronic Obstructive Pulmonary Disease (GOLD) also classifies the degree of disease severity, from GOLD stage I to IV, based on the predicted FEV_1, which is the percentage of the predicted FEV_1 value in a patient according to age, sex, height and ethnicity (**Table 1.1**).

Classification	**Disease Severity**	**Post-bronchodilator FEV_1**
GOLD I	Mild	$FEV_1 \geqslant 80\%$ of predicted
GOLD II	Moderate	$50\% \leqslant FEV_1 < 80\%$ of predicted
GOLD III	Severe	$30\% \leqslant FEV_1 < 50\%$ of predicted
GOLD IV	Very severe	$FEV_1 < 30\%$ of predicted

Table 1.1: Stratification of COPD severity according to GOLD classification [2]

1.1.1 Risk factors of COPD

Cigarette smoking is the main environmental risk factor of COPD. Smokers have a greater prevalence of lung abnormalities, respiratory symptoms and an accelerated decline in lung function, as well as a greater mortality rate due to COPD compared to non-smokers [2]. However, only 20% of smokers develop COPD, and non-smokers may also develop chronic airflow limitation, which indicates the existence of other drivers of disease [9]. Occupational exposure to particles, such as organic and inorganic dusts, chemical agents and fumes, and exposure to indoor pollutants, such as biomass combustion gases, are also associated with COPD pathogenesis [2]. Non-environmental risk factors have also been identified. Genetic predisposition may explain why only some smokers develop COPD. The most common genetic variation associated to COPD is in the *SERPINA1* gene, which encodes for alpha-1 antitrypsin (AAT), the main inhibitor of the serine protease neutrophil elastase [2, 10]. This genetic variation is associated with a deficiency of AAT, which results in an protease/anti-protease imbalance leading to parenchymal destruction

and emphysema [10]. This will be further described in the following section. Genome wide association studies (GWAS) have identified other genetic variations that are associated with increased susceptibility to COPD, such as variations in the genes encoding hedgehog-interacting protein, α-nicotinic acetylcholine receptor and iron-responsive element binding protein [11]. COPD typically affects people over 40 years of age [7], which suggests age is a risk factor. However, it is unclear how ageing affects disease. On the one hand, the age of onset of COPD may be a result of a cumulative exposure to disease-causing agents over many years. However, some of the structural changes observed in COPD are also seen in ageing lungs [2] and many of the hallmarks of ageing, such as cellular senescence and mitochondrial and telomere dysfunction, are more pronounced in COPD patients compared to age-matched controls [12]. This suggests that an accelerated ageing of the lungs may contribute to COPD. Viral and bacterial infections are also a known risk factor for COPD, often associated to the occurrence of exacerbations – a sustained worsening of symptoms with an acute onset that is beyond day-to-day variations [13]. Pathogens such as human rhinovirus (HRV), respiratory syncytial virus (RSV), *Haemophilus influenza*, *Moraxella catarrhalis* and *Streptococcus pneumoniae* have been detected in the lungs of COPD patients during exacerbations [14, 15]. There is currently insufficient data to establish whether infection with severe acute respiratory syndrome coronavirus 2 (SARS-CoV-2), leading to Covid-19 disease, is associated with increased risk of COPD. However, there are studies pertaining to the potential of COPD as a risk factor for Covid-19 [16, 17]. A systematic review and meta-analysis revealed that COPD was associated with an increased risk of hospitalization, ICU admission and mortality in patients diagnosed with Covid-19 [17]. While the mechanisms by which this happens are not established, a few possibilities have been described. The angiotensin converting enzyme-2 (ACE-2) is a receptor responsible for the entry of the SARS-CoV-2 virus into cells and is up-regulated in the alveoli and the small airway epithelium of COPD patients [18]. In addition, individuals with COPD have abnormal inflammatory responses and impaired clearance of respiratory viruses [19]. Other risk factors for COPD include gender, lung growth and development, socio-economic status, asthma and chronic bronchitis [2, 20]. All these risk factors can

contribute to the development of structural abnormalities in the lung, such as airway remodelling and emphysema, which, in turn, lead to airflow obstruction.

1.1.2 Pathophysiology and pathogenesis of COPD

COPD is a heterogeneous disease comprising different pathological features (**Figure 1.1**). Two important hallmarks of COPD are airway remodelling and emphysema. Airway remodelling consists of thickening of the large and small airways, which leads to narrowing of the airway lumen and consequent airflow obstruction [21, 22]. It is driven by an increase in airway wall compartments, such as the airway smooth muscle, changes in epithelial cell function, such as loss of barrier function, goblet cell metaplasia and basal cell exhaustion, as well as an increase in mucus exudates [21, 23]. Emphysema is characterised by changes in the alveolar space, such as parenchymal destruction and loss of elastic recoil. These result in reduced gas exchange and air trapping in the alveoli, which contribute to airflow obstruction [24]. Other aspects, such as pulmonary hypertension and mucus hypersecretion, can also be present in COPD [2]. Though COPD is primarily characterised as a lung disease, it is often accompanied by co-morbidities such as cardiovascular diseases, osteoporosis, depression and lung cancer [2]. Whether these are worsened by COPD or occur concomitantly as a result of similar risk factors is not clear. The degree to which the pathological features of COPD affect each individual is variable and reflects the complexity of the disease. The cellular mechanisms driving the development of these phenotypes are also intricate and can vary not only between individuals but between cell types and location in the lungs. These include, but are not limited to, abnormal inflammation, oxidative stress, protease/anti-protease imbalance, cellular senescence and apoptosis, and will be elaborated in the paragraphs below.

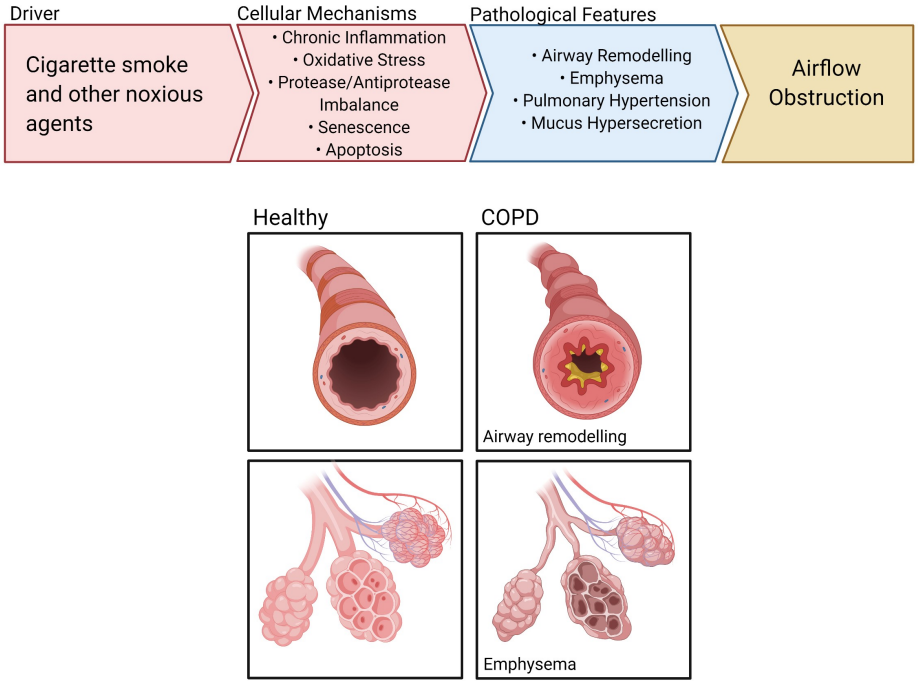

Figure 1.1: Pathogenesis of COPD. Diagram created with BioRender.com

Chronic inflammation, induced by exposure to cigarette smoke (CS) and other noxious agents, is an important cellular aspect of COPD. Whereas in healthy subjects inflammation resolves upon removal of the stimuli, in COPD, CS-induced inflammatory responses persist after smoking cessation [21]. Several factors may contribute to this. Firstly, there is an increase in the levels of both innate and adaptive immune cells, such as neutrophils, macrophages, and B and T-lymphocytes, in the airways of COPD patients, which correlates with severity of disease [21]. Moreover, many immune cells have impaired function in COPD. For example, macrophages from COPD patients display defective phagocytosis, which reduces bacterial clearance in the airways [25]. COPD neutrophils show abnormal chemotactic behaviour and migratory dynamics [26]. These may contribute to persistent inflammation in COPD. Inflammatory mediators are also increased in COPD, and can further recruit and activate immune cells. For example, chemokines, such as interleukin (IL)-8, and cytokines, such as the tumour necrosis factor α (TNF-α), are increased in sputum from COPD patients compared to smoking and non-smoking controls [27]. The cytokine IL-6 is elevated in exhaled breath condensate of COPD patients [28]. Transform-

ing growth factor β (TGF-β) is increased in the small airway epithelium of COPD patients [29]. Inflammatory mediators are secreted not only by immune cells, but also by structural cells. For example, epithelial cells are the first point of contact of disease-driving noxious agents, and the resulting epithelial damage leads to the secretion of cytokines, growth factors and danger associated molecular patterns (DAMPs) that promote inflammation [20]. Abnormal inflammation in the lungs contributes to the development of pathological features of COPD. For example, infiltration of immune cells within the bronchial wall can lead to thickening and remodelling of the airway wall [21]. Increased TGF-β, a fibrogenic factor, induces the proliferation of fibroblasts and the production of collagen and other extracellular matrix components, which also contribute to airway remodelling [29]. Chronic inflammation is also present systemically and may lead to the development of co-morbidities, such as cardiovascular disease, and exacerbations [30, 31].

Proteolytic enzymes, secreted mainly by inflammatory cells, are counter-balanced by the action of anti-proteases. However, in COPD, due to the accumulation of inflammatory cells, there is a shift in the balance between proteases and anti-proteases, which contributes to emphysema in the lungs. Proteases are upregulated in COPD. For example, matrix metalloprotease (MMP)-12, an elastase, is higher in macrophages, bronchoalveolar lavage fluid (BALF) and bronchial biopsies of COPD patients compared to healthy volunteers [32]. The accumulation of different proteolytic elastases is thought to contribute to emphysema by breaking down elastin, a component of the parenchymal extracellular matrix (ECM) that is important in maintaining lung tissue elasticity [33]. This is clearly evidenced in patients with AAT deficiency, where a loss of inhibition of neutrophil elastase leads to parenchymal destruction [10]. Other components of the ECM, such as collagens and glycosaminoglycans, are also dysregulated in COPD. For example, an increased and disorganized deposition of collagen has been reported in the lungs of COPD patients [34].

Another important cellular mechanism of COPD is oxidative stress, which occurs when oxidants are present in excess and/or the antioxidant defence mechanisms are impaired [35]. Markers of oxidative stress, such as carbon monoxide and myeloperoxidase are elevated in exhaled breath condensate from COPD patients [35]. Oxidants, such as

reactive oxygen species (ROS), are highly reactive free radicals that can oxidize different biomolecules, such as DNA, proteins and lipids, modifying their function. ROS include the superoxide anion ($O_2^{\bullet -}$), hydrogen peroxide (H_2O_2), hydroxyl radical ($^{\bullet}HO$) and hypochlorous acid (HOCl) [36]. Cigarette smoke is a major source of exogenous oxidants, where both gas and tar phases are rich in free radicals [36]. The tar phase contains 10^{17} relatively stable radical molecules per gram, such as the quinone/hydroquinone (Q/QH2) complex, which reduces molecular oxygen to produce $O_2^{\bullet -}$, leading to the subsequent formation of H_2O_2 and $^{\bullet}HO$ [36, 37]. The gas phase contains 10^{15} radicals per puff, such as nitric oxide ($NO^{\bullet}$) and peroxynitrite ($ONOO^-$) [38]. ROS are also generated endogenously by cells, primarily during aerobic respiration in the mitochondria, when electrons leak from Complex I and III of the electron transport chain (ETC) (**Figure 1.3**) [39]. Other cellular processes that generate ROS include the reduced nicotinamide adenine dinucleotide phosphate (NADPH) oxidase-driven "respiratory burst" in phagocytes [40]. Whereas at physiological levels ROS participate in different cellular mechanisms such as signalling pathways and phagocytosis, in excess, ROS can lead to oxidative damage. Oxidants can cause lipid peroxidation, modifications in proteins and DNA damage, which can in turn activate inflammatory pathways that lead to disease [36]. For example, 4-Hydroxy-2-nonenal, a product of lipid peroxidation, is increased in the lungs of patients with COPD [41] and is a chemoattractant to neutrophils [42]. ROS can activate transcription factors, such as nuclear factor-kappaB (NF-kB), that lead to an increase in the transcription of pro-inflammatory genes, thus contributing to an increase in inflammatory responses [43]. Exposure to cigarette smoke leads to oxidative stress in the lungs of patients with and without COPD. However, in COPD, as observed with inflammatory responses, oxidative stress persists after smoking cessation [44]. This may be due to both increased endogenous oxidants, as well as impaired antioxidant defences, which normally maintain ROS at non-pathological levels. Indeed, increased levels of mitochondrial ROS have been reported in COPD lungs [45, 46]. The nuclear factor erythroid 2–related factor 2 (NRF-2) regulates antioxidant responses at a transcriptional level and is downregulated in COPD [47]. Genetic polymorphisms in genes involved in the antioxidant response, such as superoxide

dismutase (SOD) and glutathione S-transferases (GST), have also been linked to COPD [48, 49].

Cellular senescence and apoptosis also contribute to COPD pathogenesis. Senescent cells, which are cells that have irreversibly lost their ability to proliferate but maintain a metabolic activity, accumulate in the lungs during ageing, but in COPD this process is accelerated. There are increased levels of senescent cells, such as endothelial and epithelial cells, in the lungs of COPD patients [50]. Senescent cells secrete a variety of mediators known as the senescent associated secretory phenotype (SASP), which include pro-inflammatory mediators and proteases that contribute to chronic inflammation in COPD [51]. There is also an increase in apoptotic cells (epithelial, mesenchymal and endothelial cells) and apoptotic markers in the lungs of patients with emphysema [52]. Apoptosis is important in the maintenance of normal tissue homeostasis. However, in COPD, there is an imbalance between apoptosis and replenishment of new tissue, which contributes to emphysema. Necroptosis, a regulated form of necrosis, is also increased in the lungs of patients with COPD, and is further induced by exposure to CS [53]. Necroptosis not only causes loss of tissue but also promotes inflammation as a result of the release of DAMPs. Interestingly, whereas in the alveoli there is an increase in apoptosis and senescence, leading to parenchymal destruction [54], in the airways there is hyperproliferation of airway smooth muscle cells and fibroblasts which contributes to airway thickening and remodelling [45]. These contrasting phenotypes between cell types and/or localization in the lungs highlight the complexity of COPD pathogenesis. In addition to these well-described cellular mechanisms, other aspects, such as changes in the microbiome, auto-immunity and epigenetics are emerging as contributing factors to COPD pathogenesis [24, 55–58].

1.1.3 Current therapies

The complex and heterogenous pathogenesis of COPD makes the development of effective therapies a challenge. Current therapies for COPD are limited to alleviating symptoms of disease rather than treating the underlying conditions and reversing disease phenotypes. Smoking cessation is the most effective approach to reduce disease progression [2]. Pharmacological therapies are also used to reduce symptoms. Bronchodilators, such as β2-agonists and anti-muscarinic agents, increase FEV_1 by reducing contraction of the airway smooth muscle. Such drugs include short- and long-acting β2-agonists (SABA and LABA) and short- and long-acting muscarinic antagonists (SAMA and LAMA) that can be used in different combinations [59]. Anti-inflammatory agents, such as inhaled corticosteroids and phosphodiesterase-4 inhibitors, act by reducing chronic inflammation in the lungs. Other drugs, such as mucolytic and antioxidant agents, target mucus hypersecretion and oxidative stress, respectively. Vaccinations and antibiotics are used to reduce the rate of exacerbations in COPD patients [2]. Finally, non-pharmacological interventions such as pulmonary rehabilitation and mechanical ventilation are also used as a therapy. Patients can be treated with one or more of the above therapies depending on severity of disease and other factors [2]. Potential new therapies include the use of monoclonal antibodies to target and reduce specific cytokines and chemokines involved in COPD pathology [59] as well as senolytics that induce apoptosis and the removal of senescent cells in the lungs [60]. Still, the current treatments are limited and do not reverse the pathological features that lead to airflow obstruction, such as emphysema and airway remodelling. Elucidating the changes in different cell types that drive these pathological features will unveil new therapeutic targets. In my thesis, I focus on the role of airway smooth muscle cells in COPD.

1.1.4 Airway smooth muscle in COPD

The airway smooth muscle (ASM) is a structural component of the airways located from the trachea to the terminal bronchioles. Airway smooth muscle cells (ASMCs) can exert different functions such as contraction, proliferation, migration and secretion of mediators [61, 62].

ASMCs exhibit phenotypic plasticity *in vitro*, changing function in response to extrinsic and intrinsic cues. Halayko *et al* showed that, upon isolation, canine tracheal smooth muscle cells exhibit a contractile phenotype associated with the expression of markers such as smooth muscle myosin heavy chain, calponin, h-caldesmon, transgelin. After five days in culture the cells become proliferative, expressing markers such as non-muscle myosin heavy chain, i-caldesmon and vimentin [63]. Interestingly, prolonged serum-starvation induces a "hyper-contractile" phenotype in ASMCs [64]. This suggests that ASMCs can undergo a phenotypic switch *in vitro*, though whether this is also observed *in vivo* is not known. The functions of ASMCs are not mutually exclusive and overlapping populations exits. For example, both proliferative and non-proliferative ASMCs can have a synthetic phenotype, secreting cytokines [65].

The function and phenotype of ASMCs is modulated by different cues, such as ECM proteins, growth factors, serum-deprivation and mechanical strain [63, 66–68]. For example, TGF-β induces proliferation of ASMCs in the presence of serum [67]. ECM proteins differentially regulate ASM phenotype: collagen I enhances cellular proliferation whereas laminin reduces it [66]. It has also been shown that interaction with other cell-types in the airways can affect ASM function. For example, co-culture of ASMCs with epithelial cells leads to a reduction in ASMC contractility while increasing proliferation [69]. Neutrophil elastase, secreted by neutrophils and macrophages in the airways, promotes an inflammatory and synthetic phenotype in ASMCs [70]. Phenotypic plasticity of ASMCs is regulated by intracellular pathways that are activated in response to extrinsic cues. For example, the serum response transcription factor (SRF) regulates the transcription of contractile genes in ASM in response to serum starvation [71]. The mitogenic effect of TGF-β is mediated by the Smad pathway, kinases such as Phosphoinositide 3-kinases

(PI3K), extracellular signal-regulated kinase (ERK) and c-Jun N-terminal kinases (JNK) and the transcription factor Nf-kB [67]. Epigenetic changes may also have a role in the transcriptional regulation of ASM function: in vascular smooth muscle, inhibition of histone deacetylase, an epigenetic regulator, reduces cellular proliferation [72]. Calcium is a master regulator of ASM contractility thus changes in pathways or organelles involved in calcium homeostasis can affect ASM function. The sarco/endoplasmic reticulum Ca^{2+} ATPase (SERCA) is required for the reuptake of calcium by the endoplasmic reticulum (ER). A reduction in SERCA leads to accumulation of calcium in the cytosol, which is associated with induction of a synthetic and proliferative phenotype in ASMCs [73]. Altered calcium homeostasis also promotes mitochondrial biogenesis, which in turn induces proliferation of ASMCs [22]. Although the role of phenotypic plasticity in physiological conditions is not clear, some changes in ASM function are associated with pathological conditions such as asthma and chronic obstructive pulmonary disease (COPD).

Airway smooth muscle (ASM) dysfunction contributes to airway remodelling in COPD (**Figure 1.2**). ASM dysfunction in COPD is characterised by an increase in smooth muscle layer thickness, contractility, and secretion of inflammatory mediators. An increased ASM layer thickness has been observed in the small, central and large airways of patients with COPD, and correlates with severity of disease [21, 22, 74, 75]. Two main mechanisms may contribute to ASM thickening: hyperproliferation of ASMCs and increased ECM deposition. Liu *et al* reported that there is an increase in the levels of the proliferative marker proliferating cell nuclear antigen (PCNA) and in cell number in ASM in small airway sections of COPD patients, suggesting an increase in proliferation of ASMCs [75]. *In vitro*, ASMCs from COPD patients show a higher induction of proliferation in response to mitogenic stimuli (TGF-β and foetal bovine serum) compared to healthy controls [76]. Disease-relevant stimuli, such as cigarette smoke, can also induce proliferation of ASMCs [77]. In addition to hyperproliferation, mild hypertrophy has also been reported in ASMCs in the large airways of COPD patients, and may also contribute to thickening of the ASM layer [78]. In contrast, it has been shown that the ECM volume fraction within the ASM bundles, but not ASMCs size or number, is negatively correlated with $FEV_1\%$ in both

small and large airways [79]. COPD patients show increased levels of the ECM protein laminin in ASM, which also negatively correlates with severity of disease [75, 80]. CS induces the release of collagen by ASMCs and this is more pronounced in ASMCs from COPD patients [81]. ASMCs from COPD patients have decreased levels of hyaluronic acid, an ECM component that regulates tissue flexibility [82]. Although the relative contribution of hyperproliferation of ASMCs and ECM deposition is not fully understood, evidence suggests that both processes may be involved in ASM layer thickening.

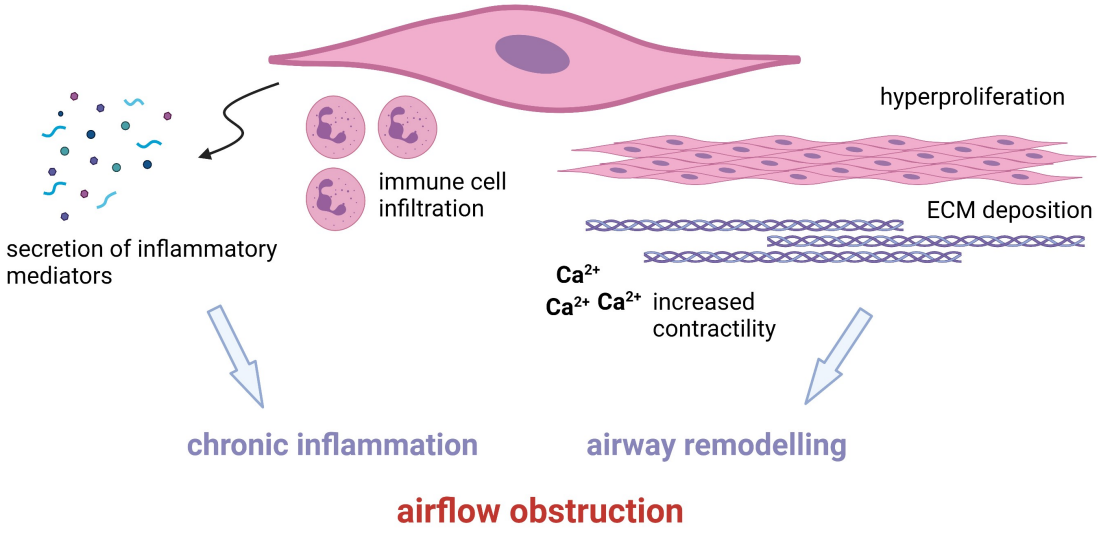

Figure 1.2: Airway smooth muscle dysfunction in COPD. Schematic showing the phenotypes that have been described in airway smooth muscle in COPD. Diagram created with BioRender.com.

Altered contractility of ASM may also contribute to COPD pathogenesis. ASM from small airway sections from COPD patients show increased force generation compared to non-COPD patients, and this is negatively correlated with FEV_1/FVC [83]. In addition, ASMCs from non-smoker patients treated with CS show an increase in expression of calcium regulatory proteins and an increase in agonist-induced calcium levels, which is required for force generation [77]. COPD is characterised by chronic inflammation. ASMCs can secrete inflammatory mediators and this response is increased in COPD. Airways from COPD patients show increased levels of the inflammatory mediators C-

X-C motif chemokine 10 (CXCL-10) and TGF-β, which localized within the ASM [75, 84]. There is also an increase in infiltration of immune cells in the ASM bundles, such as neutrophils, which may be a result of increased chemokine secretion [85]. Indeed, *in vitro*, ASMCs from COPD patients secrete higher levels of the chemokine IL-8, which is a neutrophil chemoattractant, and the pro-inflammatory cytokine IL-6, compared to ASMCs from non-smoker patients [45]. CS treatment leads to increased secretion of IL-8 in ASMCs from both healthy and COPD subjects and of C-X-C Motif Chemokine Ligand 1 (CXCL-1) in COPD ASMCs only [81].

Phenotypic changes of ASMCs, including increased proliferation, ECM deposition, contractility and secretion of inflammatory mediators contribute to airway remodelling and inflammation in COPD (**Figure 1.2**). Therefore, reversing these phentoypes could be an approach to curb disease progression. The ASM is the main target of current COPD therapies, such as bronchodilators, which lead to ASM relaxation. However, these therapies are only effective in alleviating symptoms and do not stop progression of disease [2]. To find new and more effective therapies, it is important to investigate the cellular and molecular underpinnings regulating ASM function. As mentioned before, different extrinsic and intrinsic pathways can regulate ASM function. Studies have suggested mitochondria may play an important role in this regulation, and this will be elaborated in the following sections.

1.2 Introduction to mitochondria

Mitochondria are double membrane intracellular organelles that, according to endosymbiotic theories for the origin of eukaryotic cells, originated from the endocytosis of a proteobacterium by an anaerobic prokaryotic or eukaryotic cell [86, 87]. Often depicted as the "power-house of the cell", mitochondria are responsible for the production of ATP via oxidative phosphorylation (OXPHOS), which is the major source of energy in mammals. Besides this canonical role, mitochondria are central in several other cellular processes, including redox homeostasis, calcium regulation, apoptosis and other signalling pathways.

1.2.1 Structure of mitochondria

Mitochondria are composed of an inner and outer membrane, which define the compartments of the mitochondria. The mitochondrial matrix, the innermost compartment, is surrounded by the inner mitochondrial membrane (IMM) and the intermembrane space is located between the IMM and the outer mitochondrial membrane (OMM). The IMM forms invaginations known as cristae, which is where the proteins of the ETC and ATP synthase are located and where oxidative phosphorylation takes place. Mitochondria have their own DNA (mtDNA), which is 16,569 base-pairs long and encodes for 13 proteins of the ETC, 22 tRNAS and 2 rRNAS [88]. Instead of paired chromosomes, mtDNA is organised in a circular structure resembling plasmids, of which there are multiple copies per cell [87]. The genotypes of these copies can vary in what is called heteroplasmy: the occurrence of multiple variants of mtDNA within a cell or population of cells. Interestingly, despite having their own DNA, most of the mitochondrial proteins are encoded by nuclear DNA.

1.2.2 Mitochondrial respiration, ROS and membrane potential

Mitochondrial respiration is the process by which macronutrients are converted to energy in the form of ATP. Mitochondrial ROS (mtROS) and mitochondrial membrane potential ($\Delta\Psi$m) are generated primarily during aerobic respiration in the mitochondria, as

will be described below and is depicted in **Figure 1.3**. Glycolysis, which takes place in the cytosol, is a catabolic process whereby glucose is converted to pyruvate required for production of ATP in the mitochondria. Pyruvate translocates to the mitochondrial matrix, where it is converted to acetyl-CoA, which feeds into the Krebs cycle. The Krebs cycle produces reducing intermediates, such as NADH and $FADH_2$, which transfer electrons through complexes I-IV of the ETC and finally to oxygen. Mitochondrial respiration can be assessed using a Seahorse Analyser which measures oxygen consumption rate (OCR) and extracellular acitification rate (ECAR) (**Section 2.10**). In mammalian cells, oxygen consumption takes place primarily during oxidative phosphorylation in the mitochondria [39]. Sequential addition of different inhibitors of the ETC, and their effects on the OCR, allow for the quantification of different parameters of mitochondrial respiration. Oligomycin inhibits ATP synthase, determining the proportion of basal respiration coupled to ATP production. Proton leak is determined as the proportion of basal mitochondrial respiration not coupled to ATP production. Carbonyl cyanide-p-trifluoromethoxyphenylhydrazone (FCCP) is an uncoupling agent that disrupts the mitochondrial membrane potential. This leads to uninterrupted flow of electrons through the ETC, causing respiration to reach a maximum. Maximal respiration rate allows the calculation of spare respiratory capacity, which is the difference between maximal and basal respiration, and reflects the ability of cells to respond to stress. Rotenone and antimycin A inhibit complex I and III, respectively, fully attenuating mitochondrial respiration and enabling the calculation of non-mitochondrial oxygen consumption (NMOC). CO_2 produced by mitochondrial respiration and lactate, a product of glycolysis, contribute to extracellular acidification, which is determined by the ECAR levels. The Seahorse Analyzer generates real-time OCR and ECAR data and the Seahorse Wave Software automatically calculates different parameters of respiration based on the generated data and the inhibitors used in the assay. In the Seahorse Cell Mito Stress Test oligomycin, FCCP and Rotenone/Antimycin A are added sequentially allowing for the calculation of maximal respiration, spare respiratory capacity, ATP-linked respiration, non-mitochondrial respiration and proton leak.

The transfer of electrons during oxidative phosphorylation is coupled to proton pumping by the ETC. Complex I, III and IV of the ETC generate a proton motive force (Δp) by pumping protons towards the intermembrane space of the mitochondria [89]. The proton motive force consists of both an electrical and a proton (pH) gradient, and leads to a negative charge environment in the mitochondrial matrix. The resulting potential across the IMM, known as the $\Delta\Psi$m, favours the flow of protons from the intermembrane space to the matrix through ATP synthase, which is coupled to the generation of ATP [39]. Mitochondrial ROS are a by-product of oxidative phosphorylation, derived from superoxide radicals generated by the leakage of electrons during electron transfer [39]. This occurs in specific locations, such as complex I and complex III of the ETC. ROS generation by complex I can occur during electron transfer from NADH to complex I well as in the reverse electron transfer from succinate through complex II to complex I. Other mitochondrial enzymes, such as the flavoenzymes α-ketoglutarate dehydrogenase, glycerol phosphate dehydrogenase and monoamine oxidases, are also important sources of mtROS [90]. mtROS are important signalling messengers and participate in a number of biochemical reactions in the cell, including cellular responses to low oxygen, regulation of inflammatory responses and autophagy pathways [91]. Mitochondria have anti-oxidant systems that maintain mtROS at physiological levels, such as the manganese superoxide dismutase (mnSOD) that converts superoxide ions to hydrogen peroxide, which is then converted to water by catalase (**Figure 1.3**).

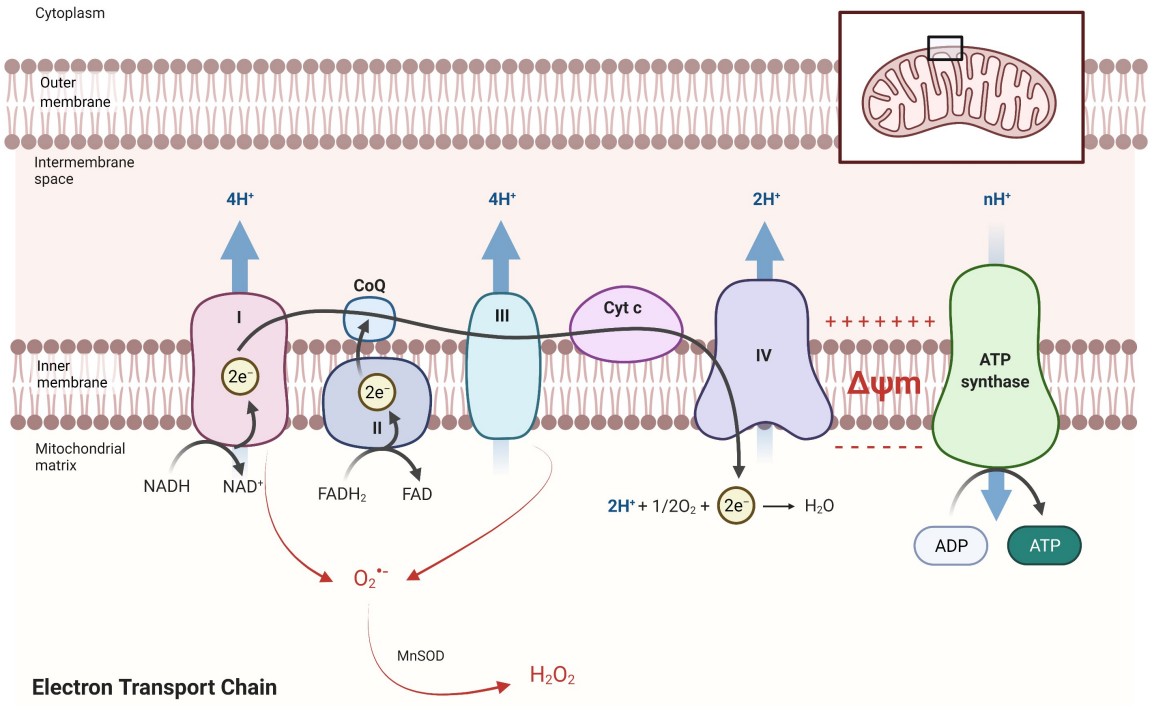

Figure 1.3: Generation of mtROS and Δψm during oxidative phosphorylation. NADH and $FADH_2$, derived from the Krebs cycle, donate electrons to complex I and II, respectively. The electrons are transferred through complexes I-IV (represented by the blue arrows), until being accepted by oxygen, forming water. During this process, electrons can leak from complexes I and III giving rise to ROS. The free radicals formed ($O_2^{\bullet-}$) are converted to H_2O_2 by mitochondrial superoxide dismutase. The flow of electrons is coupled to the pumping of protons by complex I, III and IV from the mitochondrial matrix to the intermembrane space. This generates the mitochondrial membrane potential ($\Delta\psi m$) which favours the transport of protons through ATP synthase, coupled to the production of ATP. Adapted from "Electron Transport Chain" template, by BioRender.com (2022).

Whereas at physiological levels both mtROS and $\Delta\Psi m$ are important in cellular homeostasis and function, sustained changes to these are deleterious and can be both a cause and consequence of mitochondrial damage. For example, damage to the IMM can lead to proton leak - the flow of protons across the IMM through other mechanisms other than ATP synthase - which can dissipate the $\Delta\Psi m$. In turn, this affects ATP production in the mitochondria, as the electrical gradient is required for the functioning of ATP synthase [39]. Mitochondria are not only the source but also a target of, mtROS, where they can cause oxidative damage to phospholipids and mtDNA. This can compromise mitochondrial function. For example, it can lead to the acquirement of mutations in mtDNA that can affect the function of ETC proteins encoded by mtDNA, further increasing elec-

tron leakage and mtROS production [92]. Damage to the mitochondria can also occur as a result of nuclear DNA mutations, deprivation or oversupply of mitochondrial fuel substrates, changes in iron and calcium homeostasis and exposure to exogenous ROS [93].

1.2.3 Mitochondrial quality control

Mitochondria are dynamic organelles and have quality control mechanisms, including re-shaping, re-building and recycling processes that support the maintenance of optimal mitochondrial function in response to stressors (**Figure 1.4**).

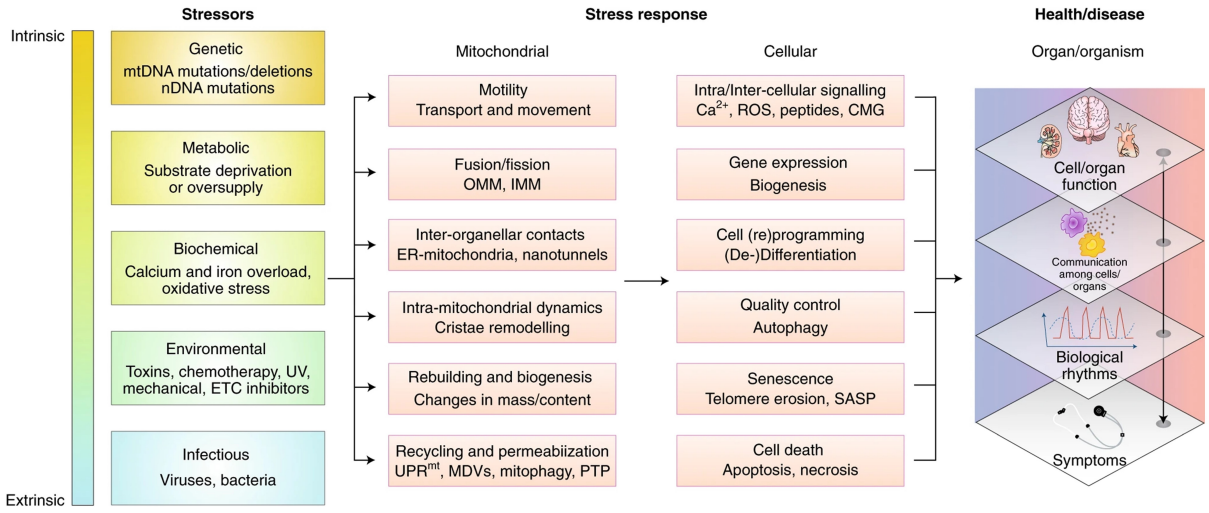

Figure 1.4: Mitochondrial stress responses and associated cellular effects. Reprinted with permission from Eisner *et al* [93] (see Table A1).

Though often depicted as single entities, mitochondria exist in tubular networks that can change in shape and size. Fusion of adjacent mitochondria can occur in response to mitochondrial damage to "dilute" this damage and prevent possible deleterious effects. Mitofusins (MFN)-1 and -2 mediate the fusion of the OMM, whereas optic atrophy protein 1 (OPA1) is required for IMM fusion [94]. Fission of mitochondria, mediated by dynamin-related protein 1 (DRP1), occurs for differing purposes, including re-distribution during cell division as well as segregation of damaged mitochondria for consequent degradation [93]. Mitochondria are degraded through mitophagy, where, in response to damage signals, such as a drop in $\Delta\Psi$m, the mitochondria are targeted to autophagosomes [95].

Damaged regions of mitochondria can also be removed via mechanisms such as the degradation of mitochondrial proteins in the mitochondrial unfolded protein response and the release of mitochondrial derived vesicles containing damaged cargo [93]. When mitochondria are degraded, compensatory mechanisms are required to ensure the quantity of mitochondria in the cells is maintained at physiological levels. *De novo* synthesis of mitochondria occurs through mitochondrial biogenesis. This involves a coordinated synthesis of mitochondrial and nuclear proteins, lipids and mtDNA replication, regulated by the mitochondrial transcription factor A (TFAM) and the transcriptional co-activators, the peroxisome proliferator-activated receptor gamma coactivator 1-alpha and -beta (PGC1-α and PGC1-β) [96].

Mitochondria can move within cells. This is well described in the context of neuronal biology, where mitochondria move to energy-demanding distal compartments such as synapses and axonal branches [97]. Mitochondria can move along microtubules or actin-filaments (**Figure 1.5**). In microtubule-based transport, the motor protein dynein mediates retrograde movement (towards the nucleus) whereas anterograde transport (towards the plasma membrane) is mediated by proteins in the kinesin family, such as kinesin-related protein 5 (KIF5). These proteins associate with the adaptor proteins trafficking kinesin (TRAK)-1 and -2, which bind to the mitochondrial membrane receptors mitochondrial Rho GTPase (MIRO) -1 and -2. Mitochondrial movement along actin filaments is mediated by myosins, such as Myosin XIX (MYO19) [97]. Not all mitochondria are motile; in neurons, two-thirds of mitochondria are stationary and this is facilitated by docking proteins such as syntaphilin [98]. Other mitochondrial proteins, typically involved in different processes, can also regulate mitochondrial movement. For example, the PTEN-induced kinase 1 (PINK1)/Parkin complex, which is best known for its role in mitophagy, can phosphorylate MIRO1, targeting it for degradation and arresting mitochondrial movement [99]. The fusion protein MFN-1 can form complexes with MIRO1 and facilitates axonal movement of mitochondria [100]. Movement of mitochondria can be either random or directional, and is modulated by different stimuli, such as ADP, calcium and glucose [101, 102]. Intracellular mitochondrial movement has been well described

in neurons, but whether the same mechanisms are present in other cell types, such as ASMCs, is less well elucidated.

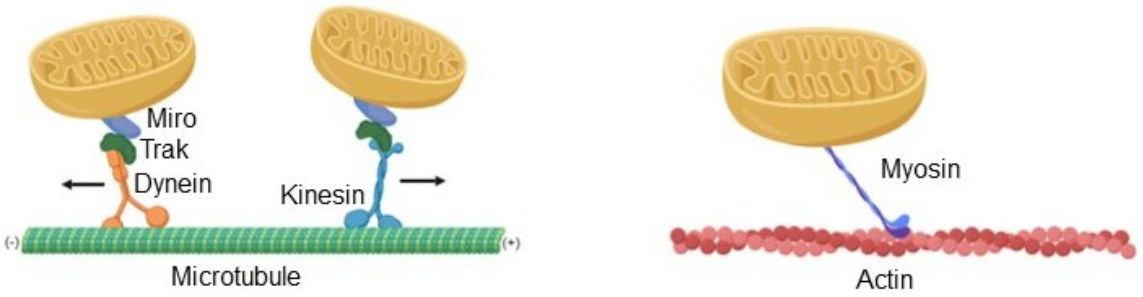

Figure 1.5: Intracellular movement of mitochondria Schematic showing movement of mitochondrial along microtubules and actin filaments. Created with BioRender.com.

Other mitochondrial quality control mechanisms include cristae remodelling and changes in contact sites with other organelles, such as the endoplasmic reticulum, as depicted in **Figure 1.4** [93]. Together, these responses allow cells to regulate the quality and the quantity of mitochondria at a given time.

Extensive damage to the mitochondria and/or impaired quality control mechanisms can result in sustained mitochondrial dysfunction. In consequence, this can affect the plethora of cellular mechanisms in which mitochondria play a pivotal role, including ATP production, redox homeostasis and calcium regulation, and lead to the development of disease. Mitochondrial diseases are a clinically heterogeneous group of disorders caused by mutations in nuclear or mitochondrial DNA which predominantly affect mitochondrial oxidative phosphorylation. These tend to affect energy-demanding tissues such as the heart, skeletal muscle and the brain. Examples of such disorders include mitochondrial encephalomyopathy, lactic acidosis and stroke-like episodes (MELAS), Leigh and Kearns-Sayre syndrome [103, 104]. In addition, mitochondrial abnormalities have also been associated with several noncommunicable chronic diseases, such as type 2 diabetes mellitus, lung cancer, cardiovascular diseases and neurodegenerative conditions such as Alzheimer's and Parkinson's [103, 105]. There is evidence of mitochondrial dysfunction in COPD, and this will be elaborated in the following section.

1.2.4 Mitochondrial dysfunction in COPD

Mitochondrial dysfunction has been reported in the lungs and cells of patients with COPD, and therefore may play a role in driving the cellular mechanisms that underly COPD pathogenesis, such as inflammation and oxidative stress. For example, large aggregates of mitochondria are found in diaphragm muscle fibres of patients with COPD [106]. Mitochondria isolated from bronchial biopsies of COPD patients have increased levels of mtROS and decreased $\Delta\psi m$ compared to samples from healthy donors, and there is a correlation between $\Delta\psi m$ and FEV_1 (% predicted) [46]. *In vitro*, epithelial cells from COPD patients show abnormalities in mitochondrial structure, such as excessive branching of the mitochondria and cristae depletion, mitochondrial swelling and elongation and increased levels of mtDNA damage [107, 108]. Mitochondrial dysfunction might be driven by exposure to cigarette smoke, as it is the major source of exogenous oxidants in COPD. Indeed, cigarette smoke has been shown to alter mitochondrial function, though the effects vary depending on the experimental set-up and the cell types used. Long-term exposure to CS (6-months) leads to fragmentation and branching of cristae in a bronchial epithelial cell line (BEAS-2B) [107]. In contrast, short-term (6 to 48 hours) exposure to CS leads to mitochondrial hyperfusion in murine lung epithelial (MLE)-12 and primary mouse alveolar epithelial cells, mediated by an increased expression of MFN2 [109]. CS leads to an increase in mtROS and decrease in membrane potential in the bronchial epithelial cell line BEAS-2B, and this induces mitophagy through stabilization of PINK1 [110]. CS also induces mitophagy in primary human bronchial epithelial cells [111] which is contrary to what is seen in primary fibroblasts and small airway epithelial cells where CS leads to a reduction in Parkin translocation, thereby impairing mitophagy [112].

Although CS induces mitochondrial dysfunction, only a proportion of smokers develop COPD. Increased susceptibility to CS might contribute to the higher levels of mitochondrial dysfunction detected in COPD lungs. What underlies this susceptibility, however, is not known. With regards to the mitochondria, this may be due to inherent differences in mitochondrial function and structure, or maladaptive mitochondrial responses to stress. Genetic predisposition may increase the susceptibility of COPD patients to

mitochondrial damage. For example, the iron regulatory protein 2 (*IREB2*) is a major COPD susceptibility gene [113] and has been shown to promote mitochondrial dysfunction in a mouse model of COPD [114]. As mentioned before, mitochondria have quality control mechanisms to maintain optimal function in response to stress. In COPD, some of these are impaired. For example, mitochondrial dynamics mechanisms might be dysregulated in COPD. Specifically, the prohibitin complexes (PHB), which help maintain mitochondrial stability and normal function as part of the mitochondria fusion machinery, are downregulated in lung tissue of smokers and COPD patients. Expression of PHB correlates with airway obstruction (FEV_1 %) [115]. COPD epithelial cells also show impaired Parkin mitochondrial translocation, which is required for mitophagy to occur, and Parkin expression is lower in the lungs of COPD patients compared to healthy controls [111, 112]. Reduced expression of Parkin and increased mitochondrial mass in COPD fibroblasts indicates these cells might also have impaired mitophagy [116].

Importantly, there is some evidence showing that changes in mitochondrial function are associated with the development of cellular phenotypes that drive COPD pathogenesis. In epithelial cells, CS-induced cellular senescence is increased when mitophagy is impaired, either by knockdown of PINK1 or by using the mitochondrial division inhibitor (Mdivi) -1 [111, 112]. This suggests that impaired mitophagy, which has been reported in COPD lungs, may drive senescence in these cells. Damaged mitochondria can release mitochondrial (mt)-DAMPS, such as ATP and mtDNA, which in turn can induce inflammation through activation of Toll-like receptors [117]. Increased levels of ATP are found in BALF from COPD patients, which correlates with severity of disease. Moreover, COPD neutrophils and macrophages respond to ATP stimulation by secretion of pro-inflammatory and tissue-degrading mediators [118]. Cell-free mtDNA detected in urine and plasma also correlates with distinct COPD phenotypes [119, 120]. Mitochondrial dysfunction also induces necroptosis and ferroptosis, two forms of cell death that promote inflammation. For example, increased levels of mtROS lead to the autophosphorylation of the receptor-interacting protein kinase 1, which in turn activates the necroptosis pathway [110]. Interestingly, PINK1 knockdown and Mdivi-1 protect epithelial cells from

CS-induced necroptosis, suggesting that, in this case, mitophagy, which is thought to be protective, may promote this phenotype [110]. Further studies are required to establish the role of mitochondrial dysfunction in driving disease phenotypes.

There is also evidence of alterations in mitochondrial function in the ASM of COPD patients. ASMCs from smokers, with or without COPD, show mitochondrial dysfunction and reduced oxidative phosphorylation compared to healthy non-smoker cells [45]. These findings indicate a role of smoking in ASMC mitochondrial dysfunction, in line with studies reporting that CS causes mitochondrial fragmentation, mtROS production and a decrease in $\Delta\psi m$ in ASMCs from healthy non-smoker patients [76, 121]. However, ASMCs from COPD patients also show inherent differences in mitochondrial function compared to ASMCs from healthy ex-smoker subjects. Michaeloudes *et al* showed that ASMCs from COPD patients have a distinct metabolic phenotype compared to ASMCs from ex-smoker and non-smoker patients, which is characterised by an accumulation of metabolites involved in glycolysis, and fatty acid and glutamine metabolism [76]. Under H_2O_2-induced oxidative stress, COPD ASMCs have increased levels of mtROS compared to ASMCs from healthy smoker and non-smoker subjects [45]. Therefore COPD ASMCs may show impaired or maladaptive responses to oxidative stress-induced mitochondrial dysfunction. Whether COPD ASMCs also show increased susceptibility to CS-induced mitochondrial dysfunction is not known.

The role of mitochondrial function in determining ASM phenotypes has yet to be fully elucidated. The mtROS scavenger MitoQ inhibits mitogenic-induced proliferation of healthy ASMCs as well as of COPD ASMCs, though to a lesser extent in the latter [45]. Contrastingly, another study reported that the glutathione synthesis inhibitor buthionine sulfoximine increased mtROS levels but also inhibited mitogenic-induced proliferation of COPD ASMCs [76]. Furthermore,inhibition of glycolysis and glutamine depletion attenuate mitogenic-induced proliferation in COPD ASMCs [76]. The link between mitochondrial function and other ASM phenotypes relevant to COPD, such as contractility, secretion of mediators and ECM deposition should be further explored.

As highlighted in the paragraphs above, mitochondrial dysfunction may play a key role

in COPD pathogenesis. Whilst cigarette smoke drives mitochondrial dysfunction in different models, cells from COPD patients may be more sensitive to CS-induced mitochondrial damage. This could explain why only some smokers develop COPD. Understanding the mechanisms of increased susceptibility to CS can help identify therapeutic targets for the treatment of COPD. One possibility is that patients with COPD have impaired mitochondrial adaptation or quality control mechanisms, such as mitophagy, which would result in a failure to preserve mitochondrial function in response to damaging stimuli. Transfer of mitochondria between cells is a recently described mitochondrial quality control mechanism. However, it is not known whether this happens between lung structural cells, nor whether it's impairment can lead to the development of disease, such as COPD.

1.3 Introduction to mitochondrial transfer

Mitochondria possess a number of quality control mechanisms in order to preserve optimal function, as described in **Section 1.2.3**. Recent evidence suggests that in addition to intracellular dynamics, inter-cellular mitochondrial movement may also play an important role in cellular homeostasis and responses to stress. The observation that cells can share mitochondria was first shown by Spees *et al* in 2006. Cells (A549 cell line) with non-functional mitochondria acquired mitochondria from mesenchymal stem cells (MSCs) and skin fibroblasts, and this restored their mitochondrial respiration [122]. Since then, several studies have demonstrated transfer of mitochondria between different cell types [123–128]. Mitochondrial transfer between cells occurs in many different contexts, from development to disease [123, 129, 130]. However, many questions regarding this process, such as how, when and why it happens, still remain. In the following sections, I will summarise the current literature on mitochondrial transfer between cells.

1.3.1 Detection of mitochondrial transfer

Mitochondrial transfer has been observed both *in vitro* and *in vivo* using different experimental approaches. The most commonly used protocol to detect mitochondrial transfer is the use of MitoTracker dyes to stain and track mitochondria from one specific cell population (mitochondria "donor" cells). If mitochondria from the "donor" cells are taken up by other cells, then the fluorescence of MitoTracker dyes can be detected in the "recipient cells" by flow cytometry or fluorescence microscopy. MitoTracker dyes have a positively charged thiol-reactive chloromethyl moiety, which allows them to accumulate in active mitochondria due to negative charge of the mitochondrial matrix. Thus, changes in $\Delta\psi m$ can affect the staining with these dyes. Some types of MitoTracker dyes, however, such as MitoTracker Green FM, bind covalently to mitochondrial proteins and are therefore less likely to be affected by changes in $\Delta\Psi m$ [131]. Another caveat for these dyes is that they can leak from cells, and in this case the detection of MitoTracker fluorescence in recipient cells may be a consequence of dye leakage rather than transfer [132, 133]. It is important to control for this possibility by, for example, co-culturing donor and recipi-

ent cells in systems that impair cell-cell contact and the transfer of intact mitochondria, whilst allowing transfer of free dye (e.g. transwell plates). To circumvent the issue of dye leakage, it is also possible to track mitochondria from donor cells by tagging them with fluorescent proteins. There are several plasmids encoding mitochondrial targeted fluorescent proteins that have been used to tag mitochondria of donor cells, which have thereafter been detected in recipient cells in co-cultures [123, 125, 134, 135]. However, this protocol is not as effective in tagging mitochondria as MitoTracker staining, since transfection efficiency may be low. Further, transfecting primary cells can be especially challenging and it is not possible to stably transfect these as they can only be used at limited passage numbers. Genetic approaches can also be used to detect donor mitochondria in recipient cells. Mitochondrial DNA from different cells can be differentiated by identifying the presence or absence of specific mutations unique to a certain cell line [122, 136, 137]. If a donor-specific mutation is detected in recipient cells, this indicates uptake of donor mtDNA by the recipient cell. These mutations can be detected by sequencing or by qPCR methods, such as the amplification refractory mutation system (ARMS)-qPCR [138]. This approach cannot be used to assess mitochondrial transfer between cell-lines or primary cells from the same patient, as they will have the same mtDNA sequence. Finally, detection of species-specific mitochondrial genes or proteins can be used to assess transfer of mitochondria between cells from different species [123, 127, 132, 139–141]. While using MitoTracker dyes and fluorescent proteins have experimental drawbacks, detection of mtDNA genes, mitochondrial proteins or mtDNA does not indicate transfer of whole mitochondria. Therefore, multiple methods should be used to confidently detect and quantify mitochondrial transfer.

1.3.2 Cell types known to exchange mitochondria

Mitochondrial transfer has been reported between different cell types. Most studies to date focus on the transfer of mitochondria from stem cells, such as mesenchymal stem cells, to structural and immune cells, such as epithelial cells, macrophages, cardiomyocytes, neurons and ASMCs [123, 127, 142–144]. Mitochondrial transfer has also been shown

to occur from structural cells, such as cardiomyocytes and adipocytes, to immune cells such as macrophages [124, 145, 146]. Different cancer cells can receive mitochondria from immune and stem cells [147–149]. Interestingly, cells do not need to be in close contact to transfer mitochondria: in a murine model, adipocytes can transfer their mitochondria to cardiomyocytes in the heart [150]. Not all cell types can exchange mitochondria. For example, whereas MSCs, ASMCs, and fibroblasts can transfer mitochondria to lung epithelial cells, movement of mitochondria in the reverse direction has not been detected [125]. Studies investigating transfer of mitochondria between the same cell type are limited, and this has only been demonstrated in vascular smooth muscle cells and MSCs [151, 152]. It is not known whether other structural cells can exchange mitochondria. In addition, while some studies have demonstrated transfer of mitochondria to occur in *in vivo* murine models [123, 124, 150], many studies are limited to *in vitro* observations. Whether mitochondrial transfer occurs within and between tissues in the human body remains unknown.

1.3.3 Mechanisms of mitochondrial transfer

Two main routes of mitochondrial transfer have been described: tunnelling nanotubes (TNTs) [125, 136, 141, 143, 153] and extracellular vesicles (EVs) [126, 127, 154]. TNTs are thin membrane protrusions that extend from one cell to another and transport different cargoes, such as electrical signals, calcium, pathogens, lysosomes, lipid droplets and mitochondria [155, 156]. TNTs can form by outgrowth of filopodia-like protrusions towards the target cell or through the outward dislodgment of connected cells where TNTs maintain the cell connection [155]. TNTs vary in their size, composition and duration, which may be related to their specific function. For example, macrophages can form both F-actin-containing small TNTs (<0.7µm) as well as larger TNTs (>0.7µm), which contain both F-actin and microtubules. Mitochondria are found in the latter only [157]. Live cell imaging has shown that mitochondrial move along TNTs [125] and several studies have reported that impairing TNT formation abrogates mitochondrial transfer [141, 148, 153, 158]. For example, knockdown of TNF Alpha Induced Protein 2 (TNFAIP2), a protein

involved in TNT formation reduces mitochondrial transfer from MSCs to epithelial cells [125]. Cytochalasin B, an inhibitor of actin polymerisation, also leads to a reduction in TNT formation and in the transfer of mitochondria from MSCs to epithelial cells [140]. Some proteins involved in intra-cellular movement, such as MIRO1 and KIF5B, are required for TNT-mediated mitochondrial transfer [125, 158]. However, the mechanisms is involved in TNT formation are not completely understood.

Extracellular vesicles are cell-derived membranous structures that can also transport different cargoes between cells. There are different types of EVs, classified based on their origin. Microvesicles (100-2000nm) are released from membrane budding, whereas exosomes (40-100nm) are released from multivesicular endosomes [159]. A third type of EVs are apoptotic bodies (1-4µm), which are formed during apoptosis. Whole mitochondria have been observed in EVs by electron microscopy [126, 127]. It has been shown that cells can take up mitochondria from other cells via EV-containing conditioned media (CdM) [154], as well as from EVs isolated from CdM [146, 160]. Studies have also reported that inhibiting uptake of EVs reduces mitochondrial transfer. For example, dynasore, an endocytosis inhibitor, blocks transfer of mitochondria from MSCs to alveolar epithelial cells [123]. Treatment of macrophages with the phagocytic inhibitor dextran sulphate blocked the uptake of MSC-derived microvesicles containing mitochondria [127]. While EVs have been described as a route for mitochondrial transfer, the origin, and therefore classification, of mitochondria-carrying EVs is less clear. These have been shown to vary in size and composition. Astrocytes secrete extracellular particles containing mitochondria, spanning from 300 to 1,100 nm [126]. Markers typically found in exosomes (e.g. ALG-2-interacting protein X (ALIX) and tumour susceptibility gene (TSG)-101) [146, 150, 160] as well as in microvesicles (e.g. caveolin-1 and β-integrin) [126, 161] have been detected in EVs carrying mitochondria.

TNTs and EVs are important mechanisms of mitochondrial transfer, but they may not be the only ones. Cancer cells are able to take up free mitochondria [132, 162] and respiratory-competent free mitochondria have been detected in circulating blood [163] and in conditioned media of cultured cells [126, 146]. Mitochondria can also be trans-

ferred through gap junctions [144, 164] and through ring canals that join sister germ cells [129]. Different mechanisms of mitochondrial transfer may mediate distinct cell-cell communication processes.

1.3.4 Modulation of mitochondrial transfer

Different stimuli can regulate the rate of mitochondrial transfer between cells. Treatment of co-cultures with stress inducers, such as hydrogen peroxide and cigarette smoke extract, have been shown to increase transfer from MSCs to acute myeloid leukaemia (AML) blasts and ASMCs, respectively [143, 148]. In contrast, anti-oxidants, such as n-acetylcysteine (NAC) and glutathione, reduced transfer from MSCs to AML blasts [148]. This supports the idea that mitochondrial transfer is a quality control mechanism that is induced in response to stress. It is not clear whether these responses are mediated by effects of the stimuli in the mitochondria "donor" or "recipient" cells, or both. Transfer of mitochondria from MSCs to epithelial cells increases when the latter are treated with rotenone or antimycin, inhibitors of the ETC. However, this effect is reduced or no effect is seen when MSCs, the mitochondrial donor cells, are treated with rotenone [125, 135]. Interestingly, reduced ROS production by AML blasts, as a consequence of NADPH oxidase (NOX-2) knockdown, inhibited transfer of mitochondria from MSCs to the AML blasts, suggesting that regulation of this process involves an interplay between the two cell types, mediated by ROS [148]. While stimuli can modulate mitochondrial transfer, cells may also exhibit inherent differences in the ability of donating and receiving mitochondria, as highlighted in **Section 1.3.2**. MSCs from patients with rheumatoid arthritis have a lower ability to donate mitochondria [130], and transfer of mitochondria from adipocytes to macrophages is reduced in a murine model of obesity [145]. This suggests that disease status can affect mitochondrial transfer between cells, though whether this is a consequence or cause is not known.

1.3.5 Functional impact of mitochondrial transfer

Recent evidence suggests that transfer of mitochondria between cells is an important process in regulating mitochondrial and cellular function [123, 125, 127, 130, 143, 148]. It has been widely described that mitochondrial transfer leads to an increase in ATP production by recipient cells [126, 141, 147, 148, 165]. Further, this process can rescue cells from stress-induced mitochondrial dysfunction. For example, transfer of mitochondria from MSCs to epithelial cells led to a reduction in rotenone-induced mtROS production [125]. H_2O_2-induced mitochondrial ROS and fission in MSCs is also rescued by mitochondrial transfer [166]. In COPD, there is evidence suggesting that transfer of mitochondria from induced pluripotent stem cell derived MSCs (iPSC-MSCs) to ASMCs and to airway epithelial cells rescues these cells from oxidative stress-induced mitochondrial damage [140, 143]. Contrastingly, some studies have reported that transfer of mitochondrial can have a detrimental effect on mitochondrial function. For example, transfer of mitochondria from adipocytes to macrophages leads to an increase in mtROS and decrease in $\Delta\Psi$m in the latter [145]. One possible explanation for these contrasting responses is the status of the donated mitochondria.

Are cells donating their "healthy" mitochondria or ridding themselves of damaged mitochondria? In some models, transfer of intact and functional mitochondria has been shown [126, 146, 154]. However, dysfunctional mitochondria released by damaged cells can also be taken up by neighbouring cells [124, 127]. Another important factor in understanding the response of cells to transfer of mitochondria is the fate of the transferred the mitochondria in the recipient cell. Phinney *et al* showed that MSCs shed microvesicles containing depolarized mitochondria, which are then taken up by macrophages where they integrate in the host network and are repurposed to enhance cellular bioenergetics [127]. Mitochondria transferred from neural stem cells to macrophages and from adipocytes to cardiomyocytes also fuse to the mitochondria network in the host cell [146, 150]. In contrast, another study reported that mitochondria shed from retinal ganglion cells are internalized and degraded by adjacent astrocytes [134]. Similarly, macrophages take up and degrade damaged mitochondria from cardiomyocytes and this is required to maintain

metabolic homeostasis in the heart [124]. The different nature and fate of transferred mitochondria may dictate the functional impact elicited in the recipient cell. The precise mechanisms mediating the functional impact of mitochondrial transfer are not known.

One promising observation is that mitochondrial transfer reverses not only mitochondrial damage, but also cellular dysfunction and pathological features in different *in vitro* and *in vivo* models [123, 125, 130, 143]. Mitochondria from untreated pheochromocytoma 12 (PC12) cells to UV-treated PC12 cells rescues the latter from UV-induced apoptosis [153]. Transfer of mitochondria from MSCs to T helper 17 (Th17) cells leads to a reduction in the production of interleukin-17, which is associated with pro-inflammatory phenotypes characteristic of autoimmune conditions [130]. *In vivo*, transfer of mitochondria from airway-instilled MSCs to the alveolar epithelium reduced lipopolysaccharide (LPS)-induced acute lung injury in mice, characterised by leukocytosis and protein leak [123]. MSCs over-expressing MIRO1, which is associated with increased transfer, are more effective in reversing hyperresponsiveness and airway remodelling in a mouse model of allergic airway inflammation, when compared to normal MSCs or MSCs with MIRO1 knockdown [125]. Alveolar macrophages treated with MSC-derived EVs, which contain mitochondria, ameliorate LPS-induced lung injury in mice [154]. Moreover, iPSC-MSCs prevent lung inflammation and emphysema in *in vivo* models of COPD, possibly through the transfer of mitochondria [143]. In contrast, in cancer models, cancer cells can hijack mitochondria from stem cells and immune cells and this favours disease progression [132, 137, 147–149, 167]. For example, AML cells become resistant to the chemotherapeutic agent cytarabine after receiving mitochondria from stem cells [147]. Cancer cells that acquire mitochondria from MSCs show increased migration, invasion capacity and proliferation [132]. The effects of transfer of mitochondria from damaged to healthy cells has not been explored; can it lead to disease propagation?

Modulating mitochondrial transfer may be used as an approach to treat different pathological conditions. For example, cell-based therapies based on the transfer of mitochondria from stem cells to structural cells can be used to reverse disease phenotypes. Alternatively, inhibition of mitochondrial transfer in cancer models could be used to pre-

vent disease progression. The role of mitochondrial transfer between structural cells in health and in disease, and its' potential as a therapeutic target, has yet to be elucidated.

1.4 Aims of the study

COPD is a heterogeneous disease that has a significant health and economic burden. There is an urgent need for developing new treatments for COPD, as current therapies only reduce symptoms without treating the driving mechanisms of disease. The main cause of COPD is cigarette smoking, however, only a proportion of smokers develop COPD. Understanding the mechanisms underlying COPD susceptibility to disease-causing agents may help identify new therapeutic targets.

The pathophysiology of COPD is complex and involves chronic inflammation associated with emphysema and remodelling of the airways. Abnormal ASM layer thickening, possibly due to ASMC hyperplasia and/or ECM deposition, contributes to airway remodelling and airflow obstruction in COPD. There is also evidence of defective mitochondria in the lungs and in cultured ASMCs from patients with COPD, which may drive airway inflammation and remodelling. However, the mechanisms driving mitochondrial dysfunction and how this leads to abnormal cellular responses and lung pathology is not fully understood.

Homeostatic mechanisms to preserve mitochondrial function may be impaired in COPD, leading to persistence of disease phenotypes. Mitochondrial transfer from stem cells to lung cells rescues the latter from mitochondrial dysfunction and reverses lung inflammation and emphysema in animal models of lung disease [123, 125, 140]. However, it is not known whether lung structural cells can exchange mitochondria, nor what role this process plays in modulating mitochondrial and cellular function in normal tissue homeostasis as well as in disease.

Based on the above evidence, I hypothesise that: **Mitochondrial transfer is a homeostatic mechanism that modulates mitochondrial and cellular function in ASMCs, which is impaired in COPD leading to sustained mitochondrial dysfunction in response to stress.** This is illustrated in **Figure 1.6**.

To address this hypothesis, the aims of this study are to:

- Characterise mitochondrial and cellular function in ASMCs from healthy and COPD subjects under conditions of CS-induced stress
- Assess mitochondrial transfer between ASMCs, under baseline and CS exposed conditions, and assess the functional impact of this process
- Investigate whether mitochondrial transfer is impaired in COPD ASMCs
- Elucidate the mechanisms of mitochondrial transfer between ASMCs

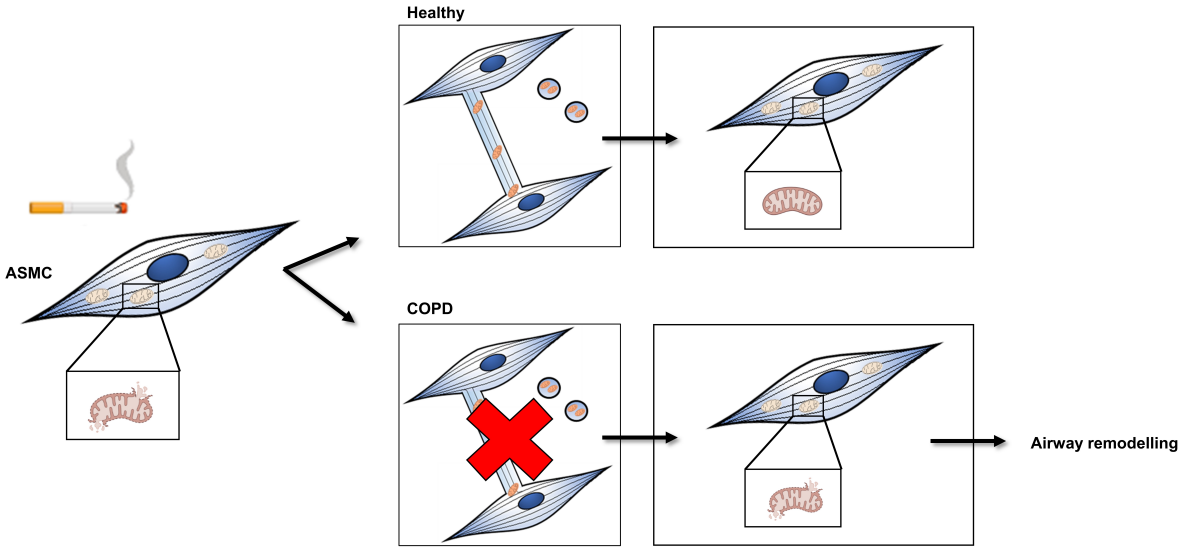

Figure 1.6: Proposed hypothesis of ASM dysfunction in COPD. Mitochondrial transfer acts as a homeostatic mechanism to rescue ASMCs from mitochondrial damage induced by, for example, cigarette smoke. In COPD mitochondrial transfer is impaired. This leads to sustained mitochondrial dysfunction, which contributes to changes in ASM function, such as proliferation, secretion of inflammatory mediators and ECM deposition. These result in airway remodelling, such as thickening of the airway wall, which lead to airflow obstruction seen in COPD. Created with BioRender.com.

Chapter 2

Materials and Methods

Assay optimizations performed during my PhD study are described throughout the thesis. All other assays were either optimized previously within the group or did not require optimization (e.g. followed manufacturer's instruction). All optimizations were performed on ASMCs from healthy subjects unless otherwise stated.

2.1 Culture of ASMCs

ASMCs were isolated from non-cancerous tissue obtained from surgical resections of main bronchi (2nd-to-4th generation) of nine COPD and nine non-COPD ("healthy") ex-smoker patients with a diagnosis of adenocarcinoma (**Table 2.1**). Non-smoker healthy ASMCs were not used in this study, and therefore all mentions of healthy ASMCs refer to ASMCs from healthy ex-smoker subjects, unless otherwise stated. ASMCs grown to passage 2 were kindly provided by Professor Andrew Halayko (University of Manitoba, Canada). ASMCs were cultured in High-Glucose Dulbecco's Modified Eagle's Medium (DMEM; Sigma Aldrich, St. Louis, Missouri, United States) supplemented with a solution of 10 units/ml Penicillin and 10 µg/ml Streptomycin (Sigma Aldrich), 2.5 µg/ml Amphotericin B (Sigma Aldrich), 4 mM L-Glutamine (Sigma Aldrich) and 10% Foetal Bovine Serum (FBS) (also referred to as complete medium). Serum-free media consisted of Dulbecco's Modified Eagle's Medium (DMEM) without Phenol Red (Thermo Fisher Scientific, Waltham, Massachusetts, United States) supplemented with a solution of 10 units/ml Penicillin and 10 µg/ml Streptomycin, 2.5 µg/ml Amphotericin B, 4 mM L-

Glutamine, 0.1% Bovine Serum Albumin (Sigma Aldrich) and 1% Non-Essential Amino Acids (Sigma Aldrich). Cultures were maintained in a 5% CO2 and 37° C humidified incubator. Cell culture media was changed every 2-3 days and cells were passaged at 80-100% confluency with 1X Trypsin-EDTA Solution (Sigma Aldrich). All experiments were performed with ASMCs grown to passage 5 or 6.

	Healthy	**COPD**
Number of Subjects	9	9
Age (years)	67.89 ± 3.297	59.56 ± 3.962
Gender (male/female)	3/6	8/1
FEV_1 (% of predicted)	98.44 ± 3.618	57.56 ± 5.268****
FEV_1/FVC (%)	79.56 ± 2.028	58.22 ± 3.487****
Smoking (Pack Years)	24.58 ± 3.643	56.78 ± 14.91
GOLD stage (I/II/III/IV)	N/A	0/7/1/1

Table 2.1: Demographics of subjects from whom ASMCs were obtained. Abbreviations: FEV_1 – forced expiratory volume in 1 second, FEV_1 predicted - according to age, sex, height and ethnicity, FVC – forced vital capacity, Pack Years – packs smoked per day*years of smoking, GOLD stage: classification of airflow limitation severity in COPD by the Global Initiative for Chronic Obstructive Lung Disease [2], N/A – not applicable; ****p<0.0001 relative to Healthy. Data presented as mean ± SEM.

2.2 Cigarette smoke media (CSM) preparation

To prepare CSM, cigarette smoke from one Marlboro Red cigarette (13 mg TAR and 1 mg nicotine) was pumped at 60 rpm into 25 ml of serum-free media using a peristaltic pump (Longer Pump). Absorbance was measured at 320 nm with a Spectra Max Plus 384 Spectrophotometer (Molecular Devices, San Jose, California, United States) and adjusted to 1.1 absorbance units. The medium was filtered through a 0.22 µm filter and stored in frozen aliquots. Working concentrations of 10% and 25% were freshly prepared by diluting the stock (100%) in serum-free media. The same batch of frozen CSM aliquots

was used in each experiment.

2.3 Cell viability assay

Cell viability was assessed by Annexin and propidium iodide (PI) staining (Thermo Fisher Scientific), as per the manufacturer's instructions. PI enters the cells when the plasma membrane is compromised, which is indicative of necrosis. Annexin V binds to phosphatidylserine when it is located to the outer plasma membrane, which happens during apoptosis. Late apoptotic cells will also have a compromised plasma membrane and will stain for PI as well as Annexin V. As a positive control, cells were treated with 500 µM hydrogen peroxide for 4 hours to induce cell death. Briefly, cells were harvested and re-suspended in 1X annexin-binding buffer with 100 µg/mL PI. After this, 5 µl of FITC-annexin V was added to 100 µl of cells and incubated at room temperature for 15 minutes, followed by addition of 400 µl of 1X annexin-binding buffer. Samples were kept on ice while quantification of fluorescence in the phycoerythrin (PE) and fluorescein (FITC) channels was performed by flow cytometry, using the FACSCanto II flow cytometer (BD Biosciences, Franklin Lakes, New Jersey, United States) (**Table 2.2**). Analysis was performed on the FlowJo 10.4 Software (BD Biosciences), as follows. Firstly, forward vs side scatter (FSC vs SSC) gating was used to differentiate cells from cell debris, and FSC-height vs FSC-amplitude gating was used to exclude doublets. Unstained controls were used to draw quadrant gates in a FITC x PE dot plot, creating the quadrants: FITC-negative/PE-negative, FITC-positive/PE-negative, FITC-negative/PE-positive and FITC-positive/PE-positive. The percentage of cells positive for Annexin V and/or PI was quantified based on the percentage of events in each quadrant.

Channel	Excitation Laser Line	Filter
Phycoerythrin (PE)	488 nm	575/26
Fluorescein (FITC)	488 nm	530/30
Pacific Blue	405 nm	440/50

Table 2.2: Optical channel configurations used for flow cytometry

2.4 Proliferation assays

To assess proliferation, cells were plated in 96-well plates (3,000 cells/well) and were washed with HBSS and dry frozen at -80°C at days 1-6 after plating. Total DNA was measured as a surrogate for cell number using the CyQuant Assay (Invitrogen, Waltham, Massachusetts, United States), as per manufacturer's instructions. Fold-change in total DNA from day 1 to day 6 was calculated to evaluate changes in cell number and hence proliferation.

Proliferation was also assessed by measuring BrdU incorporation using the Cell Proliferation ELISA kit (Roche, Basel, Switzerland), according to the manufacturer's instructions. Briefly, cells were plated at 3,000 cells/well in a 96-well plate. Cells were treated as appropriate and cultured for 24 to 72 hours. BrdU was added to the cells 24 hours before collection, thus allowing for measurement of DNA synthesis of proliferating cells during this period of time. Cells were then fixed, and an enzyme-conjugated anti-BrdU antibody was added. The immune complexes were detected by a substrate reaction and the reaction product was quantified by measuring luminescence using a spectrophotometer (Molecular Devices).

Cell-cycle analysis was performed using propidium iodide staining. Following stimulation, cells were fixed with ethanol at the appropriate time-point, and then were stained with 3 µM propidium iodide (Thermo Fisher Scientific) in phosphate buffered saline (PBS) containing 100 µg/ml RNAse A for 30 minutes. Fluorescence was measured by flow cytometry in the PE channel using the Accuri C6 flow cytometer (BD Biosciences), and the

percentage of cells in the G0/G1, S and G2M phases were quantified by gating the left, middle and right peak, respectively, of the frequency histograms (see **Figure 4.1**. Cell debris and doublets were excluded as described in **Section 2.3**. Analysis was performed using the FlowJo software.

2.5 Gene expression analysis by quantitative reverse transcription PCR (RT-qPCR)

To measure gene expression, total RNA was extracted from cell lysates using the QIAshredder to homogenize the samples and RNeasy Plus Mini Kits for RNA purification (Qiagen, Hilden, Germany). Genomic DNA was removed using an RNase-Free DNase Set (Qiagen), as per manufacturer's instructions. Concentration and purity of RNA was measured using a Nanodrop1000 Spectrophotometer (Thermo Fisher Scientific). Reverse transcription was performed to obtain cDNA. Briefly, 0.5 µg of extracted RNA was denatured at 70°C for 5 minutes, after which a master mix containing 1 µl AMV reverse transcriptase (Promega, Madison, Wisconsin, United States), 4 µl AMV buffer (Promega), 1 µl Recombinant RNAsin ribonuclease inhibitor (Promega), 1 µl random primers (Promega), 2 µl of 10mM dNTPs (Bioline, London, UK) and 1 µl sterile water was added. Samples were then added to a heat-block (G-Storm Thermal Cycler PCR) and the following cycle was performed: 42°C for 60 minutes (DNA polymerisation), 90°C for 4 minutes (enzyme deactivation), 4°C for storage. Samples were stored at -80°C.

Quantitative PCR was performed on the cDNA, diluted 1:200, using a SYBR Green Master Mix (Qiagen), as per manufacturer's instructions. In-house designed or Qiagen pre-designed primers were used (**Table 2.4**). Sequences of in-house designed primers were obtained using the PrimerBLAST (NCBI) and OligoEvaluator (Sigma Aldrich) tools. Cycling and data acquisition was performed using the ABI 7500 Real-Time PCR System, with the parameters described in **Table 2.3**. The annealing temperatures yielding the best amplification plots were selected and the formation of primer dimers was assessed by performing dissociation curve analysis following the completion of the PCR cycles,

with cycling parameters automatically set by the ABI 7500 Real-Time PCR System. The obtained cycle threshold (Ct) values of the house-keeping 18S gene was subtracted from the Ct values of the genes of interest to obtain the ΔCt, and the $2^{-\Delta\Delta Ct}$ method ($2^{-(\Delta Ct \text{ (treated sample)} - \Delta Ct \text{ (control sample)})}$) was used to represent gene expression relative to controls. When comparing healthy and COPD samples without treatment, the mean ΔCt for healthy samples was used as the (ΔCt (control sample)).

Step	**Temperature (°C)**	**Time**	**Cycles**
Activation	95	15 min	1
Denaturation	94	15s	45-50
Annealing	55-60	30s	
Extension (Data Acquisition)	72	30s	

Table 2.3: Cycling parameters for RT-qPCR.

Gene	Design	Forward primer (5'-3')	Reverse primer (5'-3')	Probe (5'-3')
			cDNA	
18S	In-house	CTTAGAGGGACAAGTGGCG	ACGCTGAGCCAGTCAGTGTA	n/a
HAPLN3	Qiagen	n/a	n/a	n/a
LAMC2	Qiagen	n/a	n/a	n/a
ELN1	Qiagen	n/a	n/a	n/a
KIF5B	In-house	TTCCCTGCAAGACTGAGCG	CATAAGGCTTGGACGCGAT	n/a
KIF1B-α	In-house	ACAGCGGGGAAGTTATCGTG	GTCTTCTCTCGCTCAGCTCG	n/a
MIRO1	In-house	TCTTGCGGGGAAGCAACTG	ACTCTAGGTTCTCCCACCAGC	n/a
MIRO2	In-house	AGAAATCCTGCTTTGGGCAC	GAGGAAACCATCCAGGGTCAG	n/a
TRAK1	In-house	ATGTCTGCACATGGCATTGG	TGCACACATCACAGGCGTTT	n/a
TRAK2	In-house	GCCGAACCACTCCAGTCAT	GACATCCGTAGCAACGAGCA	n/a
DYNC1H1	In-house	CAGTTTTGAACCCGGTGCTG	TGGTGGGAACTCGACAGTTG	n/a
MYO19	In-house	CAGAGAGGAGCTTAGAAGAGGA	CCAAACTTAAGTGGCGTGGC	n/a
PGC1-α	Qiagen	n/a	n/a	n/a
PGC1-β	Qiagen	n/a	n/a	n/a
DRP1	[121]	ATGTCTGCACATGGCATTGG	TGCACACATCACAGGCGTTT	n/a
MFN1	[121]	GCCGAACCACTCCAGTCAT	GACATCCGTAGCAACGAGCA	n/a
MFN2	[121]	CAGTTTTGAACCCGGTGCTG	TGGTGGGAACTCGACAGTTG	n/a
OPA1	[121]	CAGAGAGGAGCTTAGAAGAGGA	CCAAACTTAAGTGGCGTGGC	n/a
			DNA	
β-ACTIN	In-house	TCACCCACACTGTGCCCATCTACGA	CAGCGGAACCGCTCATTGCCAATGC	n/a
MT-CO2	In-house	CCTGCGACTCCTTGACGTTG	AGCGGTGAAAGTCGTTTGGTT	n/a
mt.3531=G (ARMS-qPCR)	In-house	CTCTACATCACCGCC**A**CG	GCCTAGGTTGAGGTTGACC	FAM-CACCATCGCTCTTCTACTATGAACCCC-BHQ1
mt.11719=G (ARMS-qPCR)	In-house	CTCATAATCGCCCAC**T**GG	GGGAGTAGAGTTTGAAGTCCTT	FAM-GCAAACTCAAACTACGAACGCACTCAC-BHQ1

Table 2.4: Sequences of primer pairs used in qPCR and ARMS-qPCR experiments.

2.6 Quantification of protein expression by western blot

To extract total protein, cells in 6-well plates or T75 flasks were washed with ice-cold PBS and scraped in PBS using a cell-scraper. Samples were centrifuged at 7000 rpm for 3 minutes at 4°C and re-suspended in radioimmunoprecipitation (RIPA) buffer (Santa Cruz, Dallas, Texas, USA) supplemented with 1X protease inhibitor cocktail (Roche) by pipetting and vortexing. Lysates were incubated on ice for 30 minutes and stored at –80°C. Once thawed, samples were centrifuged at 13000 rpm for 15 minutes at 4°C to remove remaining cell debris, and supernatants were transferred into new pre-chilled tubes. Protein quantification was performed using the Pierce BCA Protein Assay (Thermo Fisher Scientific), as per manufacturer's instructions. Samples (10-40 µg) were diluted in RIPA buffer, containing 1X NuPage Laemmli loading buffer (Invitrogen) and 2-mercaptoethanol (diluted 1:26), and were denatured at 95°C for 5 minutes. Proteins were separated by size by running at 100 V through a NuPage 4-12% Bis-Tris gel (Invitrogen), alongside an Amersham ECL Full-Range Rainbow ladder (Sigma Aldrich), and transferred to a nitrocellulose membrane using an iBlot Stack and Gel Transfer Device (Thermo Fisher Scientific). Membranes were blocked with 5% non-fat milk in Tris-buffered saline containing Tween 20 (TBS-T; 0.15 M NaCl, 0.01 M Tris HCl, 0.05% Tween 20) for 30 minutes and incubated with primary antibodies as appropriate (**Table 2.5**) for either 2 hours at room temperature or overnight at 4°C in a shaker. After being washed with TBS-T (3x, 5 minutes), membranes were incubated with HRP-linked secondary antibodies (Agilent, Santa Clara, California, United States) for 1 hour and then washed again with TBS-T (4x, 10 minutes). The ECL Plus (Thermo Fisher Scientific) chemiluminescent horseradish peroxidase (HRP) substrate was added to the membranes to detect protein bands using the Odyssey Fc Imaging System (Licor Biosciences, Lincoln, NE, United States). Quantification of bands was performed using Image Studio Lite (Licor Biosciences) and were normalised to the levels of β-actin.

Antibody	Supplier	Dilution
Western Blotting		
Total OXPHOS Human WB Antibody Cocktail	Abcam	1 in 600
TOM20	Cell Signalling	1 in 1000
LC3B-I/II	Novus Biologicals	1 in 2000
MIRO1	Abcam	1 in 250
ATG12	Cell Signalling	1 in 500
ALIX	Abcam	1 in 500
Calnexin	Abcam	1 in 500
HRP-linked β-Actin	Santa Cruz	1 in 10,000
HRP-linked Goat Anti-Rabbit (secondary)	Agilent	1 in 2000
HRP-linked Goat Anti-Mouse (secondary)	Agilent	1 in 2000
Immunofluorescence		
TOM20	Santa Cruz	1 in 100
488 Goat Anti-mouse (secondary)	Thermo Fisher Scientific	1 in 600

Table 2.5: Antibodies used for western blot and immunofluorescence.

2.7 Protein quantification by enzyme-linked immunosorbent (ELISA) and Luminex assays

For quantification of secreted proteins, 100 µl of supernatant obtained from 10,000 cells plated in a 96-plate, was collected after centrifugation of the plate for 5 minutes at 1500 rpm (to remove cell debris). Media only controls were also collected in parallel. Samples were stored at -20°C. Quantification of IL-8 and IL-6 was performed using enzyme-linked immunosorbent assay (ELISA) kits (R&D Systems, Minneapolis, Minnesota, United States), as per the manufacturer's instructions. Briefly, samples and standards were added into 96-well plates coated with capture antibody. The plate was washed and incubated with detection antibody followed by streptavidin conjugated with horseradish peroxidase (HRP). Addition of the HRP substrate tetramethylbenzidine (TMB; BD Biosciences) led to a colorimetric reaction, which was inhibited by addition of 2N

H_2SO_4. The optical density of the product was measured at 450/570 nm in a microplate reader (FLUOstar Optima, BMG Labtech). CXCL-1, MMP-1, CXCL-10 and granulocyte-macrophage colony-stimulating factor (GM-CSF) were quantified using a custom Human Magnetic Luminex Assay Kit (BioTechne, Minneapolis, Minnesota, United States). Primary antibodies for these analytes were coated onto color-coded microparticles and added to a 96-well plate alongside standards and samples. Detection antibodies were then added, followed by a streptavidin-phycoerythrin conjugate that binds to the former. Washing steps were included between steps, where a magnetic separator was used to pull down the microparticles and bound samples, while the wash was tipped off the plate. After a final wash, samples were re-suspended in a buffer provided by the manufacturer and read using the Luminex MAGPIX Instrument System. The concentration of the analytes in both assays was calculated automatically based on a standard curve stipulated from the standards.

2.8 Gene silencing by small interfering (si)RNA

Gene knockdowns in ASMCs were performed using siRNAs. Target (MIRO1) or scramble siRNAs (Dharmacon, Lafayette, Colorado, United States) were diluted in transfection media (High-Glucose DMEM supplemented with 4 mM L-Glutamine only). Different concentrations of siRNA were tested (10 – 50 nM). The HiPerfect Transfection reagent (12 µl) (Qiagen) was added to 100 µl of siRNAs and these were incubated for 10 minutes at room temperature to allow the formation of complexes. The complexes of siRNA with HiPerfect Transfection reagent were added dropwise to ASMCs cultured in 6-well plates in 1 ml complete media. A mock control (no siRNA) and an untransfected control were also included. After 3 hours of incubation at 37°C, the volume of media was adjusted to 2 ml. RNA or protein was collected after 24 to 72 hours to measure gene expression and protein levels, as described in **Section 2.5** and **Section 2.6**. Alternatively, cells were re-plated for further experiments.

2.9 Fluorescence microscopy

All imaging was performed at the Facility for Imaging by Light Microscopy (NHLI, Faculty of Medicine, Imperial College London), with guidance and advice from Stephen Rothery.

Fluorescent labelling of live ASMCs was performed by staining cells with dyes (MitoTracker Green and CellTrace Violet), or by transfecting cells with green fluorescent protein (GFP), as described in **Section 2.13**. Alternatively, fluorescent labelling was performed on fixed cells by immunofluorescence as follows. Cells were cultured in coverslips fitted in 12- or 24-well plates and then fixed with 4% formaldehyde for 15 minutes. To perform further immunofluorescence, cells were permeabilized with 10% Triton-X and probed with appropriate primary antibodies (**Table 2.5**) for 2 hours at room temperature or overnight at 4°C. After washing, fluorescent secondary antibodies were added for 45 minutes at room temperature (**Table 2.5**). Once staining was complete, coverslips were transferred to slides with Vectashield and sealed with nail polish. To image extracellular vesicles, these were collected as described in (**Table 2.15**), and loaded as a monolayer directly onto a microscope slide by centrifugation of the sample at 1000 rpm for 10 minutes using a cytospin centrifuge (Thermo Shandon Cytospin 3 Centrifuge, Marshall Scientific, Hampton, New Hampshire, United States). Samples were allowed to air-dry and a hydrophobic pen was used to delineate the location of the samples and allow for liquid retention within this region. Immunofluorescence was performed as described above.

Single plane or Z-stack images of samples were acquired using either the Leica SP5 MP Inverted (confocal) or the Widefield Zeiss Axio Observer Microscope. All samples fixed and transferred to slides before imaging, as described in the previous paragraph, except for ASMCs stained with MitoTracker Green, which were imaged live as this dye is not retained after fixation. Live imaging was performed on cells cultured in Mattek dishes (Mattek Life Sciences, Ashland, MA, United States). During acquisition, live cells were kept in a chamber at 37^{o}C and 5% CO2. All images were processed with ImageJ (NIH and Laboratory for Optical and Computational Instrumentation, University of Wisconsin, United States), where brightness and contrast were adjusted and extra processing, such as background subtraction, were performed as required. Images were manipulated to improve

visualisation but did not eliminate, mask, or misrepresent any information present in the original image. Final images were prepared using the "Presentation" Macro developed by FILM at Imperial College London.

2.10 Assessment of mitochondrial respiration

Mitochondrial respiration was assessed by measuring OCR and ECAR using a Seahorse Analyzer (Xp or XFe96, Agilent Biosciences), and the Seahorse Cell Mito Stress Assay Kit (Agilent Biosciences) (see **Section 1.2.2**).

All reagents used were purchased from Agilent Biosciences unless stated otherwise. Cells were plated at a density of 62,500 cells/ml (80 µl volume) in 8- or 96-well Seahorse cell culture plates. On the day before the assay, Extracellular Flux Packs were hydrated with XF Calibrant Solution. On the day of the assay, cells were washed and incubated with Assay Media (Seahorse DMEM medium supplemented with 4 mM L-Glutamine, 1 mM sodium pyruvate and 4500 mg/L glucose) for 1 hour in a 37°C non-CO_2 incubator. The appropriate inhibitor drugs (1 µM oligomycin, 2 µM FCCP and 0.5 µM Rotenone/Antimycin A) were added to the drug ports in the Extracellular Flux Pack, which was then calibrated in the Seahorse Analyzer. After calibration, the cell culture plates were added to the Seahorse Analyzer and the assay was run according to the machine configuration. Optimal cell densities and inhibitor drug concentrations were optimized previously by Charalambos Michaeloudes.

The OCR measured is affected by the number of cells in each well. Therefore, it is required to normalise OCR to cell number. Two surrogates for cell number were used: total protein and total DNA. To measure total protein, upon completion of the Seahorse assay, cells were lysed with RIPA buffer supplemented with a protease inhibitor cocktail, containing protease inhibitor cocktail, and frozen at -20°C. Total protein was measured using the Pierce BCA Protein Assay, according to the manufacturer's instruction. Alternatively, cells were dry-frozen at -80°C and total DNA was measured using the CyQuant Assay, according to the manufacturer's instructions.

Maximal respiration, spare respiratory capacity, ATP-linked respiration, non-mitochondrial

respiration and proton leak were calculated automatically using the Seahorse Wave Software as shown in **Table 2.6**.

Parameter	Calculation
Non-Mitochondrial Respiration	Minimum rate measurement after rotenone/ antimycin injection
Basal Respiration	(Last rate measurement before first injection)-(Non-Mitochondrial Respiration rate)
Maximum Respiration	(Maximum respiration rate measurement after FCCP injection)-(Non-Mitochondrial Respiration)
Proton Leak	(Minimum rate measurement after oligomycin injection) - (Non-Mitochondrial Respiration)
ATP Production	(Last rate measurement before oligomycin injection) - (Minimum rate measurement after oligomycin injection)
Spare Respiratory Capacity	(Maximal Respiration) - (Basal Respiration)

Table 2.6: Calculation of mitochondrial respiration parameters based on measurements from the Seahorse Cell MitoStress Test.

2.11 Relative quantification of mtROS and $\Delta\psi$m

Mitochondrial ROS was measured by staining cells with MitoSOX Red Mitochondrial Superoxide Indicator (Molecular Probes), which specifically accumulates in the mitochondria and emits fluorescence when oxidised by superoxide. To measure $\Delta\psi$m, cells were stained with Tetramethylrhodamine, Methyl Ester, Perchlorate (TMRM) (Molecular Probes, Eugene, Oregon, United States), which is a dye that accumulates in mitochondria with an active membrane potential. Therefore, the TMRM signal decreases upon a reduction in $\Delta\psi$m. Cells in culture were incubated with 5 µM MitoSOX diluted in Hanks' balanced

salt solution (HBSS) containing Ca^{2+}/Mg^{2+} (Sigma Aldrich), or with 100 nM TMRM diluted in complete media (with FBS, see **Section 2.1**), for 30 minutes. Cells were collected by trypsinisation and their fluorescence in the PE channel was measured by flow cytometry (BD FACSCanto II). Cell debris and doublets were excluded as described in **Section 2.3**, and the MFI in the PE channel of the gated population was determined. Median fluorescence intensity (MFI) of unstained cells was subtracted from the MFI of stained cells to control for changes in laser status and background fluorescence. Data were analysed using the FlowJo 10.4 Software.

2.12 Quantification of relative mtDNA copy number

Total DNA was extracted from cell pellets with a phenol-chloroform extraction protocol optimized in-house. Briefly, cells were collected by trypsinisation and pellets were frozen in dry ice and stored at -80°C. After thawing, lysis buffer (1 M Tris pH 8, 0.5 M EDTA pH 8, 10% SDS and 20 mg/ml protease K in PBS) was added to the pellets for 2 hours at 56°C. Extraction of DNA was performed by adding an equal volume of phenol: chloroform: isoamyl alcohol and mixing by inversion. After centrifugation the top aqueous phase containing DNA was transferred to a new tube and 2 volumes of chloroform were added. Again, the sample was mixed by inversion, centrifuged and the top phase was separated. 1/10 volume of sodium acetate solution (2 M pH 4.6) and 2 volumes of ice-cold 100% ethanol were added to the sample which was then kept at -20°C overnight to allow for precipitation of the DNA. On the following day, the samples were centrifuged at high speed (10 min at 13,000 rpm at 4°C), re-suspended in 70% ethanol, and centrifuged once more. After the final centrifugation, the supernatant was removed and samples were left to air-dry and then eluted in DNAse-free water. Concentration and purity of DNA was measured using a Nanodrop Spectrophotometer. Real-time quantitative PCR using SYBR Green (Qiagen) was performed, as described in **Section 2.5**, to measure the relative amount of the mitochondrial gene cytochrome oxidase 2 (*MT-CO2*) and the nuclear gene *β-ACTIN*. Primer sequences can be found in **Table 2.4**. Relative mtDNA copy number was calculated by normalising the quantity of *MT-CO2* to β-ACTIN using

the ΔCt method (Ct(*MT-CO2*) – Ct(*β-ACTIN*)) and the equation $2^{*}(2^{\Delta Ct})$ [168].

2.13 Detection and quantification of mitochondrial transfer

2.13.1 MitoTracker dyes

To detect and quantify mitochondrial transfer, cells in suspension were incubated for 30 minutes with either 0.2 µM MitoTracker Green (Molecular Probes), which specifically stains mitochondria, or with 5 µM of the cytoplasmic CellTrace dye (Molecular Probes). After staining, MitoTracker-stained and Cell-Trace stained cells were washed and incubated in complete media for 10 minutes to remove unbound dye and directly co-cultured at a 1:1 ratio. After 24 hours of culture, cells were collected by trypsinisation and fluorescence in the FITC (MitoTracker Green) and Pacific Blue (CellTrace) channels was measured by flow cytometry (BD Biosciences FACSCanto II). Fluorescence of stained and unstained cells in single culture was also measured. Data were analysed using the FlowJo 10.4 Software. Briefly, cell debris and doublets were excluded as described in **Section 2.3**. Unstained samples were used as negative controls for both FITC and Pacific Blue to set quadrant gates in a FITC x Pacific Blue dot plot. These gates were then applied to all samples. Mitochondrial donor cells were positive for FITC only, whereas mitochondria recipient cells were positive for Pacific Blue. Double positive cells (FITC-positive/Pacific Blue-positive) represent recipient cells that received mitochondria from donor cells (see **Figure 5.1B**. To exclude the possibility of the detected double positive cells being a result of leakage of the MitoTracker dye, cells were also cultured in a transwell system. Specifically, MitoTracker-stained cells were cultured in porous cell culture inserts (0.4 µm pore size; Sigma-Aldrich), which were fitted onto the wells of 6 well plates, where CellTrace-stained cells were seeded. Since mitochondria are typically larger than the pore size of 0.4 µm, this would impair transfer of intact mitochondria whilst allowing for transfer of free dye. As a second control for dye leakage, supernatants of stained donor cells were

collected after the last wash step of the staining protocol, filtered with a 0.4 µm filter, and added to CellTrace stained cells. The percentage of MitoTracker-positive recipient cells was measured by flow cytometry as described above. To visualise mitochondrial transfer, co-cultures of MitoTracker Green- and CellTrace-stained cells were imaged live by fluorescence microscopy as described in **Section 2.9**.

2.13.2 Mitochondrial-targeted fluorescent proteins

To tag mitochondria with a green fluorescent protein (GFP), two approaches were used. Firstly, CellLight Mitochondria-GFP, BacMam 2.0 (Thermo Fisher Scientific) was used to transfect ASMCs with a construct expressing GFP fused to the leader sequence of E1 alpha pyruvate dehydrogenase. The vector was packaged in the insect virus baculovirus in a ready-to-use reagent. ASMCs was transfected by adding the CellLight Mitochondria-GFP reagent directly to the cells for 24 hours. Different quantities of particles per cell (PPC) were tested to ensure optimal transfection (**Figure 5.3A**).

In a second approach, ASMCs were transfected with 500 ng of the pCT-Mito-GFP vector (Cambridge Biosciences, Cambridge, United Kingdom), which encodes for the mitochondrial protein cytochrome oxidase VII (COX8) tagged with GFP, using lipofectamine LTX transfection (Thermo Fisher Scientific). Briefly, the pCT-Mito-GFP vector was diluted in transfection media and incubated for 10 minutes with 1 or 1.5 µl of the lipofectamine LTX reagent and 0.5 µl of PLUS reagent (provided by the supplier). The complexes were added drop-wise to the cells, cultured in 24-well plates, for 24 hours. Transfection efficiency was assessed by measuring fluorescence in the FITC channel by flow cytometry (**Figure 5.3B**). Transfected cells were cultured for 24 hours and washed three times, after which CellTrace-stained (recipient) cells were added to the culture at a 1:1 ratio for another 24 hours. The percentage of GFP-positive donor and recipient cells was measured by flow cytometry and GFP-positive recipient cells were visualised by fluorescence microscopy, as described in sections **Section 2.13.1** and **2.9**, respectively.

2.13.3 Detection of mtDNA mutations

Mitochondrial transfer was also assessed by detecting the presence of donor-specific mtDNA in recipient cells. Since most of the mtDNA is transcribed [169], transcriptome data can be used to analyse the sequence of mtDNA and identify patient-specific mtDNA mutations. This allows for a distinction of the mtDNA from ASMCs from different subjects. Transcriptomics data from ASMCs from seven healthy and seven COPD patients cultured in complete media was obtained in previous experiments performed by our research group (unpublished). RNA-seq reads were aligned to the reference mtDNA sequence (rCRS NC012920.1) using the HiSat2 package for Linux command line. The aligned reads (BAM files) were uploaded to the Integrative Genomics Viewer (IGV, Broad Institute) where mutations were identified (see **Figure 5.5A**).

Co-cultures of MitoTracker (donor)- and CellTrace (recipient)-stained ASMCs with distinct mtDNA mutations were plated. Recipient cells that received mitochondria from donor cells (Mito+) were separated from those that did not (Mito-) by fluorescence-activated single cell sorting (FACS), as described in **Section 2.14**. These cells, alongside single culture controls of recipient cells, were re-plated and DNA was extracted after 48 hours, as described in **Section 2.12**. Alternatively, Mito+, Mito- and single culture controls were sorted into single cells in 96-well plates and flash frozen. Single cells were lysed by incubating in a solution containing 50 mM Tris-HCl [pH 8.5], 1 mM EDTA, 0.5% Tween 20, and 200 µg/ml Proteinase K, for 2 hours at 55°, followed by 96° for 10 min to inactivate Proteinase K.

Amplification-refractory mutation system qPCR was used to detect the presence of mtDNA with a mutation specific to donor cells. Briefly, for each sample two qPCRs were performed: one that specifically amplified the mutant mtDNA sequence (discriminatory assay) and one that amplified a mtDNA housekeeping gene (*MT-CO2*) to measure total mtDNA. The discriminatory assay was performed using a mastermix containing the Hot FirePol DNA polymerase (Solis BioDyne, Tartu, Estonia) (**Table 2.7**), and the cycling parameters described in **Table 2.8**.

Reaction Component	Concentration/amount	Volume (µl)
$MgCl_2$	2.25 mM	1.35
HOT FIREPol 10X Buffer B2	1X	1.5
dNTP	0.2 mM	0.3
Forward Primer	0.13 µM	0.1
Reverse Primer	0.13 µM	0.1
Probe	0.13 µM	0.1
HOT FIREPol	1U	0.2
DNA	2.5 ng	2
Water	n/a	9.35
Total	n/a	15

Table 2.7: Contents of the master mix used in the discriminatory assay of ARMS-qPCR.

Primers and probes were designed in-house (**Table 2.4**). The 3'-end nucleotide of the forward primer was aligned to the mutation of interest, and a mismatch was introduced in the penultimate nucleotide of this primer (highlighted in red in **Table 2.4**). This resulted in a specificity that allowed for the amplification of mtDNA containing the mutation only: the binding of the primers to the mtDNA was only possible when the mutation was present. In mtDNA without the mutation of interest, the alignment of the primer to the sequence is poor and does not for allow primer binding and consequent amplification.

Step	Temperature (°C)	Time	Cycles
Activation	95	15 min	1
Denaturation	95	15 s	45
Annealing and Extension (Data Acquisition)	62	60 s	

Table 2.8: Cycling parameters for the discriminatory assay of the ARMS-qPCR.

The total mtDNA assay was performed using a SYBR green master mix, with primers for the *MT-CO2* gene, as described in **Section 2.12**. The quantity of mutant and total mtDNA were calculated automatically based on a standard curve prepared from a positive control sample (donor ASMCs bearing the mutation of interest) using the QuantStudio Software (Thermo Fisher Scientific). The amount of mutant DNA relative to total mtDNA was calculated based on the equation 100*(quantity of mutant mtDNA/quantity of total mtDNA) [138]. The efficiency of the ARMS-qPCR assay was assessed as described in **Section 5.2.1**.

2.14 Isolation of Mito+ and Mito- cells by FACS

Using the same co-culture and staining conditions as in **Section 2.13.1**, MitoTraker-negative (Mito-) and MitoTracker-positive (Mito+) CellTrace-stained cells were isolated from the co-cultures by FACS using the BD ARIA II flow cytometer (see **Figure 5.6B**). Briefly, cells were collected in HBSS with 1% FBS and filtered through a 35 µm mesh to avoid clumps. Unstained cells were used to set gates as before and recipient cells were sorted according to their MitoTracker (FITC) fluorescence using a 100 µm nozzle and 2.0 filter. Isolated cells were collected in polystyrene tubes, centrifuged and re-suspended in complete media. Single culture controls were also sorted to control for the effect of sorting. Cells were counted and re-plated as appropriate for further experiments.

2.15 Isolation of extracellular vesicles

Conditioned media obtained from 1.5 million ASMCs cultured over 24 hours, was subjected to successive centrifugations (300g for 5 min at 20°C; 3,000g for 10 min at 4°C; 20,000g for 30 min at 4°C and 100,000g for 2 hours at 4°C) to isolate different sized vesicles. Low speed centrifugations were performed using a bench-top centrifuge whereas a Micro Ultracentrifuge (Hitachi, Tokyo, Japan) was used for high-speed centrifugations. The pellets from the different centrifugations were re-suspended in 1ml of PBS and centrifuged again using the same settings, and then re-suspended in different reagents depending

on the subsequent applications. For imaging, pellets were re-suspended in 100 µl PBS and loaded onto slides as described in **Section 2.9**. For western blotting, samples were re-suspended in 20 µl RIPA with protease inhibitors. Due to limited sample amount, protein quantification was not performed, and the whole sample was used for loading on the western blot running gel. For mtDNA quantification, pellets were dry-frozen after the last centrifugation and kept at -80^{o}C, before they were digested using the same protocol as for single cells, described in **Section 2.13.3**. Finally, to use EVs as cell treatments, samples were re-suspended in 1ml of warm complete media.

2.16 Statistical analyses

Statistical analyses were performed using the GraphPad Prism 7.0 software (San Diego, California). Sample size was determined based on power calculations performed previously by members of my research group. Data from primary cells are highly variable, and the small sample size used (n=3-7) does not allow for accurate assessment of normality [170]. Therefore, non-parametric tests were used. Where more than two groups were present, data were analysed using a Friedman's test (paired data) or Kruskall-Wallis (unpaired data), followed by Dunn's multiple comparisons. When only two groups were compared, a Wilcoxon signed-rank test was used for paired data and a Mann-Whitney test for unpaired data. Data points comparing different conditions of ASMCs from the same patient was considered paired data, whereas data from ASMCs from different patients was treated as unpaired data. Replicates refer to data points obtained from ASMCs from different subjects. Data was presented as either raw values or normalised to appropriate controls, plus/minus standard error of the mean (SEM). A p-value <0.05 was deemed statistically significant.

Chapter 3

Mitochondrial function of ASMCs from healthy and COPD subjects

3.1 Introduction

Mitochondrial dysfunction has been reported in different cell types in COPD, such as epithelial cells [107, 110, 112] and macrophages [25]. There is also some evidence suggesting mitochondria and metabolic changes play a role in ASM dysfunction in COPD [45, 76, 171]. For example, under serum-starved conditions, COPD ASMCs show an increase in the levels of lactate and alanine as well as an increase in the mRNA expression of pyruvate dehydrogenase kinase 1 (*PDK1*) compared to ASMCs from healthy ex-smoker subjects [76], which suggest an altered glycolytic metabolism.

Cigarette smoke is the main environmental risk factor of COPD [2] and has been shown to lead to mitochondrial damage in different ways, such as mitochondrial fragmentation [107], loss of $\Delta\psi m$ [172] and impaired mitophagy [112]. In ASMCs from healthy subjects, a 24-48 hour exposure to 0.5-2% CSM leads to mitochondrial fragmentation and a reduction in ATP-linked respiration and maximal and spare respiratory capacity [121]. In addition, these cells show an increase in mtROS and a decrease in $\Delta\psi m$ when treated with 10-25% CSM for 4 hours [143]. The effect of CSM on mitochondrial function of ASMCs from COPD subjects has not been studied. COPD ASMCs may be more sensitive to oxidative stress-induced mitochondrial dysfunction, as the increase in mtROS induced by H_2O_2 is higher in COPD ASMCs compared to healthy ex- and non-smoker ASMCs [45].

One of the characteristics of COPD is that cigarette smoke-induced responses, such as oxidative stress and chronic inflammation, persist after smoking cessation [21]. It is not clear whether CS-induced mitochondrial dysfunction is also sustained once the stressor is removed. In epithelial cells CS-induced fragmentation, changes in the expression of ETC proteins and induction of Mn-SOD are reversible after removal of CS, though other aspects, such as CS-induced branching, are maintained [107]. In a murine model of CS exposure, CS-induced changes to metabolism, such as a reduction in glycolysis, and redox balance were reversed after a recovery period [173]. Finally, the activity of complex III and IV is restored in peripheral lymphocytes of smokers after smoking cessation [174]. It is possible that, in COPD, the ability of cells to reverse CS-induced mitochondrial dysfunction is impaired.

In summary, there is evidence of mitochondrial dysfunction in COPD ASM. This may be driven by exposure to cigarette smoke, but only a proportion of smokers develop COPD. Therefore, ASMCs from COPD patients may be more susceptible to CS-induced mitochondrial damage. In addition, sustained changes in mitochondrial function in response to stressors, such as CS, may contribute to the persistence of COPD phenotypes after smoking cessation. With this in mind, the main aims of this chapter are the following:

- Optimise both an acute and smoking cessation model of cigarette smoke treatment to be used for all future experiments
- Investigate the effect of CSM on mitochondrial function of healthy and COPD ASMCs

3.2 Results

3.2.1 Optimisation of CSM treatment

Two CSM-treatments were initially optimised. In an acute treatment model, cells were treated with 10% or 25% of cigarette smoke media for 4 hours, whilst untreated controls were kept in serum-free media. Alternatively, in a "smoking cessation" model, after the 4 hour treatment cells were washed and re-plated in complete media for 24 or 48 hours.

The effect of cigarette smoke media treatment on the viability of ASMCs from healthy subjects was assessed by Annexin V/PI staining (described in **section 2.3**). Experiments performed in previous studies in the laboratory showed that treatment of healthy ASMCs with 50% CSM leads to a significant reduction in cell viability [143], therefore only 10 and 25% CSM were tested here. A 4 hour treatment with 500 µM hydrogen peroxide was used as a positive control to induce cell death. Hydrogen peroxide led to an increase in the percentage of necrotic and late apoptotic cells from less than 1% to ∼20%, confirming the expected effect (**Figure 3.1A-B**). There was no change in the percentage of necrotic, early and late apoptotic cells when ASMCs were treated with 10% or 25% CSM for 4 hours compared to controls, and this was also true after cells were re-plated in complete media for 24 hours (**Figure 3.1**). This indicated that, in both CSM treatment models, 10% and 25% CSM had no significant effects on cell viability and were therefore suitable for further studies.

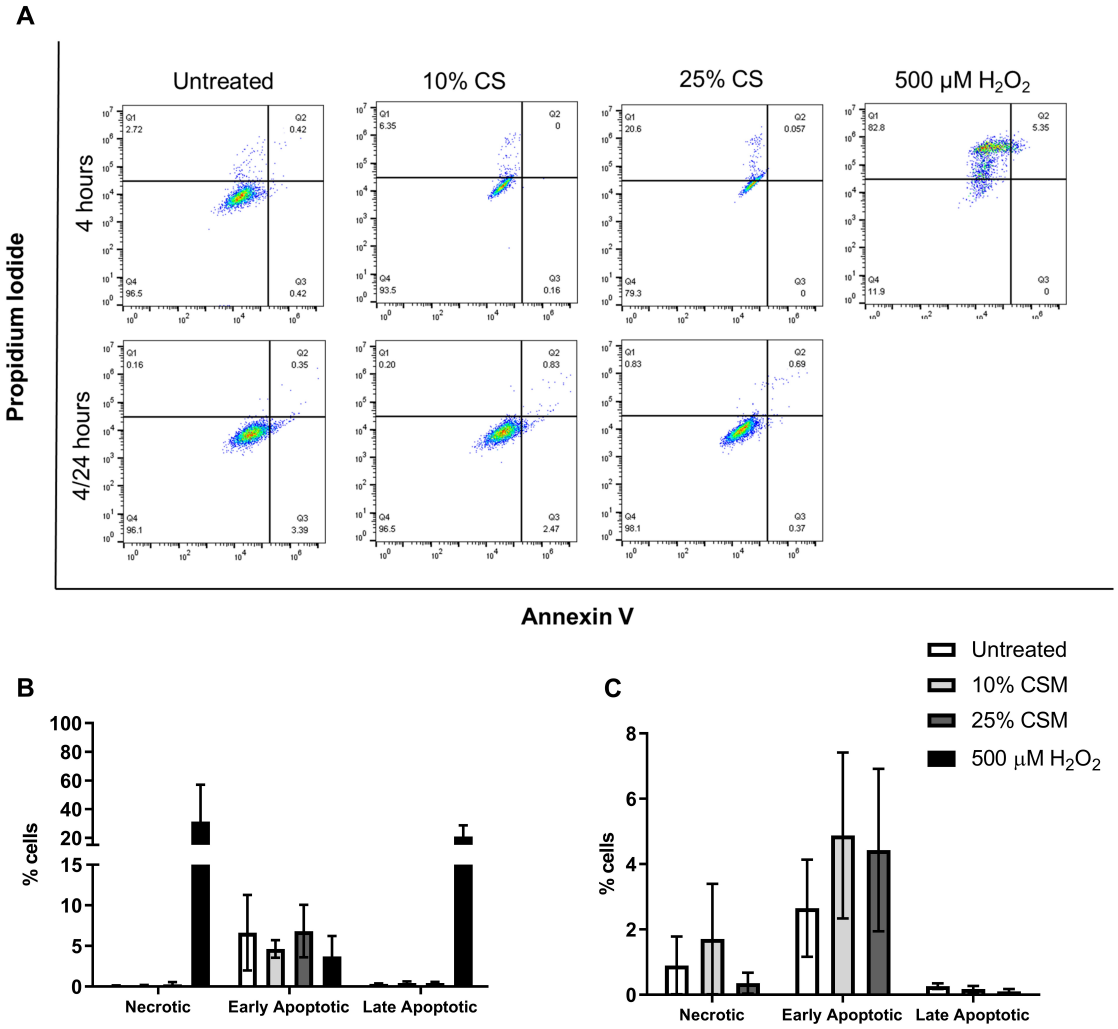

Figure 3.1: Effect of cigarette smoke on cell viability. (A) Representative flow cytometry dot plots of cells stained with Annexin V/PI under different conditions. Quantification of the percentage of necrotic, early apoptotic and late apoptotic ASMCs from healthy subjects either (B) cultured in serum-free media with or without cigarette smoke 4 hours, or (C) re-plated in complete media for 24 hours after treatment. Data presented as mean ± SEM. N=3.

Cigarette smoke contains many chemicals that are auto-fluorescent, such as benzene, naphthalene and other polycyclic aromatic hydrocarbons [175]. Since several of the assays used to evaluate mitochondrial function are based on fluorescent probes, the auto-fluorescence properties of CSM were assessed. As shown in **Figure 3.2A-C**, there was an increase in the fluorescence intensity measured in the PE, FITC and Pacific Blue channels of the BD FACS Canto II flow cytometer when cells were treated with 25% CSM for 4 hours. This indicates that this treatment leads to auto-fluorescence and could affect readings of the fluorescent-probe assays performed. However, the auto-fluorescence was

no longer observed when cells were re-plated in complete media for 24 hours (**Figure 3.2D-F**).

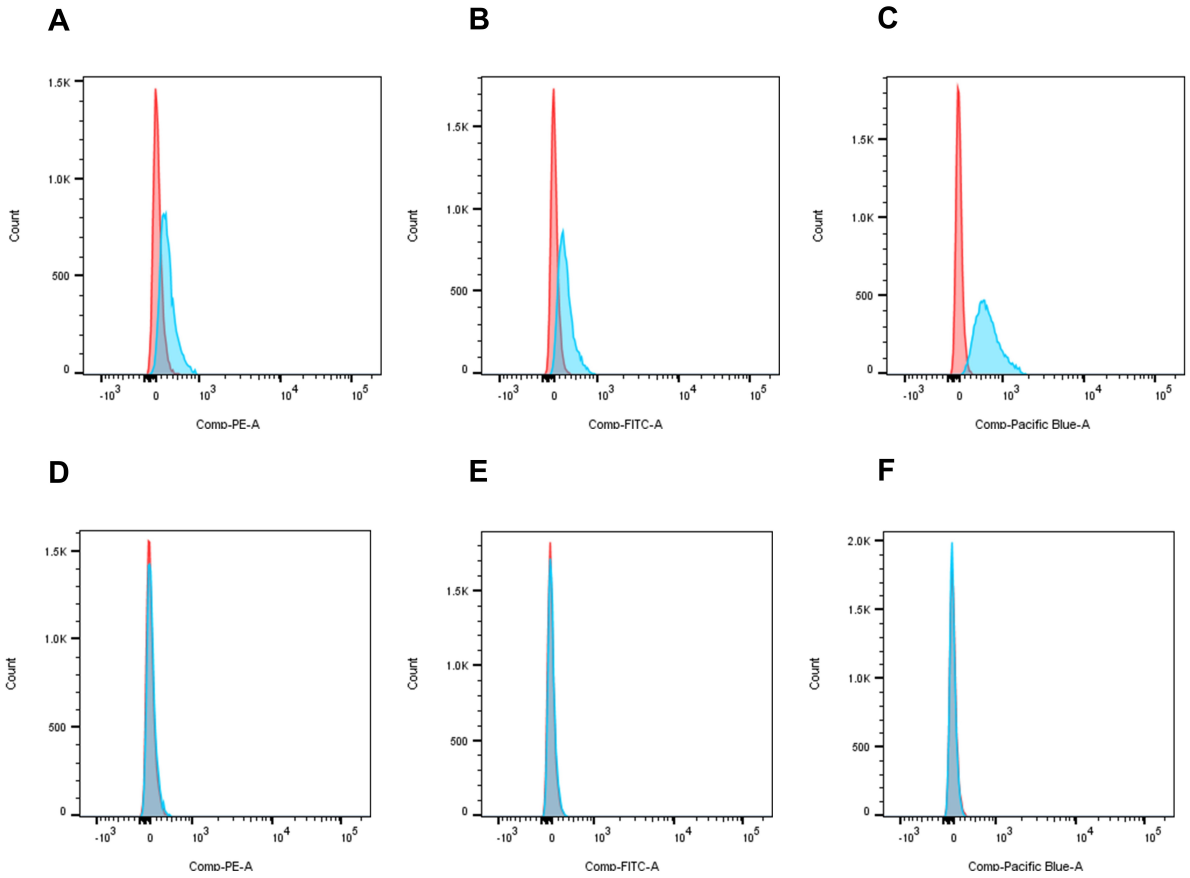

Figure 3.2: Auto-fluorescence of cigarette smoke medium. Unstained ASMCs treated with 25% CSM (blue) or serum-free media (red) (A-C) for 4 hours, or (D-F) for 4 hours and re-plated in complete media for 24 hours. Fluorescence in the (A,D) PE, (B,E) FITC and (C,F) Pacific Blue channels was measured by flow cytometry. N=1.

The auto-fluorescence of CSM in the acute model hinders the interpretation of the results obtained from assays based on fluorescent probes. In addition, it is already known that acute CSM treatment induces mitochondrial dysfunction in healthy ASMCs [143]. Therefore, I opted for continuing my study using only the "smoking cessation" model, as this circumvented the issue of auto-fluorescence and would add information on the duration of the acute damage once the stimuli is removed.

3.2.2 COPD ASMCs are more sensitive to stress-induced changes in mitochondrial function

To assess mitochondrial function in healthy and COPD ASMCs, mitochondrial respiration, mtROS, $\Delta\psi$m and mitochondrial protein levels were measured under baseline conditions and upon exposure to cigarette smoke media.

TMRM staining for measurement of $\Delta\psi$m was optimised using the uncoupler carbonyl cyanide m-chlorophenylhydrazone (CCCP) as a positive control for mitochondrial membrane depolarisation. The concentration of 100 nM provided the best staining, and a clear response to CCCP (**Figure 3.3**), and therefore was chosen for further assays. Higher concentrations of TMRM could also be tested, though these may alter the functioning of the dye [39]. The remaining assays were previously optimized by Charalambos Michaeloudes, and the determined optimal conditions were used for the experiments described below.

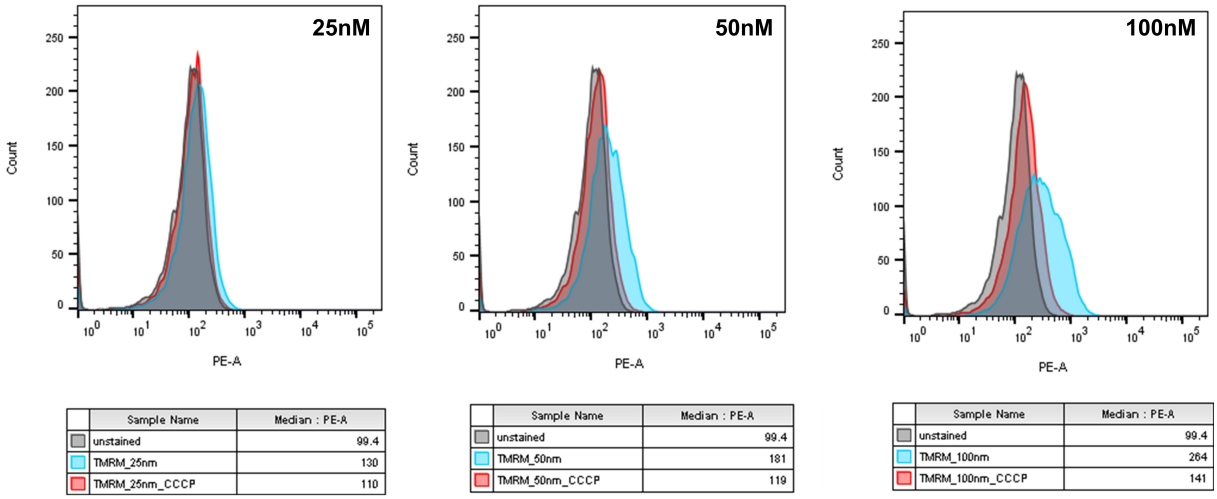

Figure 3.3: Optimization of TMRM staining for quantification of $\Delta\psi$m. ASMCs stained with different concentrations of TMRM for 30min. Cells were pre-treated with 50 µM CCCP to induce depolarization as a control. N=1.

Mitochondrial function was first assessed under baseline conditions, in which cells were serum-starved for 4 hours and re-plated in complete media for 24 hours. This experimental set-up was used to match the conditions used in the CSM-treatment experiments. There was no difference in most parameters of mitochondrial respiration between the two

groups, except for NMOC, which was significantly lower in COPD ASMCs (∼40% reduction, $p<0.05$, **Figure 3.4**). ASMCs from COPD patients displayed a ∼30% lower $\Delta\psi m$ compared to healthy ASMCs (**Figure 3.5A**). Although this did not reach significance, the reduced $\Delta\psi m$ in COPD ASMCs was consistent across all experiments, which were always performed in pairs. The lack of significance may be due to the spread of the data points, which itself may be a result of the variability in laser intensity of the flow cytometer on differing days. The internal variability of staining in an individual patient cell was not assessed, but may also contribute to the lack of significance. No differences were seen in the levels of mtROS between the two groups (**Figure 3.5B**). ASMCs from COPD patients showed a significantly lower expression of complex III (∼45%; $p<0.05$, **Figure 3.6D**) of the ETC and a trend towards lower expression of complex V (∼30%, $p=0.08$, **Figure 3.6F**). There was no difference in the expression of complexes I, II and IV (**Figure 3.6B, C and E**). In addition, the expression of TOM20, an outer mitochondrial membrane protein used to assess relative mitochondrial mass, did not differ between groups, indicating that differences in $\Delta\psi m$ and expression of complex III and V are not a result of different mitochondrial mass (**Figure 3.6G**).

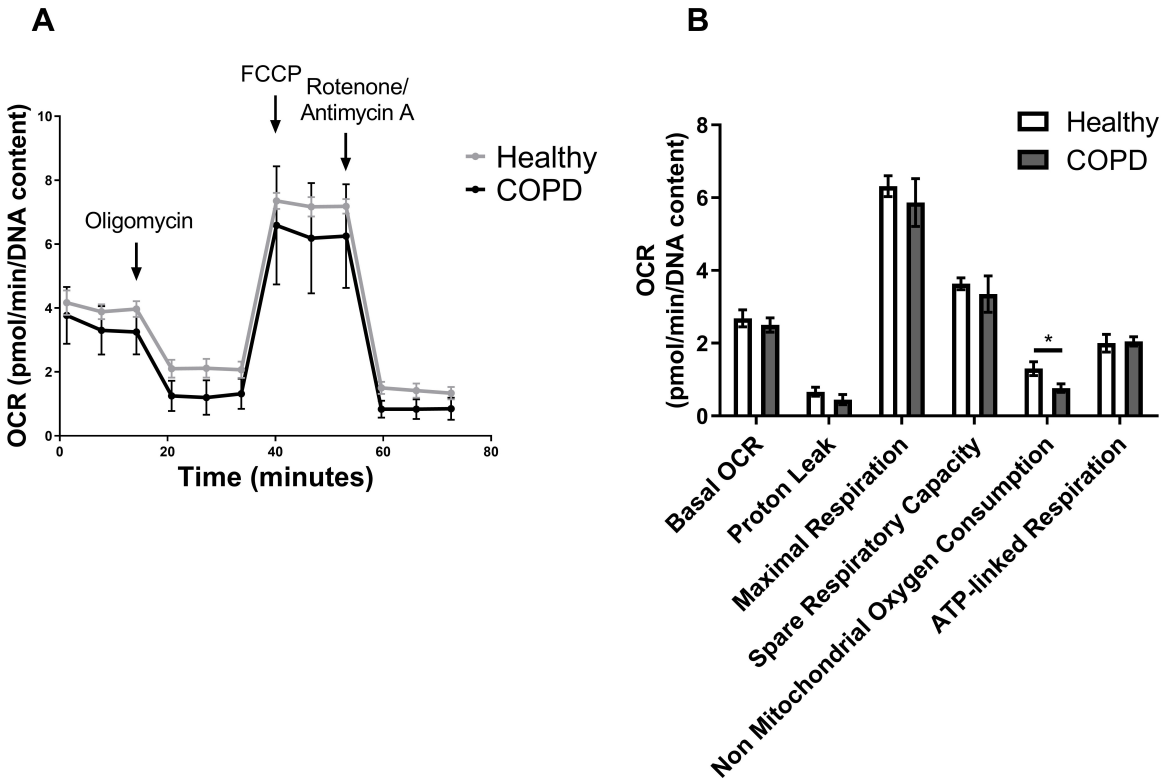

Figure 3.4: Mitochondrial respiration in ASMCs from healthy and COPD subjects. Quantification of oxygen consumption rate (OCR) in ASMCs from healthy and COPD subjects serum-starved for 4 hours and re-plated in complete media for 24 hours. (A) Time-course of OCR changes over during of the assay and in response to OXPHOS-targeting drugs. (B) Parameters of mitochondrial respiration calculated from OCR data. Data presented as mean ± SEM. *$p<0.05$, N=6.

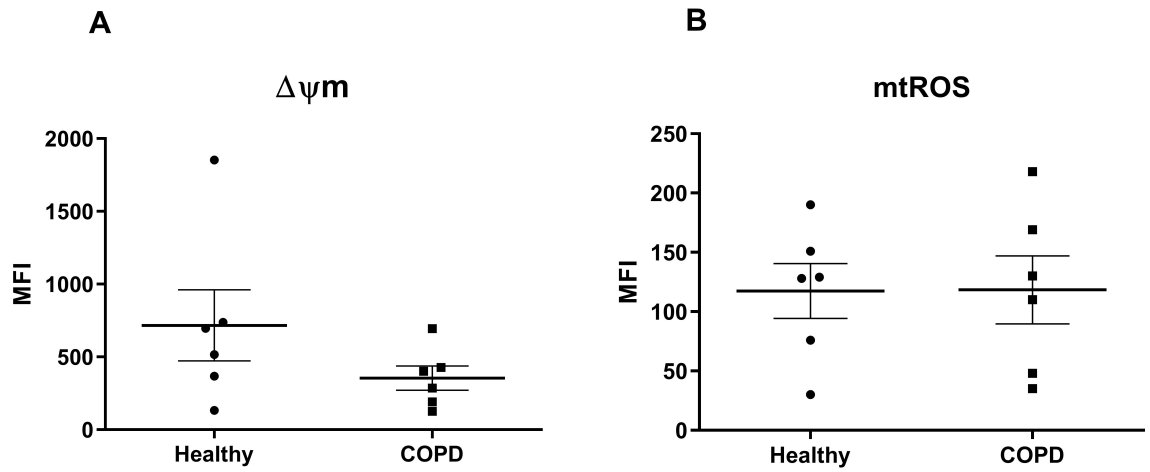

Figure 3.5: Mitochondrial membrane potential and mitochondrial ROS in ASMCs from healthy and COPD subjects. Quantification of relative levels of (A) $\Delta\psi$m and (B) mtROS in ASMCs from COPD and healthy subjects serum-starved for 4 hours and re-plated in complete media for 24 hours. Data shown is the median intensity fluorescence (MFI) in the PE-A channel and is presented as mean ± SEM. *$p<0.05$, N=6.

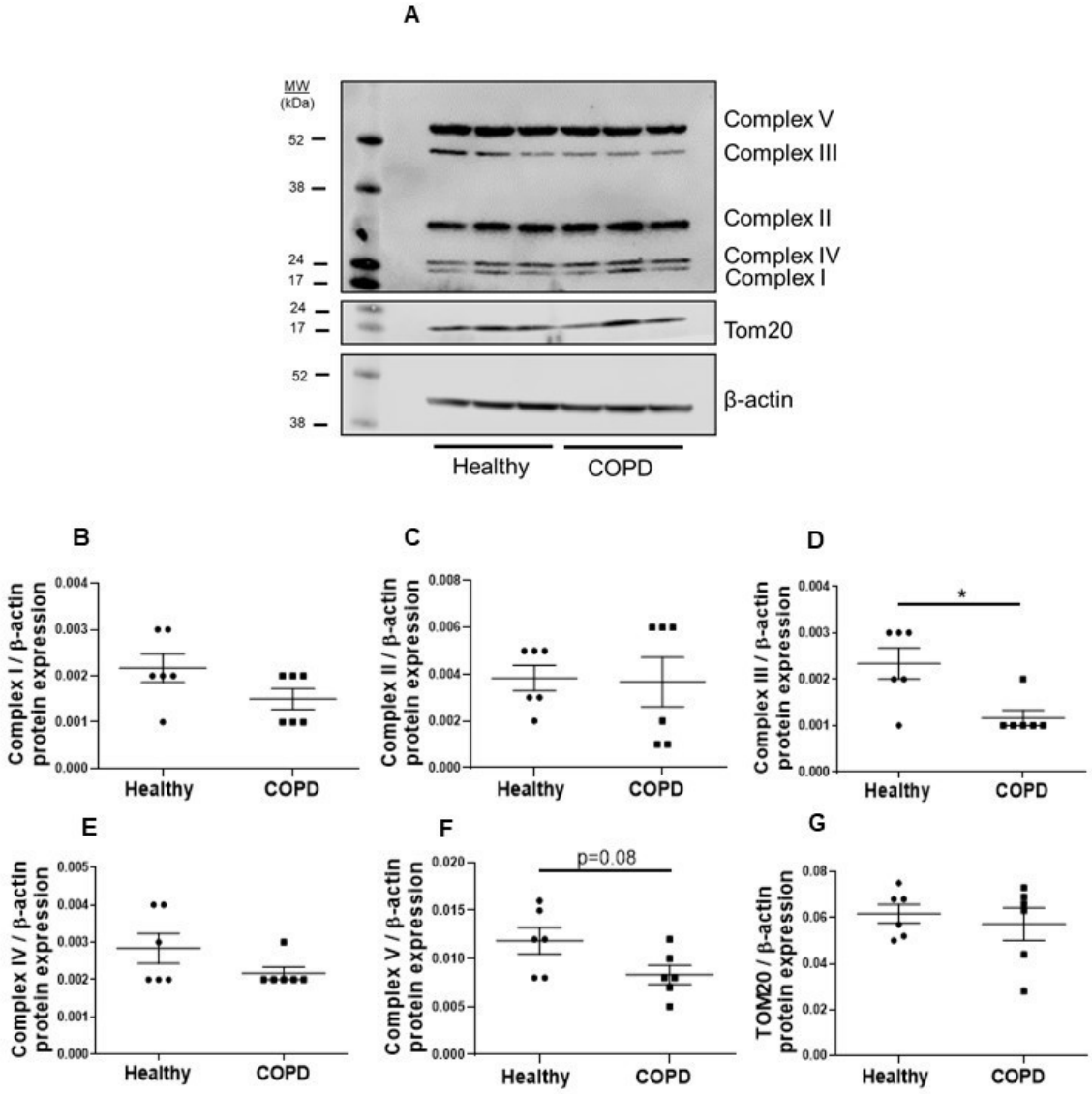

Figure 3.6: Expression of mitochondrial proteins in ASMCs from healthy and COPD subjects. (A) Representative western blot membrane depicting protein levels of ASMCs from COPD and healthy subjects serum-starved for 4 hours and re-plated in complete media for 24 hours. Quantification of (B-F) Complexes I-V of OXPHOS and (G) TOM20, all normalized to β-actin. Data presented as mean ± SEM. *$p<0.05$, N=6.

I then assessed the effect of CSM on the same parameters on ASMCs from both healthy subjects and COPD patients, using the "smoking cessation" treatment model. At 24 hours post-treatment, 25% CSM led to a significant reduction in ATP-linked respiration (20%; $p<0.05$ **Figure 3.7B**), as well a trend towards a 20% decrease in basal OCR, maximal respiration and spare respiratory capacity in COPD ASMCs but not in healthy ASMCs (**Figure 3.7A,C and D**). There was also a trend towards an increase in non-mitochondrial oxygen consumption in CSM-treated COPD ASMCs (**Figure 3.7F**).

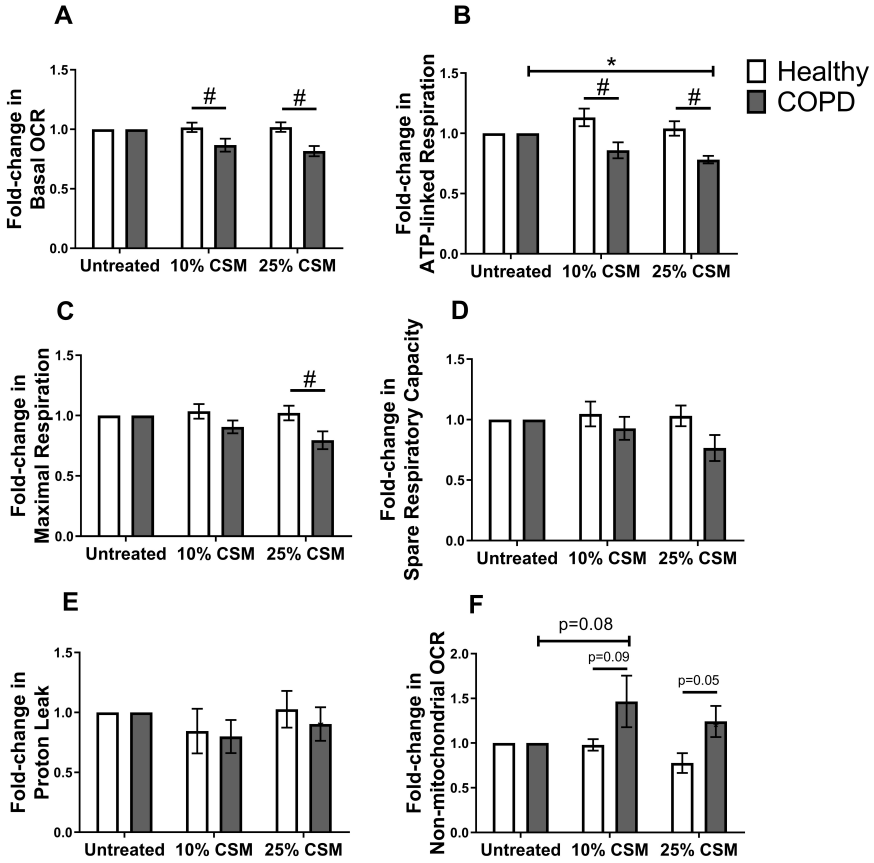

Figure 3.7: Effect of cigarette smoke on mitochondrial respiration in ASMCs from healthy and COPD subjects. Quantification of (A) basal OCR (B) ATP-linked respiration (C) baximal respiration (D) spare respiratory capacity (E) proton leak and (F) non-mitochondrial oxygen consumption in ASMCs from healthy and COPD subjects, cultured in serum-free media in the presence or absence of 10 or 25% CSM for 4 hours and re-plated in complete media for 24 hours. Data normalised to untreated and presented as mean ± SEM. Statistical analyses performed on non-normalised data. *$p<0.05$, #$p<0.05$. N=6.

Treatment of 25% CSM led to a significant decrease in $\Delta\psi$m in both healthy and COPD ASMCs (∼20%, p<0.05) but had no effect in mtROS (**Figure 3.8**). Similar to what was observed in baseline conditions, $\Delta\psi$m was lower in COPD ASMCs treated with 25% CSM compared to healthy ASMCs, and there was no difference in mtROS (non-normalised data not shown).

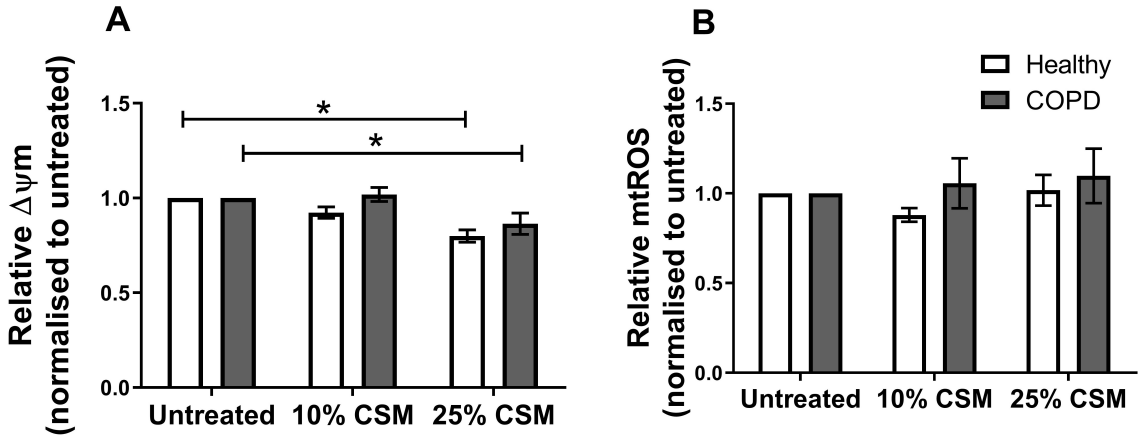

Figure 3.8: Effect of cigarette smoke on mitochondrial function in ASMCs from healthy and COPD subjects. Quantification of relative levels of (A) $\Delta\psi$m and (B) mtROS in ASMCs from COPD and healthy subjects, cultured in serum-free media in the presence or absence of 10 or 25% CSM for 4 hours and re-plated in complete media for 24 hours. Data shown is the fold-change in median intensity fluorescence (MFI) in the PE-A channel compared to untreated and is presented as mean ± SEM. Statistical analyses performed on non-normalised data. *p<0.05. N=6.

Finally, the expression of complex III was decreased by 25% CSM in COPD ASMCs only (∼40%, p=0.06, **Figure 3.9C**), whereas the expression of other complexes and TOM20 remained unchanged upon CSM treatment (**Figure 3.9**).

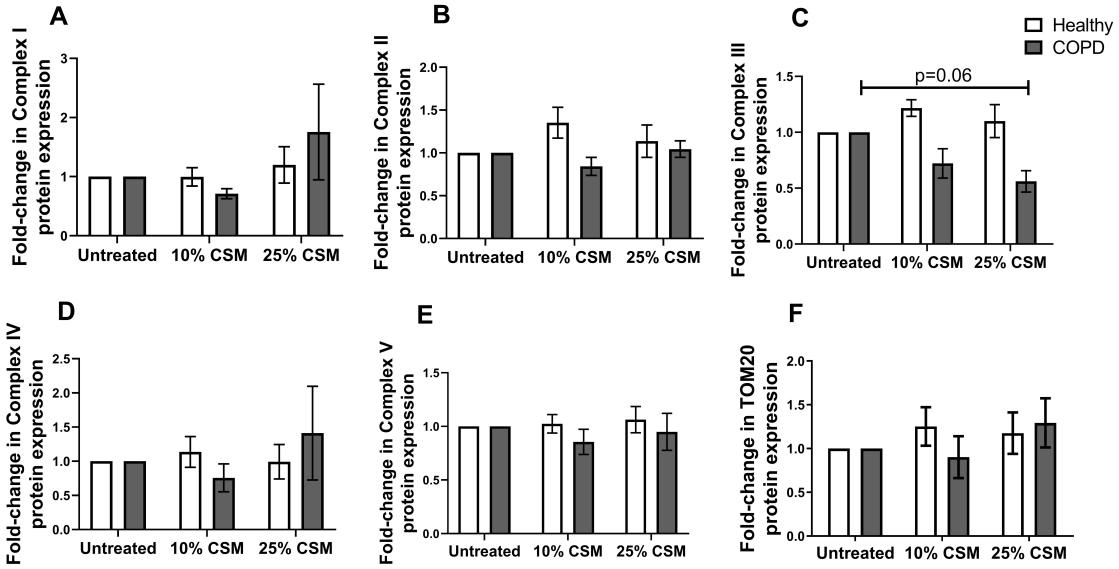

Figure 3.9: Effect of cigarette smoke on the expression of mitochondrial proteins in ASMCs from healthy and COPD subjects. Quantification of (A-E) Complexes I-V of OXPHOS and (F) TOM20 in ASMCs from healthy and COPD subjects, cultured in serum-free media in the presence or absence of 10 or 25% CSM for 4 hours and re-plated in complete media for 24 hours. Data normalised to untreated and presented as mean ± SEM. Statistical analyses performed on non-normalised data. N=6.

To assess the long-term effect of CSM, the same parameters were measured in healthy and COPD ASMCs 48 hours after treatment. Here, the effects of CSM on COPD ASMCs were no longer detected, suggesting the existence of homeostatic stress-response mechanisms (**Figure 3.10-3.12**). Interestingly, healthy, but not COPD, ASMCs maintained a reduced $\Delta\psi m$ 48 hours post-treatment (10% CSM: ∼20% reduction, $p<0.05$; 25% CSM: ∼20% reduction, $p<0.01$; **Figure 3.11A**).

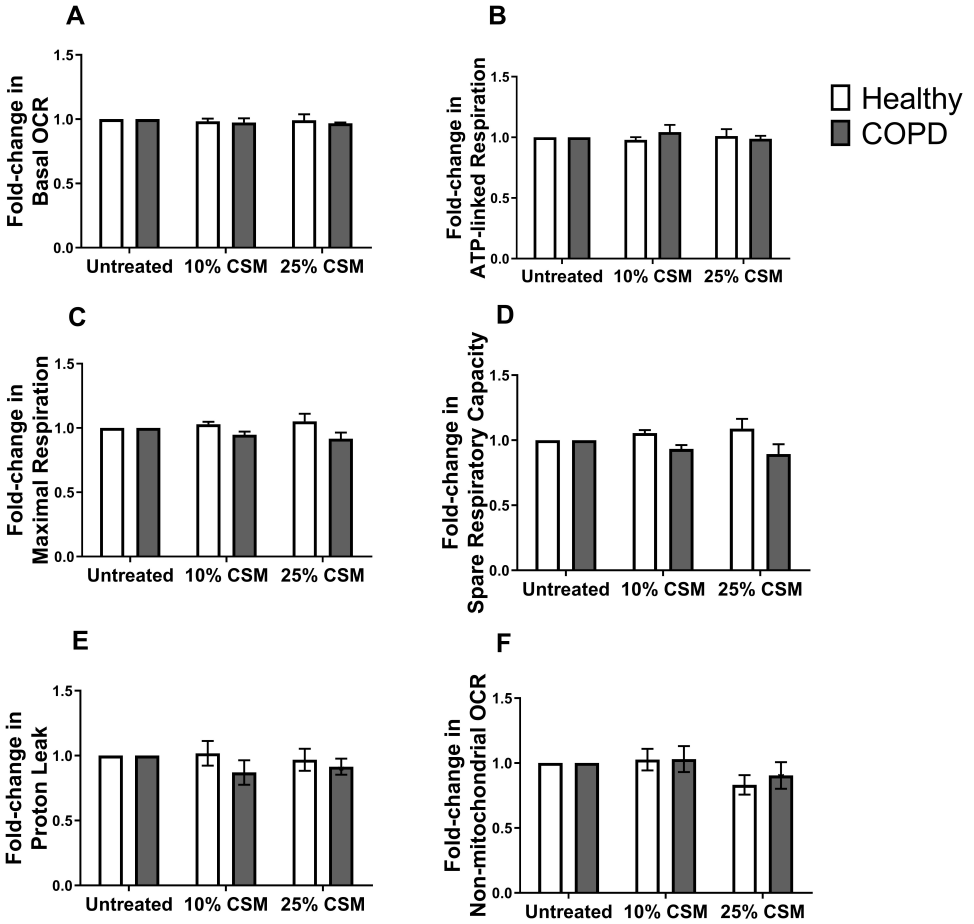

Figure 3.10: Long-term effect of cigarette smoke on mitochondrial respiration in ASMCs from healthy and COPD subjects. Quantification of (A) basal OCR (B) ATP-linked respiration (C) baximal respiration (D) spare respiratory capacity (E) proton leak and (F) non-mitochondrial oxygen consumption in ASMCs from healthy and COPD subjects, cultured in serum-free media in the presence or absence of 10 or 25% CSM for 4 hours and re-plated in complete media for 48 hours. Data normalised to untreated and presented as mean ± SEM. Statistical analyses performed on non-normalised data. *$p<0.05$, #$p<0.05$. N=6.

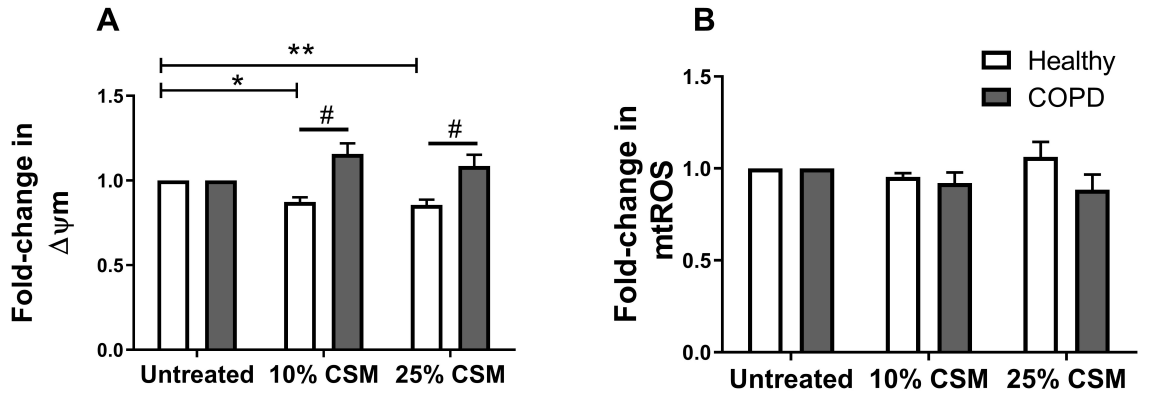

Figure 3.11: Long-term effect of cigarette smoke on mitochondrial function in ASMCs from healthy and COPD subjects. Quantification of relative levels of (A) $\Delta\psi$m and (B) mtROS in ASMCs from COPD and healthy subjects, cultured in serum-free media in the presence or absence of 10 or 25% CSM for 4 hours and re-plated in complete media for 48 hours. Data shown is the fold-change in median intensity fluorescence (MFI) in the PE-A channel compared to untreated and is presented as mean ± SEM. Statistical analyses performed on non-normalised data. *p<0.05 **p<0.01, #p<0.05. N=6.

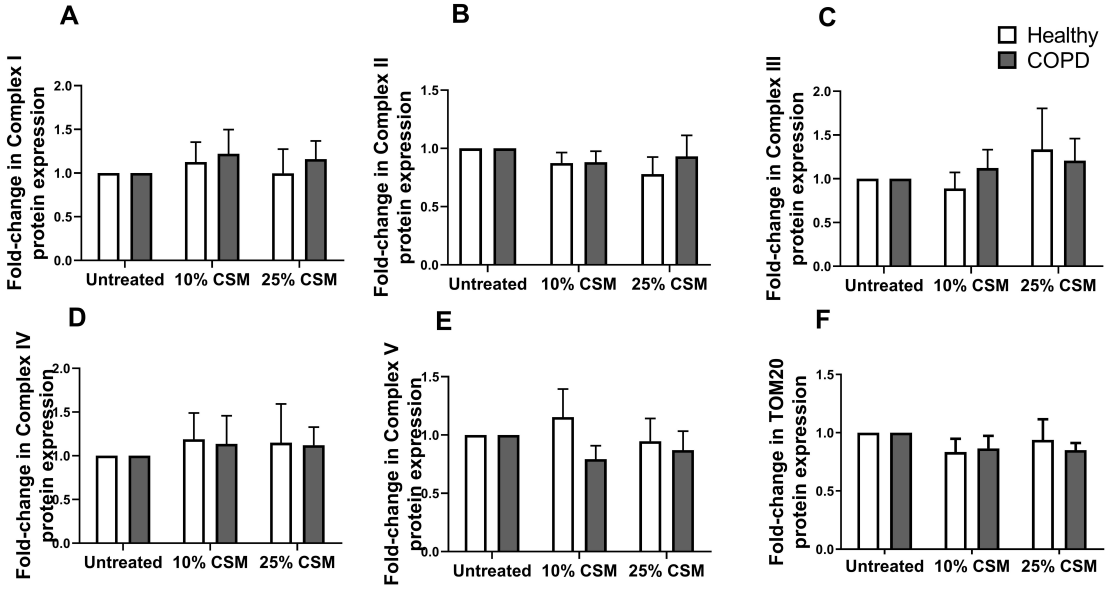

Figure 3.12: Long-term effect of cigarette smoke on the expression of mitochondrial proteins in ASMCs from healthy and COPD subjects. A. Quantification of (A-E) Complexes I-V of OXPHOS and (F) TOM20 in ASMCs from healthy and COPD subjects, cultured in serum-free media in the presence or absence of 10 or 25% CSM for 4 hours and re-plated in complete media for 48 hours. Data normalised to untreated and presented as mean ± SEM. Statistical analyses performed on non-normalised data. N=6.

3.3 Discussion

Changes in mitochondrial function, in response to cigarette smoke exposure, may drive ASM dysfunction in COPD. To assess this, I characterised mitochondrial function in primary ASMCs from healthy and COPD subjects, under baseline conditions and upon exposure to CS. The results of this Chapter demonstrate that CSM leads to mitochondrial damage, which is more pronounced in COPD ASMCs, suggesting these are more sensitive to CS-induced mitochondrial dysfunction.

Under baseline conditions, the mitochondrial function of healthy and COPD ASMCs differed in some aspects only. A non-significant, but consistent, reduction in TMRM fluorescence, representative of $\Delta\Psi$m, was observed in COPD ASMCs, indicative of an altered mitochondrial function. Mitochondrial membrane potential is controlled by different factors such as substrate availability, proton leakage across the IMM, ATP synthesis, electron flux through the respiratory chain and ion transport [176]. COPD ASMCs showed a reduced expression of complex III and V, which may affect electron flux and thereby $\Delta\Psi$m. It is important to note that the ETC complexes consist of different subunits, and the antibodies used to measure protein levels are specific to only one of the subunits for each complex. Whether the expression of other subunits or even the activity of the individual complexes is altered in COPD ASMCs was not assessed. In addition, it is not known what contributes to the reduced expression of complex III and V in COPD ASMCs. Mutations in mtDNA can lead to defects in the expression of complex proteins and can hence also affect $\Delta\Psi$m [177]. In the case of complex III, the measured subunit is the ubiquinol-cytochrome C reductase core protein 2 (UQCRC2) and mutations in the gene encoding this protein have been associated with mitochondrial disease [178]. In a southwestern Han Chinese population, different mtDNA haplogroups have been associated to increased susceptibility to COPD [179]. Therefore, mutations in mtDNA may be an important driver of mitochondrial dysfunction in COPD. NMOC was also lower in COPD ASMCs when compared to healthy cells. Whilst the majority of oxygen consumption takes place in the mitochondria, there are other cellular processes that also use oxygen. For example, cell surface oxygen consumption occurs in the trans-plasma

membrane electron transport (tPMET) and allows for re-oxidisation of NADH which is required for glycolysis [180]. Professional phagocytes use oxygen to produce ROS, during the pathogen-targeting respiratory burst, using the non-mitochondrial oxidases NADPH oxidases (NOX). NOX enzymes transfer electrons from NADPH, across biological membranes, to molecular oxygen generating superoxide ions [181]. NOX homologues, such as NOX4, are also present in non-phagocytic cells, including ASMCs, and could contribute to the observed differences in NMOC. A reduction in NMOC could be a result of a decrease in NOX4 activity, but conflictingly, NOX4 is upregulated in COPD ASM, and this expression correlates with severity of disease [75, 171]. The cause of reduced NMOC in COPD ASMCs remains unknown. No differences in mitochondrial mass, respiration or ROS were detected in between untreated healthy and COPD ASMCs.

The limited differences in mitochondrial function between healthy and COPD ASMCs could be a result of the culture conditions used in this study. Under H_2O_2-induced oxidative stress, COPD ASMCs show an increase in the levels of mtROS compared to healthy ex-smoker and non-smoker controls [45] whereas, upon mitogenic stimulation, COPD ASMCs have lower levels of mtROS [76]. This indicates that the choice of culture and treatment conditions affects mitochondrial function in these cells. Here, experiments were carried out after 4 hours of serum starvation followed by culture in medium containing 10% FBS, which may minimise cellular stress. The culture media also contained phenol red, which has anti-oxidant properties [182], and may affect the levels of ROS detected. In addition, the healthy ASMCs used in my study were isolated from ex-smoker subjects, which can be intrinsically different to cells from healthy never smokers, and more similar to COPD ASMCs. For example, serum-starved ASMCs from both COPD and ex-smoker subjects show a lower ATP-linked respiration compared to never smokers [45]. Therefore, some level of mitochondrial dysfunction may be present in cells from healthy ex-smoker subjects compared to cells from non-smokers. However, in this study I did not have access to ASMCs from non-smokers and could not evaluate this.

As highlighted above, *in vitro* systems have limitations, and it is important to confirm whether observations also represent what occurs *in vivo*. There is some evidence in *ex-vivo*

studies indicating mitochondrial dysfunction in COPD ASM. For example, *NOX-4* is up-regulated in ASM bundles and in immunohistochemistry analysis of small airway sections of COPD patients, suggesting an alteration in redox homeostasis [75, 171]. Mitochondrial dysfunction (e.g. decreased $\Delta\Psi$m and increased mtROS) was observed in bronchial biopsies of COPD patients compared to never or ex-smoker healthy controls [46], though the contribution of ASMCs to this phenotype is not clear. More studies on ASM bundles or airway sections should be performed to confirm this.

Acute exposure to cigarette smoke-conditioned medium induces mitochondrial dysfunction in healthy ASMCs [121, 143]. Due to the auto-fluorescence of CSM, I did not measure the differential effect of acute CSM treatment on healthy and COPD ASMCs. However, I show that some aspects of mitochondrial dysfunction are present after CS is removed, a phenomenon that this is more pronounced in COPD ASMCs. Previous studies in our group have shown that 4 hour exposure of CSM leads to a reduction $\Delta\Psi$m and an increase in mtROS in healthy ASMCs [143]. In this study I show that, in both healthy and COPD ASMCs, the reduced $\Delta\Psi$m is maintained for 24 hours after the stimuli is removed, indicating that CS-induced mitochondrial damage is sustained. However, the effect of CSM on mtROS was no longer observed. Again, the detection of mtROS may be hindered by the phenol-containing media, and further experiments in phenol-free media should be performed in order to confirm this. There was no difference in mitochondrial respiration in CSM-treated healthy cells compared to controls, indicating that either CSM had no effect initially, or that the cells recovered during the 24 hours of culture without CSM. In contrast, after 24 hours, COPD ASMCs showed a decrease in mitochondrial respiration parameters in response to CSM, as well as a reduction in the expression of complex III. Interestingly, 48 hours after stimuli removal, the effects of CSM were lost in COPD ASMCs whereas healthy ASMCs maintained a reduced $\Delta\Psi$m. This could be part of an adaptive response to CS in healthy ASMCs, which may be impaired in COPD. Mild uncoupling of the mitochondria has been shown to reduce oxidant production [183], so this may be a mechanism by which healthy ASMCs cope with increased CS-induced oxidative stress.

The results from this Chapter indicate that COPD ASMCs are more susceptible to CSM-induced mitochondrial dysfunction, compared to healthy cells, but what drives this is not known. One possibility is that the acute effect of CS is higher in COPD ASMCs. While this was not assessed in this study, it has been shown that COPD ASMCs are more susceptible to acute H_2O_2-oxidative stress induced damage, as shown by an increase in mtROS production [45]. This may be mediated by inherent differences in mitochondrial function, such as a the lower $\Delta\Psi m$ and expression of complex III detected in untreated COPD ASMCs. Another possibility is that mitochondrial responses to CSM are impaired in COPD ASMCs. My findings indicate that CSM-treated COPD cells show a trend towards lower spare respiratory capacity, a measure of metabolic adaptation to stress, compared to healthy ASMCs. Healthy ASMCs may have effective quality control mechanisms, explaining why at 24 hours minimal mitochondrial damage is observed. However, in COPD, these may be impaired leading to a delayed restoration of normal mitochondrial function. Impaired mitochondrial quality control mechanisms have been reported in COPD. For example, small airway epithelial cells from COPD subjects show reduced levels of Parkin, a protein required for mitophagy, suggesting this process may be impaired [112]. Reduced Mn-SOD is associated with increased susceptibility to CS-induced mitochondrial damage [184] and in ASMCs, TGF-β, which is upregulated in COPD airways, leads to a reduction in the expression of Mn-SOD [185]. Therefore, impaired anti-oxidant responses in COPD ASMCs may also contribute to an increased sensitivity to CSM. Understanding the cellular and molecular mechanisms that underpin the differential responses of healthy and COPD ASMCs to CSM could help explain why only some smokers develop COPD.

To understand differential responses to CS, it is important to clarify how cigarette smoke causes damage. Cigarette smoke is the major exogenous source of ROS in the lungs [36]. It is therefore conceivable that oxidative stress mediates CS-induced mitochondrial damage, and there is some evidence supporting this. For example, CS-induced changes to mitochondrial structure in epithelial cells are rescued by anti-oxidants [107]. CS also induces mitochondrial fragmentation in ASMCs via upregulation of *DRP1*, which occurs in response to different signalling pathways involving ROS [121]. It is not clear what are

the specific components of cigarette smoke that are responsible for these effects, but some have been shown to cause mitochondrial damage individually. Acrolein causes mtDNA damage and leads to a decrease in mitochondrial respiration [186, 187] whereas benzene can affect mtDNA copy number [188]. Finally, it is worth noting that the level of exposure to CSM in the ASM *in vivo* is not clear. Epithelial cells are the first to be exposed to cigarette smoke in the airways, but some lipid-soluble components of CS can diffuse through membranes and reach other compartments [189]. In addition, in COPD there is a loss of epithelial barrier function [190] which may allow for CS to leak through and reach the ASM.

In summary, in line with the hypothesis of this Chapter, CS leads to sustained changes in mitochondrial function, which are greater in COPD ASMCs, suggesting these are more sensitive to CS-induced mitochondrial dysfunction. This could be due to intrinsic differences in mitochondrial function of COPD ASMCs, or impaired recovery mechanisms. Hence, mitochondria may be targeted for therapies in COPD. However, to further assess this, it is important to investigate the functional consequences of mitochondrial dysfunction in COPD. How do changes in mitochondrial function affect cellular phenotypes associated to disease, such as proliferation and secretion of inflammatory mediators? The following chapter will address this questions.

Chapter 4

Funtional studies on ASMCs from healthy and COPD subjects

4.1 Introduction

The ASM is a structural component of the airways and its abnormal function has been associated with lung pathologies, such as asthma and COPD [191]. In COPD, changes in the phenotype of ASMCs may contribute to airway remodelling and chronic inflammation. Specifically, increased ASMC proliferation, hypertrophy and ECM deposition in COPD are thought to contribute to the thickening of ASM layer and subsequent narrowing of the airways [21, 22, 74, 75]. Increased levels of the proliferation marker PCNA and an increase in the number of ASMCs have been detected in small airway sections of COPD patients [75]. *In vitro*, ASMCs from COPD patients show a higher proliferative capacity in response to mitogenic stimuli [45]. Alterations to ECM structure and composition have been reported in COPD: elastic fibres, fibronectin, collagens, tenascin-C and versican are dysregulated in COPD throughout all lung compartments [192]. The ECM has several components with different roles in the lung. Collagens (I, II, III, V, XI) contribute to the structure of the lung whereas elastin and microfibrils (made of glycoproteins) provide the lung with elasticity required for elastic recoil during breathing [193]. Proteoglycans, such as glycosaminoglycans (GAGs), are also major components of the ECM, and provide hydration and swelling pressure to the tissue. In addition, there are many ECM modulating enzymes, such as MMPs, that affect the function and structure of ECM. Although an increase in ECM volume within the ASM layer is associated with a decrease in FEV_1 [79],

there is conflicting evidence regarding the ECM composition within the ASM in COPD. While Pini *et al* showed no difference in the levels of different ECM markers between healthy and COPD ASM [74], other studies have reported increased levels of laminin and collagen [75, 81]. Another important phenotype of ASMCs in COPD is increased secretion of inflammatory mediators that contributes to airway inflammation. Increased levels of the chemokine CXCL-10 and of the growth factor TGF-β have been detected in the ASM of COPD airways [75, 84]. IL-8 is a potent neutrophil chemoattractant and is secreted at higher levels by COPD ASMCs either at baseline conditions, or in response to stressors such as cigarette smoke [45]. GM-CSF, an important survival factor for both macrophages and neutrophils in the lung, is secreted at higher levels by COPD ASMCs compared to healthy ex- and non-smoker controls [45]. Pro-inflammatory cytokines, such as IL-6, are also secreted by ASMCs and this is higher in COPD [45].

Airway smooth muscle cells exhibit phenotypic plasticity in response to external cues [68]. As with mitochondrial dysfunction, changes in the cellular function of COPD ASMCs may be driven by exposure to CS. For example, CS induces proliferation [77, 194, 195] and secretion of inflammatory mediators, such as IL-8, CXCL-1 and TNF-α, of ASMCs [77, 81]. CS also modulates the ECM in ASMCs, leading to an increased secretion of MMP-1, MMP-6 and collagen (COL)9A1 [81]. Importantly, some of these responses, such as the secretion of CXCL-1, MMP-1 and COL8A1, are more pronounced in COPD ASMCs [81]. This indicates that COPD ASMCs have increased susceptibility to CS, and this may contribute to the development of pathological features in COPD. In **Chapter 3**, I show that CS-induced mitochondrial dysfunction is sustained after stimuli removal, and this is more pronounced in COPD ASMCs. However, it is not known whether the same is observed with disease-related phenotypes in ASMCs, nor what is the role of mitochondrial dysfunction in driving these changes in cellular function. To address these questions, the aims of this Chapter are to:

- Characterise cellular proliferation, changes in ECM deposition and secretion of inflammatory mediators in ASMCs from healthy and COPD subjects under baseline conditions and in response to CSM

- Investigate the link between mitochondrial and cellular function in ASMCs from healthy subjects

4.2 Results

4.2.1 CSM modulates cellular function in both healthy and COPD ASMCs

To characterise differences in cellular function between healthy and COPD ASMCs, these were cultured in the same conditions as **Chapter 3**. Cells from the same donors were used as much as possible (always from a pool of the same nine donors). Cellular function of ASMCs was first assessed under baseline conditions: cells were serum-starved for 4 hours and re-plated in complete medium. Cellular proliferation was assessed using three different assays, as described in **section 2.4**. First, total DNA was measured as a surrogate for cell number. Differences in the proliferation of cells can be inferred by comparing the increase in total DNA, as a surrogate for cell number, from day 1 to day 6 of culture (see **Section 2.4**). From day 1 to day 4, ASMCs from healthy and COPD patients showed no difference in the fold-change in total DNA. At day 5, however, the total DNA was further increased in COPD ASMCs, whereas it reached a plateau in healthy ASMCs. There was a significantly greater increase in DNA from day 4 to day 5 in COPD ASMCs ($p<0.05$), suggesting a higher proliferative rate. At day 6, the total DNA in COPD ASMCs also reached a plateau (**Figure 4.2A**). The rate of DNA synthesis was measured after 24 hours of culture, using a BrdU incorporation assay. To control for differences in cell number, that affect the BrdU assay readings, the data obtained from the BrdU assay was normalised to total DNA of the same cells, quantified using the CyQuant assay. Albeit not significant, there was an averaged 1.8-fold increase in BrdU incorporation in COPD ASMCs, again suggesting a higher proliferative rate in these cells (**Figure 4.2B**). The lack of significance may result from high variability and low replicate number, and additional experimentation is required to confirm whether these differences are indeed real. Finally, to assess cell-cycle in ASMCs, PI staining was performed in healthy and COPD ASMCs after 24 hours of culture. To assess the efficiency of the assay, a control with cells treated with mitogenic stimuli (1 ng/µl of TGF-β and 2.5% FBS) was used. There was a shift from the G0/G1 phase in untreated cells to the S and G2M phases

in treated cells, confirming the detection of the mitogenic effect of the stimuli (**Figure 4.1**). When assessing cell-cycle in healthy and COPD ASMCs, no significant differences were observed in the percentage of cells at G0/G1, S and G2M phases between the two groups, although a higher number of replicates (only N=3 used here) would be required to confirm this (**Figure 4.2C**). Overall, despite the differences observed being small, these data suggest COPD ASMCs are more proliferative than healthy ASMCs when cultured in complete media.

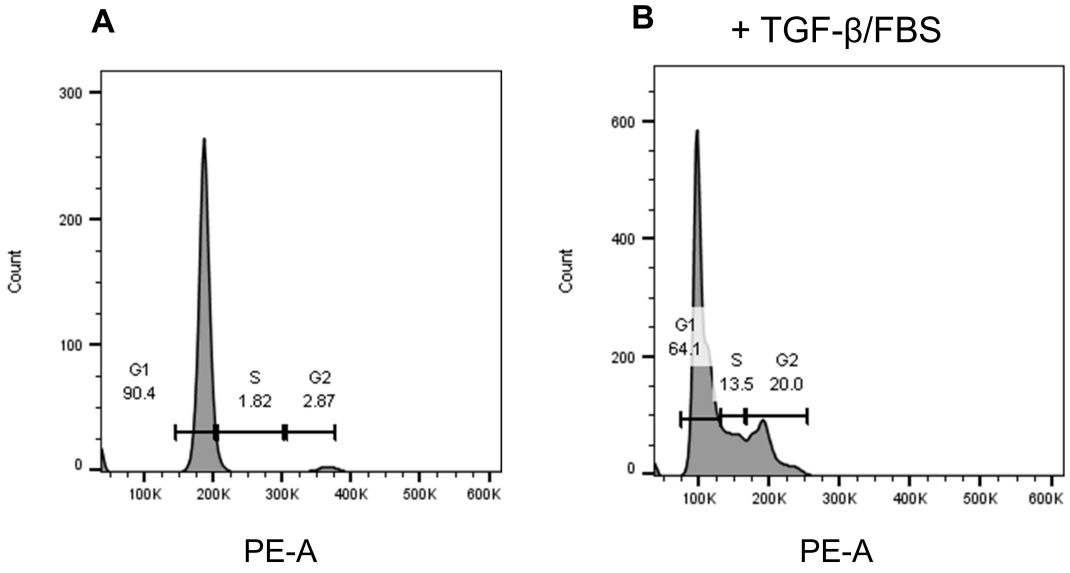

Figure 4.1: Cell cycle analysis by propidium iodide staining. Propidium iodide staining of ASMCs cultured for 24 hours in serum-free media in the (A) absence or (B) presence of mitogenic stimulation (1ng/µl of TGF-β and 2.5% FBS). Graphs show flow cytometry histograms. N=1.

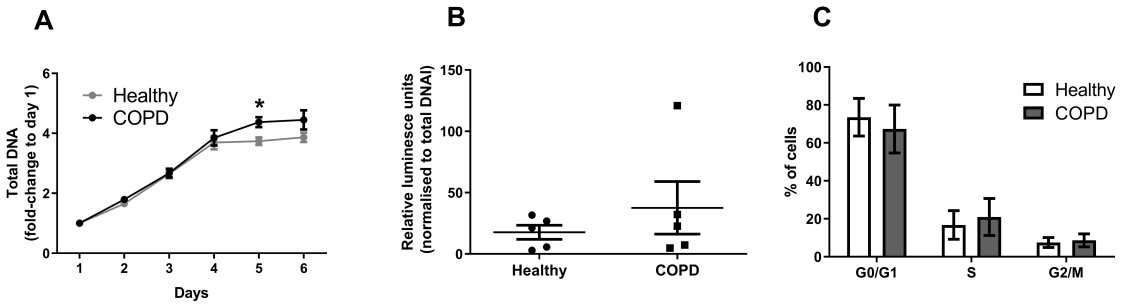

Figure 4.2: Cellular proliferation in ASMCs from healthy and COPD subjects. Assessment of proliferation in ASMCs from COPD and healthy subjects, serum-starved for 4 hours and re-plated in complete media for 24 hours using: (A) CyQuant assay to measure change in total DNA, N=8; (B) BrdU incorporation to measure DNA synthesis, N=5; and (C) propidium iodode staining to assess cell-cycle, N=3. Data presented as mean ± SEM.*$p<0.05$.

I then quantified the secretion of inflammatory mediators in healthy and COPD ASMCs. The mediators measured were chosen based on current evidence suggesting secretion of these is altered in COPD ASMCs [45, 81, 84]. However, in my experiments I saw no difference in the baseline secretion of the mediators measured - IL-8, IL-6, CXCL-1, CXCL-10 and GM-CSF - between the two groups, except for a non-significant increase in MMP-1 in COPD ASMCs (p=0.057) (**Figure 4.3**).

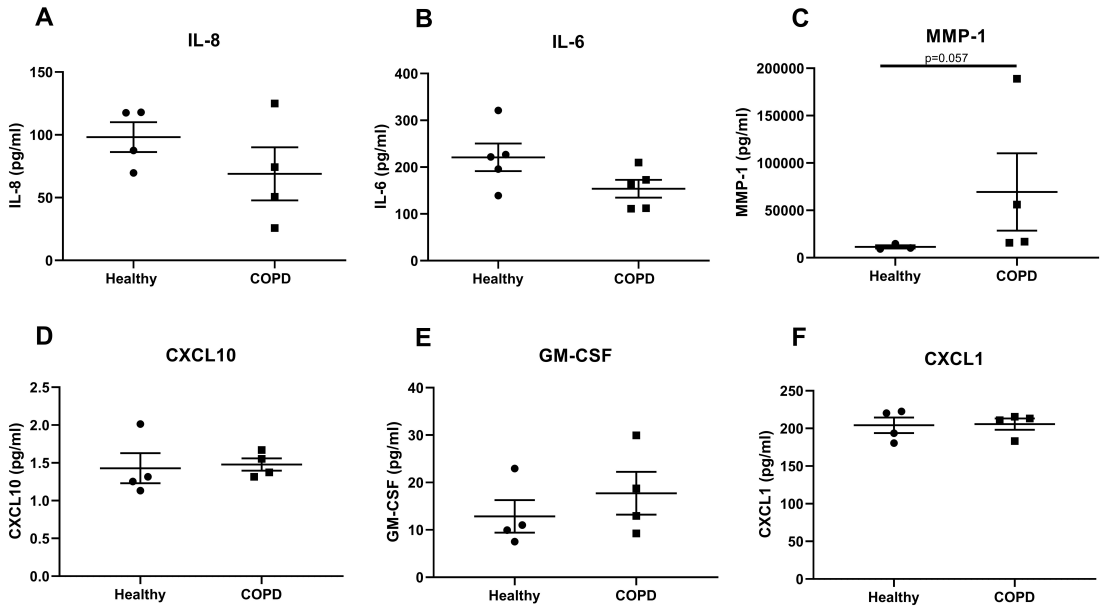

Figure 4.3: Secretion of inflammatory mediators in ASMCs from healthy and COPD subjects. Quantification of levels of (A) IL-8 (B) IL-6 (C) MMP-1 (D) CXCL-10 (E) GM-CSF and (F) CXCL1 in supernatant collected from ASMCs from COPD and healthy subjects, serum-starved for 4 hours and re-plated in complete media for 24 hours. Data presented as mean ± SEM.*$p<0.05$. N=4-5.

Transcriptomics data was previously obtained from ASMCs from seven healthy and seven COPD subjects cultured in complete media (unpublished). The cells were cultured and RNA was extracted by myself and Charalambos Michaeloudes and the sequencing and analysis was performed by Novogene Co. These data showed that extracellular matrix and structure organisation were the biological processes with the highest number of differentially regulated genes (34 genes) between healthy and COPD ASMCs, though the differential expression of individual genes did not reach statistical significance (in terms

of the adjusted p-value). (**Figure 4.4A**). I sought to assess the expression of the top differentially expressed genes (**Figure 4.4B**) by qPCR. No differences were seen in the mRNA levels of the 3 genes selected, elastin (*ELN*), hyaluronan and proteoglycan link protein 3 (*HAPLN3*) and laminin subunit gamma 2 (*LAMC2*), between the two groups (**Figure 4.5**).

A

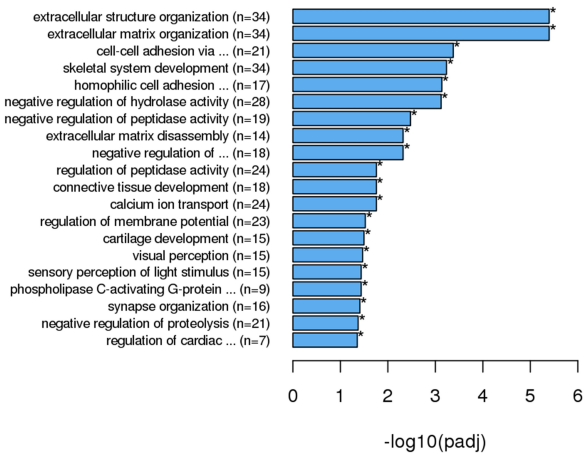

B

gene_name	COPD_FPKM	Healthy_FPKM	log2FoldChange	P-value	P-value (adjusted)
ELN	13.54189314	99.46506571	-3.127884	0.000123	0.109417
ACAN	0.625475	3.564213429	-2.706498	0.000139	0.109663
LAMC2	0.410568143	3.140310714	-3.236994	0.000143	0.109663
HAPLN3	1.308533714	4.167939714	-1.866465	0.000411	0.180118
COL22A1	0	0.025430571	-11.17348	0.000499	0.207448
ITGA11	0.388852857	1.320283143	-2.044777	0.003116	0.481729
COL18A1	8.241309857	14.15135714	-0.836447	0.007138	0.654008

Figure 4.4: Transcriptome analysis of ASMCs from healthy and COPD subjects. (A) Gene ontology enrichment analysis for biological processes (BP): differentially expressed genes between healthy and COPD ASMCs fall into the shown categories of BPs. (B) Top 7 differentially expressed genes related to extracellular matrix, showing Fragments Per Kilobase of transcript per Million mapped reads (FPMK) and the changes between the two groups. N=7.

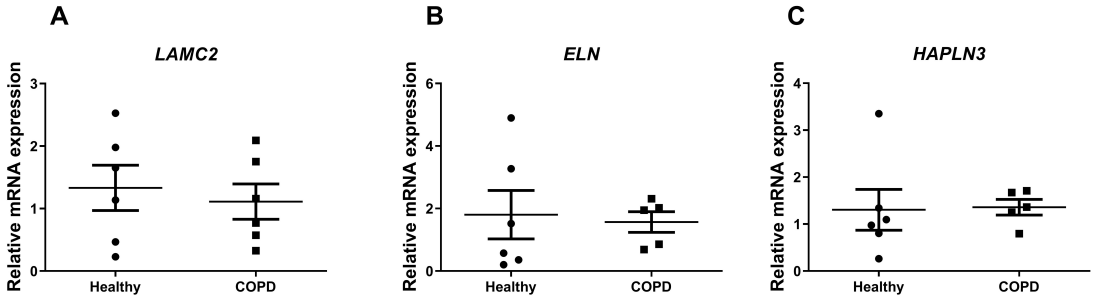

Figure 4.5: Expression of ECM genes in ASMCs from healthy and COPD subjects. Quantification fo mRNA levels of extracellular matrix genes (A) *LAMC2* (B) *ELN1* and (C) *HAPLN3* in ASMCs from COPD and healthy subjects serum-starved for 4 hours and re-plated in complete media for 24 hours. Data presented as $2^{-\Delta\Delta Ct}$ to healthy cells and as mean ± SEM. *p<0.05. N=6.

To assess the effect of CSM on ASMC function, cells were treated with 25% CSM for 4 hours, whilst untreated controls were kept in serum-free media, and re-plated in complete media for 24 hours or for the appropriate duration of the assays ("smoking cessation" CSM treatment model). Since in **Chapter 3** minimal effects were seen with 10% CSM, only the 25% CSM treatment was used for these experiments, unless otherwise stated. Cellular proliferation was inhibited by CSM in all assays performed. There was a reduction in the increase of total DNA over time in both healthy and COPD ASMCs, with differences between treated and untreated significant at day 4 to 6 (**Figure 4.6A-B**). BrdU incorporation was lower in CSM-treated healthy and COPD cells at 24 hours post-treatment, though this did not reach statistical significance. This effect was lost over time, with no differences detected at 72 hours (**Figure 4.6C-E**). Similarly, CSM led to a trend towards an increase in cells at the G0/G1 phase and a reduction in cells in the S-phase at 24 hours, in both healthy and COPD ASMCs. This effect was again lost at 48 and 72 hours (**Figure 4.6F-K**).

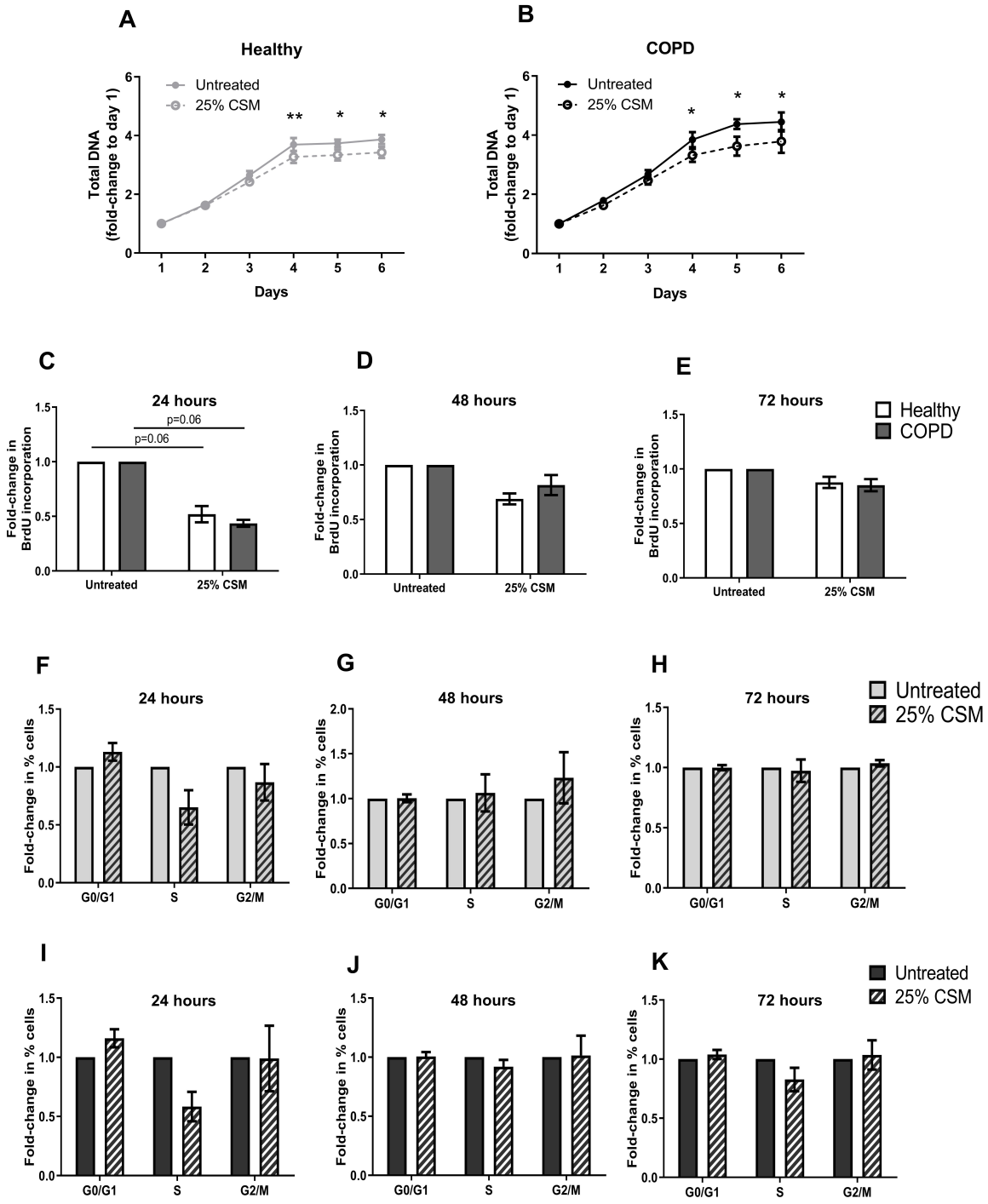

Figure 4.6: Effect of cigarette smoke medium on proliferation of ASMCs from healthy and COPD subjects. Assessment of proliferation in ASMCs from COPD and healthy subjects cultured in serum-free media in the presence or absence of 25% CSM for 4 hours and re-plated in complete, media using: (A) CyQuant assay to measure change in total DNA after 1-6 days, N=8; (B) BrdU incorporation to measure DNA synthesis after 24-72 hours, N=3; and (C) propidium iodide staining to assess cell cycle after 24-72 hours, N=3. (A,B) Data presented as fold-change to day 1. (C-K) Data normalised to untreated. All data is presented as mean ± SEM. Statistical analyses performed on non-normalised data. *p<0.05, **p<0.01, relative to 25% CSM.

The effect of CSM on the secretion of inflammatory mediators after 24 hours was varied. Whilst there was an increase in the secretion of IL-8 and a trend towards an increase in CXCL10 and MMP-1, no effects were detected in the secretion of IL-6, CXCL-1 and GM-CSF (**Figure 4.7**). Finally, CSM did not alter the mRNA levels of *ELN*, *HAPLN3* and *LAMC2* at 24 hours post-treatment (**Figure 4.8**). In all the assays, there was no significant difference in the effects of CSM between healthy and COPD ASMCs.

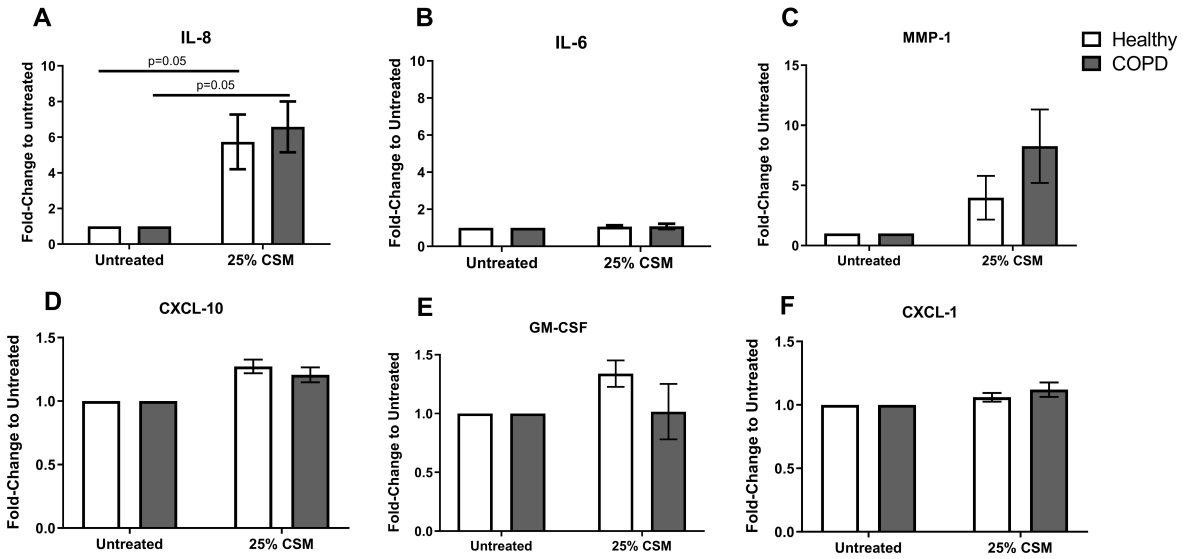

Figure 4.7: Effect of cigarette smoke on the secretion of inflammatory mediators in ASMCs from healthy and COPD subjects. Quantification of levels of (A) IL-8 (B) IL-6 (C) MMP-1 (D) CXCL-10 (E) GM-CSF and (F) CXCL-1 in supernatant collected from ASMCs from COPD and healthy subjects, cultured in serum-free media in the presence or absence of 25% CSM for 4 hours and re-plated in complete media for 24 hours. Data normalised to untreated and presented as mean ± SEM. Statistical analyses performed on non-normalised data. N=4-5.

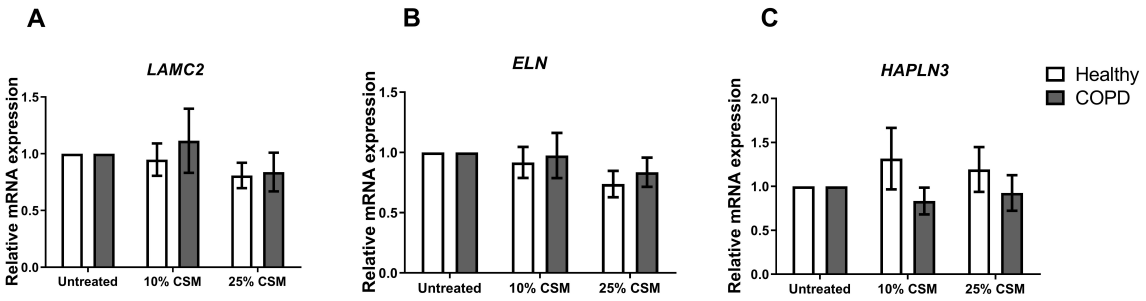

Figure 4.8: Effect of cigarette smoke on the expression of ECM genes of ASMCs from healthy and COPD subjects. Quantification fo mRNA levels of extracellular matrix genes (A) *LAMC2* (B) *ELN1* and (C) *HAPLN3* in ASMCs from COPD and healthy subjects, cultured in serum-free media in the presence or absence of 10-25% CSM for 4 hours and re-plated in complete media for 24 hours. Data presented as $2^{-\Delta\Delta Ct}$ to untreated controls and as mean ± SEM. Statistical analyses performed on non-normalised data. N=6.

The culture conditions used for the experiments described above might be masking differences in cellular function between healthy and COPD ASMCs (See **section 4.3**). For this reason, experiments were also performed with cells re-plated in complete media without phenol and with reduced FBS (2.5%). Under these conditions, however, no differences were seen in proliferation of healthy and COPD ASMCs as shown by the changes in total DNA over time and BrdU incorporation at 24 hours (**Figure 4.9**). Similarly, there was no difference in the secretion of IL-8, IL-6, MMP-1, CXCL1, CXCL10 and GM-CSF between the two groups (**Figure 4.10**).

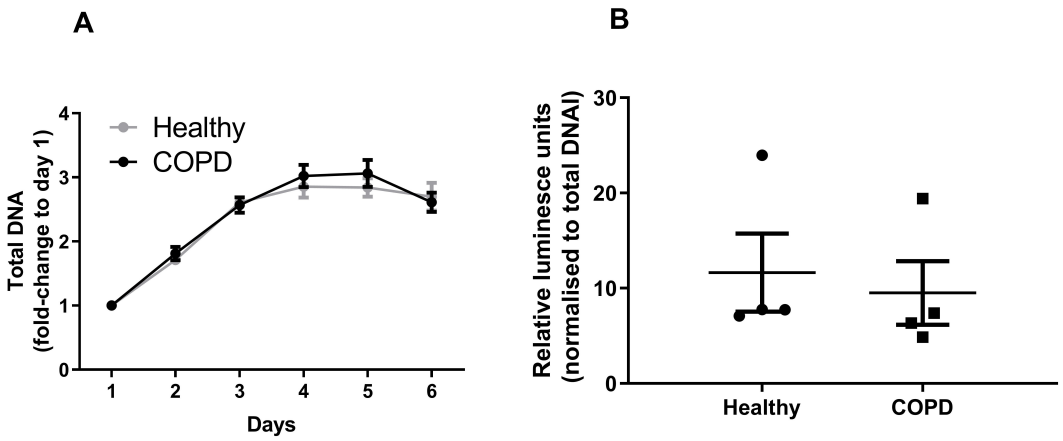

Figure 4.9: Cellular proliferation of ASMCs from healthy or COPD subjects under conditions of reduced serum. Assessment of proliferation in ASMCs from healthy and healthy subjects serum-starved for 4 hours and re-plated in 2.5% FBS phenol-free complete media, using: (A) CyQuant assay to measure change in total DNA afte 1-6 days, N=6; (B) BrdU incorporation to measure DNA synthesis after 24 hours, N=4; Data presented as mean ± SEM.

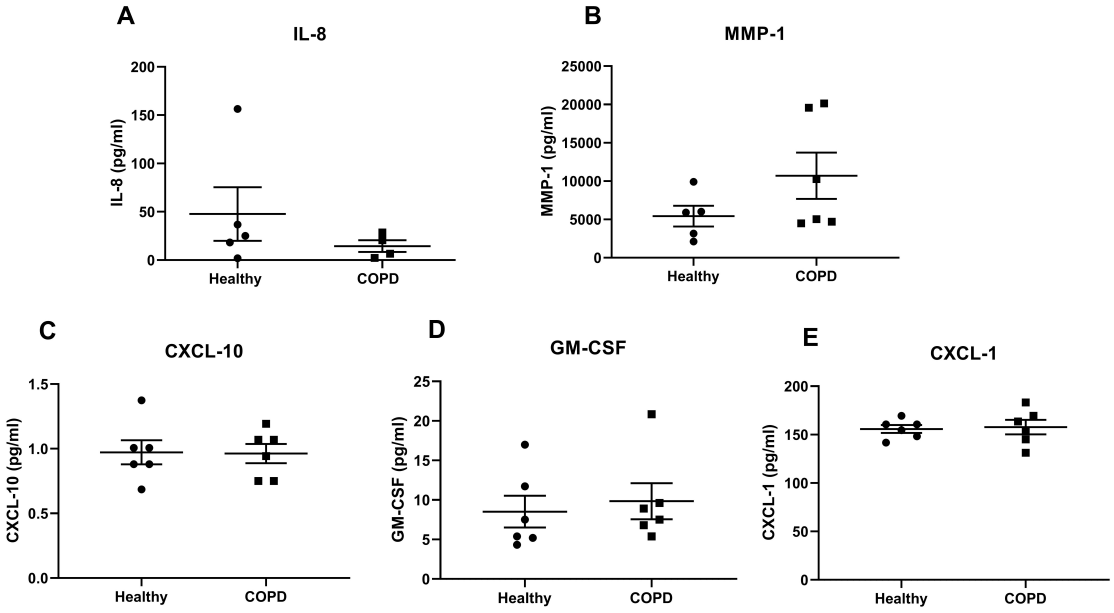

Figure 4.10: Secretion of inflammatory mediators in ASMCs from healthy and COPD subjects under conditions of reduced serum. Quantification of levels of (A) IL-8 (B) MMP-1 (C) CXCL-10 (D) GM-CSF and (E) CXCL1 in supernatant collected from ASMCs from COPD and healthy subjects, serum-starved for 4 hours and re-plated in 2.5% FBS phenol-free complete media for 24 hours. Data presented as mean ± SEM. n=5-6.

When the cells were pre-treated with CSM, there was a reduction in the proliferation of both groups as seen before. Contrary to what was observed when cells were re-plated in complete media, here, the effect of CSM on BrdU incorporation appeared to be maintained until 72 hours, which could indicate that the previous culture conditions were facilitating the recovery of the cells (**Figure 4.11**). The effect of CSM on the secretion of inflammatory mediators was also more pronounced in this experimental set-up: there was a significant increase in IL-8, MMP-1, CXCL10 and GM-CSF in healthy and COPD CSM-treated cells (**Figure 4.12**).

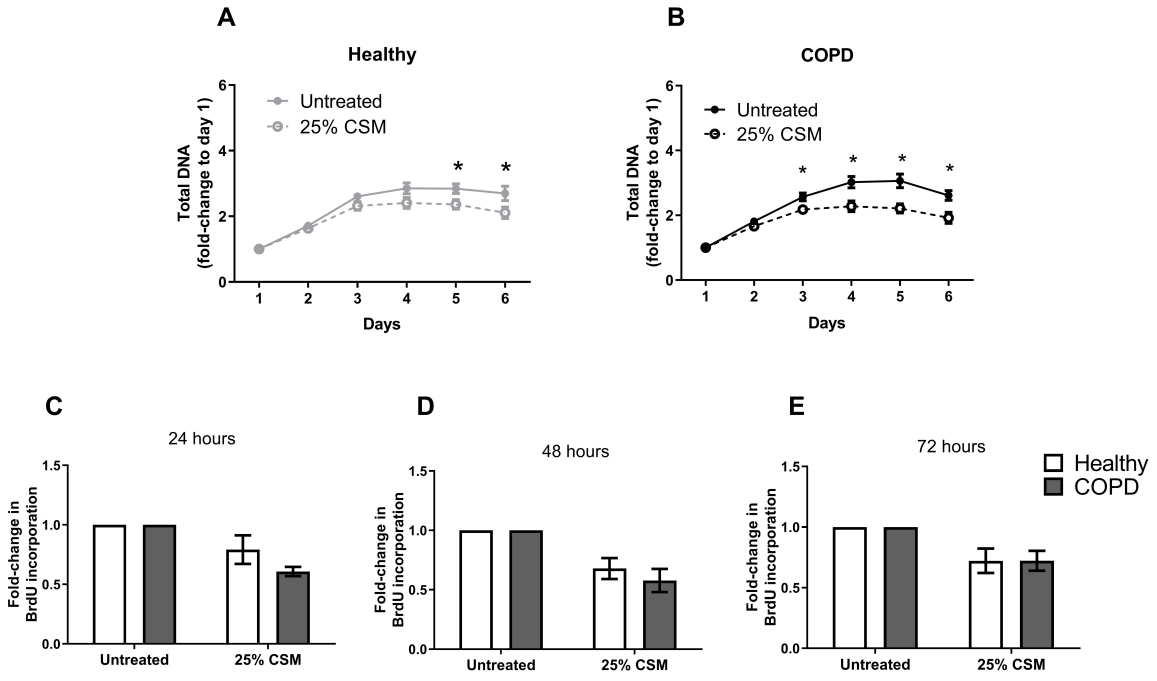

Figure 4.11: Effect of cigarette smoke on proliferation of ASMCs from healthy and COPD subjects under conditions of reduced serum. Assessment of proliferation in ASMCs from COPD and healthy subjects, cultured in serum-free media in the presence or absence of 25% CSM for 4 hours and re-plated in 2.5% FBS phenol-free complete media using: (A-B) Change in CyQuant assay (n=6) and (C-E) BrdU incorporation. N=4. (A,B) Data presented as fold-change to day 1. (C-E) Data normalised to untreated. All data is presented as mean ± SEM. Statistical analyses performed on non-normalised data. *p<0.05, relative to 25% CSM.

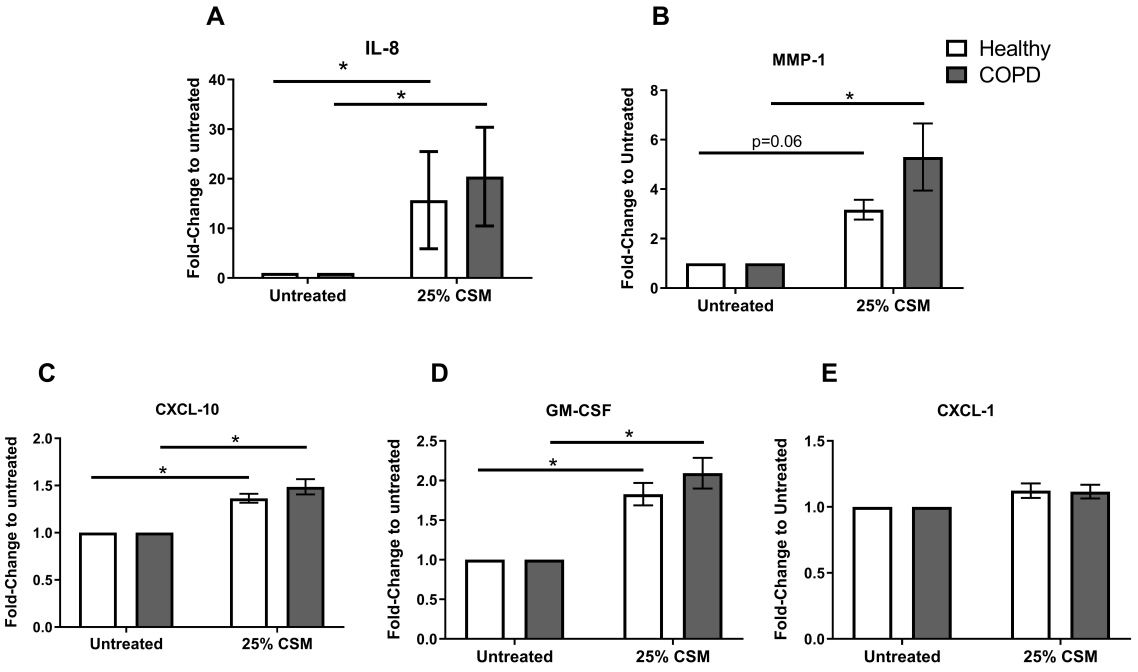

Figure 4.12: Effect of cigarette smoke on secretion of inflammatory mediators of ASMCs from healthy and COPD subjects under conditions of reduced serum. Quantification of levels of (A) IL-8 (B) MMP-1 (C) CXCL-10 (D) GM-CSF and (E) CXCL-1 in supernatant collected from ASMCs from COPD and healthy subjects, cultured in serum-free media in the presence or absence of 25% CSM for 4 hours and re-plated in 2.5% FBS phenol-free complete media for 24 hours. Data normalised to untreated and presented as mean ± SEM. Statistical analyses performed on non-normalised data. N=4-5.

4.2.2 Changes in $\Delta\psi$m are associated to distinct cellular phenotypes in healthy ASMCs

I next examined the link between mitochondrial function and cellular phenotypes in healthy ASMCs. To achieve this, I compared the cellular phenotype of cells with distinct mitochondrial membrane potential. ASMCs from healthy subjects were stained with TMRM as a measure of $\Delta\psi$m. FACS was used to isolate cells with high $\Delta\psi$m from cells with low $\Delta\psi$m, by separating cells with high a low TMRM staining as shown in **Figure 4.13A**. The same number of cells with high and low TMRM staining were collected, and plating for the different assays was performed as described in **Chapter 2**. Assessment of mitochondrial respiration confirmed that these two groups had different mitochondrial function: cells with high $\Delta\psi$m had a higher basal OCR, spare respiratory,

ATP-linked and maximal respiration and a lower proton leak compared to cells with low $\Delta\psi$m (**Figure 4.13B**). With regards to cellular phenotype, cells with high $\Delta\psi$m were less proliferative and had a lower secretion of IL-8 compared to cells with low $\Delta\psi$m, indicating differences in cellular phenotype (**Figure 4.13C-D**). This was a preliminary experiment, and completion of more replicates is required to reach statistical significance. In addition, while there is an evident correlation between mitochondrial function and the phenotypes assessed, the causal link between these remains unknown and requires further investigation.

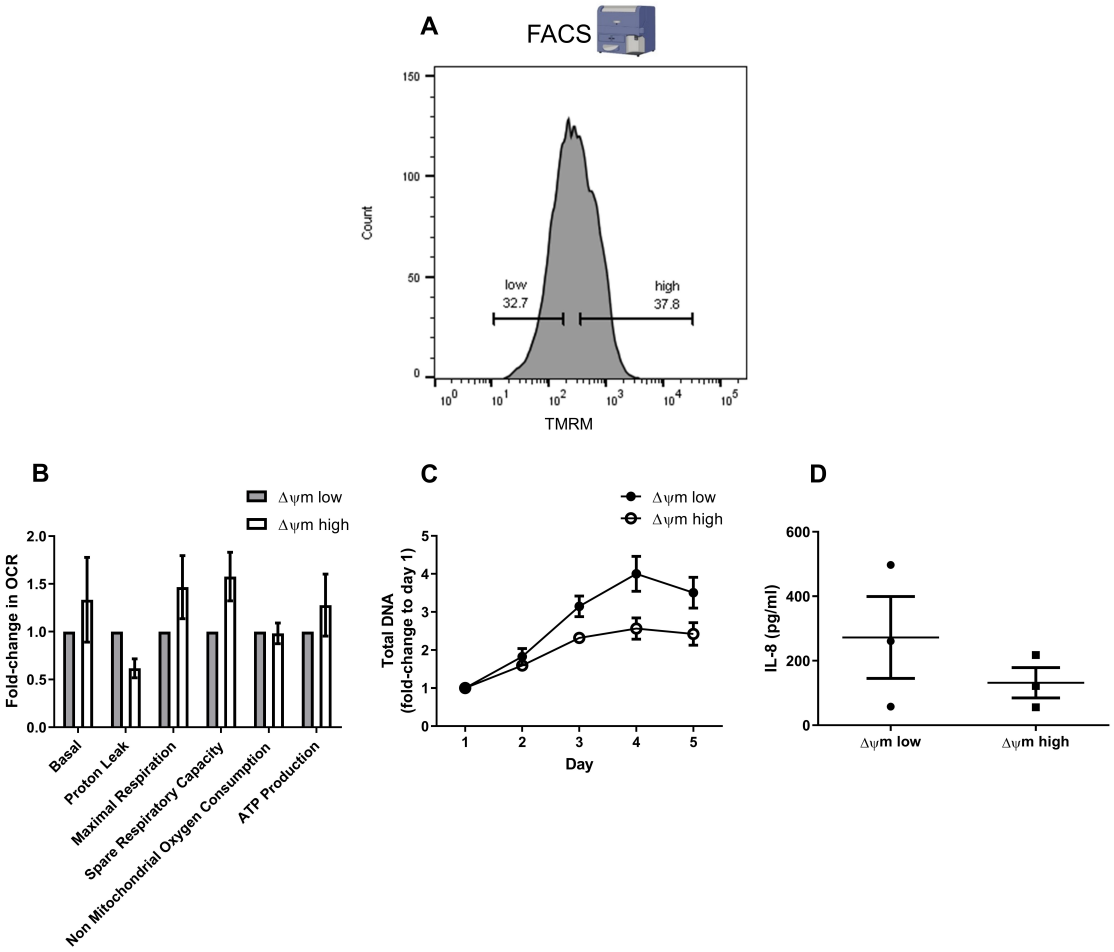

Figure 4.13: Characterisation of mitochondrial and cellular function in ASMCs from healthy subjects with high and low $\Delta\psi$m. (A) Isolation of cells with high and low $\Delta\psi$m by FACS based on TMRM staining. Assessment of (B) Mitochondrial respiration, (C) proliferation by CyQuant assay and (D) secretion of IL-8 in high vs low $\Delta\psi$m cells. Proliferation was measured from day 1-5 post-isolation; other assays were performed 48h post-isolation. Data presented as mean ± SEM. N=3.

4.3 Discussion

Mitochondria participate in several cellular processes. To investigate the functional consequences of mitochondrial dysfunction described in **Chapter 3**, in this Chapter I evaluated different aspects of the cellular phenotype of ASMCs. The results described show that COPD ASMCs are hyperproliferative, and that modulation of mitochondrial function is accompanied by changes in cellular function. However, the causal link between these changes requires further investigation.

There is evidence that ASM dysfunction, such as hyperproliferation and secretion of inflammatory mediators, contributes to COPD pathogenesis [45, 75, 81, 84]. In this study, similar to what was observed with regards to mitochondrial function, only some aspects of cellular function were different between healthy and COPD ASMCs under baseline conditions. Specifically, COPD ASMCs showed an altered cellular proliferation. While the growth curve for healthy and COPD cells was similar from day 1 to 4, at day 5 COPD ASMCs continued to proliferate whereas healthy cells reached a plateau. At day 4, cells were visibly confluent, and therefore contact inhibition might prevent healthy cells from proliferating. In COPD, however, cells continue to grow which could suggest that contact inhibition is lost. Loss of contact inhibition is associated to abnormal proliferation of cancerous cells, a mechanism which is orchestrated by different signalling pathways including ECM-induced activation of the Hippo-YAP/TAZ pathway [196]. In ASMCs, the ECM component Fibulin-5, which is upregulated in COPD lung tissue, induces proliferation of cells through activation of the Hippo-YAP/TAZ pathway [197], which therefore may involve loss of contact inhibition. Although the differences in proliferation detected in other assays did not reach statistical significance, there are some visible trends that may be indicative of a higher proliferation rate in COPD ASMCs. It is worth noting that cell-cycle synchronisation was not performed prior to experiments, and the readings of the assays performed can be affected by the cell-cycle phase. Cell-cycle synchronisation could be achieved by increasing the serum-starvation period to 24 hours [198]. Another important phenotype of ASMCs in COPD is the secretion of inflammatory mediators, which contributes to chronic inflammation in the lungs. However, here, there was no dif-

ference in the secretion of IL-8, IL-6, CXCL-10, CXCL-1 and GM-CSF between healthy and COPD ASMCs. ECM plays an important role in the pathogenesis of COPD [192, 193], and there is some evidence that ASMCs contribute to ECM changes in the lung [75, 81]. In this study, there was a non-significant increase in the secretion of MMP-1 by COPD ASMCs compared to healthy cells. Though MMP-1 is thought to be mostly secreted by bronchial epithelial cells, type II pneumocytes and alveolar macrophages [199], it has also been found in ASM [81]. MMP-1 breaks down collagen and cleaves pro-MMP-2 and -9 to their active form, playing an important role in modulating ECM composition in the lung. It is overexpressed in the lungs of patients with emphysema [200]. Furthermore, it has been shown to mediate ECM-induced proliferation [201] and contraction [202] of ASMCs. Gene expression profiling from previous experiments performed by my research group revealed that the most differentially expressed genes between COPD and healthy ex-smoker ASMCs were consistent with biological process involving ECM, suggesting this is indeed an important aspect of ASM dysfunction. However, when assessing the expression of individual genes, both by RNA-seq and qPCR, no statistical differences were found between the two groups. Therefore, while changes in the ECM seem to be an important aspect of COPD, the identification of individual genes involved in this requires further investigation. Whereas differences at a transcriptional level were not detected, protein levels or post-translational modifications (PTMs) might still differ and affect function. In other conditions, such as cancer and lung fibrosis, PTMs play an important role in modifying ECM function [203, 204]. Whether this also occurs in COPD is not known.

Cigarette smoke is the main cause of COPD, and CS-induced pathological features, such as inflammation and oxidative stress persist after smoking cessation in COPD [21]. In **Chapter 3**, I showed that CS induces mitochondrial dysfunction, which is sustained after removal of the stressor. In this Chapter, I show that these responses are accompanied by changes in cellular function. Firstly, CSM led to a reduction of proliferation in both healthy and COPD ASMCs. This was an unexpected finding since cigarette smoke has been shown to induce proliferation of ASMCs [77, 194, 195], which may contribute to hyperplasia of ASMCs seen in COPD. This disparity might reflect differences

in the treatment models used, since previous studies have assessed the effect of continuous exposure to lower doses of CS (1-5% CS for 12-72 hours) [77, 81], whereas here I assess cellular function after removal of the stimuli. Nevertheless, it is still not clear how CSM would inhibit proliferation. Guan *et al* reported that CSM induces proliferation by decreasing the activation of the transcription factor CCAAT/enhancer-binding protein alpha (C/EBP-α), which normally inhibits proliferation [195]. Studying the transcriptional responses of ASMCs to the CSM treatment model used in my studies could provide clues as to how proliferation is inhibited. When assessed by BrdU incorporation and cell cycle analysis, the reduction in cellular proliferation caused by CSM was evident at 24 hours post-treatment but this effect was lost over time, as was observed with CS-induced mitochondrial dysfunction. This indicates there may be homeostatic mechanisms that restore normal cellular function after exposure to CS. With regards to the effect on inflammation and ECM deposition, CSM led to a non-significant increase in the secretion of IL-8 and MMP-1 in both healthy and COPD ASMCs. No differences were seen in the secretion of other inflammatory mediators, nor in the expression of the ECM genes measured. One unexpected finding was that there was no significant difference in the effect of CSM on healthy and COPD ASMCs in the assays performed, unlike what was observed with regards to mitochondrial function, where CS-induced changes were greater in COPD ASMCs.

The lack of significant differences may be due to the cell culture conditions used, which can affect the phenotype of cells. For example, phenol red, which is typical component of standard cell culture media, has anti-oxidant properties and therefore can mask oxidative stress-induced effects on cells [182]. The levels of serum can also alter cellular function: serum starvation leads to changes in cell phenotype including increased ROS production, reduced mitochondrial function and inhibition of cell proliferation [45]. Therefore, the presence of growth factors and other FBS components in the medium used in my study could mask differences in the cellular phenotype between healthy and COPD ASMCs. However, the phenotype of ASMCs cultured in phenol-free media with reduced FBS was similar to those cultured in standard conditions. The proliferation rate of ASMCs from

healthy and COPD subjects was again unchanged from day 1-4, though the difference observed at day 5 in normal cultured conditions was lost. The reduced FBS content might be a limiting factor for proliferation. There was also no difference in secretion of inflammatory mediators between healthy and COPD ASMCs. Moreover, under these conditions, cigarette smoke likewise led to a reduction in cellular proliferation and an increase in the secretion of IL-8 and MMP-1. There was a significant CSM-induced increase in the secretion of CXCL-10 and GM-CSF, which was not observed before, but might be a result of an increased number of repeats (from 4 to 6 replicates). Overall, changing the culture conditions had no significant effect on the phenotype of these cells. In the future, other culture conditions, such as serum-starvation and reduced glucose levels should be tested.

As with mitochondrial function, changes in cellular function may be more evident when comparing ASMCs from healthy non-smoker patients, but I did not have access to these. In addition, though the phenotypes assessed were chosen based on current evidence in the literature, there are other important cellular mechanisms, such as senescence and apoptosis, which may be different in COPD ASMCs. Gene expression profiling suggested that changes in ECM play an important role in ASM dysfunction in COPD, and further studies regarding this are an important avenue to pursue. However, studying ECM is complex: ECM components can be difficult to discern from intracellular proteins, and, as they are often found as large oligomeric proteins, they can be insoluble in many solvents impairing their use in different assays [205]. Furthermore, the ECM is composed of ∼300 proteins [193] and therefore high-throughput analysis using mass spectrometry/proteomics is required for a better understanding of the role of ECM in ASM dysfunction in COPD. This was beyond the scope of this study.

Mitochondrial dysfunction has been widely reported in COPD [25, 45, 46, 107, 112, 206]. However, the functional consequences of mitochondrial dysfunction are not fully understood. Here, exposure to cigarette smoke leads to mitochondrial dysfunction, such as a drop in $\Delta\psi m$, which is accompanied by a reduction in cellular proliferation and an increase in the secretion of some inflammatory mediators. I have also shown that healthy ASMCs

with low $\Delta\psi$m and mitochondrial respiration have a distinct phenotype when compared to cells with high $\Delta\psi$m. Cells with low $\Delta\psi$m show a higher secretion of IL-8, comparable to what happens when cells are treated with CSM. However, cells with low $\Delta\psi$m are hyperproliferative which is the opposite of what is observed in CSM-treated cells. Hence, the signalling pathways involved in these responses may differ. It is worth noting that the correlation between mitochondrial dysfunction and cellular phenotypes observed in my experiments does not necessarily implicate causation. Further mechanistic studies are required to assess whether there is a causal link between these concomitant events. However, given the pleiotropic roles of mitochondria, it is likely that changes in mitochondrial function can indeed affect different cellular processes, and several studies have reported such observations. For example, known as the Warburg effect, cancer cells switch to a glycolytic metabolism to support growth and proliferation, an occurrence which is mediated by mitochondrial uncoupling and proton leak [207]. Similarly, mitogenic stimulation induces proliferation of ASMCs as well as increased glycolytic metabolism, and this is more pronounced in COPD [76]. Whether this occurs through similar signalling pathways as the Warburg effect is not known. In contrast, other models have reported that proliferation is associated with increased mitochondrial respiration, and requires proteins involved in mitochondrial quality control such as MFN2 [208]. Proliferation can also be regulated by other mitochondrial by-products, such as mtROS. In ASMCs, the anti-oxidant MitoQ inhibits mitogenic-induced proliferation suggesting a role for mtROS in modulating this phenotype [45]. ROS can regulate signalling cascades involved in proliferation by inhibiting the action of protein tyrosine phosphatases, which contain redox-sensitive cysteine residues in their catalytic domain and are inactivated by ROS-induced oxidation [209]. For example, ROS can induce the growth-promoting PI3-K signalling pathway by inhibiting the phosphatase and tensin homolog (PTEN) [210]. Mitochondrial function can also modulate the secretion of inflammatory mediators. Antimycin A and oligomycin, which inhibit complex III and V of oxidative phosphorylation, respectively, induce the secretion of IL-8 in chondrocytes, and this is reversed by ROS inhibitors [211]. Release of intracellular mtDNA induces IL-8 and IL-6 in ARPE-19 cells. This occurrs by activation of the

DNA-sensing cGAS-STING pathway that activates the transcription factor NF-kB to induce transcription of pro-inflammatory genes [212]. More mechanistic studies are required to determine the link between mitochondrial function and cellular phenotypes in ASMCs. An approach to do so could be to modulate different aspects of mitochondrial function, particularly the ones described in COPD ASMCs. For example, since the expression of complex III of the ETC was decreased in COPD ASMCs, the effect of its function on proliferation and secretion of inflammatory mediators could be assessed by inhibiting its function with antimycin A or knocking down the different proteins that comprise it.

In summary, no remarkable differences were observed in the cellular phenotype of healthy and COPD ASMCs. Nevertheless, these phenotypes were modulated by cigarette smoke, which occurred concomitantly to changes in mitochondrial function. As hypothesised, the effects of CSM on both mitochondrial and cellular function were observed for 24 hours after removal of the stressor, relatable to the persistence of pathological features in COPD patients after smoking cessation. However, after 48 hours, many of these effects were lost, suggesting the presence of homeostatic mechanisms that restore normal cellular function. In the following chapter, I will describe the process of mitochondrial transfer between cells as a possible cell-cell communication mechanism to maintain mitochondrial and cellular homeostasis.

Chapter 5

Mitochondrial transfer in ASMCs from healthy and COPD subjects

5.1 Introduction

Mitochondria have quality control mechanisms that regulate their quality and quantity. For example, in response to different cues, cells can increase mitochondrial number through activation of biogenesis, alter their morphology by modulating fusion and fission, and remove defective mitochondria by mitophagy [93]. Mitochondria also show random and directed intracellular movement [97]. Recently, it has been shown that mitochondria can move, not only within, but also between cells. This was first shown by Spees and colleagues who demonstrated that MSCs and fibroblasts could transfer their mitochondria to A549 epithelial cells devoid of mtDNA in a co-culture. This rescued the ability of the mitochondria-recipient cells to undergo aerobic respiration, which was impaired as a consequence of mtDNA depletion [122]. Since then, a number of studies have reported mitochondrial transfer between different cells types, such as from MSCs to structural or immune cells [123, 125, 130, 135, 143, 147, 213], and structural cells to macrophages [124, 127, 145, 146]. Interestingly, not all cell types are capable of exchanging mitochondria. For example, epithelial cells can receive mitochondria from MSCs, but cannot donate their own [125].

The physiological role of mitochondrial transfer is not clear. Some studies have reported that transferred mitochondria are damaged [124, 127, 150] and are degraded by

the recipient cells [124, 130, 134], suggesting this may be a quality control mechanism to remove dysfunctional mitochondria. Others report that donation of mitochondria from healthy cells, such as MSCs, has beneficial effects in the recipient cells, such as enhancing mitochondrial function by an increase in ATP production and a decrease mtROS [123, 125, 130, 141, 143]. Importantly, several studies have shown that this process can reverse pathogenic phenotypes in different disease models, including lung disorders such as acute lung injury [123], allergic airway inflammation [125], acute respiratory distress syndrome [165] and asthma [214]. For example, transfer of mitochondria from airway-instilled MSCs to the lung epithelium protects against LPS-induced lung injury by decreasing leucocytosis and protein leak in a murine model of acute lung injury [123]. MSCs can also reverse airway remodelling through mitochondrial transfer in a mouse model of allergic airway inflammation [125]. Overall, the existing evidence suggests that mitochondrial transfer may be an important process in maintaining both mitochondrial and cellular homeostasis, though the mechanisms may vary depending on the cell type and conditions. However, there is limited understanding regarding transfer of mitochondria between structural cells within a tissue. Airway smooth muscle cells can receive mitochondria from MSCs [143] and can donate their mitochondria to epithelial cells [125]. Whether ASMCs themselves can exchange mitochondria and the contribution of this process to tissue homeostasis has yet to be determined. Moreover, it is not known whether impairment of mitochondrial transfer can contribute to mitochondrial dysfunction seen in different conditions, such as COPD.

In this Chapter, I hypothesise that airway structural cells, namely ASMCs, can exchange mitochondria and this is impaired in COPD leading to the persistence of mitochondrial dysfunction. The aims of the Chapter are to:

- Assess whether ASMCs are capable of exchanging mitochondria
- Investigate differences in mitochondrial transfer between healthy and COPD ASMCs, under baseline conditions and in response to CSM
- Assess the functional impact of mitochondrial transfer between ASMCs

5.2 Results

5.2.1 ASMCs can exchange mitochondria

To assess the ability of ASMCs from healthy subjects to exchange mitochondria, I co-cultured MitoTracker- (donor) with CellTrace- (recipient) stained ASMCs from the same subject. This allowed me to track the stained mitochondria from MitoTracker-stained cells and establish whether these were transferred and hence detected in CellTrace-stained cells (**Figure 5.1A**). The percentage of CellTrace-stained cells positive for MitoTracker (i.e. cells that receive mitochondria) was quantified by flow cytometry (**Figure 5.1B**). After 24 hours of co-culture, 32.33 % $\pm$ 3.6 of CellTrace-stained cells were positive for MitoTracker, indicating uptake of mitochondria (**Figure 5.1C**). The doublet exclusion performed confirmed that these were single cells (See **Section 2.3**). The same co-cultures were imaged live by fluorescence microscopy, and MitoTracker-positive recipient cells were observed (white arrows in **Figure 5.1D**). It is important to note that it is likely that the CellTrace-stained cells are also simultaneously transferring mitochondria to the MitoTracker-stained cells. However, due to the experimental set-up, it was only possible to track transferred mitochondria from MitoTracker- to CellTrace-stained cells.

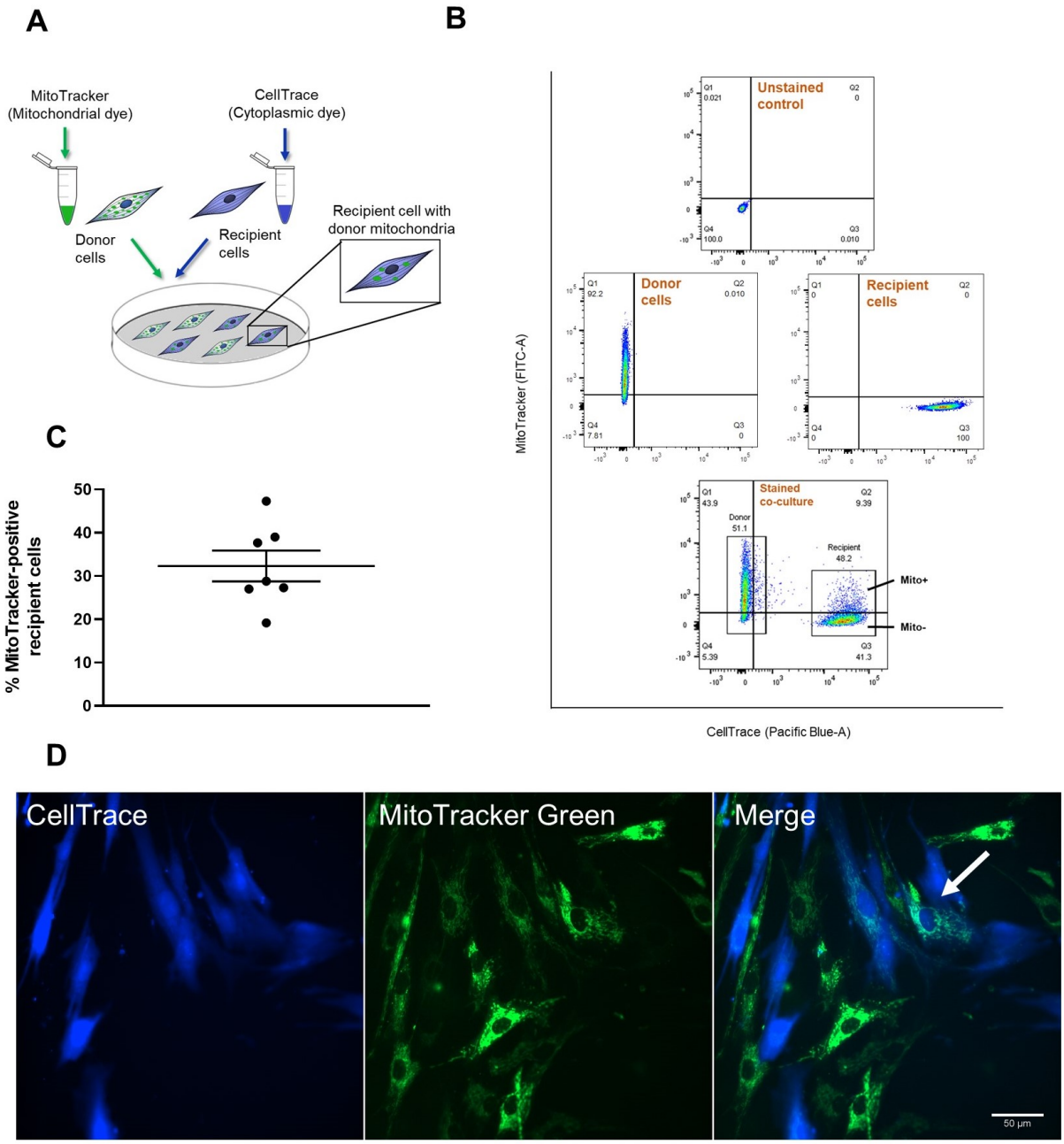

Figure 5.1: Detection of mitochondrial transfer between healthy ASMCs. (A) Schematic representation of co-culture of MitoTracker-stained (donor) cells and CellTrace-stained (recipient) ASMCs. (B) Representative flow cytometry dot plot showing detection of MitoTracker-positive recipient ASMCs. (C) Quantification of MitoTracker-positive recipient cells following direct co-culture for 24 hours, N=7. (D) Representative image of MitoTracker-positive recipient cells visualised by fluorescence microscopy.

MitoTracker dyes can leak from cells [133] and therefore I set up two different controls to assess this possibility (described in detail in **section 2.13**). In a first control, the supernatant resulting from the last wash step of the MitoTracker staining procedure was filtered using a 0.4 µM porous filter and added onto CellTrace-stained cells for 24 hours. Alternatively, cells were cultured in a transwell system, where MitoTracker-stained cells were cultured in inserts with 0.4 µM pores that were placed over wells where CellTrace-stained cells were cultured. Since mitochondria are typically larger than 0.4 µM, these set-ups would impair transfer of intact mitochondria whilst allowing for transfer of leaked free dye. In parallel, MitoTracker-stained cells were cultured with CellTrace-stained cells as before. After 24 hours, the percentage of MitoTracker-positive recipient cells in normal co-cultures was of ∼30% whereas this was negligible in the two controls (**Figure 5.2A**). However, one data-point for the filtered supernatant control showed a value of 13.30%, indicating that leakage may have occurred in this situation. This may be due to a poorly executed staining procedure (e.g. in the washing step), and therefore special attention was taken thereafter when doing so. The effect of cigarette smoke media on MitoTracker leakage was also assessed by treating MitoTracker-stained ASMCs with CSM for 4 hours before plating. As seen in **Figure 5.2B**, the controls showed no MitoTracker-positive recipient cells.

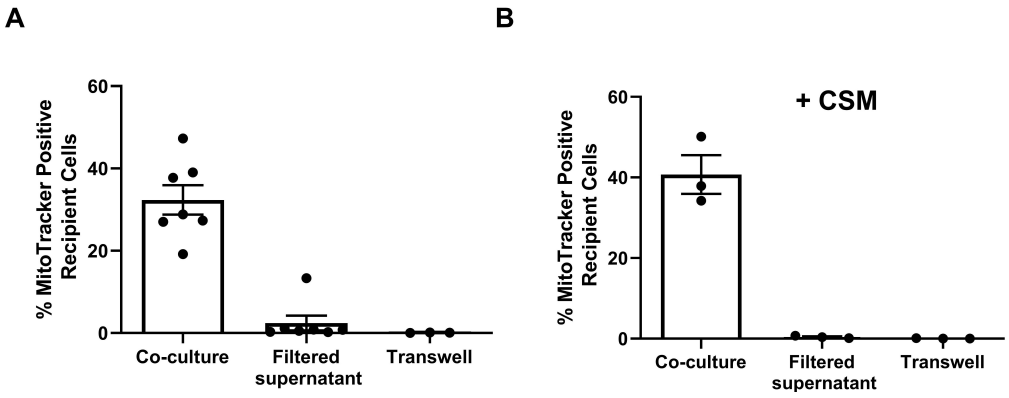

Figure 5.2: Controlling for leakage of the MitoTracker dye. Flow cytometry quantification of MitoTracker signal in CellTrace-stained cultured with: MitoTracker-stained cells directly, filtered supernatant of MitoTracker-stained cells (collected after the last wash step of staining) or MitoTracker-stained cells in a transwell system. MitoTracker-stained cells were either (A) serum-starved or (B) treated with 25% CS for 4 hours, before staining and plating. N=3-7

Two additional methods were used as an alternative to MitoTracker dyes to assess mitochondrial transfer between ASMCs. Firstly, mitochondria were tagged with GFP, using two approaches. Cells were transfected with either a plasmid containing either a GFP-tagged pyruvate dehydrogenase (CellLight Mitochondria-GFP) or a GFP-tagged cytochrome c oxidase subunit 8 (pCT-Mito-GFP). Both these proteins are expressed in the mitochondria, which causes the GFP to be targeted to the mitochondria. The CellLight Mitochondria-GFP construct is packaged within the insect virus baculovirus, and 50 particles per cell (PPC) was the most efficient multiplicity of infection for transfecting the cells, with 26% of cells expressing GFP (**Figure 5.3A**). The pCT-Mito-GFP vector was transfected using lipofectamine LTX, and 1.5 µl of the latter resulted in the best transfection efficiency, with 50% of cells transfected (**Figure 5.3B**). Transfected cells were co-cultured with CellTrace-stained (recipient) cells for 24 hours (as described in **Section 2.13.2**. GFP-positive recipient cells were detected by flow cytometry, but the percentage of cells receiving mitochondria was considerably lower than what was observed with MitoTracker (1.2% ± 0.6 for CellLight Mitochondria-GFP and 3.2% ± 0.7 for pCT-Mito-GFP transfected cells). However, whereas MitoTracker-stained cells showed around 90% of staining efficiency (data not shown), the transfection efficiency for both plasmids was much lower (32% ± 11 for CellLight Mitochondria-GFP and 47% ± 3.9 for pCT-Mito-GFP), which could explain the lower rates of mitochondrial transfer detected (**Figure 5.4A and C**). Confocal imaging confirmed the presence of GFP-positive recipient cells (**Figure 5.4B and D**).

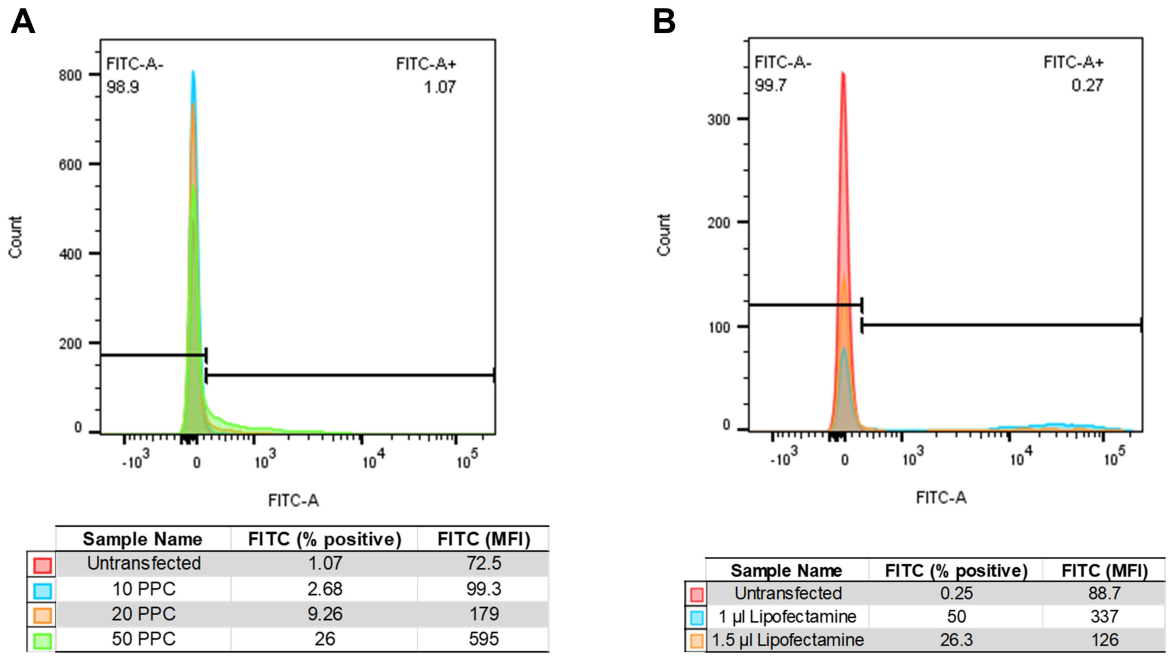

Sample Name	FITC (% positive)	FITC (MFI)
Untransfected	1.07	72.5
10 PPC	2.68	99.3
20 PPC	9.26	179
50 PPC	26	595

Sample Name	FITC (% positive)	FITC (MFI)
Untransfected	0.25	88.7
1 µl Lipofectamine	50	337
1.5 µl Lipofectamine	26.3	126

Figure 5.3: Optimization of expression of mitochondria-targeted GFP. Flow cytometry quantification of fluorescence in the FITC-A channel of ASMCs from healthy subjects 24 hours after either (A) transfection with CellLight Mitochondria-GFP at 10, 25 and 50 particles per cell (PPC), or (B) transfection with pCT-Mito-GFP vector with either 1 or 1.5 µl of lipofectamine LTX. Tables show percentage of positive cells and median fluorescence intensity of FITC-A fluorescence. N=1.

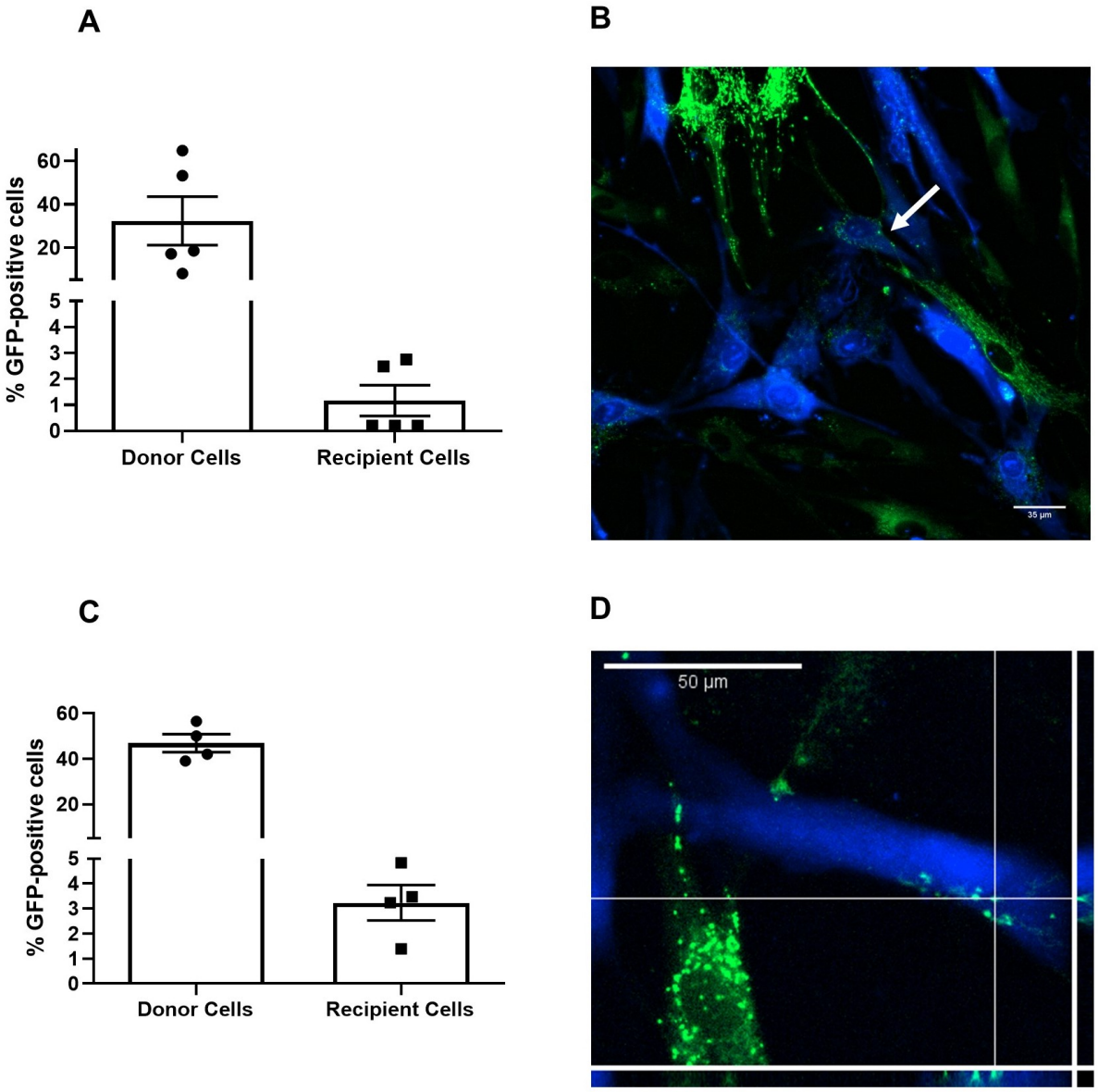

Figure 5.4: Detection of mitochondrial transfer using mitochondrial-targeted GFP. Detection of mitochondrial transfer in 24-hour co-cultures of CellTrace-stained ASMCs and mitochondria donor cells transfected with either (A-B) CellLight Mitochondria-GFP or (C-D) pCT-Mito-GFP vector. (A and C) The percentage of GFP-positive donor and recipient cells was quantified by flow cytometry, N=4-5; and (B and D) mitochondrial uptake by recipient cells (blue) was visualised by confocal microscopy, N=1.

The final method used to assess mitochondrial transfer was the detection of patient-specific mtDNA mutations using ARMS-qPCR (described in detail in **section 2.13**). Patient-specific mtDNA polymorphisms were identified from transcriptomic data obtained previously by my research group, and two were selected for the assay: m.3531A<G and m.11719A<G (**Figure 5.5A and B**). The ARMS-qPCR assays were designed to detect the m.3531=G and m.11719=G genotypes. The efficiency of the assay was tested by mixing mtDNA from cells with or without these genotypes at known proportions: 5%/95%, 25%/75%, 50%/50%, 75%/25%, which rendered samples with different levels of these specific polymorphisms (i.e. different heteroplasmy levels). The measured heteroplasmy was plotted againts the predicted heteroplasmy and a linear regression was fitted. As seen in **Figure 5.5C**, the linear regression of the m.3531=G detection assay resulted in an R^2 of 0.96, indicating a good assay efficiency. The m.11719=G detection assay was less efficient with an R^2 of 0.85 (**Figure 5.5D**). Therefore, further experiments were performed using the former assay only.

A

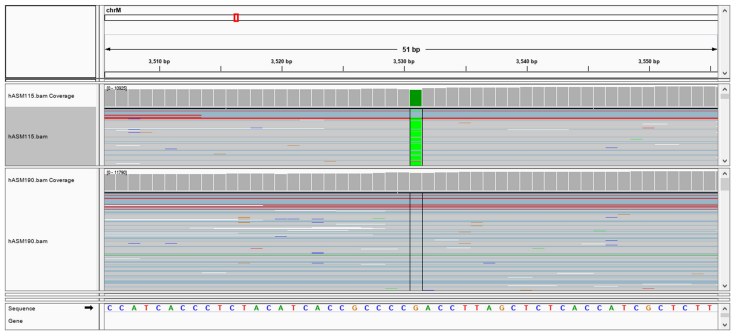

B

Loci in mtDNA	Genotype in:					Gene
	Reference genome	hASM115	hASM190	hASM145	hASM188	
m.3531	G	A	G	G	G	*MT-ND1*
m.3639	A	A	G	A	A	*MT-ND1*
m.3666	G	G	C	G	G	*MT-ND1*
m.3721	A	G	A	A	A	*MT-ND1*
m.4216	T	C	C	C	T	*MT-ND1*
m.4580	G	G	G	G	A	*MT-ND2*
m.5147	G	G	G	A	G	*MT-ND2*
m.5198	A	G	A	A	A	*MT-ND2*
m.8697	G	G	G	A	G	*MT-ATP6*
m.8994	G	A	G	G	G	*MT-ATP6*
m.11251	A	G	G	G	A	*MT-ND4*
m.11719	G	A	A	A	G	*MT-ND4*
m.11812	A	A	A	G	A	*MT-ND4*
m.14905	G	G	G	A	G	*MT-CYB*
m.15064	A	A	G	A	A	*MT-CYB*

C

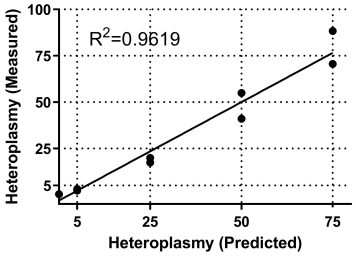

D

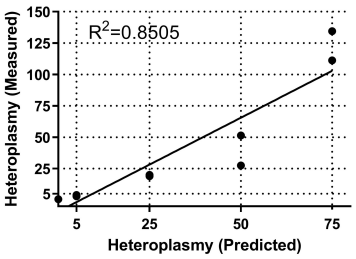

Figure 5.5: Optimization of the ARMS-qPCR assay. (A) Representative image of aligned reads from RNA-seq analysis visualised on IGV for identification of loci with distinct genotypes. Green lines indicate the genotype differs from the reference genome. (B) mtDNA polymorphisms identified between two pairs of ASMCs; the polymorphisms selected for the assay are shown in yellow. (C) Assessment of the efficiency of the ARMS-qPCR assay for the quantification of mtDNA mutations. DNA from patients with or without the selected mutation were mixed at known proportions (5, 25, 50 and 75% of DNA from donor with the mutation of interest vs remaining of DNA from ASMCs without the mutation). The predicted heteroplasmy was plotted against the measured heteroplasmy.

MitoTracker-stained ASMCs from a patient with the specific polymorphism (m.3531=G) were co-cultured with CellTrace-stained ASMCs from a patient with a distinct genotype (m.3531=A) (**Figure 5.6A**). After 24 hours, MitoTracker-positive (Mito+) were isolated from MitoTracker-negative (Mito-) recipient cells by FACS (**Figure 5.6B**). The optimized ARMS-qPCR assay was performed to detect the presence of the donor-specific mutation in the recipient cells, using DNA from the donor cells to prepare a standard curve. Donor-specific mtDNA was detected in Mito+ cells (6.5% $\pm$ 0.5), but not in Mito- nor in the single culture control, suggesting the uptake of donor mtDNA in the former (**Figure 5.6C**). However, when analysing the flow cytometry dot plots, it was noted that a proportion of donor cells ($\sim$5%) was consistently isolated with the Mito+ cells during cell sorting (Quadrant 1 of Mito+ dot plot in **Figure 5.6B**). Therefore, the detected heteroplasmy could be a result of the presence of the donor cells. In order to address this issue, Mito+, Mito- and single cultured controls were also isolated as single cells into 96-well plates. As seen in **Figure 5.6D**, whereas the control and Mito- cells showed negligible presence of the donor mutation, a proportion of Mito+ cells were positive for it. Some Mito+ cells had heteroplasmy levels close to 100%, suggesting these may indeed be donor cells. However, there was a range of cells with heteroplasmy of $\sim$5% to 30%, which would be too low for donor cells but consistent with recipient cells that receive mitochondria from donor cells. Confirmation that these were indeed single cells would be important to further validate these findings. Taken together, these data confirm that ASMCs can exchange mitochondria.

A

Sample	Genotype at locus m.3531
hASM115 (recipient)	A
hASM190 (donor)	G
hASM71 (donor)	G

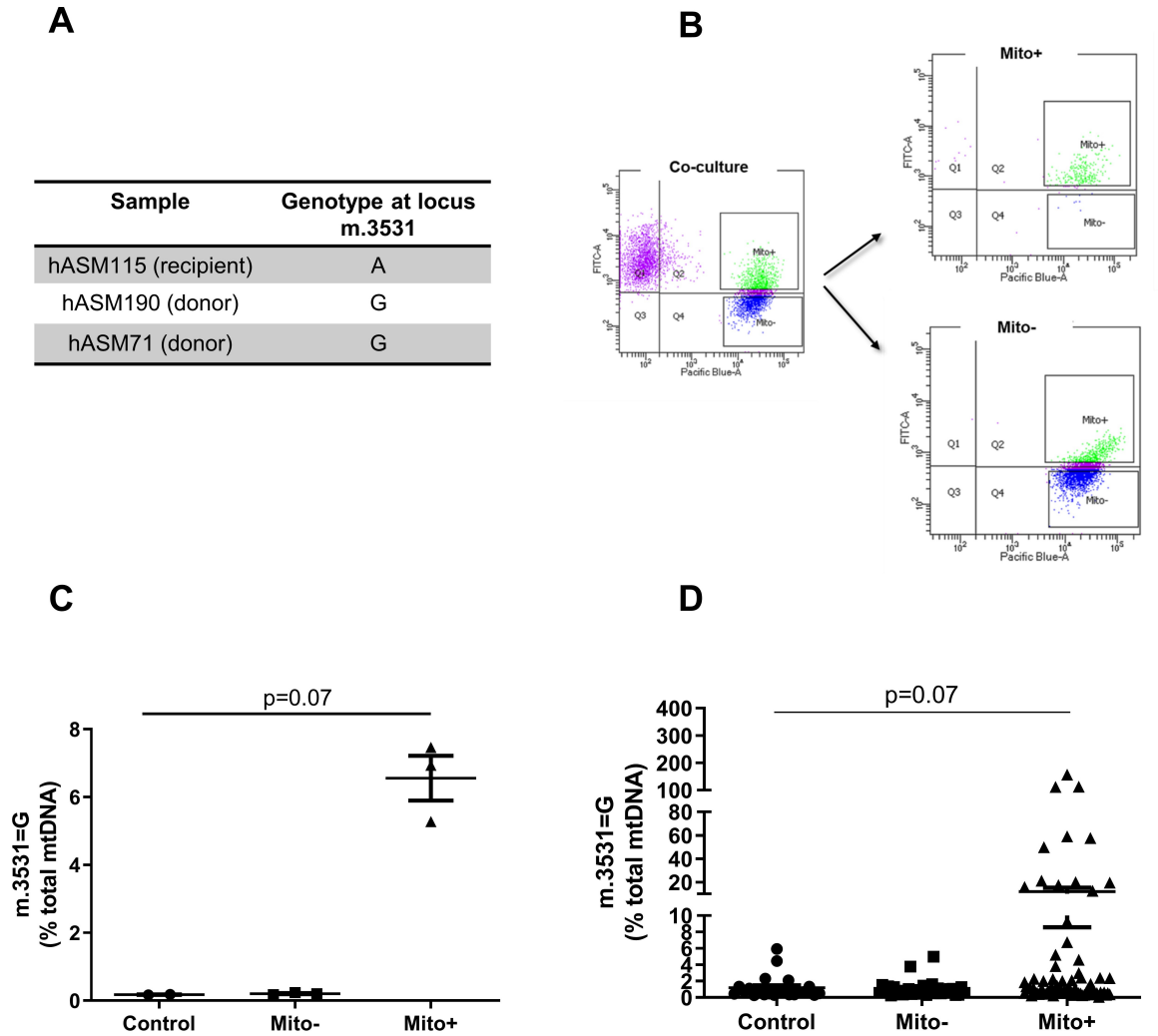

Figure 5.6: Detection of mitochondrial transfer using ARMS-qPCR. A) Genotype of mitochondrial donor and recipient ASMCs at the m.3531 loci. (B) Representative dot plots showing co-culture of MitoTracker- and CellTrace-stained ASMCs, and MitoTracker-positive and –negative CellTrace-stained cells isolated by FACS. (C-D) ARMS-qPCR quantification of the percentage of mtDNA carrying the m.3531=G mutation in (C) cells isolated in bulk and cultured for 48 hours or (D) single cells isolated immediately after isolation.

5.2.2 Cigarette smoke medium increases mitochondrial transfer in both healthy and COPD ASMCs

As shown in **Chapter 3**, ASMCs from COPD patients show mitochondrial dysfunction, which is more pronounced under conditions of stress. Therefore, I sought to investigate whether transfer of mitochondria would be different in ASMCs from COPD patients and under conditions of stress, such as upon cigarette smoke exposure. There was no difference in the ability of COPD and healthy cells to exchange mitochondria. In paired experiments, co-cultures with healthy ASMCs had 15 ± 2.5% MitoTracker-positive recipient cells, whereas this value was of 19 ± 5.7% in COPD ASMCs, with no significant difference between the groups (**Figure 5.7A**). To assess the effect of cigarette smoke, either the donor or the recipient cells were pre-treated with 10 or 25% CSM for 4 hours as in previous experiments. These were then stained and co-cultured with untreated donor or recipient cells in complete media. Whereas pre-treating recipient cells had no effect on mitochondrial transfer, pre-treatment of the donor cells with 25% CSM led to a significant increase in mitochondrial transfer in both healthy (13% ± 2.2 to 23% ± 2.3 MitoTracker-positive recipient cells, $p<0.05$) and COPD ASMCs (19.8% ± 5.1 to 30% ± 6.6 MitoTracker-positive recipient cells, $p<0.01$) (**Figure 5.7B**). This finding suggests that cellular stress may induce donation of mitochondria from ASMCs, irrespective of the cell phenotype.

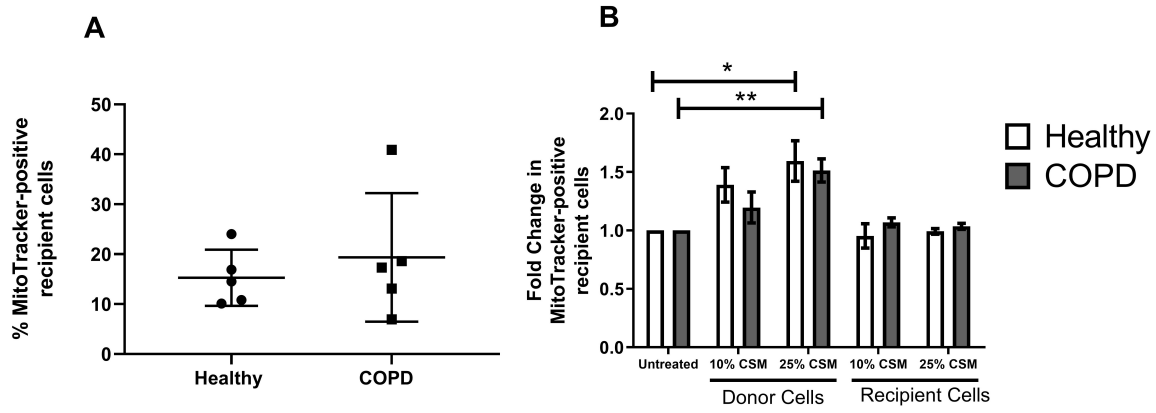

Figure 5.7: Mitochondrial transfer in ASMCs from healthy and COPD subjects in the presence or absence of cigarette smoke medium. Quantification of mitochondrial transfer by flow cytometry in: (A) untreated healthy or COPD ASMCs co-cultured for 24 hours; (B) ASMCs from healthy or COPD subjects where donor or recipient cells were pre-treated with cigarette smoke medium for 4 hours and co-cultured for 24 hours; data normalised to untreated. All data presented as mean ± SEM. Statistical analyses performed on non-normalised data. *p<0.05, **p<0.01. N=5.

Given that CSM treatment induces mitochondrial membrane depolarisation in both healthy and COPD ASMCs (**Figure 3.8A**), I hypothesised that a drop in $\Delta\psi m$ could mediate the increase in mitochondrial transfer seen in response to CSM. To further assess this, I pre-treated ASMCs from healthy subjects with CCCP to induce depolarisation and measured the effect on $\Delta\psi m$ and mitochondrial transfer. As expected, CCCP led to a ∼20% drop in $\Delta\psi m$ (**Figure 5.8A**), a response similar to that observed with CSM treatment. Interestingly, 2.5 µM but not 5 µM CCCP led to an ∼20% increase in mitochondrial transfer suggesting that at low concentrations CCCP mediates this process, but at higher concentrations it does not (**Figure 5.8B**).

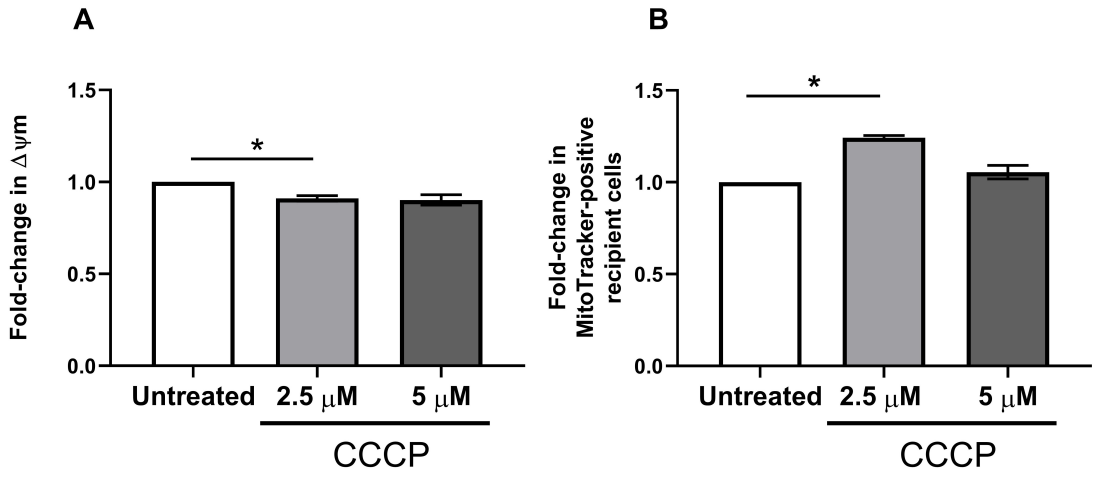

Figure 5.8: Effect of Δψm on mitochondrial transfer. Quantification of (A) Δψm and (B) mitochondrial transfer, in ASMCs from healthy patients pre-treated with CCCP (2.5 or 5μM), or left untreated, for 1 hour and then re-plated in complete media for 24 hours. Only mitochondria donor cells were pre-treated with CCCP, whereas recipient cells were kept untreated. Data normalised to untreated and presented as mean ± SEM. Statistical analyses performed on non-normalised data. *$p<0.05$. N=3-5.

5.2.3 Uptake of exogenous mitochondria modulates recipient ASMC bioenergetics and proliferation

To investigate the functional effects of mitochondrial transfer, I next examined the cellular bioenergetics and mitochondrial state of the recipient ASMCs. Given the mitochondrial dysfunction in COPD ASMCs observed in **Chapter 3**, I also assessed whether uptake of mitochondria from COPD ASMCs would elicit a different response compared to uptake from healthy ASMCs. To achieve this, I co-cultured MitoTracker-stained healthy or COPD donor cells, with CellTrace-stained healthy recipient cells. I then isolated MitoTracker-positive (Mito+) and Mito-negative (Mito-) recipient cells by FACS (**Figure 5.6B**) and assessed their cellular function 48 hours post-isolation. The process of isolating live cells by FACS can affect the function of cells, as these have to go through a 100 μm nozzle and are often kept in suspension for a few hours whilst sorting. To assess the effect of the cell sorting procedure on cellular function, single culture controls were either plated directly or FACS-sorted before plating. There was no significant difference between

the two groups in mitochondrial respiration, ROS and membrane potential, nor in cellular proliferation (**Figure 5.9A-D**). Nevertheless, for better accuracy, the FACS-sorted single cultures were used as controls in the following experiments.

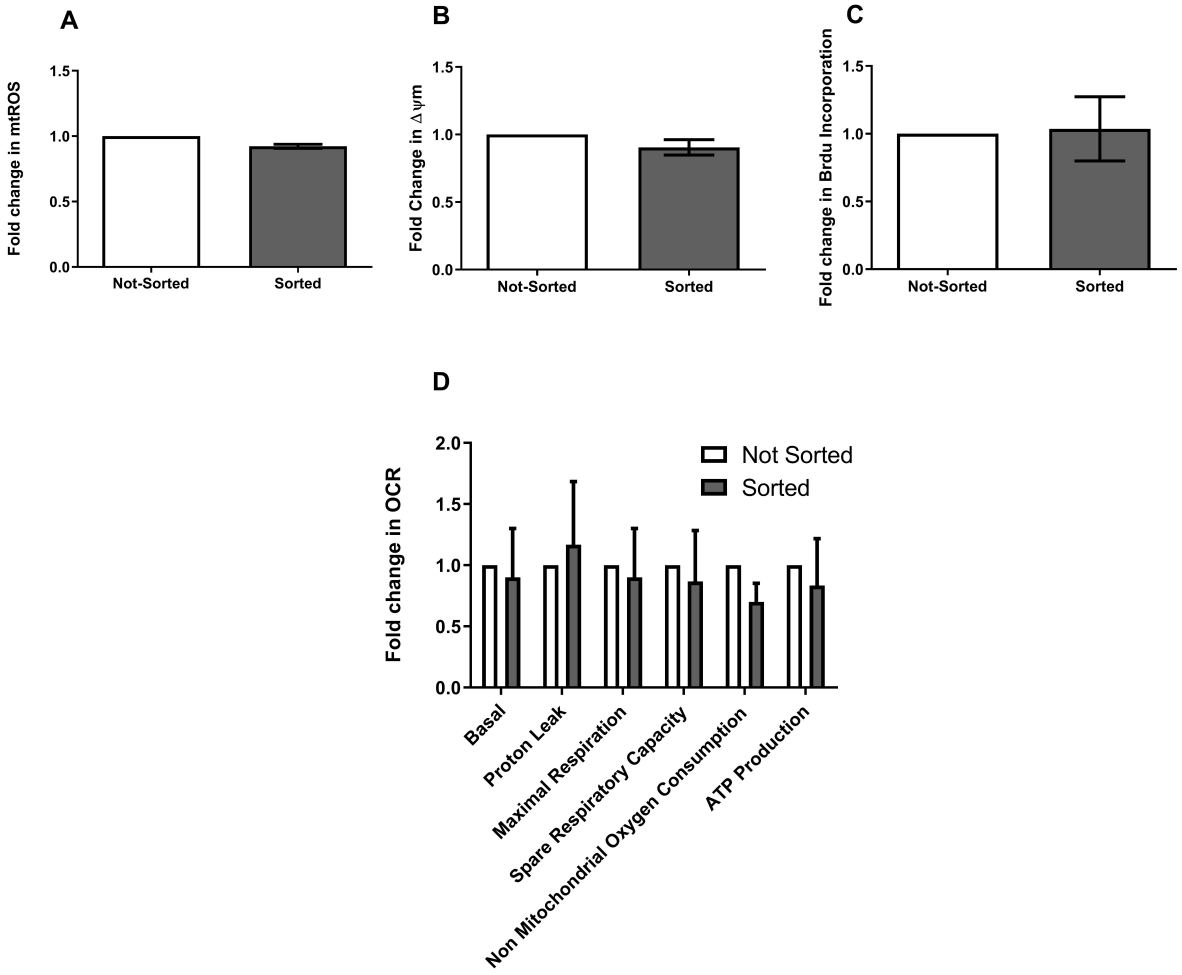

Figure 5.9: Effect of cell sorting on ASMC function. Assessment of (A) $\Delta\psi$m (B) mtROS (C) proliferation (BrdU incorporation) and (D) mitochondrial respiration, in ASMCs from healthy subjects subjected to cell sorting by FACS (sorted) or plated directly (not-sorted). After cell sorting and plating, cells were cultured for 48 hours before assays were performed. Data normalised to not-sorted controls and presented as mean ± SEM. N=3-4.

First, I assessed whether mitochondrial transfer would affect mitochondrial respiration in ASMC recipient cells. Mito+ cells showed an increased basal OCR, spare respiratory capacity, maximal and ATP-linked respiration compared to Mito- cells, irrespective of whether mitochondria were donated by healthy or COPD ASMCs (**Figure 5.10A-D**). A similar effect was observed in the mitochondrial membrane potential (∼3-fold increase in

Mito+ cells, p<0.01) whereas mtROS was increased (∼3-fold, p<0.05) in cells receiving mitochondria from healthy ASMCs only (**Figure 5.10E-F**).

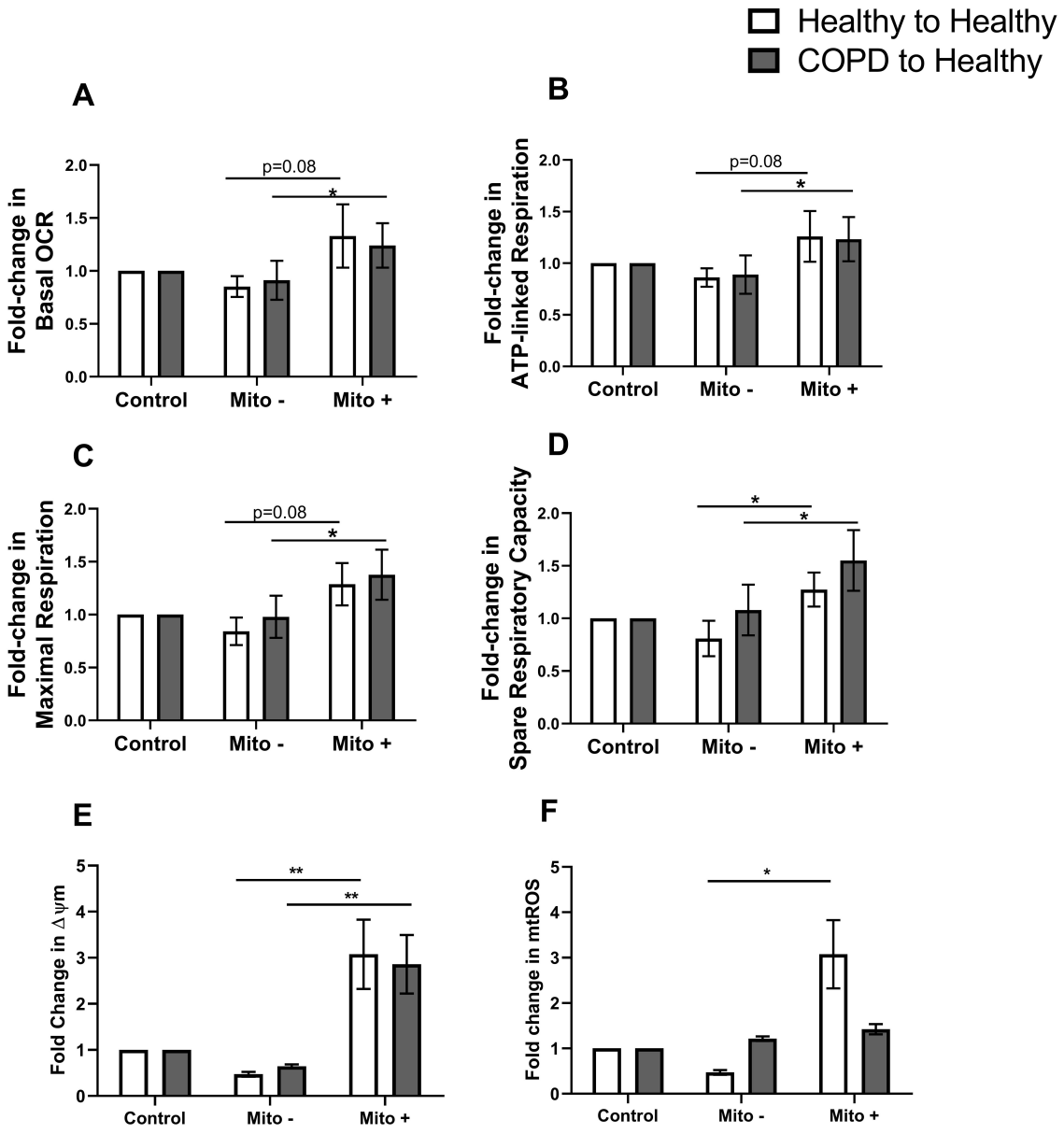

Figure 5.10: Effect of mitochondrial transfer on the bioenergetics of ASMCs. Quantification of (A) basal OCR (B) ATP-linked respiration (C) Maximal respiration (D) Spare respiratory capacity (E) mitochondrial membrane potential and (F) mtROS, in Mito+ and Mito- recipient healthy ASMCs isolated from 24-hour co-culture with MitoTracker-stained healthy or COPD donor cells. Cells were cultured for 48 hours before assays were performed. Single culture controls were also subjected to FACS sorting. Data were normalised to single culture controls and presented as mean ± SEM. Statistical analyses performed on non-normalised data.*p<0.05, **p<0.01. N=4-5, Healthy to Healthy; N=7, COPD to Healthy.

To assess whether this was a consequence of an increased mitochondrial content in Mito+ cells, I measured relative mtDNA copy number, as a surrogate for the quantity of mitochondria in cells, and found that it was increased in Mito+ cells (∼1.5-fold); however, this only reached statistical significance when mitochondria were donated by healthy cells ($p<0.05$) (**Figure 5.11C**). Expression of the biogenesis marker *PGC1-α* was also increased by ∼1.5-fold in ASMCs that received mitochondria from both healthy ($p<0.05$) and COPD ($p=0.06$) donors. Interestingly, whilst there was a trend for an increase in *PGC1-β* in cells that receive mitochondria from healthy ASMCs, this was significantly reduced when mitochondria were donated by COPD ASMCs ($p<0.05$) (**Figure 5.11A,B**).

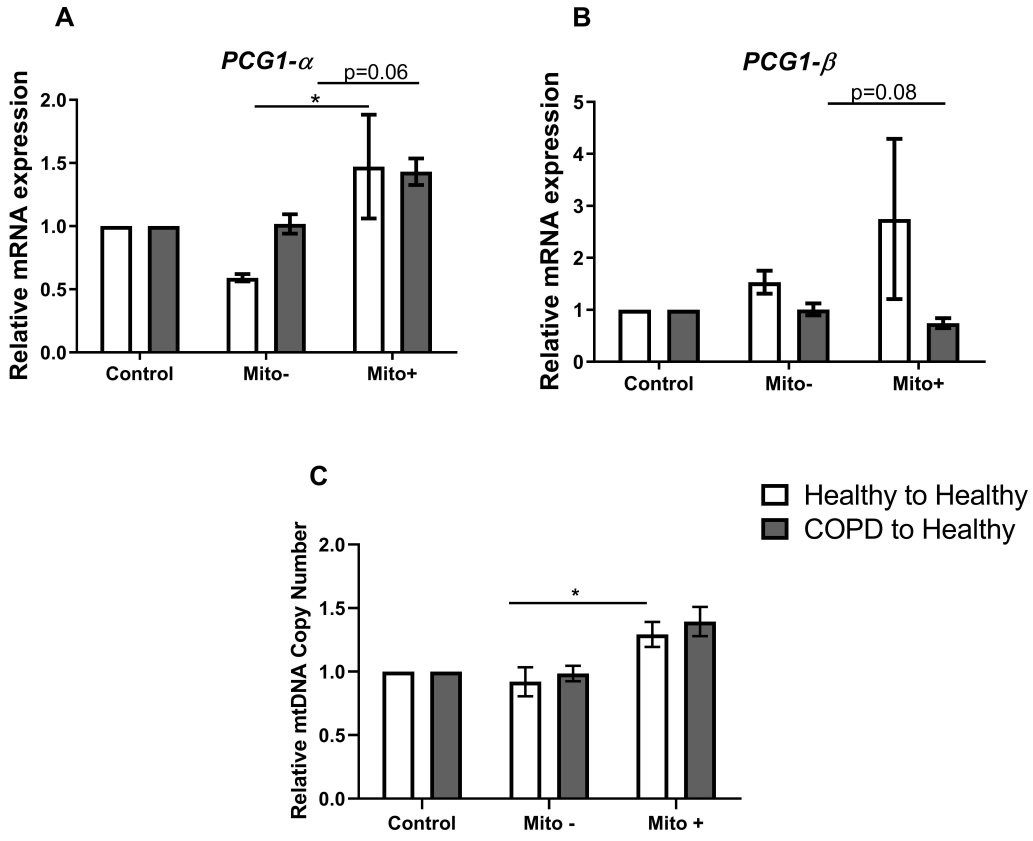

Figure 5.11: Effect of mitochondrial transfer on mitochondrial biogenesis. Measurement of relative mRNA levels of (A) *PGC1-α* or (B) *PGC1-β* and (C) relative mtDNA copy number, in Mito+ and Mito- recipient healthy ASMCs isolated from 24-hour co-culture with MitoTracker-stained healthy or COPD donor cells. Cells were cultured for 48 hours before DNA and RNA was collected. Single culture controls were also subjected to FACS sorting. Data presented as $2^{-\Delta\Delta Ct}$ relative to controls and as mean ± SEM. Statistical analyses performed on non-normalised data. *$p<0.05$. N=3-4, Healthy to Healthy; N=7, COPD to Healthy.

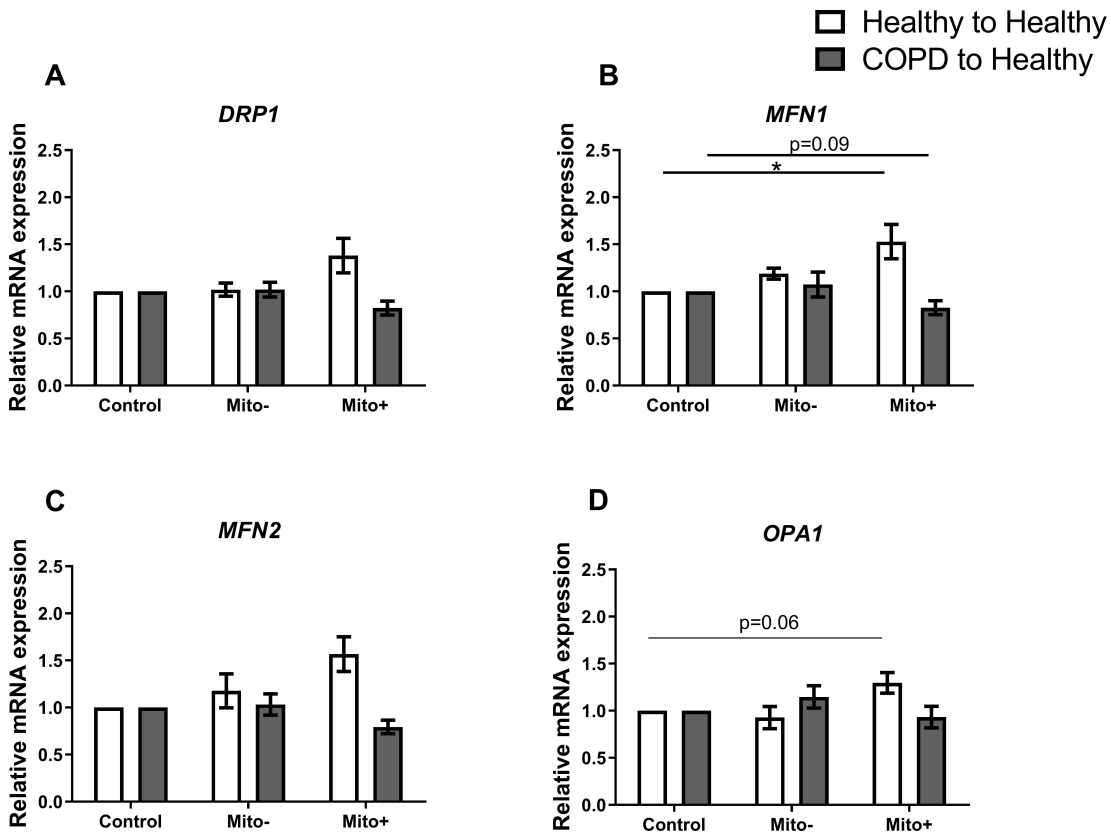

Figure 5.12: Effect of mitochondrial transfer on the expression of mitochondrial fusion and fission genes. Measurement of relative mRNA levels of (A) DRP1, (B) MFN1, (C) MFN2 and (D) OPA1 in Mito+ and Mito- recipient healthy ASMCs isolated from 24-hour co-culture with MitoTracker-stained healthy or COPD donor cells. Cells were cultured for 48 hours before RNA was collected. Single culture controls were also subjected to FACS sorting. Data presented as $2^{-\Delta\Delta Ct}$ relative to controls and as mean. ± SEM. Statistical analyses performed on non-normalised data. *p<0.05. N=3, Healthy to Healthy; N=7, COPD to Healthy.

The expression levels of different mitochondrial morphology genes were also measured in Mito+, Mito- and single culture controls. There was a significant increase in the mRNA levels of the fusion gene *MFN1* in Mito+ cells compared to control when mitochondria were donated by healthy ASMCs (∼1.5-fold, p<0.05). An opposite effect was observed when mitochondria were donated by COPD ASMCs (p=0.09). Though not significant, similar trends were present in the expression levels of other fusion genes (*MFN2* and *OPA1*), and well as, to a lesser extent, the fission gene *DRP1* (**Figure 5.12A-D**).

ASMCs are proliferative cells that respond to mitogenic stimulation [45]. I therefore assessed the effect of mitochondrial transfer on mitogenic-induced proliferation of ASMCs.

After 48 hours of stimulation with 1 ng/µl TGF-β and 2.5% FBS, Mito+ cells showed a 20% lower BrdU incorporation rate compared to Mito- cells, both when mitochondria were donated by healthy ($p<0.05$) and COPD ($p<0.05$) ASMCs (**Figure 5.13A**). At 72 hours post-stimulation, this difference was no longer significant (**Figure 5.13B**). These data indicate that mitochondrial transfer increases the mitochondrial respiration and ATP production of ASMCs, potentially due to an increase in mitochondrial mass, while reducing cellular proliferation.

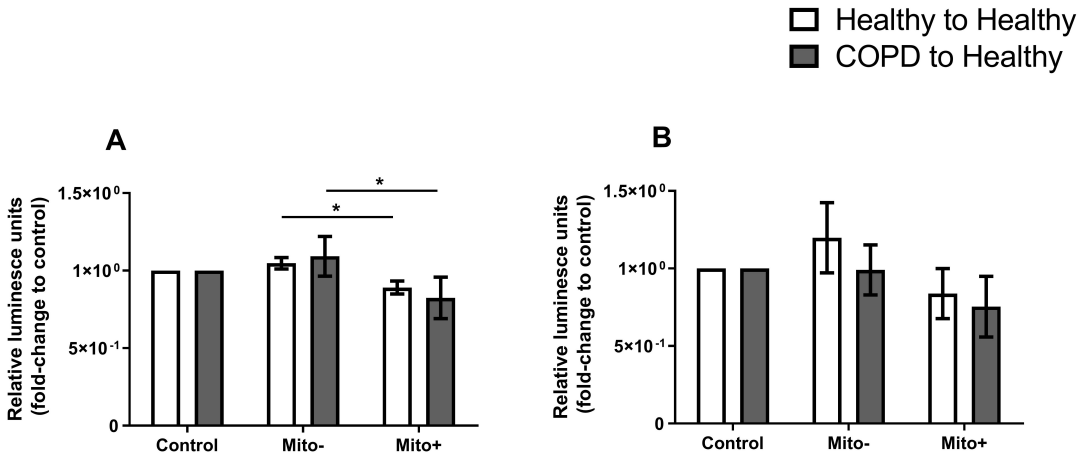

Figure 5.13: Effect of mitochondrial transfer on proliferation of ASMCs. Measurement of BrdU incorporation in Mito+ and Mito- recipient healthy ASMCs isolated from 24-hour co-culture with MitoTracker-stained healthy or COPD donor cells. Cells were serum-starved for 12 hours and stimulated with 1 ng/µl TGF-β and 2.5% FBS for (A) 48 hours and (B) 72 hours. BrdU incorporation was measured in the last 24 hours of culture. Single culture controls were also subjected to FACS sorting. Data were normalised to single culture controls and presented as mean ± SEM. Statistical analyses performed on non-normalised data. *$p<0.05$; N=3, Healthy to Healthy; N=7, COPD to Healthy.

5.3 Discussion

Transfer of mitochondria between cells is a recently described form of cell-cell communication. In this Chapter, I demonstrate that structural cells in the lung, namely ASMCs, are capable of exchanging mitochondria, and that this is a mechanism regulating mitochondrial and cellular function. However, despite an increased susceptibility to cigarette smoke-induced mitochondrial dysfunction, COPD ASMCs maintain their ability to exchange mitochondria.

ASMCs can exchange mitochondria, and this was shown using different experimental approaches. Approximately 30% of cells receive mitochondria in a co-culture, when quantified using Mitotracker dyes. These dyes have been shown to leak from cells [133], which could lead to false positive detection of mitochondrial transfer. For this reason, I performed different control experiments to ensure the signal I observed was not because of dye leakage. From these experiments, only one data-point suggested leakage may occur. This may be a result of a poor washing procedure after staining in this specific repeat, and a stringent washing procedure was performed thereafter. All other data-points indicate no leakage of the dye. Fluorescent imaging of MitoTracker-positive recipient cells shows widespread MitoTracker signal. It is possible that the MitoTracker signal spreads once mitochondria are transferred, either by fusion of mitochondria to the recipient network, or by degradation of mitochondria and release of free dye. Mitochondrial transfer was also detected using other experimental approaches, such as tracking GFP-tagged mitochondrial proteins or patient-specific mtDNA mutations. The percentage of cells receiving mitochondria as detected by these approaches was considerably lower than when using Mitotracker, which may be due to limitations of the experimental procedures. For example, the transfection efficiency of the plasmid encoding the mitochondria-targeted GFP in donor cells was only 40%, and therefore not all the mitochondria from the donor cell could be tracked. Recipient cells that received mitochondria from donor cells, isolated based on their MitoTracker fluorescence, had only 5% of donor-specific mtDNA mutation, which may indicate that the number of transferred mitochondria is low. However, when measured at the single-cell level there was a range in the percentage of donor mtDNA

detected in recipient cells, suggesting the number of transferred mitochondria is variable. This is similar to what is observed when mitochondrial transfer is detected using MitoTracker, where there is a range of MitoTracker fluorescence intensity in cells receiving mitochondria, indicating variability in the amount of transferred mitochondria. Despite the caveats for each experimental approach, together, these results confirm that ASMCs can exchange mitochondria.

Stressing the mitochondria donor, but not the recipient cells with cigarette smoke leads to an increase in mitochondrial transfer, in both healthy and COPD ASMCs. Hence, donation of mitochondria might be a stress response mechanism, induced by CSM exposure. Cigarette smoke induces mitochondrial fragmentation in healthy non-smoker ASMCs [121], which may facilitate the transport of mitochondria. In addition, as shown in **Chapter 3**, CSM depolarises mitochondria and could therefore suggest that the induction of mitochondrial transfer is mediated by damage to the mitochondria. In line with this notion, I show that mitochondrial membrane depolarisation in response to low levels of CCCP also induces donation of mitochondria. This response, however, was not observed at the higher concentration of CCCP. The reason for this unexpected finding is unclear, but it could be due to off-target effects of the compound, which at high concentrations can induce cell death [215, 216]. It is also possible that at higher concentrations, CCCP induces mitophagy instead of mitochondrial transfer. Nevertheless, this data indicates that CS-induced stress and/or mitochondrial damage triggers donation of mitochondria. It has been shown that oxidative stress, such as CS or hydrogen peroxide, increases transfer of mitochondria from MSCs to ASMCs and to acute myeloma cells [143, 148]. Moreover, mitochondria damage to the donor cell specifically, such as cardiomyocytes and adipocytes leads to an increased secretion of mitochondria-containing extracellular vesicles that are taken up by macrophages [124, 150]. In contrast, other studies have reported that improved mitochondrial function of mitochondria-donating MSCs, as a result of anti-oxidant treatment, can increase mitochondrial transfer [166]. In addition, contrary to my findings, damaging recipient cells can induce transfer of mitochondria in other models. Specifically, transfer of mitochondria from MSCs to epithelial cells increases when the latter is treated

with ETC inhibitors, such as rotenone and antimycin A [125, 135]. The specific mechanisms that underpin the induction of mitochondrial transfer are not clear. Golan and colleagues showed that mitochondrial transfer from hematopoietic stem cells to MSCs is mediated by ATP levels via activation of the purinergic receptor P2RX7 and AMPK signalling [217]. However, the signalling pathways driving mitochondrial transfer in response to stress and mitochondrial dysfunction are still elusive and may depend on many factors, including cell type, quantity and duration of stress and severity of mitochondrial damage.

Mitochondrial transfer between healthy ASMCs leads to increased mitochondrial biogenesis and respiration, associated with augmented mitochondrial membrane potential and ROS production. These findings suggest that mitochondrial transfer may have a homeostatic role, modulating mitochondrial function in recipient cells. Other studies have reported improved mitochondrial function in cells that receive mitochondria, such as increased ATP production and decreased ROS [123, 125, 130, 141, 143]. Increased mtROS production in mitochondria-recipient ASMCs appears to contradict the hypothesis that mitochondrial transfer improves mitochondrial function. However, it is not known whether the changes in mtROS are sustained as this was only measured at one time-point. In addition, whereas at high levels mtROS can cause damage, fluctuations at physiological levels are required for cellular signalling. The induction of mtROS may be a protective mechanism. For example, it may trigger a hormesis effect, as has been demonstrated in transfer of mitochondria from adipocytes to cardiomyocytes, where increased ROS generation in mitochondria-recipient cells induces anti-oxidant responses [150]. Mitochondria-recipient ASMCs also show a decrease in cellular proliferation, though this is contradictory to other studies that have reported an induction of proliferation in response to mitochondrial transfer [151, 217]. Whether this response is linked to the changes in mitochondrial function is not known. In **Chapter 4**, I showed that cells with increased $\Delta\psi m$ show decreased proliferation, and this correlation is also observed in cells that receive mitochondria. The causal link between the two should be further investigated. Nevertheless, a reduction in proliferation in response to mitochondrial transfer is an important finding as it suggests that this process could be used to modulate cellular phenotypes that contribute to air-

way remodelling in COPD, such as hyperproliferation of ASMCs [45]. In other cell types, changes in other phenotypes associated with COPD, such as apoptosis [125, 153, 158] and secretion of inflammatory mediators [130, 154] of mitochondria recipient cells have been reported. Though beyond the scope of my study, investigating the effect of mitochondrial transfer between ASMCs on these cellular mechanisms would bring further evidence to the potential of this process in modulating disease phenotypes.

I hypothesised that COPD ASMCs have impaired mitochondrial transfer, which would contribute to sustained stress-induced mitochondrial dysfunction, as observed in **Chapter 3**. However, when comparing healthy and COPD ASMCs, there was no difference in their ability to exchange mitochondria. This was contrary to what other models have reported, where mitochondrial transfer is impaired in disease. Transfer from adipocytes to macrophages is decreased in a murine obesity model [145], and MSCs from patients which rheumatoid arthritis have a lower ability to transfer mitochondria compared to healthy controls [130]. This process might differ in ASMCs from non-smoker healthy controls; unfortunately, I did not have access to these.

The effect of uptake of mitochondria in healthy ASMCs was similar regardless of whether the mitochondria were donated by healthy or COPD ASMCs: there was an increase in mitochondrial respiration, $\Delta\psi m$, mtDNA copy number and a decrease in proliferation. However, the increase in mtROS, expression of PGC1-β and fusion genes was only observed when mitochondria were donated by healthy ASMCs. Hence, mitochondria from COPD ASMCs can elicit some but not all responses associated with mitochondrial transfer, suggesting this process is somewhat altered in disease. Why this occurs is not known. It is possible that this is a result of the nature of mitochondria being transferred, as COPD ASMCs show some mitochondrial dysfunction at baseline (**Chapter 3**). Characterising the nature of transferred mitochondria would help understand these discrepancies. Apart from transfer of intact and functional mitochondria [126, 154], dysfunctional mitochondria released by damaged cells can also be taken up by neighbouring cells [124, 127, 150]. Studies have also shown that the effects of mitochondrial transfer are impaired when the donated mitochondria are damaged. MSCs are unable to revert dis-

ease phenotypes in epithelial cells (e.g. apoptosis) through mitochondrial transfer when they are pre-treated with rotenone to induce mitochondrial dysfunction [125]. The effect of uptake of MSCs mitochondria by epithelial cells (e.g. increase in alveolar ATP) is abrogated when mitochondrial function of MSCs is impaired by siRNA knockdown of the Rieske iron-sulfur protein (RISP) of complex III [123]. Interestingly, COPD cells show a lower expression of complex III compared to healthy ASMCs (**Figure 3.6**), so it is possible that this can affect the functional impact of mitochondrial transfer. One unaddressed question is whether this functional effect is also observed when COPD ASMCs take up mitochondria. Are the responses to mitochondrial transfer impaired in COPD cells? Transfer of mitochondria from MSCs to diseased cells rescues these from different pathogenic phenotypes [123, 125, 130, 143], but we do not know if this also happens in transfer between structural cells. In addition, whilst the impact of mitochondrial transfer on the recipient cell has been widely described, the effect on the donor cell is not clear. It has been shown that impairing the donation of mitochondria by cardiomyocytes, to be taken up by macrophages, leads to the accumulation of damaged mitochondria in these cells, suggesting this is also important in maintaining mitochondrial homeostasis in the donor cell [124]. What happens in other cell types is not known.

The mechanisms eliciting the functional effects observed in mitochondria-recipient cells have yet to be investigated. Increased mitochondrial membrane potential can favour mitochondrial respiration and consequent mtROS production [39], but what modulates these in response to mitochondrial transfer is not known. I demonstrated that healthy ASMCs that receive mitochondria have increased mtDNA and *PGC1-α* and *–β* expression, which suggests an increase in mitochondrial biogenesis and mass. Increased mitochondrial content might account for the augmented mitochondrial respiration observed. It could also account for the increased $\Delta\psi$m and mtROS observed, as a higher number of mitochondria would result in higher staining with the dyes used to measure these parameters. Additional experiments, such as normalisation to the quantity of mitochondria, would be required to confirm the changes in these parameters. Other studies have also shown that mitochondria-recipient cells show increased mitochondrial content and biogenesis [128,

145, 147, 217]. This could be due to incorporation of the transferred mitochondria into the host network resulting in an increase in mitochondrial mass, as has been reported in some systems [127, 146, 150]. Incorporation into the host network would require mitochondrial fusion events and ASMCs that receive mitochondria from healthy cells show increased expression of fusion genes. In contrast, studies have also reported that transferred mitochondria can be degraded in the recipient cell [124, 130, 134], in which case the increase in mitochondrial mass would not be a direct consequence of the uptake of mitochondria. Instead, the recipient cells might respond to this by increasing the biogenesis of their own mitochondrial network; the increase in *PGC1-α* and *–β* in mitochondria-recipient ASMCs suggests this is a possibility. Understanding the fate of transferred mitochondria in ASMCs might help uncover how the responses to mitochondrial transfer are elicited.

My observations cannot exclude the possibility that the detected changes in mitochondrial function and proliferation are a cause and not a consequence of mitochondrial transfer. Brestoff and colleagues showed that macrophage status can dictate their ability to take up mitochondria from adipocytes [145]. In addition, as mentioned above, other studies show that inhibiting ETC complex protein activity in recipient cells can alter the rate of mitochondrial transfer [125, 135]. Hence, mitochondrial function might affect the ability of cells to take up mitochondria. In ASMCs, it is possible that cells with an improved mitochondrial function are more prone to receiving mitochondria. However, treating ASMCs with CS, which causes damage to the mitochondria, does not affect their ability to receive mitochondria, nor is it different in COPD ASMCs, which also show mitochondrial dysfunction. This suggests that mitochondrial function does not dictate the ability of ASMCs to take up mitochondria, as would be the case if the phenotype of mitochondria-recipient cells was a "cause" of mitochondrial transfer. In addition, the function of mitochondria-recipient cells differed when mitochondria were transferred from COPD ASMCs instead of healthy ASMCs, suggesting that these phenotypes are dependent on the origin of mitochondria.

The results from my study suggest that transfer of mitochondria between ASMCs is important in maintaining bioenergetic homeostasis in the airways. This process might also

occur in other cell types in the lungs. Ahmad and colleagues showed that, in addition to MSCs, ASMCs and fibroblasts can also transfer their mitochondria to lung epithelial cells [125]. Several studies have also reported the uptake of mitochondria from different cell types by macrophages [124, 127, 145]. In the lungs, neutrophils can take up mitochondria from epithelial cells [161]. The role of this cell-cell communication in maintaining lung health and whether its impairment is associated to the development of disease should be investigated.

In summary, ASMCs are capable of exchanging mitochondria and this leads to improved bioenergetics and a decrease of cellular proliferation. This process may be a stress response mechanism, as it is induced by CS and damage to the mitochondria. It is possible that mitochondrial transfer acts as a quality control mechanism and participates in the reversal of mitochondrial and cellular dysfunction induced by CS. However, this process was not significantly impaired in COPD, as hypothesised, and hence might not be involved in increased susceptibility to CS-induced mitochondrial dysfunction. Nevertheless, mitochondrial transfer appears to be an important cell-cell communication mechanism and could still be exploited as an endogenous mechanism to reverse mitochondrial dysfunction and hyperproliferation present in COPD. Elucidating the mechanisms of mitochondrial transfer is essential to understand how this process can be modulated, and this is explored in the following Chapter.

Chapter 6

Mechanisms of mitochondrial transfer between ASMCs

6.1 Introduction

Mitochondrial transfer between cells is a form of cell-cell communication that regulates mitochondrial and cellular homeostasis. In **Chapter 5**, I have shown that structural cells in the lung, from both healthy and COPD subjects, can exchange mitochondria and this leads to improved bioenergetics and reduced proliferation. Therefore, this process could be exploited to reverse COPD disease phenotypes such as mitochondrial dysfunction and hyperproliferation. One approach could be to modulate mitochondrial transfer by, for example, further inducing this process in the airways of patients with COPD. In order to achieve this, it is important to understand how mitochondrial transfer occurs.

Different mechanisms of mitochondrial transfer have been described. Tunnelling nanotubes are a type of cellular protrusions formed by microtubules or actin filaments that temporarily join two cells [153, 156, 157]. Amongst other cargoes, mitochondria are transported along TNTs from one cell to another. TNTs mediate mitochondrial transfer from MSCs to epithelial [125, 135, 214, 218], acute myeloid lymphoma [148], endothelial [219] and ASM cells [143], between pheochromocytoma 12 cells [153], and from cardiac myofibroblasts to cardiomyocytes [158]. Another frequently described mechanism of mitochondrial transfer are extracellular vesicles. These have been shown to mediate transfer of mitochondria from MSCs [127] and neural stem cells [146] to macrophages, from adipocytes to cardiomyocytes [150], from astrocytes to neurons [126], and from

MSCs to cardiomyocytes, epithelial and endothelial cells [128, 213]. The nature of the mitochondria-carrying EVs is less clear. The typical size of exosomes (40-100 nm) is unlikely to allow for the transport of intact mitochondria, which normally exceed the size of 100 nm [220, 221]. However, studies have reported the presence of exosomal markers such as ALIX, TSG101, and CD63 in mitochondria-carrying EVs [146, 150, 160], suggesting that either the exosomes are larger or the mitochondria are smaller than the typical size. Indeed, Crewe *et al* showed that mitochondria-derived vesicles as opposed to intact mitochondria are packaged in exosomes [150], while other studies reported that the exosomes carrying mitochondria are large in size (0.04 to 1 µm) [146]. Microvesicles are typically larger in size (0.1 to 1 µm) and EVs with microvesicle markers, such as caveolin-1 and β-integrin, have been shown to carry mitochondria [126, 161]. In addition to TNTs and EVs, other mechanisms of mitochondrial transfer have also been described, such as extracellular free mitochondria [132, 146, 162], exospheres [124], gap junctions [123] and ring canals [129].

Mechanisms of intracellular mitochondrial dynamics, such as movement and morphology, may also be required for inter-cellular mitochondrial transfer. For example, blocking microtubule-based transport of mitochondria, by inhibiting microtubule formation or reducing the expression of proteins that participate in this process, such as MIRO1 and KIF5B, abrogates TNT-mediated transfer [125, 158].

The purpose of this Chapter is to characterise the mechanisms of mitochondrial transfer between ASMCs. The aims are to:

- Determine the participation of TNTs and extracellular vesicles in mitochondrial transfer between ASMCs
- Assess the role of genes and proteins that participate in mitochondrial movement and morphology in the transfer of mitochondria between ASMCs

6.2 Results

6.2.1 Extracellular vesicles mediate transfer of mitochondria between ASMCs

Mitochondrial transfer has been shown to occur through TNTs and EVs. In ASMCs, mitochondria were detected in both these structures, as shown in **Figure 6.1A**. Live-imaging microscopy also showed mitochondria in EV-like structures and moving along TNTs (data not shown). To further assess this, I treated co-cultures of Mitotracker-stained and Celltrace-stained ASMCs with a dynamin-dependent endocytosis inhibitor (dynasore) to inhibit EV-mediated transfer, and a microtubule (nocodazole) or an actin (cytochalasin B) inhibitor to prevent TNT-mediated transfer. After 4 hours of treatment, mitochondrial transfer was significantly inhibited by 70 and 100 µM dynasore but did not change in response to nocodazole and cytochalasin B (**Figure 6.1B**).

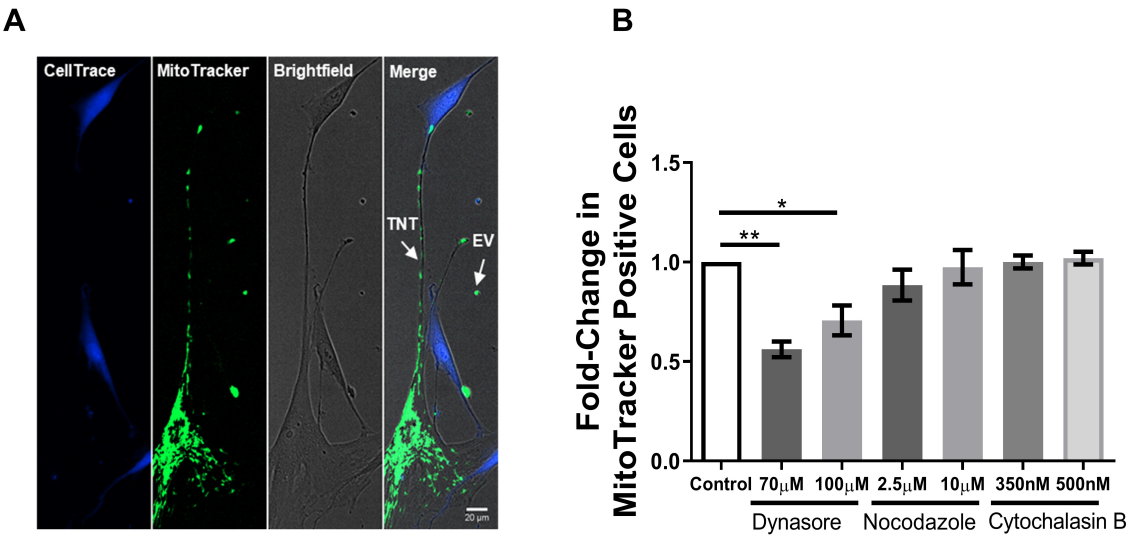

Figure 6.1: Mitochondria are found within TNTs and EVs. (A) Fluorescent microscopy of co-cultures of MitoTracker- and CellTrace-stained healthy ASMCs showing the presence of mitochondria in TNTs and EVs. N=1. (B) Quantification of mitochondrial transfer in co-cultures treated with different concentrations of dynasore, nocodazole or cytochalasin B for 4 hours. Data presented as mean ± SEM, normalised to untreated controls. Statistical analyses performed on non-normalised data. *p<0.05, **p<0.01. N=5.

Visually, nocodazole abrogated the formation of TNTs whereas cytochalasin B had no visible effect on TNT formation (data not shown). Inhibition of dynamin-mediated endocytosis by dynasore suggests that EVs may mediate transfer between ASMCs. However, dynasore also inhibits the mitochondrial dynamin DRP1 [222], so it is possible that the inhibition of mitochondrial transfer by dynasore is due to inhibition of DRP1-mediated mitochondrial fission. Therefore, the role of EVs in mitochondrial transfer was further assessed using alternative approaches.

Extracellular vesicles were isolated from the conditioned media (CdM) of healthy ASMCs by differential centrifugation for a size-dependent separation. Dead cells and apoptotic bodies were pelleted in initial centrifugations of 300g for 5 minutes and 3,000g for 10 minutes, respectively. A 20,000g centrifugation for 30 minutes was used to pellet microvesicles, and exosomes were pelleted using a further 100,000g centrifugation for 2 hours. To assess the composition of the pellets, two extracellular vesicle markers were used – ALIX and calnexin. ALIX is an endosomal sorting complexes required for transport (ESCRT) protein and participates in endosomal pathways through which exosomes are formed. Calnexin is an endoplasmic reticulum marker and should not be present in EVs of exosomal origin but can be present in in larger vesicles, such as microvesicles [223]. As expected, calnexin was not detected in the 100,000g pellet but was detected in all the other pellets. Moreover, the exosomal marker ALIX was strongly expressed in the 100,000g pellet and to a lesser extent in the 20,000g pellet, whilst it was absent in the 3,000g pellet (**Figure 6.2A**). These findings suggest that the 100,000g pellet is likely to contain exosomes, as expected, whereas the other fractions contain larger EVs, which may be apoptotic bodies or microvesicles, though exosomes may also be present in the 20,000g pellet. The presence of other EV markers, such as CD9 and CD40, was also assessed, but no protein bands were detected by western blot, likely as a result of low expression and/or poor antibody quality (data not shown). To evaluate whether the isolated vesicles contain mitochondria, I assessed the presence of mitochondrial proteins in the different fractions. I detected complex V (ATP synthase) in all fractions. The other mitochondrial proteins measured (complexes I-IV of the ETC and TOM20) were only

detected in the 300g and the 20,000g pellet, and at low levels in the 3,000g pellet. These were not detected in the exosome fraction (100,000g), suggesting these do not carry intact mitochondria. Therefore, no further experiments were performed using this fraction.

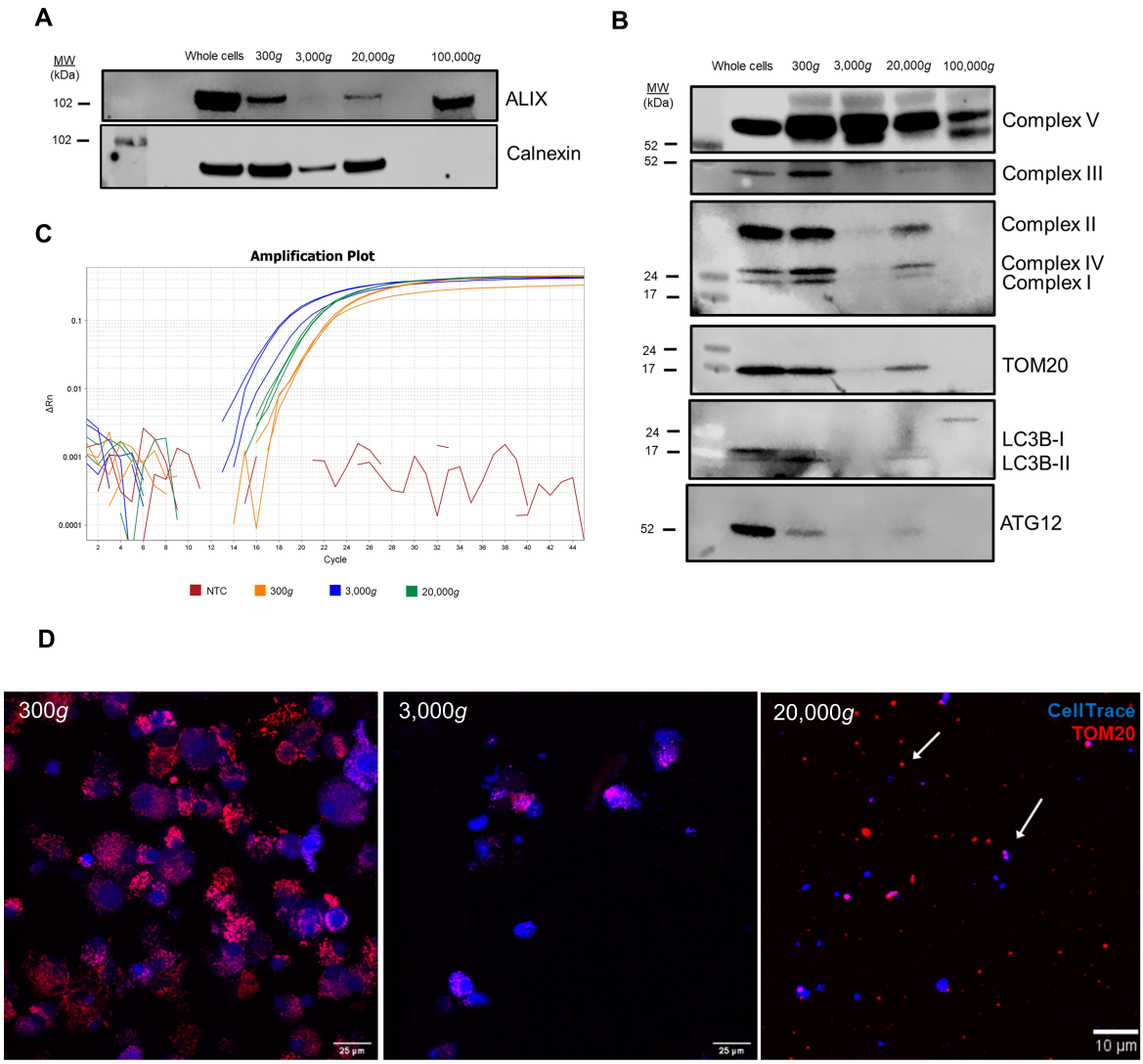

Figure 6.2: Presence of mitochondria in EVs from ASMCs. (A) EV markers in pellets obtained by differential centrifugation (B) Detection of mitochondrial and autophagy-related proteins in pellets isolated by differential centrifugation. (C) qPCR amplification plot for the *MT-CO2* mitochondrial gene in DNA extracts from pellets obtained by differential centrifugation. (D) Representative fluorescence microscopy image of EVs collected from Celltrace-stained cells and probed for TOM20; white arrows show mitochondria within EVs or free mitochondria. EVs were isolated from conditioned media of 1.5 million cells cultured for 24 hours. N=1.

Immunoblotting also revealed the presence of autophagy-related proteins such as LC3B-II and ATG-12 in the 300g and the 20,000g pellet, suggesting these may be targeted to degradation through autophagy-like pathways (**Figure 6.2B**). I investigated the presence of mtDNA in the 300g, 3,000g and 20,000g fractions by assessing amplification of the mitochondrial gene *MT-CO2* by qPCR. Whereas no amplification was detected in the no template control (NTC), *MT-CO2* was amplified in all the samples, indicating the presence of mtDNA (**Figure 6.2C**). To visualise the presence of mitochondria in the 300g, 3,000g and 20,000g pellet, these were also imaged by confocal microscopy. EVs collected from CellTrace-stained cells were loaded onto a microscope slide and probed for TOM20 using immunofluorescence. As expected, the size of the EVs decreased with higher speeds of centrifugation, confirming an efficient size separation. In the 300g and 3,000g pellets, EVs were large and their appearance suggested that these may be cell debris or large apoptotic bodies. The 20,000g centrifugation pelleted smaller sized vesicles. TOM20 (red) was detected in all the pellets, indicating the presence of mitochondria. Interestingly, in the 20,000g pellet, both EV-encapsulated and free mitochondria (not within EVs) were observed (white arrows in **Figure 6.2D**). Together, these data indicate that different sized pellets contain mitochondria.

I then investigated whether the mitochondria-containing EVs could be taken up by other cells, thus mediating mitochondrial transfer. I assessed this using the EVs isolated in the 20,000g pellet only as they were positive for all mitochondrial proteins and they likely contain microvesicles, which have been shown to transport mitochondria between cells in other systems [123, 127]. Uptake of mitochondria via EVs was assessed using three different approaches. Firstly, EVs isolated from cells stained with MitoTracker and CellTrace were added onto unstained cells for 4 hours. These cells were then collected and uptake of the mitochondria-containing vesicles was measured by flow cytometry. As seen in **Figure 6.3A**, a proportion of the EV-treated cells were positive for CellTrace (0.77% of cells in quadrant 3) or CellTrace and MitoTracker (0.30% cells in quadrant 4), indicating uptake of EVs and mitochondria-containing EVs, respectively. However, the percentage of cells taking up mitochondria-containing EVs was low, especially in comparison to the

amount of mitochondrial transfer detected in previous co-culture experiments (∼30%, **Figure 5.1C**). To exclude the possibility that the detected fluorescence was not a result of background noise, nor dye leakage, the isolated pellets used to treat cells were filtered using a 0.2 µm filter to remove EVs. Here, the percentage of MitoTracker and/or CellTrace-positive cells was markedly reduced, suggesting EVs are required for fluorescence to be detected in unstained treated cells (**Figure 6.3A**). It is possible that the sensitivity of the flow cytometer is not sufficient to detect the uptake of small quantities of EVs, or that the fluorescence of EVs is lost in the process of differential centrifugation.

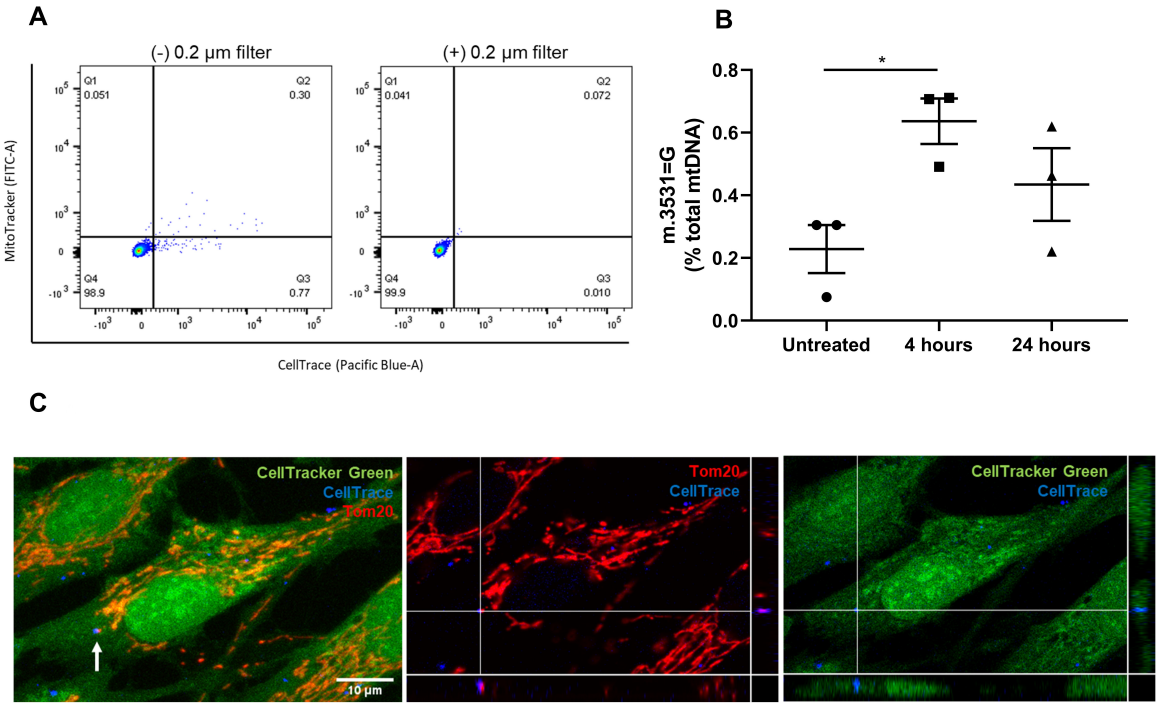

Figure 6.3: Mitochondria are transported between healthy ASMCs through EVs. (A) Flow cytometry dot plots of unstained cells treated with EVs isolated from CellTrace- and Mitotracker-stained cells, ± 0.2 µm filtration, for 4 hours . N=1. (B) Percentage of mtDNA positive for the mitochondrial donor-specific variant (m.3531=G) in cells that do not carry this variant treated with EVs from donor ASMCs for 4 and 24 hours. *$p<0.05$. N=3. (C) Representative confocal microscopy image of CellTracker Green-stained cells treated with EVs isolated from CellTrace-stained cells for 4 hours and then probed with a fluorescent anti-TOM20 antibody (maximal intensity Z-stack projection with orthogonal views). N=1. For all experiments, EVs were isolated from conditioned media of 1.5 million cells cultured for 24 hours, using a 20,000g centrifugation.

Using a different approach, EVs were isolated from ASMCs bearing a specific mtDNA mutation (m.3531=G) and added onto ASMCs from three different patients that do not carry this mutation. The percentage of the mtDNA bearing the donor-specific mutation increased from 0.2% in untreated cells to 0.6% in EV-treated cells. Though this change was low in amplitude, it was statistically significant, indicating uptake of mtDNA via EVs. Interestingly, after 24 hours the levels of the mutation appear to decrease and, though this was not significant, it indicates that EVs may be degraded in the recipient cells (**Figure 6.3B**). Finally, EV-mediated mitochondrial transfer was also visualised by confocal microscopy. In this experiment, CellTracker Green-stained cells were treated with EVs isolated from CellTrace-stained cells for 4 hours. Mitochondria were visualised by immunostaining with TOM20. CellTrace-stained EVs containing mitochondria were detected within CellTracker Green-stained cells, as shown in the orthogonal views in **Figure 6.3C**.

6.2.2 Effect of CSM on the expression of mitochondrial movement and morphology genes in ASMCs

Next, I investigated whether genes associated to mitochondrial movement and morphology may participate in mitochondrial transfer between ASMCs. As shown in **Chapter 5**, cigarette smoke treatment significantly increases the donation of mitochondria to other cells. Therefore, to assess the involvement of mitochondrial dynamic genes in mitochondrial transfer, I measured how the expression of these was altered in response to CSM. ASMCs from healthy subjects were treated with CSM for 4 hours and RNA was collected either immediately after treatment or after 24 hours of culture in serum-free media. I measured the mRNA levels of genes involved in intracellular mitochondrial movement through microtubules, namely *KIF5B*, *KIF1A*, *MIRO1*, *MIRO2*, *TRAK1*, *TRAK2* and Dynein cytoplasmic 1 heavy chain 1 (*DYNC1H1*), or through actin filaments, *MYO19* [97] (**Figure 6.4**). Of these, CSM treatment only affected the expression of *MIRO1*: at 24-hours post-treatment there was a significant increase in the mRNA levels of this gene ($\sim$1.3-fold, $p<0.05$) (**Figure 6.4D**).

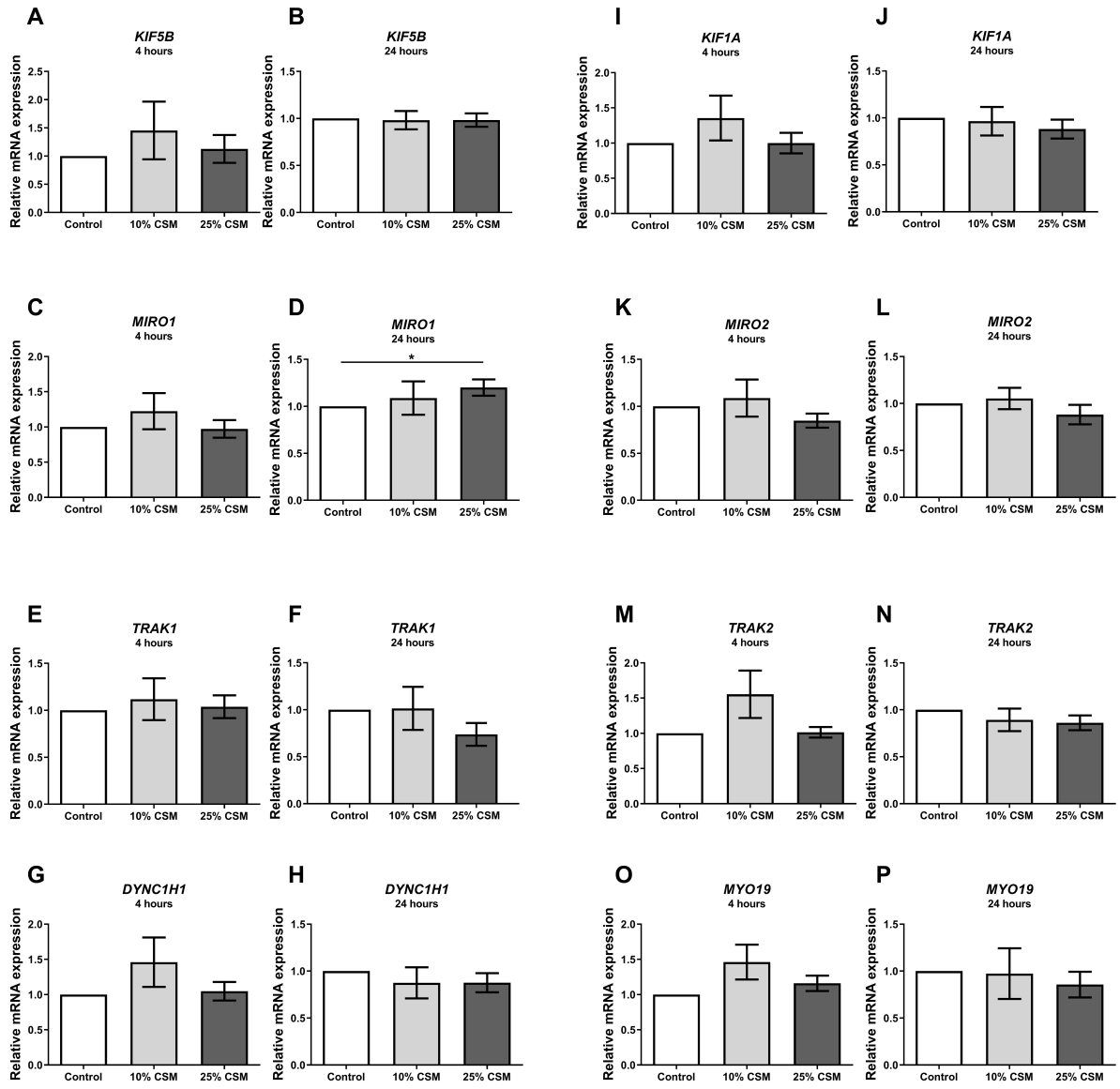

Figure 6.4: Effect of CSM on the expression of mitochondrial transport genes. Relative mRNA levels of mitochondrial transport genes in ASMCs from healthy subjects treated with 10 or 25% CSM for 4 hours. RNA was collected immediately after treatment or 24 hours after culture in serum-free media. Data presented as mean $2^{-\Delta\Delta Ct}$ relative to controls ± SEM. *p<0.05. N=6.

Cigarette smoke has been shown to modulate fusion and fission in ASMCs [121], and these processes may be important in mitochondrial transfer. I therefore investigated the effect of cigarette smoke on the expression of the fission gene *DRP1* and the fusion genes *MFN1*, *MFN2* and *OPA1*. Whilst no effect was seen on the expression of *MFN1*, *MFN2* and *OPA1*, at 4 hours post-treatment there was a trend towards a reduction in the expression of *DRP1* (**Figure 6.5**). This effect was, however, lost after 24 hours.

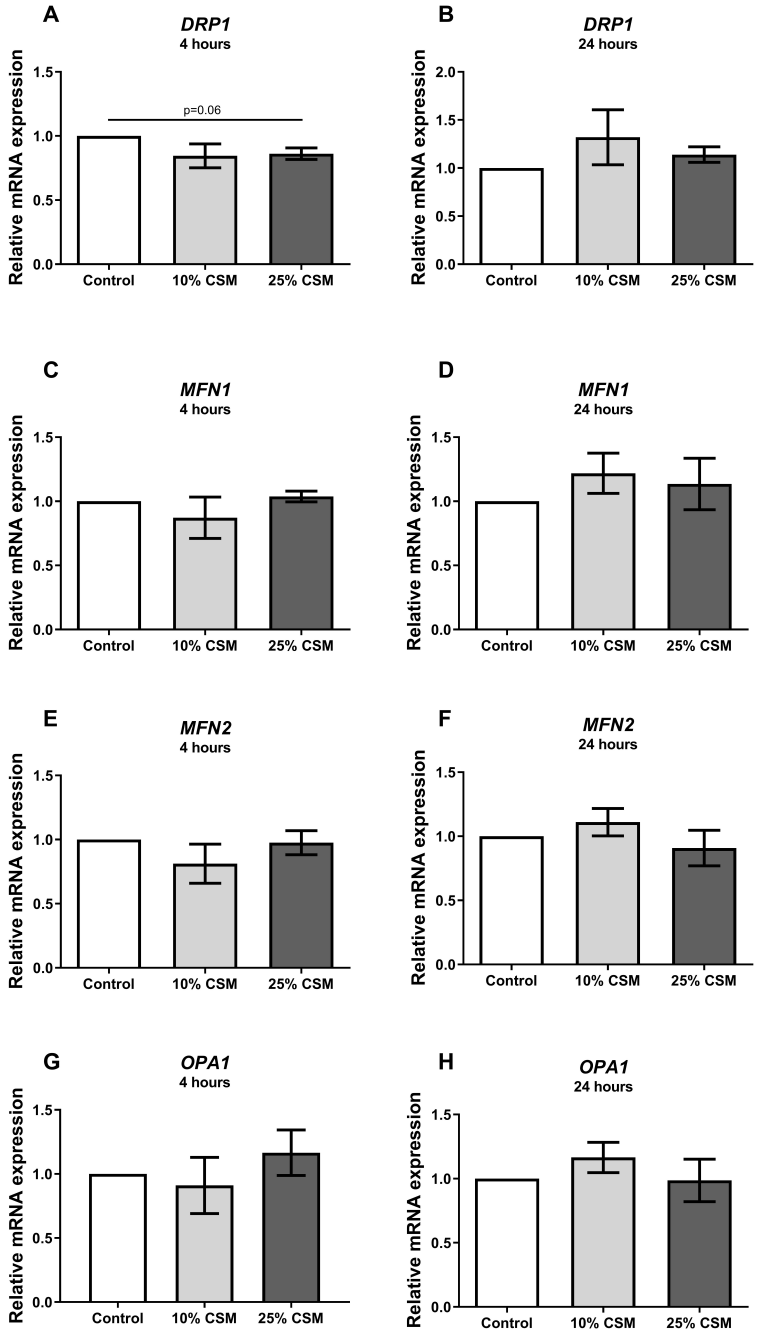

Figure 6.5: Effect of CSM on the expression of mitochondrial fusion and fission genes. Relative mRNA levels of genes in ASMCs from healthy subjects treated with 10 or 25% CSM for 4 hours. RNA was collected immediately after treatment or 24 hours culture in serum-free media. Data presented as mean $2^{-\Delta\Delta Ct}$ relative to controls ± SEM. N=6.

6.2.3 MIRO1 does not participate in mitochondrial transfer between ASMCs

Given the effect of CSM treatment on the expression of *MIRO1*, which is known to be involved in inter-cellular mitochondrial transfer [125, 141], I assessed whether depletion of this protein had an effect on mitochondrial transfer between ASMCs. I first evaluated the optimal conditions (time-point and siRNA concentration) for an effective knock-down of MIRO1 in healthy ASMCs. This was assessed by quantifying the mRNA and protein levels of MIRO1 in cells transfected with MIRO1 siRNA as well as in cells transfected with a scramble siRNA, a mock control (i.e. transfection without RNA) and an untransfected control. At 24 hours post-transfection there was a ∼60% reduction of *MIRO1* mRNA levels in cells transfected with MIRO1 siRNA at different concentrations (10, 20 and 50 nM) compared to untransfected controls, though the expression of *MIRO1* increased in the mock and scramble siRNA controls (**Figure 6.6A**). At 48 hours post-transfection, *MIRO1* mRNA levels were reduced by ∼80% in cells transfected with MIRO1 siRNA at different concentrations compared to all three controls (**Figure 6.6B**). Protein levels were reduced in the MIRO1 siRNA-transfected cells compared to the controls at 72 hours post-transfection, whereas at 48 hours this effect was less noticeable (**Figure 6.6C-E**). An ∼80% reduction was observed in all three concentrations of MIRO1 siRNA (10, 20 and 50nM) compared to untransfected controls at 72 hours post-transfection. The protein expression of MIRO1 was also reduced in the mock and scramble siRNA controls, indicating that the experimental procedure can affect MIRO1 protein levels (**Figure 6.6E**). Based on these results, I opted for using the 10nM concentration of MIRO1 siRNA for further experiments, using the same concentration of scramble siRNA as a control.

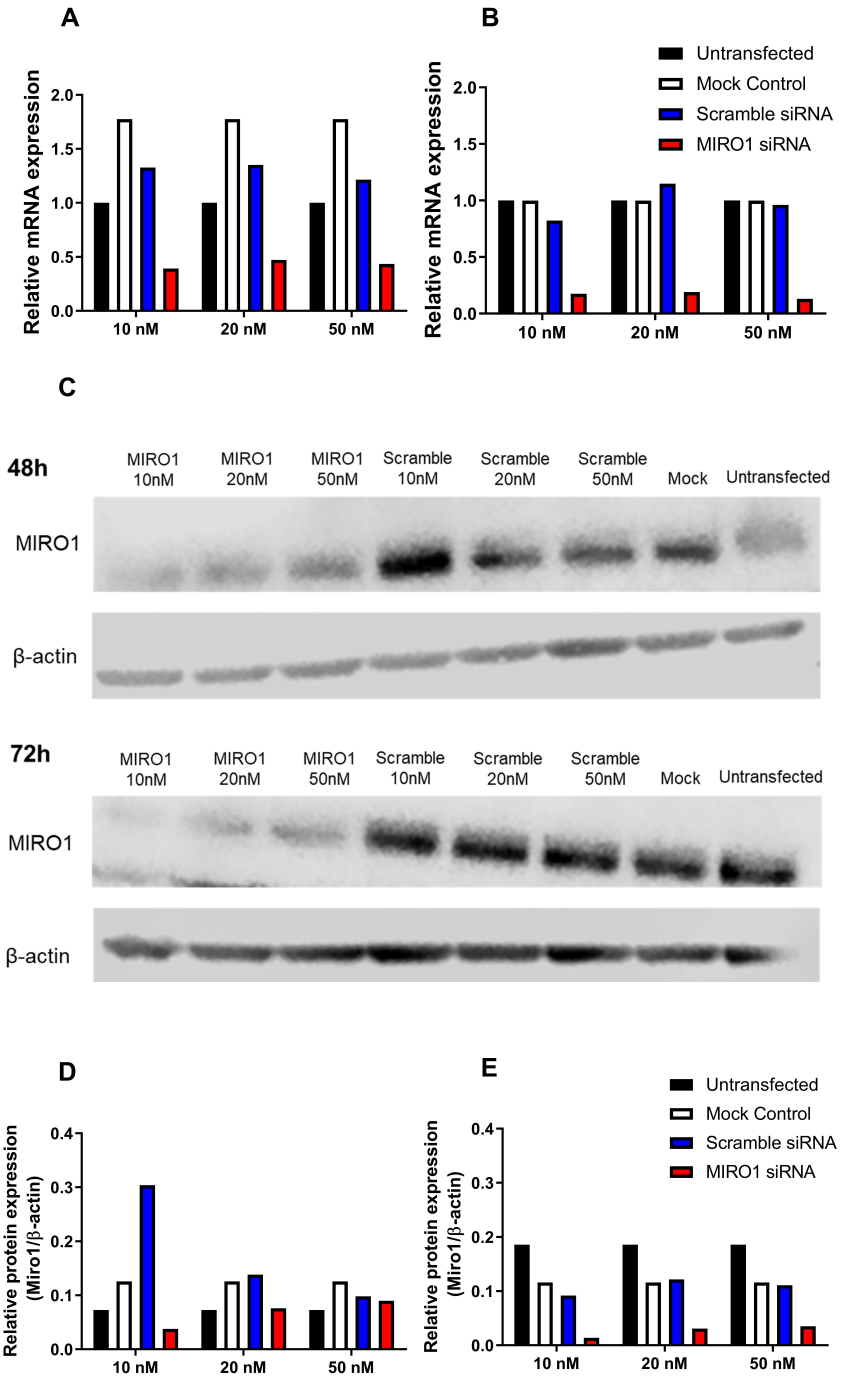

Figure 6.6: Optimization of MIRO1 knock-down by siRNA. Relative MIRO1 (A-B) mRNA and (C-E) protein levels in ASMCs from healthy subjects transfected with MIRO1 siRNA, or appropriate controls, at different concentrations. Gene expression levels of *MIRO1* were measured by qPCR (A) 24 and (B) 48 hours post-transfection. Data presented as $2^{-\Delta\Delta Ct}$ relative to controls. Relative protein expression of MIRO1 was measured (D) 48 and (E) 72 hours post-transfection and was normalised to β-actin. N=1.

Cells were transfected with MIRO1 siRNA for 48 or 72 hours, after which they were stained with MitoTracker Green and co-cultured with untransfected CellTrace-stained cells, or vice-versa. This would provide information as to whether mitochondrial transfer requires the expression of MIRO1 in either mitochondrial donor or recipient cells. There was no significant difference in the percentage of MitoTracker-positive recipient cells in co-cultures where MIRO1 was depleted (in either the donor or the recipient cells), compared to controls transfected with scramble siRNA **Figure 6.7**. This suggests that MIRO1 may not be involved in mitochondrial transfer between ASMCs.

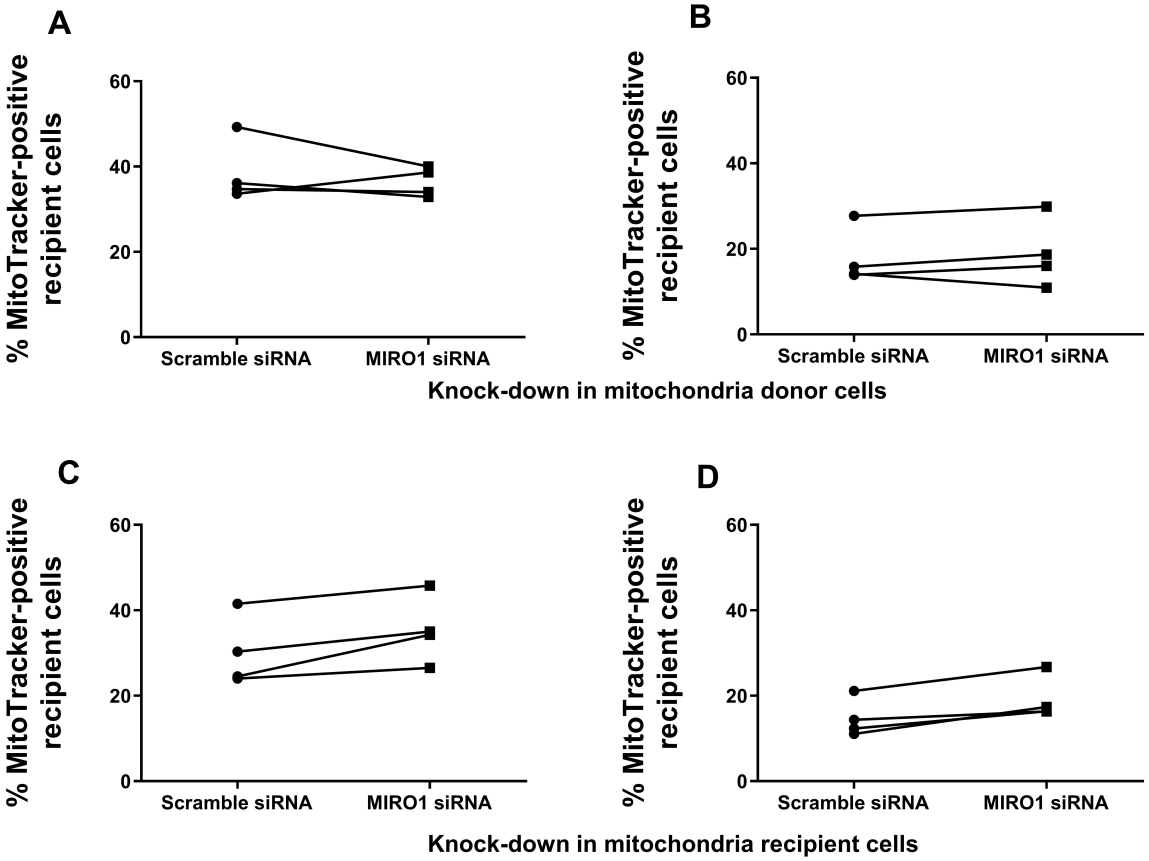

Figure 6.7: Effect of MIRO1 knockdown on mitochondrial transfer. Percentage of MitoTracker-positive recipient cells in co-cultures of MitoTracker- and CellTrace-stained healthy ASMCs, where either the (A, B) donor or the (C, D) recipient cells were transfected with 10 nM scramble or MIRO1 siRNA. Transfection was performed (A, C) 48 or (B,D) 72 hours before co-culture. N=4.

6.3 Discussion

ASMCs from both healthy and COPD subjects can exchange mitochondria, and this is associated with improved bioenergetics and reduced proliferation. In this Chapter, I demonstrate that this happens, at least partly, through extracellular vesicles. However, the molecular machinery that mediates the inter-cellular exchange of mitochondria remains unknown.

The most commonly reported mechanisms of mitochondrial transfer are TNTs and EVs. In ASMCs, mitochondria were frequently observed in TNTs, however, actin and microtubule inhibitors failed to inhibit mitochondrial transfer. The actin inhibitor, cytochalasin B, had no visible effect on TNT formation, which may indicate that the concentrations used were not sufficient, or that actin does not participate in TNT formation. On the other hand, nocodazole, a microtubule inhibitor, abrogated TNTs but did not attenuate mitochondrial transfer, indicating that TNTs may not be involved in this process. A possible explanation is that the induction of compensatory mechanisms, such as increased transfer through EVs or cell-cell adhesion, may compensate for the loss of TNTs. Alternatively, the localisation of mitochondria in TNTs may serve another purpose. Depletion of ATP impairs TNT-mediated cargo transfer between rat kidney cells [224], so it is possible that mitochondria are required in TNTs to power the transport of other cargo. Another important point is that despite numerous studies reporting TNT-mediated mitochondrial transfer [125, 157, 225] it is still not clear whether these structures form *in vivo*. A few studies have reported TNTs *in vivo* in mice, in the cornea and in brain tumours [164, 226], but whether the *in vitro* observations of TNT-mediated mitochondrial transfer can be replicated *in vivo* is not known.

The dynamin inhibitor dynasore, which inhibits endocytosis and vesicular trafficking, led to a decrease in mitochondrial transfer. Despite other non-specific effects of dynasore, such as inhibition of the mitochondrial dynamin DRP1 [222], this suggested a role for EVs in mitochondrial transfer, which was confirmed using different approaches. EVs are an important form of cell-cell communication in both health and disease. On the one hand, EVs can contribute to disease propagation. For example, microvesicles from murine BALF

and epithelial cells, secreted in response to hyperoxia-induced oxidative stress, lead to the activation of macrophages *in vitro* and promotes the recruitment of immunomodulatory cells in mice [227], contributing to pro-inflammatory responses. BALF from patients with COPD contains neutrophil-derived exosomes that express surface neutrophil elastase. These exosomes lead to collagen degradation and cause emphysema in mice [228]. On the other hand, EVs can also be protective against disease phenotypes. Conditioned media from MSCs protects against ASMCs and fibroblasts from cigarette smoke-induced damage [143, 229]. EVs from MSCs also have regenerative capacities in murine models of stroke and acute traumatic brain injury [230, 231]. In fact, recent studies suggest that the EVs are equally or more effective than MSCs themselves in cell-based therapies [232]. EVs might also mediate distal communication between different organs. In murine models, EVs containing inflammatory cytokines can travel in the blood and reach different organs [233].

Here, I show that EV-mediated mitochondrial transfer may also contribute to cell-cell communication within the lung. Size and EV marker expression suggest that the mitochondria-carrying EVs are possibly microvesicles. However, characterisation of sub-groups of EVs is challenging as these can overlap in size and expression of surface markers [223, 234]. Understanding how these EVs are formed can help clarify their nature. Blocking autophagy inhibits the release of mitochondria-containing exospheres from cardiomyocytes [124]. It is therefore possible that mitochondria may be encapsulated in EVs through autophagy-like pathways. Indeed, my findings show that the EVs isolated from ASMCs express autophagy markers, an observation also reported in EVs from MSCs and cardiomyocytes [124, 127]. Interestingly, the formation of autophagosomes can overlap with the endosomal pathway, through which exosomes are formed. For example, ESCRT proteins, such as TSG101, typically involved in exosome formation, have also been detected in autophagy processes [235]. The autophagy markers in the mitochondria-containing EVs also suggest these may be targeted for degradation in recipient cells, as has been reported in different systems [127, 134]. In line with these reports, I show that mtDNA taken up by ASMCs through EVs decreased over time in culture, suggest-

ing degradation of mitochondria after transfer. Therefore, EV-mediated mitochondrial transfer may be a mechanism for outsourcing mitophagy, though the benefit of this is unclear. Recycling of metabolites via autophagy supports respiration and cellular homeostasis [236, 237]. Degradation of transferred mitochondria may also provide metabolites to support the increased mitochondrial bioenergetics observed in response to transfer, and this may maybe be a mechanism to equalise energy status amongst neighbours. Alternatively, donation of mitochondria by ASMCs may act as a compensatory mechanism in response to impaired mitophagy in the donor cells. Cigarette smoke, which induces the donation of mitochondria by ASMCs, impairs mitophagy in small airway epithelial cells [112]. Whether this also occurs in ASMCs warrants further investigation. Donation of mitochondria is triggered by damage to the mitochondria, as shown in **Chapter 5**, where both CSM and CCCP induce mitochondrial transfer. Therefore, it is possible that mitochondria within EVs are dysfunctional. Though the nature of mitochondria in EVs from ASMCs is not known, mitochondria in exospheres from cardiomyocytes are damaged, showing a loss of cristae integrity and membrane potential [124]. This would corroborate the hypothesis of trans-cellular degradation of mitochondria.

Whilst EVs mediated mitochondrial transfer between ASMCs, they may not be the only mechanism: the levels of mitochondrial transfer detected through EVs were much lower than those observed in direct co-cultures, and inhibiting EV uptake with dynasore did not fully ablate transfer. In addition to EV-encapsulated mitochondria, free mitochondria were also detected in the conditioned media from ASMCs. Functional intact free mitochondria have been detected in blood [163] and uptake of free mitochondria by human osteosarcoma cells through micropinocytosis has also been reported [162]. Whether these free mitochondria are also taken up by ASMCs remains an unanswered question, but they may contribute to inflammatory responses in the lung. Indeed, free mitochondria can release their contents, such as mtDNA, fatty acids and ATP, which are sensed by other cells as DAMPs triggering inflammatory cascades [238]. Mitochondrial DAMPS may be important in COPD pathogenesis. For example, the levels of ATP are higher in BALF from COPD patients, and this correlates with disease severity. Neutrophils and macrophages

from COPD patients respond to ATP stimulation by secretion of pro-inflammatory and tissue-degrading mediators [118]. Other means of inter-cellular movement of mitochondria, such as cell-cell adhesion processes, may also be important in ASMCs, but were not investigated in this study.

To assess whether the intracellular mitochondrial motility machinery is required for the exchange of mitochondria between ASMCs, I measured how these are altered at the gene expression level in response to CSM, which induces the donation of mitochondria by ASMCs. CSM led to an increase in the mRNA levels of *MIRO1*, an outer mitochondrial membrane receptor, that facilitates the binding of mitochondria to molecular motor complexes and their movement along microtubules [97]. This protein is required for movement of mitochondria from MSCs to epithelial cells and cardiomyocytes [125, 141]. However, in ASMCs, depletion of MIRO1 had no effect in the ability of cells to donate or receive mitochondria. Therefore MIRO1-dependent movement of mitochondria along microtubules might not be essential for mitochondrial transfer between ASMCs. This is further corroborated by the fact that microtubule inhibition with nocodazole also had no effect on mitochondrial transfer. However, though this was not assessed, it is possible that expression of the isoform *MIRO2* is induced as a compensatory mechanism for the loss of MIRO1, preventing a reduction in mitochondrial transfer. In addition, whereas MIRO1 does not appear to be required for this process in untreated cells, it is possible that this changes under conditions of stress, such as upon exposure to CSM. Assessing the effect of *MIRO1* silencing on CSM-induced mitochondrial transfer would be important in future studies.

I hypothesised that mitochondrial morphology may also be important in mitochondrial transfer. For example, fragmentation of mitochondria may be required for encapsulation in EVs and subsequent transfer. In addition, mitochondrial fission and fusion proteins also participate in the movement of mitochondria within cells. The fusion protein MFN1 can form complexes with MIRO1 and facilitates axonal movement [100] and mouse models targeting MFN2 show impaired mitochondrial movement, though knockout of OPA1, another fusion protein, has no effect in mitochondrial motility [93, 100]. DRP1 is also important

in intracellular mitochondrial transport, where it is required for dendritic distribution of mitochondria and enhances microtubule-based mitochondrial transport in skeletal muscle [239, 240]. In this study, CSM led to a reduction in the expression of the mitochondrial fission gene *DRP1*. This was unexpected given that CSM has been previously reported to increase the expression of *DRP1* and reduce the expression of *MFN-1* and *-2* in ASMCs, leading to mitochondrial fragmentation [121]. However, whereas in this study cells were treated with 0.5 – 2% CSM for 24 to 48 hours, in my model the treatment was acute, which this can result in different effects. Nevertheless, given the requirement of DRP1 in mitochondria fission and movement, it is not clear how a reduction in *DRP1* can induce mitochondrial transfer. It is important to note that despite CSM leading to a reduction in *DRP1*, it is not known whether it affects mitochondrial fragmentation, movement or transfer. In addition, it is not known whether the effect of CSM at a gene expression level translates into changes in protein levels. CSM might also induce post-translational modifications that can affect these proteins' function. CSM can lead to modifications in redox homeostasis, altering the function of mitochondrial morphology proteins via non-transcriptional pathways [241]. For example, nitric oxide, induced in response to acute exposure to CSM, can lead to S-nitrosylation of DRP1 which promotes mitochondrial fragmentation [242, 243]. The results of these preliminary experiments are inconclusive, and the role of intracellular mitochondrial dynamics processes in mitochondrial transfer remains unclear.

Cigarette smoke induces the secretion of EVs by epithelial and basal airway cells [244, 245]. The effect of CSM on the secretion of EVs and formation of TNTs in ASMCs should be further investigated. Furthermore, CSM is not the only modulator of mitochondrial transfer. Other disease-relevant stimuli such as hydrogen peroxide and the pro-inflammatory cytokines TNF-α and IL-13, can modulate transfer in other systems [125, 219]. A high throughput assessment of transcriptional changes in response to CSM and other modulators of mitochondrial transfer would therefore provide a better insight into the mechanisms by which cells exchange mitochondria.

Whilst the molecular machinery that regulates mitochondrial transfer between ASMCs

remains unclear, the results from this Chapter begin to uncover the mechanisms by which this happens. The main observation is that ASMCs can exchange mitochondria through EVs. Extracellular vesicle-mediated mitochondrial transfer may be as effective in modulating recipient cell phenotypes, such as mitochondrial function and proliferation, as observed in mitochondrial transfer in direct co-cultures. Though this was not experimentally tested here, similar observations have been reported in MSC-mediated cell-based therapy models. EVs can be easily isolated from cell culture conditioned media and can be instilled in the lungs through the airways. Therefore, mitochondrial transfer via EVs could be exploited in clinical applications to reverse disease phenotypes in airway smooth muscle in COPD.

Chapter 7

General Discussion

COPD remains one of the leading causes of death globally and there are currently no treatments to reverse disease progression. It is therefore important to further elucidate the different molecular and cellular mechanisms driving COPD pathogenesis. Specifically, understanding the underpinnings of increased susceptibility to cigarette smoke, the main cause of COPD, can help identify new therapeutic targets. One important pathological aspect of COPD is airway remodelling, which involves thickening of the airway walls and narrowing of the airway lumen leading to airflow obstruction. Airway smooth muscle dysfunction, such as hyperplasia and increased ECM deposition, contributes to airway remodelling, and could be driven by CS-induced changes in mitochondrial function. In my thesis, I hypothesised that mitochondrial transfer between ASMCs is an important homeostatic mechanism to preserve mitochondrial function, and that this is impaired in COPD leading to sustained mitochondrial and cellular dysfunction in response to stress. I show that primary human ASMCs from COPD patients have increased susceptibility to CS-induced mitochondrial dysfunction, though this does not translate to differences in cell function, such as proliferation and cytokine release. ASMCs are capable of exchanging mitochondria, a process that is induced by stress and occurs, at least partly, via EVs. Contrary to my hypothesis, I did not detect differences in the ability of COPD ASMCs to exchange mitochondria, indicating this process may not underpin the increased susceptibility to CS. However, it may be exploited as an endogenous protective mechanism as it is associated with an up-regulation of mitochondrial biogenesis and respiration, and

a reduction in proliferation.

In COPD, CS-induced pathological features, such as oxidative stress and inflammation, persist after smoking cessation [21]. However, it is not known what drives this increased susceptibility to CS-induced damage. Cigarette smoke induces mitochondrial dysfunction in different cell types in the lung, including in ASMCs [107, 109, 121, 143, 246]. In this study, I show that CS-induced mitochondrial dysfunction in ASMCs is sustained after removal of the stressor, an effect which is more pronounced in ASMCs from COPD subjects. Therefore, mitochondrial dysfunction might also persist after smoking cessation and contribute to the pathological features of COPD. Increased susceptibility to CS-induced mitochondrial damage may be driven by inherent differences in mitochondrial function in COPD. For example, it has been shown that differences in mtDNA determine susceptibility to damage caused by CS-induced ROS [179]. In this study, I show that COPD ASMCs have lower $\Delta\psi$m and expression of complex III under baseline conditions compared to healthy ASMCs, and this may be linked to increased sensitivity to CS. It is also possible that homeostatic responses to stress are impaired in COPD. For example, defective anti-oxidant responses and impaired mitochondrial quality control processes, such as mitophagy, have been reported in COPD [47, 49, 111, 112]. Mitochondrial transfer between cells may be another mechanism of stress adaptation, and impairment of this process could contribute to sustained mitochondrial and cellular dysfunction seen in COPD.

Mitochondrial transfer has been reported in different organs including the lung, but also the heart, the liver and the brain [123, 124, 126, 145]. In the lung, specifically, transfer of mitochondria has been reported mainly in models of cell-based therapy, from MSCs to epithelial cells [123, 125, 140, 213], endothelial cells [213], macrophages [154, 165] and ASMCs [143]. Here, I show that this process also occurs endogenously, between structural cells in the lung: ASMCs can exchange mitochondria, a process that regulates bioenergetics and cellular function. Mitochondrial transfer between ASMCs is mediated, at least partly, by EVs, which have been widely described as important mediators of cell communication [247, 248]. Importantly, this process is induced by CS and/or mitochondrial

damage, suggesting it is indeed a stress adaptation mechanism and may be important in preserving mitochondrial function in response to stress. However, mitochondrial transfer also occurred under baseline conditions, suggesting it is also important in normal cell homeostasis. Inside the cell, a proportion of mitochondria are under constant movement, and this is dictated by homeostatic changes in, for example, calcium, ADP and glucose levels [97, 101, 249]. Similar stimuli may drive mitochondrial transfer in the absence of stressors.

Cell-cell communication is important in preserving lung homeostasis but can also contribute to disease pathogenesis. In COPD, alveolar macrophages orchestrate inflammatory responses by secreting cytokines and chemokines that recruit and activate other immune cells in the lung [250]. ASMCs themselves interact with other cell types, such as eosinophils, neutrophils and epithelial cells, through direct or indirect contact [251–254]. Importantly, these interactions can modulate ASMC phenotypes involved in disease, such as proliferation and contraction [69, 255]. EVs are an important mediator of cell communication and can spread or alleviate disease phenotypes. For example, oxidative stress-induced EVs secreted from epithelial cells can promote pro-inflammatory phenotypes in macrophages [227]. In contrast, the uptake of EVs from alveolar macrophages, containing suppressor of cytokine signalling (SOCS) proteins, reduces pro-inflammatory signalling in epithelial cells [256].

Here, I describe mitochondrial transfer, via EVs, as a novel form of cell-cell communication in the lungs. However, its role in disease pathogenesis is still not clear. Contrary to my hypothesis, I did not detect differences in the ability of COPD ASMCs to exchange mitochondria, nor in the response to stressors such as CS. Still, this does not completely exclude the possibility of this process being impaired in disease. For example, I show that, in some respects, healthy ASMCs respond differently to the uptake of mitochondria from COPD ASMCs, suggesting these may induce different metabolic effects in mitochondria recipient cells. In addition, I did not assess whether COPD ASMCs have the same ability to respond to the uptake of mitochondria as healthy ASMCs. Finally, it is also not known whether other endogenous cell types in the lung can also exchange mitochondria,

nor the physiological and pathological implications of this process. While transfer of mitochondria between ASMCs seems to be protective, this might not be the case in other cell types. For example, macrophages that take up mitochondria from adipocytes show a worsening of mitochondrial function [145], which could contribute to cellular dysfunction. In addition, mitochondrial transfer might be impaired in other cells types in COPD. Macrophages from COPD patients show impaired phagocytosis [25]; so it is possible that they also have an impaired ability to take up EVs containing mitochondria. There are also reports of mitochondrial transfer between different organs, such as between the liver and the heart [150]. This form of inter-organ communication may modulate the development of co-morbidities in COPD.

Mitochondrial transfer can be exploited as a therapeutic target for lung disorders. Several studies have shown that transfer of mitochondria from MSCs to other cell types is protective [123, 125, 143], suggesting that this process can be explored as a cell-based therapy. Moreover, here, I show that endogenous transfer of mitochondria in the lungs may reverse phenotypes associated with disease, such as mitochondrial dysfunction and hyper-proliferation, and could therefore also be targeted therapeutically. One approach to do so is to induce the mechanisms mediating this process. Chemotherapy drugs induce the release of EVs [257], but are there other pharmacological agents that can modulate this? Another approach is to target the protective pathways activated in response to transfer, instead of mitochondrial transfer itself. However, while different protective responses to transfer have been described, how these are elicited is not known. One common feature seen in response to transfer is an increase in mitochondrial biogenesis, which may contribute to the improved bioenergetics observed in mitochondria-recipient cells. Mitochondrial biogenesis is regulated by several transcription factors and transcriptional co-activators that can be induced pharmacologically. For example, *PGC1-α* is up-regulated by AMP-activated protein kinase (AMPK) agonists, such as 5-aminoimidazole-4-carboxamide ribonucleotide (AICAR), and the transcription factor peroxisome proliferator-activated receptor (PPAR)γ is activated directly by the anti-diabetic drugs pioglitazone and rosiglitazone [258]. Targeting mitochondrial trans-

fer, or mimicking its effects, in the lungs might have an effect not only in ASMCs, but also in other cell types that show mitochondrial dysfunction and may exchange mitochondria.

It is important to note that if we are to target mitochondria for therapy, it is imperative to understand how mitochondrial dysfunction drives pathogenic phenotypes in COPD. Mitochondrial function has been shown to influence phenotypes associated with COPD, such as inflammation and senescence [112, 118, 259]. In this study, changes in mitochondrial function, in response to CS exposure, were accompanied by changes in cellular function, such as proliferation and secretion of inflammatory mediators, but the link between these responses has yet to be established. Moreover, no remarkable differences were observed in the phenotypes assessed between healthy and COPD ASMCs. While this may be due to limitations of the experimental set-up, it also raises questions about the implication of ASM in COPD pathogenesis. The current literature describing the phenotype of ASM in COPD is sometimes contradictory. For example, some studies report no change in ECM proteins in COPD ASM, whereas others indicate that there is a negative correlation between ECM volume and airflow limitation [74, 79]. In addition, current therapies for COPD, such as bronchodilators, target the ASM, leading to relaxation of ASM tone, but have little impact on reversing airflow limitation [79]. It is therefore crucial to further study the changes in ASM that are associated with COPD. These observations, however, do not reduce the importance of my findings of mitochondrial transfer as a form of cell-cell communication between ASMCs. Studying this process is important for extending our understanding of ASMC biology, and cellular metabolism in general, both under physiological conditions, as well as in a disease context. This is important not only for COPD, but also in other lung conditions where mitochondrial dysfunction plays a role, such as asthma and lung fibrosis [260, 261].

7.1 Limitations of the study

This study has a few unaddressed questions, as a consequence of time-constrains, experimental limitations, or hindsight realisations. The main limitations of this study pertain to the *in vitro* culture system. Firstly, the healthy ASMCs used in this study were not "true" healthy as they were isolated from ex-smoker patients that had a diagnosis of adenocarcinoma. Though tissue was isolated from non-cancerous regions in the lung, it is possible that their function is affected by the cancer environment as well as by previous exposure to cigarette smoke. It would be important to include ASMCs from healthy never smokers in this study, but I did not have access to these. Secondly, the cell culture conditions (e.g. presence of serum) used may mask differences in the cellular phenotypes. Studies show contradicting results depending on the culture or specific treatment conditions. In lung epithelial cells, toxic doses of CS lead to reduced mitochondrial respiration whereas the opposite is observed with non-toxic doses of CS [260]. Understanding how best to mimic *in vivo* situations is important. Additions to the *in vitro* model could include the use of co-cultures with other cell types, such as epithelial cells and fibroblasts, or the use of lung organoids with ASMCs [262, 263].

I did not measure the acute effect of CSM on healthy and COPD ASMCs, and this is important as the acute effect of CSM in COPD ASMCs might be more pronounced and could explain the sustained mitochondrial dysfunction observed. Transcriptomics data suggested that ECM genes are differentially regulated in COPD ASMCs, but differences in ECM function were not further explored. The link between mitochondrial function and cellular phenotypes was also not extensively investigated, and this is a pivotal question to determine the functional consequences of mitochondrial dysfunction in COPD ASM.

With regards to mitochondrial transfer, there are many questions to be addressed, some of which would be particularly important to complement the findings of my study. Firstly, it is not clear whether the functional effect observed in mitochondria-recipient cells is a cause or consequence of this process. Though my data and the current literature suggests it is likely to be the latter, further experimental evidence is required to confidently confirm this. The effect of mitochondrial transfer was not assessed in CS-treated cells or in

COPD ASMCs. This would provide information as to the role of this process as a rescue mechanism, as well as a possible impairment in disease. EV-mediated mitochondrial transfer can also be further studied. I did not assess the effect of CS on the secretion or uptake of EVs, nor did I determine the specific contribution of mitochondria-containing EVs towards the functional impact elicited by mitochondrial transfer.

7.2 Future perspectives

Apart from the proposed work highlighted above, the results of my study open several new lines of investigation. I am the first to show that structural cells in the lung can exchange mitochondria, but many questions regarding this process remain unanswered. The precise mechanisms by which cells exchange mitochondria are not known. While EVs are a route for mitochondrial transfer, other routes, such as TNTs and other direct cell contact mechanisms might also participate in this process. In addition, the molecular machinery involved in this process is not known. A few proteins have been implicated in EV-mediated transport, such as the CD200 and Merkt receptors [124, 264]. Whether these are also important in ASMCs should be studied. Elucidating the mechanisms of mitochondrial transfer can also help understand the physiological relevance of this process. If we understand how transfer occurs, we can block it and assess the effects on cell function. Is it essential for maintaining cellular homeostasis in physiological conditions? To address this question, we can also investigate what drives mitochondrial function under normal conditions, such as physiological levels of ROS and changes in energy substrate levels. Another important question is what happens to the mitochondria in the recipient cell, and how is the functional impact of mitochondrial transfer elicited. These questions could be investigated using immortalised cell lines, rather than primary cells, as they are more easily manipulated and can be used for high throughput studies. For example, genetic screens would allow us to identify the molecular machinery mediating mitochondrial transfer and the uptake and processing of mitochondria by the recipient cells. Alternatively, studying the transcriptional responses of mitochondrial donor and recipient cells in response to known modulators of transfer, such as CS, would also provide clues in this

regard. Immortalised cell lines can be stably transfected, and this is another important advantage. This would allow, for example, for the stable expression of mitochondrial targeted GFP, circumventing the issues raised by the possibility of leakage of MitoTracker dyes. The findings in immortalised cell lines could then be confirmed in primary cells including cells from COPD patients.

In this study, I hypothesised that impaired mitochondrial transfer contributes to increased susceptibility of COPD ASMCs to CS-induced mitochondrial dysfunction. However, my findings did not support this hypothesis. Therefore, elucidating the mechanisms of increased susceptibility to CS is still required and could help identify new therapeutic targets in COPD. For example, differences in mtDNA repair or antioxidant protection can affect susceptibility to CS [108, 265, 266]. The regulation of these responses, and how these are affected by genetic or epigenetic mechanisms, should be investigated in COPD ASMCs.

While my study focused on ASMCs, other cell types, such as epithelial cells, fibroblasts and macrophages, are involved in COPD, but it is not known whether these cells can exchange mitochondria in the lungs. Recent studies have suggested an important role of uptake of mitochondria by macrophages in protecting against metabolic stress [124, 145, 146]. Macrophages play a pivotal role in COPD and also show mitochondrial dysfunction, so studying mitochondrial transfer in these cells would be of interest. Finally, it is currently unknown whether mitochondrial transfer between structural cells occurs *in vivo*. As it is not possible to study this mechanism in humans *in vivo*, a possibility would be to use established mouse models of COPD, where COPD-like phenotypes are induced by, for example, exposure to CS or intranasal administration of elastase [267, 268]. These models, however, do not accurately represent all clinical aspects of COPD.

7.3 Concluding remarks

Mitochondrial dysfunction is a prominent feature of COPD. In this thesis, I demonstrate mitochondrial transfer as a novel form of cell communication between structural cells in the lung that occurs in both normal homeostasis and under stress. Contrary to what I hypothesised, this process is not impaired in disease and therefore may not be implicated in the increased susceptibility of COPD patients to CS. However, given its role in preserving mitochondrial function in the lungs, it can still be exploited for future clinical applications. This thesis brings novel data and importantly, it is a foundation for several new avenues of research to be pursued.

Appendix

Permission to re-use figures from publicly available sources was obtained. The source and license of these items is summarised in **Table A1.**

Licensed Material	Licensor	License	Source of Material
Figure 1.4	Springer Nature Customer Service Centre GmbH	Link to license	[93]

Table A1: Source and copyright license of items included in the thesis.

References

[1] B. R. Celli and J. A. Wedzicha. Update on Clinical Aspects of Chronic Obstructive Pulmonary Disease. *N Engl J Med* 381 (2019):1257–1266. DOI: 10.1056/NEJMra1900500.

[2] GOLD. *Global Strategy for Prevention, Diagnosis and Management of COPD*. Report. 2021. Accessed at https://goldcopd.org/wp-content/uploads/2020/11/GOLD-REPORT-2021-v1.1-25Nov20_WMV.pdf.

[3] WHO. *The top 10 causes of death*. Web Page. 2019. Accessed at https://www.who.int/news-room/fact-sheets/detail/the-top-10-causes-of-death.

[4] B. L. Foundation. *The battle for breath: the impact of lung disease in the UK*. Report. 2016. Accessed at https://cdn.shopify.com/s/files/1/0221/4446/files/The_Battle_for_Breath_report_48b7e0ee-dc5b-43a0-a25c-2593bf9516f4.pdf?7045701451358472254&_ga=2.226714587.776305819.1589449063-144437535.1587116077.

[5] E. R. Society. *The Global Impact of Respiratory Disease*. Report. 2017. Accessed at https://www.who.int/gard/publications/The_Global_Impact_of_Respiratory_Disease.pdf.

[6] A. J. Guarascio, S. M. Ray, C. K. Finch, and T. H. Self. The clinical and economic burden of chronic obstructive pulmonary disease in the USA. *Clinicoecon Outcomes Res* 5 (2013):235–45. DOI: 10.2147/CEOR.S34321.

[7] C. D. Mathers and D. Loncar. Projections of global mortality and burden of disease from 2002 to 2030. *PLoS Med* 3 (2006):e442. DOI: 10.1371/journal.pmed.0030442.

[8] R. Lozano et al. Global and regional mortality from 235 causes of death for 20 age groups in 1990 and 2010: a systematic analysis for the Global Burden of Disease Study 2010. *Lancet* 380 (2012):2095–128. DOI: 10.1016/S0140-6736(12)61728-0.

[9] N. Terzikhan, K. M. Verhamme, A. Hofman, B. H. Stricker, G. G. Brusselle, and L. Lahousse. Prevalence and incidence of COPD in smokers and non-smokers: the Rotterdam Study. *Eur J Epidemiol* 31 (2016):785–92. DOI: 10.1007/s10654-016-0132-z.

[10] S. Eriksson. Pulmonary Emphysema and Alpha1-Antitrypsin Deficiency. *Acta Med Scand* 175 (1964):197–205. DOI: 10.1111/j.0954-6820.1964.tb00567.x.

[11] A. Berndt, A. S. Leme, and S. D. Shapiro. Emerging genetics of COPD. *EMBO Mol Med* 4 (2012):1144–55. DOI: 10.1002/emmm.201100627.

[12] N. Mercado, K. Ito, and P. J. Barnes. Accelerated ageing of the lung in COPD: new concepts. *Thorax* 70 (2015):482–9. DOI: 10.1136/thoraxjnl-2014-206084.

[13] S. Burge and J. A. Wedzicha. COPD exacerbations: definitions and classifications. *Eur Respir J Suppl* 41 (2003):46s–53s. DOI: 10.1183/09031936.03.00078002.

[14] E. Monso, J. Ruiz, A. Rosell, J. Manterola, J. Fiz, J. Morera, and V. Ausina. Bacterial infection in chronic obstructive pulmonary disease. A study of stable and exacerbated outpatients using the protected specimen brush. *Am J Respir Crit Care Med* 152 (1995):1316–20. DOI: 10.1164/ajrccm.152.4.7551388.

[15] D. Linden, H. Guo-Parke, P. V. Coyle, D. Fairley, D. F. McAuley, C. C. Taggart, and J. Kidney. Respiratory viral infection: a potential "missing link" in the pathogenesis of COPD. *Eur Respir Rev* 28 (2019). DOI: 10.1183/16000617.0063-2018.

[16] J. M. Leung, M. Niikura, C. W. T. Yang, and D. D. Sin. COVID-19 and COPD. *Eur Respir J* 56 (2020). DOI: 10.1183/13993003.02108-2020.

[17] F. V. Gerayeli, S. Milne, C. Cheung, X. Li, C. W. T. Yang, A. Tam, L. H. Choi, A. Bae, and D. D. Sin. COPD and the risk of poor outcomes in COVID-19: A systematic review and meta-analysis. *EClinicalMedicine* 33 (2021):100789. DOI: 10.1016/j.eclinm.2021.100789.

[18] J. M. Leung, C. X. Yang, A. Tam, T. Shaipanich, T. L. Hackett, G. K. Singhera, D. R. Dorscheid, and D. D. Sin. ACE-2 expression in the small airway epithelia of smokers and COPD patients: implications for COVID-19. *Eur Respir J* 55 (2020). DOI: 10.1183/13993003.00688-2020.

[19] R. T. McKendry, C. M. Spalluto, H. Burke, B. Nicholas, D. Cellura, A. Al-Shamkhani, K. J. Staples, and T. M. Wilkinson. Dysregulation of Antiviral Function of CD8(+) T Cells in the Chronic Obstructive Pulmonary Disease Lung. Role of the PD-1-PD-L1 Axis. *Am J Respir Crit Care Med* 193 (2016):642–51. DOI: 10.1164/rccm.201504-0782OC.

[20] K. F. Chung and I. M. Adcock. Multifaceted mechanisms in COPD: inflammation, immunity, and tissue repair and destruction. *Eur Respir J* 31 (2008):1334–56. DOI: 10.1183/09031936.00018908.

[21] J. C. Hogg, F. Chu, S. Utokaparch, R. Woods, W. M. Elliott, L. Buzatu, R. M. Cherniack, R. M. Rogers, F. C. Sciurba, H. O. Coxson, and P. D. Pare. The nature of small-airway obstruction in chronic obstructive pulmonary disease. *N Engl J Med* 350 (2004):2645–53. DOI: 10.1056/NEJMoa032158.

[22] T. Trian, G. Benard, H. Begueret, R. Rossignol, P. O. Girodet, D. Ghosh, O. Ousova, J. M. Vernejoux, R. Marthan, J. M. Tunon-de Lara, and P. Berger. Bronchial smooth muscle remodeling involves calcium-dependent enhanced mitochondrial biogenesis in asthma. *J Exp Med* 204 (2007):3173–81. DOI: 10.1084/jem.20070956.

[23] A. Higham, A. M. Quinn, J. E. D. Cancado, and D. Singh. The pathology of small airways disease in COPD: historical aspects and future directions. *Respir Res* 20 (2019):49. DOI: 10.1186/s12931-019-1017-y.

[24] E. Bagdonas, J. Raudoniute, I. Bruzauskaite, and R. Aldonyte. Novel aspects of pathogenesis and regeneration mechanisms in COPD. *Int J Chron Obstruct Pulmon Dis* 10 (2015):995–1013. DOI: 10.2147/COPD.S82518.

[25] K. B. R. Belchamber, R. Singh, C. M. Batista, M. K. Whyte, D. H. Dockrell, I. Kilty, M. J. Robinson, J. A. Wedzicha, P. J. Barnes, L. E. Donnelly, and C.-M. consortium. Defective bacterial phagocytosis is associated with dysfunctional mitochondria in COPD macrophages. *Eur Respir J* 54 (2019). DOI: 10.1183/13993003.02244-2018.

[26] E. Sapey, J. A. Stockley, H. Greenwood, A. Ahmad, D. Bayley, J. M. Lord, R. H. Insall, and R. A. Stockley. Behavioral and structural differences in migrating peripheral neutrophils from patients with chronic obstructive pulmonary disease. *Am J Respir Crit Care Med* 183 (2011):1176–86. DOI: 10.1164/rccm.201008-1285OC.

[27] V. M. Keatings, P. D. Collins, D. M. Scott, and P. J. Barnes. Differences in interleukin-8 and tumor necrosis factor-alpha in induced sputum from patients with chronic obstructive pulmonary disease or asthma. *Am J Respir Crit Care Med* 153 (1996):530–4. DOI: 10.1164/ajrccm.153.2.8564092.

[28] E. Bucchioni, S. A. Kharitonov, L. Allegra, and P. J. Barnes. High levels of interleukin-6 in the exhaled breath condensate of patients with COPD. *Respir Med* 97 (2003):1299–302. DOI: 10.1016/j.rmed.2003.07.008.

[29] H. Takizawa, M. Tanaka, K. Takami, T. Ohtoshi, K. Ito, M. Satoh, Y. Okada, F. Yamasawa, K. Nakahara, and A. Umeda. Increased expression of transforming growth factor-beta1 in small airway epithelium from tobacco smokers and patients with chronic obstructive pulmonary disease (COPD). *Am J Respir Crit Care Med* 163 (2001):1476–83. DOI: 10.1164/ajrccm.163.6.9908135.

[30] W. Macnee, J. Maclay, and D. McAllister. Cardiovascular injury and repair in chronic obstructive pulmonary disease. *Proc Am Thorac Soc* 5 (2008):824–33. DOI: 10.1513/pats.200807-071TH.

[31] K. H. Groenewegen, D. S. Postma, W. C. J. Hop, P. L. M. L. Wielders, N. J. J. Schlosser, E. F. M. Wouters, and C. S. Grp. Increased systemic inflammation is a risk factor for COPD exacerbations. *Chest* 133 (2008):350–357. DOI: 10.1378/chest.07-1342.

[32] S. Molet, C. Belleguic, H. Lena, N. Germain, C. P. Bertrand, S. D. Shapiro, J. M. Planquois, P. Delaval, and V. Lagente. Increase in macrophage elastase (MMP-12) in lungs from patients with chronic obstructive pulmonary disease. *Inflamm Res* 54 (2005):31–6. DOI: 10.1007/s00011-004-1319-4.

[33] R. M. Senior, H. Tegner, C. Kuhn, K. Ohlsson, B. C. Starcher, and J. A. Pierce. The induction of pulmonary emphysema with human leukocyte elastase. *Am Rev Respir Dis* 116 (1977):469–75. DOI: 10.1164/arrd.1977.116.3.469.

[34] G. A. Finlay, M. D. O'Donnell, C. M. O'Connor, J. P. Hayes, and M. X. FitzGerald. Elastin and collagen remodeling in emphysema. A scanning electron microscopy study. *Am J Pathol* 149 (1996):1405–15.

[35] P. A. Kirkham and P. J. Barnes. Oxidative stress in COPD. *Chest* 144 (2013):266–273. DOI: 10.1378/chest.12-2664.

[36] S. Boukhenouna, M. A. Wilson, K. Bahmed, and B. Kosmider. Reactive Oxygen Species in Chronic Obstructive Pulmonary Disease. *Oxid Med Cell Longev* 2018 (2018):5730395. DOI: 10.1155/2018/5730395.

[37] D. F. Church and W. A. Pryor. Free-radical chemistry of cigarette smoke and its toxicological implications. *Environ Health Perspect* 64 (1985):111–26. DOI: 10.1289/ehp.8564111.

[38] W. A. Pryor and K. Stone. Oxidants in cigarette smoke. Radicals, hydrogen peroxide, peroxynitrate, and peroxynitrite. *Ann N Y Acad Sci* 686 (1993):12–27; discussion 27–8. DOI: 10.1111/j.1749-6632.1993.tb39148.x.

[39] D. G. Nicholls. *Bioenergetics*. 4th Edition. Academic Press, 2013.

[40] G. T. Nguyen, E. R. Green, and J. Mecsas. Neutrophils to the ROScue: Mechanisms of NADPH Oxidase Activation and Bacterial Resistance. *Front Cell Infect Microbiol* 7 (2017):373. DOI: 10.3389/fcimb.2017.00373.

[41] I. Rahman, A. A. van Schadewijk, A. J. Crowther, P. S. Hiemstra, J. Stolk, W. MacNee, and W. I. De Boer. 4-Hydroxy-2-nonenal, a specific lipid peroxidation product, is elevated in lungs of patients with chronic obstructive pulmonary disease. *Am J Respir Crit Care Med* 166 (2002):490–5. DOI: 10.1164/rccm.2110101.

[42] I. Rahman and I. M. Adcock. Oxidative stress and redox regulation of lung inflammation in COPD. *Eur Respir J* 28 (2006):219–42. DOI: 10.1183/09031936.06.00053805.

[43] I. Rahman, B. Mulier, P. S. Gilmour, T. Watchorn, K. Donaldson, P. K. Jeffery, and W. MacNee. Oxidant-mediated lung epithelial cell tolerance: the role of intracellular glutathione and nuclear factor-kappaB. *Biochem Pharmacol* 62 (2001):787–94.

[44] N. Louhelainen, P. Rytila, T. Haahtela, V. L. Kinnula, and R. Djukanovic. Persistence of oxidant and protease burden in the airways after smoking cessation. *BMC Pulm Med* 9 (2009):25. DOI: 10.1186/1471-2466-9-25.

[45] C. H. Wiegman, C. Michaeloudes, G. Haji, P. Narang, C. J. Clarke, K. E. Russell, W. Bao, S. Pavlidis, P. J. Barnes, J. Kanerva, A. Bittner, N. Rao, M. P. Murphy, P. A. Kirkham, K. F. Chung, I. M. Adcock, and Copdmap. Oxidative stress-induced mitochondrial dysfunction drives inflammation and airway smooth muscle remodeling in patients with chronic obstructive pulmonary disease. *J Allergy Clin Immunol* 136 (2015):769–80. DOI: 10.1016/j.jaci.2015.01.046.

[46] G. Haji, C. H. Wiegman, C. Michaeloudes, M. S. Patel, K. Curtis, P. Bhavsar, M. I. Polkey, I. M. Adcock, K. F. Chung, and C. consortium. Mitochondrial dysfunction in airways and quadriceps muscle of patients with chronic obstructive pulmonary disease. *Respir Res* 21 (2020):262. DOI: 10.1186/s12931-020-01527-5.

[47] N. Mercado, R. Thimmulappa, C. M. Thomas, P. S. Fenwick, K. K. Chana, L. E. Donnelly, S. Biswal, K. Ito, and P. J. Barnes. Decreased histone deacetylase 2

impairs Nrf2 activation by oxidative stress. *Biochem Biophys Res Commun* 406 (2011):292–8. DOI: 10.1016/j.bbrc.2011.02.035.

[48] T. Ishii, T. Matsuse, S. Teramoto, H. Matsui, M. Miyao, T. Hosoi, H. Takahashi, Y. Fukuchi, and Y. Ouchi. Glutathione S-transferase P1 (GSTP1) polymorphism in patients with chronic obstructive pulmonary disease. *Thorax* 54 (1999):693–6.

[49] R. P. Young, R. Hopkins, P. N. Black, C. Eddy, L. Wu, G. D. Gamble, G. D. Mills, J. E. Garrett, T. E. Eaton, and M. I. Rees. Functional variants of antioxidant genes in smokers with COPD and in those with normal lung function. *Thorax* 61 (2006):394–399. DOI: 10.1136/thx.2005.048512.

[50] T. Tsuji, K. Aoshiba, and A. Nagai. Alveolar cell senescence in patients with pulmonary emphysema. *Am J Respir Crit Care Med* 174 (2006):886–93. DOI: 10.1164/rccm.200509-1374OC.

[51] P. J. Barnes, J. Baker, and L. E. Donnelly. Cellular Senescence as a Mechanism and Target in Chronic Lung Diseases. *Am J Respir Crit Care Med* 200 (2019):556–564. DOI: 10.1164/rccm.201810-1975TR.

[52] K. Imai, B. A. Mercer, L. L. Schulman, J. R. Sonett, and J. M. D'Armiento. Correlation of lung surface area to apoptosis and proliferation in human emphysema. *Eur Respir J* 25 (2005):250–8. DOI: 10.1183/09031936.05.00023704.

[53] Z. Lu, H. P. Van Eeckhoutte, G. Liu, P. M. Nair, B. Jones, C. M. Gillis, B. C. Nalkurthi, F. Verhamme, T. Buyle-Huybrecht, P. Vandenabeele, T. Vanden Berghe, G. G. Brusselle, J. C. Horvat, J. M. Murphy, P. A. Wark, K. R. Bracke, M. Fricker, and P. M. Hansbro. Necroptosis Signaling Promotes Inflammation, Airway Remodeling, and Emphysema in Chronic Obstructive Pulmonary Disease. *Am J Respir Crit Care Med* 204 (2021):667–681. DOI: 10.1164/rccm.202009-3442OC.

[54] R. Faner, M. Rojas, W. Macnee, and A. Agusti. Abnormal lung aging in chronic obstructive pulmonary disease and idiopathic pulmonary fibrosis. *Am J Respir Crit Care Med* 186 (2012):306–13. DOI: 10.1164/rccm.201202-0282PP.

[55] K. Ito, M. Ito, W. M. Elliott, B. Cosio, G. Caramori, O. M. Kon, A. Barczyk, S. Hayashi, I. M. Adcock, J. C. Hogg, and P. J. Barnes. Decreased histone deacetylase activity in chronic obstructive pulmonary disease. *N Engl J Med* 352 (2005):1967–76. DOI: 10.1056/NEJMoa041892.

[56] J. D. Morrow, M. H. Cho, C. P. Hersh, V. Pinto-Plata, B. Celli, N. Marchetti, G. Criner, R. Bueno, G. Washko, K. Glass, A. M. K. Choi, J. Quackenbush, E. K. Silverman, and D. L. DeMeo. DNA methylation profiling in human lung tissue identifies genes associated with COPD. *Epigenetics* 11 (2016):730–739. DOI: 10.1080/15592294.2016.1226451.

[57] Z. Wang, M. Bafadhel, K. Haldar, A. Spivak, D. Mayhew, B. E. Miller, R. Tal-Singer, S. L. Johnston, M. Y. Ramsheh, M. R. Barer, C. E. Brightling, and J. R. Brown. Lung microbiome dynamics in COPD exacerbations. *Eur Respir J* 47 (2016):1082–92. DOI: 10.1183/13993003.01406-2015.

[58] X. Ji, X. Niu, J. Qian, V. Martucci, S. A. Pendergrass, I. P. Gorlov, C. I. Amos, J. C. Denny, P. P. Massion, and M. C. Aldrich. A Phenome-Wide Association Study

Uncovers a Role for Autoimmunity in the Development of Chronic Obstructive Pulmonary Disease. *Am J Respir Cell Mol Biol* 58 (2018):777–779. DOI: 10.1165/rcmb.2017-0409LE.

[59] S. P. Lakshmi, A. T. Reddy, and R. C. Reddy. Emerging pharmaceutical therapies for COPD. *Int J Chron Obstruct Pulmon Dis* 12 (2017):2141–2156. DOI: 10.2147/COPD.S121416.

[60] J. R. Baker, L. E. Donnelly, and P. J. Barnes. Senotherapy: A New Horizon for COPD Therapy. *Chest* 158 (2020):562–570. DOI: 10.1016/j.chest.2020.01.027.

[61] P. J. Barnes. Pharmacology of airway smooth muscle. *Am J Respir Crit Care Med* 158 (1998):S123–32. DOI: 10.1164/ajrccm.158.supplement_2.13tac800.

[62] K. F. Chung. The role of airway smooth muscle in the pathogenesis of airway wall remodeling in chronic obstructive pulmonary disease. *Proc Am Thorac Soc* 2 (2005):347–54; discussion 371–2. DOI: 10.1513/pats.200504-028SR.

[63] A. J. Halayko, H. Salari, X. Ma, and N. L. Stephens. Markers of airway smooth muscle cell phenotype. *Am J Physiol* 270 (1996):L1040–51. DOI: 10.1152/ajplung.1996.270.6.L1040.

[64] A. J. Halayko, B. Camoretti-Mercado, S. M. Forsythe, J. E. Vieira, R. W. Mitchell, M. E. Wylam, M. B. Hershenson, and J. Solway. Divergent differentiation paths in airway smooth muscle culture: induction of functionally contractile myocytes. *Am J Physiol* 276 (1999):L197–206. DOI: 10.1152/ajplung.1999.276.1.L197.

[65] M. B. Sukkar, A. J. Stanley, A. E. Blake, P. D. Hodgkin, P. R. A. Johnson, C. L. Armour, and J. M. Hughes. 'Proliferative' and 'synthetic' airway smooth muscle cells are overlapping populations. *Immunology and Cell Biology* 82 (2004):471–478. DOI: 10.1111/j.0818-9641.2004.01275.x.

[66] S. J. Hirst, C. H. Twort, and T. H. Lee. Differential effects of extracellular matrix proteins on human airway smooth muscle cell proliferation and phenotype. *Am J Respir Cell Mol Biol* 23 (2000):335–44. DOI: 10.1165/ajrcmb.23.3.3990.

[67] S. Xie, M. B. Sukkar, R. Issa, N. M. Khorasani, and K. F. Chung. Mechanisms of induction of airway smooth muscle hyperplasia by transforming growth factor-beta. *Am J Physiol Lung Cell Mol Physiol* 293 (2007):L245–53. DOI: 10.1152/ajplung.00068.2007.

[68] D. B. Wright, T. Trian, S. Siddiqui, C. D. Pascoe, J. R. Johnson, B. G. J. Dekkers, S. Dakshinamurti, R. Bagchi, J. K. Burgess, V. Kanabar, and O. O. Ojo. Phenotype modulation of airway smooth muscle in asthma. *Pulmonary Pharmacology & Therapeutics* 26 (2013):42–49. DOI: 10.1016/j.pupt.2012.08.005.

[69] M. J. O'Sullivan, E. Gabriel, A. Panariti, C. Y. Park, G. Ijpma, J. J. Fredberg, A. M. Lauzon, and J. G. Martin. Epithelial Cells Induce a Cyclo-Oxygenase-1-Dependent Endogenous Reduction in Airway Smooth Muscle Contractile Phenotype. *Am J Respir Cell Mol Biol* 57 (2017):683–691. DOI: 10.1165/rcmb.2016-0427OC.

[70] A. D. Lockett, Y. Wu, and S. J. Gunst. Elastase alters contractility and promotes an inflammatory synthetic phenotype in airway smooth muscle tissues. *Am J Phys-*

iol Lung Cell Mol Physiol 314 (2018):L626–L634. DOI: 10.1152/ajplung.00334.2017.

[71] B. Camoretti-Mercado, H. W. Liu, A. J. Halayko, S. M. Forsythe, J. W. Kyle, B. Li, Y. Fu, J. McConville, P. Kogut, J. E. Vieira, N. M. Patel, M. B. Hershenson, E. Fuchs, S. Sinha, J. M. Miano, M. S. Parmacek, J. K. Burkhardt, and J. Solway. Physiological control of smooth muscle-specific gene expression through regulated nuclear translocation of serum response factor. *J Biol Chem* 275 (2000):30387–93. DOI: 10.1074/jbc.M000840200.

[72] H. Okamoto, Y. Fujioka, A. Takahashi, T. Takahashi, T. Taniguchi, Y. Ishikawa, and M. Yokoyama. Trichostatin A, an inhibitor of histone deacetylase, inhibits smooth muscle cell proliferation via induction of p21(WAF1). *J Atheroscler Thromb* 13 (2006):183–91. DOI: 10.5551/jat.13.183.

[73] K. Mahn, S. J. Hirst, S. Ying, M. R. Holt, P. Lavender, O. O. Ojo, L. Siew, D. E. Simcock, C. G. McVicker, V. Kanabar, V. A. Snetkov, B. J. O'Connor, C. Karner, D. J. Cousins, P. Macedo, K. F. Chung, C. J. Corrigan, J. P. Ward, and T. H. Lee. Diminished sarco/endoplasmic reticulum Ca2+ ATPase (SERCA) expression contributes to airway remodelling in bronchial asthma. *Proc Natl Acad Sci U S A* 106 (2009):10775–80. DOI: 10.1073/pnas.0902295106.

[74] L. Pini, V. Pinelli, D. Modina, M. Bezzi, L. Tiberio, and C. Tantucci. Central airways remodeling in COPD patients. *Int J Chron Obstruct Pulmon Dis* 9 (2014):927–32. DOI: 10.2147/COPD.S52478.

[75] X. Liu, B. Hao, A. Ma, J. He, X. Liu, and J. Chen. The Expression of NOX4 in Smooth Muscles of Small Airway Correlates with the Disease Severity of COPD. *Biomed Res Int* 2016 (2016):2891810. DOI: 10.1155/2016/2891810.

[76] C. Michaeloudes, C. H. Kuo, G. Haji, D. K. Finch, A. J. Halayko, P. Kirkham, K. F. Chung, I. M. Adcock, and Copdmap. Metabolic re-patterning in COPD airway smooth muscle cells. *Eur Respir J* 50 (2017). DOI: 10.1183/13993003.00202-2017.

[77] M. E. Wylam, V. Sathish, S. K. VanOosten, M. Freeman, D. Burkholder, M. A. Thompson, C. M. Pabelick, and Y. S. Prakash. Mechanisms of Cigarette Smoke Effects on Human Airway Smooth Muscle. *PLoS One* 10 (2015):e0128778. DOI: 10.1371/journal.pone.0128778.

[78] M. Ebina, H. Yaegashi, R. Chiba, T. Takahashi, M. Motomiya, and M. Tanemura. Hyperreactive site in the airway tree of asthmatic patients revealed by thickening of bronchial muscles. A morphometric study. *Am Rev Respir Dis* 141 (1990):1327–32. DOI: 10.1164/ajrccm/141.5_Pt_1.1327.

[79] R. L. Jones, P. B. Noble, J. G. Elliot, H. W. Mitchell, P. K. McFawn, J. C. Hogg, and A. L. James. Airflow obstruction is associated with increased smooth muscle extracellular matrix. *Eur Respir J* 47 (2016):1855–7. DOI: 10.1183/13993003.01709-2015.

[80] A. R. Kranenburg, A. Willems-Widyastuti, W. J. Moori, P. J. Sterk, V. K. Alagappan, W. I. de Boer, and H. S. Sharma. Enhanced bronchial expression of ex-

tracellular matrix proteins in chronic obstructive pulmonary disease. *Am J Clin Pathol* 126 (2006):725–35. DOI: 10.1309/jc477fael1ykv54w.

[81] L. Chen, Q. Ge, G. Tjin, H. Alkhouri, L. Deng, C. A. Brandsma, I. Adcock, W. Timens, D. Postma, J. K. Burgess, J. L. Black, and B. G. Oliver. Effects of cigarette smoke extract on human airway smooth muscle cells in COPD. *Eur Respir J* 44 (2014):634–46. DOI: 10.1183/09031936.00171313.

[82] I. Klagas, S. Goulet, G. Karakiulakis, J. Zhong, M. Baraket, J. L. Black, E. Papakonstantinou, and M. Roth. Decreased hyaluronan in airway smooth muscle cells from patients with asthma and COPD. *Eur Respir J* 34 (2009):616–28. DOI: 10.1183/09031936.00070808.

[83] A. M. Opazo Saez, C. Y. Seow, and P. D. Pare. Peripheral airway smooth muscle mechanics in obstructive airways disease. *Am J Respir Crit Care Med* 161 (2000):910–7. DOI: 10.1164/ajrccm.161.3.9903138.

[84] E. L. Hardaker, A. M. Bacon, K. Carlson, A. K. Roshak, J. J. Foley, D. B. Schmidt, P. T. Buckley, M. Comegys, J. Panettieri R. A., H. M. Sarau, and K. E. Belmonte. Regulation of TNF-alpha- and IFN-gamma-induced CXCL10 expression: participation of the airway smooth muscle in the pulmonary inflammatory response in chronic obstructive pulmonary disease. *FASEB J* 18 (2004):191–3. DOI: 10.1096/fj.03-0170fje.

[85] S. Baraldo, G. Turato, C. Badin, E. Bazzan, B. Beghe, R. Zuin, F. Calabrese, G. Casoni, P. Maestrelli, A. Papi, L. M. Fabbri, and M. Saetta. Neutrophilic infiltration within the airway smooth muscle in patients with COPD. *Thorax* 59 (2004):308–12. DOI: 10.1136/thx.2003.012146.

[86] W. F. Martin, S. Garg, and V. Zimorski. Endosymbiotic theories for eukaryote origin. *Philos Trans R Soc Lond B Biol Sci* 370 (2015):20140330. DOI: 10.1098/rstb.2014.0330.

[87] J. B. Stewart and P. F. Chinnery. The dynamics of mitochondrial DNA heteroplasmy: implications for human health and disease. *Nat Rev Genet* 16 (2015):530–42. DOI: 10.1038/nrg3966.

[88] A. D. Jayaprakash, E. K. Benson, S. Gone, R. Liang, J. Shim, L. Lambertini, M. M. Toloue, M. Wigler, S. A. Aaronson, and R. Sachidanandam. Stable heteroplasmy at the single-cell level is facilitated by intercellular exchange of mtDNA. *Nucleic Acids Research* 43 (2015):2177–2187. DOI: 10.1093/nar/gkv052.

[89] L. D. Zorova, V. A. Popkov, E. Y. Plotnikov, D. N. Silachev, I. B. Pevzner, S. S. Jankauskas, V. A. Babenko, S. D. Zorov, A. V. Balakireva, M. Juhaszova, S. J. Sollott, and D. B. Zorov. Mitochondrial membrane potential. *Anal Biochem* 552 (2018):50–59. DOI: 10.1016/j.ab.2017.07.009.

[90] E. B. Tahara, F. D. Navarete, and A. J. Kowaltowski. Tissue-, substrate-, and site-specific characteristics of mitochondrial reactive oxygen species generation. *Free Radic Biol Med* 46 (2009):1283–97. DOI: 10.1016/j.freeradbiomed.2009.02.008.

[91] T. Finkel. Signal transduction by mitochondrial oxidants. *J Biol Chem* 287 (2012):4434–40. DOI: 10.1074/jbc.R111.271999.

[92] A. Hahn and S. Zuryn. Mitochondrial Genome (mtDNA) Mutations that Generate Reactive Oxygen Species. *Antioxidants (Basel)* 8 (2019). DOI: 10.3390/antiox8090392.

[93] V. Eisner, M. Picard, and G. Hajnoczky. Mitochondrial dynamics in adaptive and maladaptive cellular stress responses. *Nat Cell Biol* 20 (2018):755–765. DOI: 10.1038/s41556-018-0133-0.

[94] D. C. Chan. Fusion and fission: interlinked processes critical for mitochondrial health. *Annu Rev Genet* 46 (2012):265–87. DOI: 10.1146/annurev-genet-110410-132529.

[95] R. J. Youle and D. P. Narendra. Mechanisms of mitophagy. *Nat Rev Mol Cell Biol* 12 (2011):9–14. DOI: 10.1038/nrm3028.

[96] K. Labbe, A. Murley, and J. Nunnari. Determinants and functions of mitochondrial behavior. *Annu Rev Cell Dev Biol* 30 (2014):357–91. DOI: 10.1146/annurev-cellbio-101011-155756.

[97] M. Y. Lin and Z. H. Sheng. Regulation of mitochondrial transport in neurons. *Exp Cell Res* 334 (2015):35–44. DOI: 10.1016/j.yexcr.2015.01.004.

[98] J. S. Kang, J. H. Tian, P. Y. Pan, P. Zald, C. Li, C. Deng, and Z. H. Sheng. Docking of axonal mitochondria by syntaphilin controls their mobility and affects short-term facilitation. *Cell* 132 (2008):137–48. DOI: 10.1016/j.cell.2007.11.024.

[99] X. Wang, D. Winter, G. Ashrafi, J. Schlehe, Y. L. Wong, D. Selkoe, S. Rice, J. Steen, M. J. LaVoie, and T. L. Schwarz. PINK1 and Parkin target Miro for phosphorylation and degradation to arrest mitochondrial motility. *Cell* 147 (2011):893–906. DOI: 10.1016/j.cell.2011.10.018.

[100] A. Misko, S. R. Jiang, I. Wegorzewska, J. Milbrandt, and R. H. Baloh. Mitofusin 2 Is Necessary for Transport of Axonal Mitochondria and Interacts with the Miro/Milton Complex. *Journal of Neuroscience* 30 (2010):4232–4240. DOI: 10.1523/Jneurosci.6248-09.2010.

[101] S. L. Mironov. ADP regulates movements of mitochondria in neurons. *Biophys J* 92 (2007):2944–52. DOI: 10.1529/biophysj.106.092981.

[102] G. Pekkurnaz, J. C. Trinidad, X. Wang, D. Kong, and T. L. Schwarz. Glucose regulates mitochondrial motility via Milton modification by O-GlcNAc transferase. *Cell* 158 (2014):54–68. DOI: 10.1016/j.cell.2014.06.007.

[103] A. H. V. Schapira. Mitochondrial diseases. *The Lancet* 379 (2012):1825–1834. DOI: 10.1016/s0140-6736(11)61305-6.

[104] O. M. Russell, G. S. Gorman, R. N. Lightowlers, and D. M. Turnbull. Mitochondrial Diseases: Hope for the Future. *Cell* 181 (2020):168–188. DOI: 10.1016/j.cell.2020.02.051.

[105] A. Diaz-Vegas, P. Sanchez-Aguilera, J. R. Krycer, P. E. Morales, M. Monsalves-Alvarez, M. Cifuentes, B. A. Rothermel, and S. Lavandero. Is Mitochondrial Dys-

function a Common Root of Noncommunicable Chronic Diseases? *Endocr Rev* 41 (2020). DOI: 10.1210/endrev/bnaa005.

[106] J. Lloreta, M. Orozco, J. Gea, J. M. Corominas, and S. Serrano. Selective diaphragmatic mitochondrial abnormalities in a patient with marked air flow obstruction. *Ultrastruct Pathol* 20 (1996):67–71.

[107] R. F. Hoffmann, S. Zarrintan, S. M. Brandenburg, A. Kol, H. G. de Bruin, S. Jafari, F. Dijk, D. Kalicharan, M. Kelders, H. R. Gosker, N. H. Ten Hacken, J. J. van der Want, A. J. van Oosterhout, and I. H. Heijink. Prolonged cigarette smoke exposure alters mitochondrial structure and function in airway epithelial cells. *Respir Res* 14 (2013):97. DOI: 10.1186/1465-9921-14-97.

[108] B. Kosmider, C. R. Lin, L. Karim, D. Tomar, L. Vlasenko, N. Marchetti, S. Bolla, M. Madesh, G. J. Criner, and K. Bahmed. Mitochondrial dysfunction in human primary alveolar type II cells in emphysema. *EBioMedicine* 46 (2019):305–316. DOI: 10.1016/j.ebiom.2019.07.063.

[109] K. Ballweg, K. Mutze, M. Konigshoff, O. Eickelberg, and S. Meiners. Cigarette smoke extract affects mitochondrial function in alveolar epithelial cells. *Am J Physiol Lung Cell Mol Physiol* 307 (2014):L895–907. DOI: 10.1152/ajplung.00180.2014.

[110] K. Mizumura, S. M. Cloonan, K. Nakahira, A. R. Bhashyam, M. Cervo, T. Kitada, K. Glass, C. A. Owen, A. Mahmood, G. R. Washko, S. Hashimoto, S. W. Ryter, and A. M. Choi. Mitophagy-dependent necroptosis contributes to the pathogenesis of COPD. *J Clin Invest* 124 (2014):3987–4003. DOI: 10.1172/JCI74985.

[111] S. Ito, J. Araya, Y. Kurita, K. Kobayashi, N. Takasaka, M. Yoshida, H. Hara, S. Minagawa, H. Wakui, S. Fujii, J. Kojima, K. Shimizu, T. Numata, M. Kawaishi, M. Odaka, T. Morikawa, T. Harada, S. L. Nishimura, Y. Kaneko, K. Nakayama, and K. Kuwano. PARK2-mediated mitophagy is involved in regulation of HBEC senescence in COPD pathogenesis. *Autophagy* 11 (2015):547–559. DOI: 10.1080/15548627.2015.1017190.

[112] T. Ahmad, I. K. Sundar, C. A. Lerner, J. Gerloff, A. M. Tormos, H. Yao, and I. Rahman. Impaired mitophagy leads to cigarette smoke stress-induced cellular senescence: implications for chronic obstructive pulmonary disease. *FASEB J* 29 (2015):2912–29. DOI: 10.1096/fj.14-268276.

[113] D. L. DeMeo, T. Mariani, S. Bhattacharya, S. Srisuma, C. Lange, A. Litonjua, R. Bueno, S. G. Pillai, D. A. Lomas, D. Sparrow, S. D. Shapiro, G. J. Criner, H. P. Kim, Z. Chen, A. M. Choi, J. Reilly, and E. K. Silverman. Integration of genomic and genetic approaches implicates IREB2 as a COPD susceptibility gene. *Am J Hum Genet* 85 (2009):493–502. DOI: 10.1016/j.ajhg.2009.09.004.

[114] S. M. Cloonan, K. Glass, M. E. Laucho-Contreras, A. R. Bhashyam, M. Cervo, M. A. Pabon, C. Konrad, F. Polverino, I. Siempos, E. Perez, K. Mizumura, M. C. Ghosh, H. Parameswaran, N. C. Williams, K. T. Rooney, Z. H. Chen, M. P. Goldklang, G. C. Yuan, S. C. Moore, D. L. Demeo, T. A. Rouault, J. M. D'Armiento, E. A. Schon, G. Manfredi, J. Quackenbush, A. Mahmood, E. K. Silverman, C. A. Owen, and A. M. Choi. Mitochondrial iron chelation ameliorates cigarette smoke-

induced bronchitis and emphysema in mice. *Nat Med* 22 (2016):163–74. DOI: 10.1038/nm.4021.

[115] N. Soulitzis, E. Neofytou, M. Psarrou, A. Anagnostis, N. Tavernarakis, N. Siafakas, and E. G. Tzortzaki. Downregulation of lung mitochondrial prohibitin in COPD. *Respir Med* 106 (2012):954–61. DOI: 10.1016/j.rmed.2012.03.019.

[116] B. Even, S. Fayad-Kobeissi, J. M. Gagliolo, R. Motterlini, J. Boczkowski, R. Foresti, and M. Dagouassat. Heme oxygenase-1 induction attenuates senescence in chronic obstructive pulmonary disease lung fibroblasts by protecting against mitochondria dysfunction. *Aging Cell* 17 (2018):e12837. DOI: 10.1111/acel.12837.

[117] A. Rodriguez-Nuevo and A. Zorzano. The sensing of mitochondrial DAMPs by non-immune cells. *Cell Stress* 3 (2019):195–207. DOI: 10.15698/cst2019.06.190.

[118] M. Lommatzsch, S. Cicko, T. Muller, M. Lucattelli, K. Bratke, P. Stoll, M. Grimm, T. Durk, G. Zissel, D. Ferrari, F. Di Virgilio, S. Sorichter, G. Lungarella, J. C. Virchow, and M. Idzko. Extracellular adenosine triphosphate and chronic obstructive pulmonary disease. *Am J Respir Crit Care Med* 181 (2010):928–34. DOI: 10.1164/rccm.200910-1506OC.

[119] W. Z. Zhang, M. C. Rice, K. L. Hoffman, C. Oromendia, I. Barjaktarevic, J. M. Wells, A. T. Hastie, W. W. Labaki, C. B. Cooper, A. P. Comellas, G. J. Criner, J. A. Krishnan, R. Paine Iii, N. N. Hansel, R. P. Bowler, R. G. Barr, S. P. Peters, P. G. Woodruff, J. L. Curtis, M. K. Han, K. V. Ballman, F. J. Martinez, A. M. Choi, K. Nakahira, S. M. Cloonan, and M. E. Choi. Association of urine mitochondrial DNA with clinical measures of COPD in the SPIROMICS cohort. *JCI Insight* (2020). DOI: 10.1172/jci.insight.133984.

[120] W. Z. Zhang, K. L. Hoffman, K. T. Schiffer, C. Oromendia, M. C. Rice, I. Barjaktarevic, S. P. Peters, N. Putcha, R. P. Bowler, J. M. Wells, D. J. Couper, W. W. Labaki, J. L. Curtis, M. K. Han, r. Paine R., P. G. Woodruff, G. J. Criner, N. N. Hansel, I. Diaz, K. V. Ballman, K. Nakahira, M. E. Choi, F. J. Martinez, A. M. K. Choi, and S. M. Cloonan. Association of plasma mitochondrial DNA with COPD severity and progression in the SPIROMICS cohort. *Respir Res* 22 (2021):126. DOI: 10.1186/s12931-021-01707-x.

[121] B. Aravamudan, A. Kiel, M. Freeman, P. Delmotte, M. Thompson, R. Vassallo, G. C. Sieck, C. M. Pabelick, and Y. S. Prakash. Cigarette smoke-induced mitochondrial fragmentation and dysfunction in human airway smooth muscle. *Am J Physiol Lung Cell Mol Physiol* 306 (2014):L840–54. DOI: 10.1152/ajplung.00155.2013.

[122] J. L. Spees, S. D. Olson, M. J. Whitney, and D. J. Prockop. Mitochondrial transfer between cells can rescue aerobic respiration. *Proc Natl Acad Sci U S A* 103 (2006):1283–8. DOI: 10.1073/pnas.0510511103.

[123] M. N. Islam, S. R. Das, M. T. Emin, M. Wei, L. Sun, K. Westphalen, D. J. Rowlands, S. K. Quadri, S. Bhattacharya, and J. Bhattacharya. Mitochondrial transfer from bone-marrow-derived stromal cells to pulmonary alveoli protects against acute lung injury. *Nat Med* 18 (2012):759–65. DOI: 10.1038/nm.2736.

[124] J. A. Nicolas-Avila, A. V. Lechuga-Vieco, L. Esteban-Martinez, M. Sanchez-Diaz, E. Diaz-Garcia, D. J. Santiago, A. Rubio-Ponce, J. L. Li, A. Balachander, J. A.

Quintana, R. Martinez-de Mena, B. Castejon-Vega, A. Pun-Garcia, P. G. Traves, E. Bonzon-Kulichenko, F. Garcia-Marques, L. Cusso, A. G. N, A. Gonzalez-Guerra, M. Roche-Molina, S. Martin-Salamanca, G. Crainiciuc, G. Guzman, J. Larrazabal, E. Herrero-Galan, J. Alegre-Cebollada, G. Lemke, C. V. Rothlin, L. J. Jimenez-Borreguero, G. Reyes, A. Castrillo, M. Desco, P. Munoz-Canoves, B. Ibanez, M. Torres, L. G. Ng, S. G. Priori, H. Bueno, J. Vazquez, M. D. Cordero, J. A. Bernal, J. A. Enriquez, and A. Hidalgo. A Network of Macrophages Supports Mitochondrial Homeostasis in the Heart. *Cell* 183 (2020):94–109 e23. DOI: 10.1016/j.cell.2020.08.031.

[125] T. Ahmad, S. Mukherjee, B. Pattnaik, M. Kumar, S. Singh, M. Kumar, R. Rehman, B. K. Tiwari, K. A. Jha, A. P. Barhanpurkar, M. R. Wani, S. S. Roy, U. Mabalirajan, B. Ghosh, and A. Agrawal. Miro1 regulates intercellular mitochondrial transport & enhances mesenchymal stem cell rescue efficacy. *EMBO J* 33 (2014):994–1010. DOI: 10.1002/embj.201386030.

[126] K. Hayakawa, E. Esposito, X. Wang, Y. Terasaki, Y. Liu, C. Xing, X. Ji, and E. H. Lo. Transfer of mitochondria from astrocytes to neurons after stroke. *Nature* 535 (2016):551–5. DOI: 10.1038/nature18928.

[127] D. G. Phinney, M. Di Giuseppe, J. Njah, E. Sala, S. Shiva, C. M. St Croix, D. B. Stolz, S. C. Watkins, Y. P. Di, G. D. Leikauf, J. Kolls, D. W. Riches, G. Deiuliis, N. Kaminski, S. V. Boregowda, D. H. McKenna, and L. A. Ortiz. Mesenchymal stem cells use extracellular vesicles to outsource mitophagy and shuttle microRNAs. *Nat Commun* 6 (2015):8472. DOI: 10.1038/ncomms9472.

[128] C. G. O'Brien, M. O. Ozen, G. Ikeda, E. Vaskova, J. H. Jung, N. Bayardo, M. R. Santoso, L. Shi, C. Wahlquist, Z. Jiang, Y. Jung, Y. Zeng, E. Egan, R. Sinclair, A. Gee, R. Witteles, M. Mercola, K. J. Svensson, U. Demirci, and P. C. Yang. Mitochondria-Rich Extracellular Vesicles Rescue Patient-Specific Cardiomyocytes From Doxorubicin Injury: Insights Into the SENECA Trial. *JACC CardioOncol* 3 (2021):428–440. DOI: 10.1016/j.jaccao.2021.05.006.

[129] L. Lei and A. C. Spradling. Mouse oocytes differentiate through organelle enrichment from sister cyst germ cells. *Science* 352 (2016):95–99. DOI: 10.1126/science.aad2156.

[130] P. Luz-Crawford, J. Hernandez, F. Djouad, N. Luque-Campos, A. Caicedo, S. Carrere-Kremer, J. M. Brondello, M. L. Vignais, J. Pene, and C. Jorgensen. Mesenchymal stem cell repression of Th17 cells is triggered by mitochondrial transfer. *Stem Cell Res Ther* 10 (2019):232. DOI: 10.1186/s13287-019-1307-9.

[131] M. Poot, Y. Z. Zhang, J. A. Kramer, K. S. Wells, L. J. Jones, D. K. Hanzel, A. G. Lugade, V. L. Singer, and R. P. Haugland. Analysis of mitochondrial morphology and function with novel fixable fluorescent stains. *J Histochem Cytochem* 44 (1996):1363–72. DOI: 10.1177/44.12.8985128.

[132] A. Caicedo, V. Fritz, J. M. Brondello, M. Ayala, I. Dennemont, N. Abdellaoui, F. de Fraipont, A. Moisan, C. A. Prouteau, H. Boukhaddaoui, C. Jorgensen, and M. L. Vignais. MitoCeption as a new tool to assess the effects of mesenchymal stem/stromal cell mitochondria on cancer cell metabolism and function. *Scientific Reports* 5 (2015). DOI: ARTN907310.1038/srep09073.

[133] M. V. Berridge, P. M. Herst, M. R. Rowe, R. Schneider, and M. J. McConnell. Mitochondrial transfer between cells: Methodological constraints in cell culture and animal models. *Anal Biochem* 552 (2018):75–80. DOI: 10.1016/j.ab.2017.11.008.

[134] C. H. Davis, K. Y. Kim, E. A. Bushong, E. A. Mills, D. Boassa, T. Shih, M. Kinebuchi, S. Phan, Y. Zhou, N. A. Bihlmeyer, J. V. Nguyen, Y. Jin, M. H. Ellisman, and N. Marsh-Armstrong. Transcellular degradation of axonal mitochondria. *Proc Natl Acad Sci U S A* 111 (2014):9633–8. DOI: 10.1073/pnas.1404651111.

[135] D. Jiang, F. Gao, Y. Zhang, D. S. Wong, Q. Li, H. F. Tse, G. Xu, Z. Yu, and Q. Lian. Mitochondrial transfer of mesenchymal stem cells effectively protects corneal epithelial cells from mitochondrial damage. *Cell Death Dis* 7 (2016):e2467. DOI: 10.1038/cddis.2016.358.

[136] K. Liu, K. Ji, L. Guo, W. Wu, H. Lu, P. Shan, and C. Yan. Mesenchymal stem cells rescue injured endothelial cells in an in vitro ischemia-reperfusion model via tunneling nanotube like structure-mediated mitochondrial transfer. *Microvasc Res* 92 (2014):10–8. DOI: 10.1016/j.mvr.2014.01.008.

[137] L. F. Dong, J. Kovarova, M. Bajzikova, A. Bezawork-Geleta, D. Svec, B. Endaya, K. Sachaphibulkij, A. R. Coelho, N. Sebkova, A. Ruzickova, A. S. Tan, K. Kluckova, K. Judasova, K. Zamecnikova, Z. Rychtarcikova, V. Gopalan, L. Andera, M. Sobol, B. Yan, B. Pattnaik, N. Bhatraju, J. Truksa, P. Stopka, P. Hozak, A. K. Lam, R. Sedlacek, P. J. Oliveira, M. Kubista, A. Agrawal, K. Dvorakova-Hortova, J. Rohlena, M. V. Berridge, and J. Neuzil. Horizontal transfer of whole mitochondria restores tumorigenic potential in mitochondrial DNA-deficient cancer cells. *Elife* 6 (2017). DOI: 10.7554/eLife.22187.

[138] V. Venegas and M. C. Halberg. Quantification of mtDNA mutation heteroplasmy (ARMS qPCR). *Methods Mol Biol* 837 (2012):313–26. DOI: 10.1007/978-1-61779-504-6_21.

[139] A. Acquistapace, T. Bru, P. F. Lesault, F. Figeac, A. E. Coudert, O. le Coz, C. Christov, X. Baudin, F. Auber, R. Yiou, J. L. Dubois-Rande, and A. M. Rodriguez. Human Mesenchymal Stem Cells Reprogram Adult Cardiomyocytes Toward a Progenitor-Like State Through Partial Cell Fusion and Mitochondria Transfer. *Stem Cells* 29 (2011):812–824. DOI: 10.1002/stem.632.

[140] X. Li, Y. Zhang, S. C. Yeung, Y. Liang, X. Liang, Y. Ding, M. S. Ip, H. F. Tse, J. C. Mak, and Q. Lian. Mitochondrial transfer of induced pluripotent stem cell-derived mesenchymal stem cells to airway epithelial cells attenuates cigarette smoke-induced damage. *Am J Respir Cell Mol Biol* 51 (2014):455–65. DOI: 10.1165/rcmb.2013-0529OC.

[141] Y. Zhang, Z. Yu, D. Jiang, X. Liang, S. Liao, Z. Zhang, W. Yue, X. Li, S. M. Chiu, Y. H. Chai, Y. Liang, Y. Chow, S. Han, A. Xu, H. F. Tse, and Q. Lian. iPSC-MSCs with High Intrinsic MIRO1 and Sensitivity to TNF-alpha Yield Efficacious Mitochondrial Transfer to Rescue Anthracycline-Induced Cardiomyopathy. *Stem Cell Reports* 7 (2016):749–763. DOI: 10.1016/j.stemcr.2016.08.009.

[142] E. Y. Plotnikov, T. G. Khryapenkova, A. K. Vasileva, M. V. Marey, S. I. Galkina, N. K. Isaev, E. V. Sheval, V. Y. Polyakov, G. T. Sukhikh, and D. B. Zorov. Cell-to-cell cross-talk between mesenchymal stem cells and cardiomyocytes in co-culture. *J Cell Mol Med* 12 (2008):1622–31. DOI: 10.1111/j.1582-4934.2007.00205.x.

[143] X. Li, C. Michaeloudes, Y. Zhang, C. H. Wiegman, I. M. Adcock, Q. Lian, J. C. W. Mak, P. K. Bhavsar, and K. F. Chung. Mesenchymal stem cells alleviate oxidative stress-induced mitochondrial dysfunction in the airways. *J Allergy Clin Immunol* (2017). DOI: 10.1016/j.jaci.2017.08.017.

[144] H. Li, C. Wang, T. He, T. Zhao, Y. Y. Chen, Y. L. Shen, X. Zhang, and L. L. Wang. Mitochondrial Transfer from Bone Marrow Mesenchymal Stem Cells to Motor Neurons in Spinal Cord Injury Rats via Gap Junction. *Theranostics* 9 (2019):2017–2035. DOI: 10.7150/thno.29400.

[145] J. R. Brestoff, C. B. Wilen, J. R. Moley, Y. Li, W. Zou, N. P. Malvin, M. N. Rowen, B. T. Saunders, H. Ma, M. R. Mack, J. Hykes B. L., D. R. Balce, A. Orvedahl, J. W. Williams, N. Rohatgi, X. Wang, M. R. McAllaster, S. A. Handley, B. S. Kim, J. G. Doench, B. H. Zinselmeyer, M. S. Diamond, H. W. Virgin, A. E. Gelman, and S. L. Teitelbaum. Intercellular Mitochondria Transfer to Macrophages Regulates White Adipose Tissue Homeostasis and Is Impaired in Obesity. *Cell Metab* (2020). DOI: 10.1016/j.cmet.2020.11.008.

[146] L. Peruzzotti-Jametti, J. D. Bernstock, C. M. Willis, G. Manferrari, R. Rogall, E. Fernandez-Vizarra, J. C. Williamson, A. Braga, A. van den Bosch, T. Leonardi, G. Krzak, A. Kittel, C. Beninca, N. Vicario, S. Tan, C. Bastos, I. Bicci, N. Iraci, J. A. Smith, B. Peacock, K. H. Muller, P. J. Lehner, E. I. Buzas, N. Faria, M. Zeviani, C. Frezza, A. Brisson, N. J. Matheson, C. Viscomi, and S. Pluchino. Neural stem cells traffic functional mitochondria via extracellular vesicles. *PLoS Biol* 19 (2021):e3001166. DOI: 10.1371/journal.pbio.3001166.

[147] R. Moschoi, V. Imbert, M. Nebout, J. Chiche, D. Mary, T. Prebet, E. Saland, R. Castellano, L. Pouyet, Y. Collette, N. Vey, C. Chabannon, C. Recher, J. E. Sarry, D. Alcor, J. F. Peyron, and E. Griessinger. Protective mitochondrial transfer from bone marrow stromal cells to acute myeloid leukemic cells during chemotherapy. *Blood* 128 (2016):253–64. DOI: 10.1182/blood-2015-07-655860.

[148] C. R. Marlein, L. Zaitseva, R. E. Piddock, S. D. Robinson, D. R. Edwards, M. S. Shafat, Z. Zhou, M. Lawes, K. M. Bowles, and S. A. Rushworth. NADPH oxidase-2 derived superoxide drives mitochondrial transfer from bone marrow stromal cells to leukemic blasts. *Blood* 130 (2017):1649–1660. DOI: 10.1182/blood-2017-03-772939.

[149] T. Saha, C. Dash, R. Jayabalan, S. Khiste, A. Kulkarni, K. Kurmi, J. Mondal, P. K. Majumder, A. Bardia, H. L. Jang, and S. Sengupta. Intercellular nanotubes mediate mitochondrial trafficking between cancer and immune cells. *Nat Nanotechnol* (2021). DOI: 10.1038/s41565-021-01000-4.

[150] C. Crewe, J. B. Funcke, S. Li, N. Joffin, C. M. Gliniak, A. L. Ghaben, Y. A. An, H. A. Sadek, R. Gordillo, Y. Akgul, S. Chen, D. Samovski, P. Fischer-Posovszky, C. M. Kusminski, S. Klein, and P. E. Scherer. Extracellular vesicle-based interorgan

transport of mitochondria from energetically stressed adipocytes. *Cell Metab* 33 (2021):1853–1868 e11. DOI: 10.1016/j.cmet.2021.08.002.

[151] K. C. Vallabhaneni, H. Haller, and I. Dumler. Vascular smooth muscle cells initiate proliferation of mesenchymal stem cells by mitochondrial transfer via tunneling nanotubes. *Stem Cells Dev* 21 (2012):3104–13. DOI: 10.1089/scd.2011.0691.

[152] Y. Guo, X. Chi, Y. Wang, B. C. Heng, Y. Wei, X. Zhang, H. Zhao, Y. Yin, and X. Deng. Mitochondria transfer enhances proliferation, migration, and osteogenic differentiation of bone marrow mesenchymal stem cell and promotes bone defect healing. *Stem Cell Res Ther* 11 (2020):245. DOI: 10.1186/s13287-020-01704-9.

[153] X. Wang and H. H. Gerdes. Transfer of mitochondria via tunneling nanotubes rescues apoptotic PC12 cells. *Cell Death Differ* 22 (2015):1181–91. DOI: 10.1038/cdd.2014.211.

[154] T. J. Morrison, M. V. Jackson, E. K. Cunningham, A. Kissenpfennig, D. F. McAuley, C. M. O'Kane, and A. D. Krasnodembskaya. Mesenchymal Stromal Cells Modulate Macrophages in Clinically Relevant Lung Injury Models by Extracellular Vesicle Mitochondrial Transfer. *Am J Respir Crit Care Med* 196 (2017):1275–1286. DOI: 10.1164/rccm.201701-0170OC.

[155] S. Abounit and C. Zurzolo. Wiring through tunneling nanotubes–from electrical signals to organelle transfer. *J Cell Sci* 125 (2012):1089–98. DOI: 10.1242/jcs.083279.

[156] M. L. Vignais, A. Caicedo, J. M. Brondello, and C. Jorgensen. Cell Connections by Tunneling Nanotubes: Effects of Mitochondrial Trafficking on Target Cell Metabolism, Homeostasis, and Response to Therapy. *Stem Cells Int* 2017 (2017):6917941. DOI: 10.1155/2017/6917941.

[157] B. Onfelt, S. Nedvetzki, R. K. Benninger, M. A. Purbhoo, S. Sowinski, A. N. Hume, M. C. Seabra, M. A. Neil, P. M. French, and D. M. Davis. Structurally distinct membrane nanotubes between human macrophages support long-distance vesicular traffic or surfing of bacteria. *J Immunol* 177 (2006):8476–83. DOI: 10.4049/jimmunol.177.12.8476.

[158] J. Shen, J. H. Zhang, H. Xiao, J. M. Wu, K. M. He, Z. Z. Lv, Z. J. Li, M. Xu, and Y. Y. Zhang. Mitochondria are transported along microtubules in membrane nanotubes to rescue distressed cardiomyocytes from apoptosis. *Cell Death Dis* 9 (2018):81. DOI: 10.1038/s41419-017-0145-x.

[159] G. Turturici, R. Tinnirello, G. Sconzo, and F. Geraci. Extracellular membrane vesicles as a mechanism of cell-to-cell communication: advantages and disadvantages. *American Journal of Physiology-Cell Physiology* 306 (2014):C621–C633. DOI: 10.1152/ajpcell.00228.2013.

[160] K. P. Hough, J. L. Trevor, J. G. Strenkowski, Y. Wang, B. K. Chacko, S. Tousif, D. Chanda, C. Steele, V. B. Antony, T. Dokland, X. Ouyang, J. Zhang, S. R. Duncan, V. J. Thannickal, V. M. Darley-Usmar, and J. S. Deshane. Exosomal transfer of mitochondria from airway myeloid-derived regulatory cells to T cells. *Redox Biol* 18 (2018):54–64. DOI: 10.1016/j.redox.2018.06.009.

[161] E. Letsiou, L. G. Teixeira Alves, D. Fatykhova, M. Felten, T. J. Mitchell, H. C. Muller-Redetzky, A. C. Hocke, and M. Witzenrath. Microvesicles released from pneumolysin-stimulated lung epithelial cells carry mitochondrial cargo and suppress neutrophil oxidative burst. *Sci Rep* 11 (2021):9529. DOI: 10.1038/s41598-021-88897-y.

[162] D. Patel, J. Rorbach, K. Downes, M. J. Szukszto, M. L. Pekalski, and M. Minczuk. Macropinocytic entry of isolated mitochondria in epidermal growth factor-activated human osteosarcoma cells. *Sci Rep* 7 (2017):12886. DOI: 10.1038/s41598-017-13227-0.

[163] Z. Al Amir Dache, A. Otandault, R. Tanos, B. Pastor, R. Meddeb, C. Sanchez, G. Arena, L. Lasorsa, A. Bennett, T. Grange, S. El Messaoudi, T. Mazard, C. Prevostel, and A. R. Thierry. Blood contains circulating cell-free respiratory competent mitochondria. *FASEB J* 34 (2020):3616–3630. DOI: 10.1096/fj.201901917RR.

[164] M. Osswald, E. Jung, F. Sahm, G. Solecki, V. Venkataramani, J. Blaes, S. Weil, H. Horstmann, B. Wiestler, M. Syed, L. Huang, M. Ratliff, K. Karimian Jazi, F. T. Kurz, T. Schmenger, D. Lemke, M. Gommel, M. Pauli, Y. Liao, P. Haring, S. Pusch, V. Herl, C. Steinhauser, D. Krunic, M. Jarahian, H. Miletic, A. S. Berghoff, O. Griesbeck, G. Kalamakis, O. Garaschuk, M. Preusser, S. Weiss, H. Liu, S. Heiland, M. Platten, P. E. Huber, T. Kuner, A. von Deimling, W. Wick, and F. Winkler. Brain tumour cells interconnect to a functional and resistant network. *Nature* 528 (2015):93–8. DOI: 10.1038/nature16071.

[165] M. V. Jackson, T. J. Morrison, D. F. Doherty, D. F. Mcauley, M. A. Matthay, A. Kissenpfennig, C. M. O'Kane, and A. D. Krasnodembskaya. Mitochondrial Transfer via Tunneling Nanotubes is an Important Mechanism by Which Mesenchymal Stem Cells Enhance Macrophage Phagocytosis in the In Vitro and In Vivo Models of ARDS. *Stem Cells* 34 (2016):2210–2223. DOI: 10.1002/stem.2372.

[166] C. J. Li, P. K. Chen, L. Y. Sun, and C. Y. Pang. Enhancement of Mitochondrial Transfer by Antioxidants in Human Mesenchymal Stem Cells. *Oxid Med Cell Longev* 2017 (2017):8510805. DOI: 10.1155/2017/8510805.

[167] J. Pasquier, B. S. Guerrouahen, H. Al Thawadi, P. Ghiabi, M. Maleki, N. Abu-Kaoud, A. Jacob, M. Mirshahi, L. Galas, S. Rafii, F. Le Foll, and A. Rafii. Preferential transfer of mitochondria from endothelial to cancer cells through tunneling nanotubes modulates chemoresistance. *J Transl Med* 11 (2013):94. DOI: 10.1186/1479-5876-11-94.

[168] V. Venegas and M. C. Halberg. Measurement of mitochondrial DNA copy number. *Methods Mol Biol* 837 (2012):327–35. DOI: 10.1007/978-1-61779-504-6_22.

[169] G. Forni, G. Puccio, T. Bourguignon, T. Evans, B. Mantovani, O. Rota-Stabelli, and A. Luchetti. Complete mitochondrial genomes from transcriptomes: assessing pros and cons of data mining for assembling new mitogenomes. *Sci Rep* 9 (2019):14806. DOI: 10.1038/s41598-019-51313-7.

[170] D. S. Fay and K. Gerow. A biologist's guide to statistical thinking and analysis. *WormBook* (2013):1–54. DOI: 10.1895/wormbook.1.159.1.

[171] F. Hollins, A. Sutcliffe, E. Gomez, R. Berair, R. Russell, C. Szyndralewiez, R. Saunders, and C. Brightling. Airway smooth muscle NOX4 is upregulated and modulates ROS generation in COPD. *Respiratory Research* 17 (2016). DOI: ARTN8410.1186/s12931-016-0403-y.

[172] N. Banzet, D. Francois, and B. S. Polla. Tobacco smoke induces mitochondrial depolarization along with cell death: effects of antioxidants. *Redox Rep* 4 (1999):229–36. DOI: 10.1179/135100099101534945.

[173] A. R. Agarwal, L. Zhao, H. Sancheti, I. K. Sundar, I. Rahman, and E. Cadenas. Short-term cigarette smoke exposure induces reversible changes in energy metabolism and cellular redox status independent of inflammatory responses in mouse lungs. *Am J Physiol Lung Cell Mol Physiol* 303 (2012):L889–98. DOI: 10.1152/ajplung.00219.2012.

[174] F. Cardellach, J. R. Alonso, S. Lopez, J. Casademont, and O. Miro. Effect of smoking cessation on mitochondrial respiratory chain function. *J Toxicol Clin Toxicol* 41 (2003):223–8. DOI: 10.1081/clt-120021102.

[175] E. S. Davis, M. F. Sassano, H. Goodell, and R. Tarran. E-Liquid Autofluorescence can be used as a Marker of Vaping Deposition and Third-Hand Vape Exposure. *Sci Rep* 7 (2017):7459. DOI: 10.1038/s41598-017-07862-w.

[176] A. C. Rego, S. Vesce, and D. G. Nicholls. The mechanism of mitochondrial membrane potential retention following release of cytochrome c in apoptotic GT1-7 neural cells. *Cell Death Differ* 8 (2001):995–1003. DOI: 10.1038/sj.cdd.4400916.

[177] J. Szczepanowska, D. Malinska, M. R. Wieckowski, and J. Duszynski. Effect of mtDNA point mutations on cellular bioenergetics. *Biochim Biophys Acta* 1817 (2012):1740–6. DOI: 10.1016/j.bbabio.2012.02.028.

[178] N. Miyake, S. Yano, C. Sakai, H. Hatakeyama, Y. Matsushima, M. Shiina, Y. Watanabe, J. Bartley, J. E. Abdenur, R. Y. Wang, R. Chang, Y. Tsurusaki, H. Doi, M. Nakashima, H. Saitsu, K. Ogata, Y. Goto, and N. Matsumoto. Mitochondrial complex III deficiency caused by a homozygous UQCRC2 mutation presenting with neonatal-onset recurrent metabolic decompensation. *Hum Mutat* 34 (2013):446–52. DOI: 10.1002/humu.22257.

[179] S. Zheng, C. Wang, G. Qian, G. Wu, R. Guo, Q. Li, Y. Chen, J. Li, H. Li, B. He, H. Chen, and F. Ji. Role of mtDNA haplogroups in COPD susceptibility in a southwestern Han Chinese population. *Free Radic Biol Med* 53 (2012):473–81. DOI: 10.1016/j.freeradbiomed.2012.05.019.

[180] P. M. Herst, A. S. Tan, D. J. Scarlett, and M. V. Berridge. Cell surface oxygen consumption by mitochondrial gene knockout cells. *Biochim Biophys Acta* 1656 (2004):79–87. DOI: 10.1016/j.bbabio.2004.01.008.

[181] K. Bedard and K. H. Krause. The NOX family of ROS-generating NADPH oxidases: physiology and pathophysiology. *Physiol Rev* 87 (2007):245–313. DOI: 10.1152/physrev.00044.2005.

[182] A. Lewinska, M. Wnuk, E. Slota, and G. Bartosz. Total anti-oxidant capacity of cell culture media. *Clin Exp Pharmacol Physiol* 34 (2007):781–6. DOI: 10.1111/j.1440-1681.2007.04637.x.

[183] S. S. Korshunov, V. P. Skulachev, and A. A. Starkov. High protonic potential actuates a mechanism of production of reactive oxygen species in mitochondria. *FEBS Lett* 416 (1997):15–8. DOI: 10.1016/s0014-5793(97)01159-9.

[184] C. M. Harrison, M. Pompilius, K. E. Pinkerton, and S. W. Ballinger. Mitochondrial oxidative stress significantly influences atherogenic risk and cytokine-induced oxidant production. *Environ Health Perspect* 119 (2011):676–81. DOI: 10.1289/ehp.1002857.

[185] C. Michaeloudes, M. B. Sukkar, N. M. Khorasani, P. K. Bhavsar, and K. F. Chung. TGF-beta regulates Nox4, MnSOD and catalase expression, and IL-6 release in airway smooth muscle cells. *Am J Physiol Lung Cell Mol Physiol* 300 (2011):L295–304. DOI: 10.1152/ajplung.00134.2010.

[186] A. R. Agarwal, F. Yin, and E. Cadenas. Metabolic shift in lung alveolar cell mitochondria following acrolein exposure. *Am J Physiol Lung Cell Mol Physiol* 305 (2013):L764–73. DOI: 10.1152/ajplung.00165.2013.

[187] R. Kasiviswanathan, I. G. Minko, R. S. Lloyd, and W. C. Copeland. Translesion synthesis past acrolein-derived DNA adducts by human mitochondrial DNA polymerase gamma. *J Biol Chem* 288 (2013):14247–14255. DOI: 10.1074/jbc.M113.458802.

[188] M. Shen, L. Zhang, M. R. Bonner, C. S. Liu, G. Li, R. Vermeulen, M. Dosemeci, S. Yin, and Q. Lan. Association between mitochondrial DNA copy number, blood cell counts, and occupational benzene exposure. *Environ Mol Mutagen* 49 (2008):453–7. DOI: 10.1002/em.20402.

[189] B. Prokopczyk, D. Hoffmann, M. Bologna, A. J. Cunningham, N. Trushin, S. Akerkar, T. Boyiri, S. Amin, D. Desai, S. Colosimo, B. Pittman, G. Leder, M. Ramadani, D. Henne-Bruns, H. G. Beger, and K. El-Bayoumy. Identification of tobacco-derived compounds in human pancreatic juice. *Chem Res Toxicol* 15 (2002):677–85. DOI: 10.1021/tx0101088.

[190] I. H. Heijink, J. A. Noordhoek, W. Timens, A. J. van Oosterhout, and D. S. Postma. Abnormalities in airway epithelial junction formation in chronic obstructive pulmonary disease. *Am J Respir Crit Care Med* 189 (2014):1439–42. DOI: 10.1164/rccm.201311-1982LE.

[191] R. L. Jones, P. B. Noble, J. G. Elliot, and A. L. James. Airway remodelling in COPD: It's not asthma! *Respirology* 21 (2016):1347–1356. DOI: 10.1111/resp.12841.

[192] R. Annoni, T. Lancas, R. Yukimatsu Tanigawa, M. de Medeiros Matsushita, S. de Morais Fernezlian, A. Bruno, L. Fernando Ferraz da Silva, P. J. Roughley, S. Battaglia, M. Dolhnikoff, P. S. Hiemstra, P. J. Sterk, K. F. Rabe, and T. Mauad. Extracellular matrix composition in COPD. *Eur Respir J* 40 (2012):1362–73. DOI: 10.1183/09031936.00192611.

[193] G. Burgstaller, B. Oehrle, M. Gerckens, E. S. White, H. B. Schiller, and O. Eickelberg. The instructive extracellular matrix of the lung: basic composition and alterations in chronic lung disease. *Eur Respir J* 50 (2017). DOI: 10.1183/13993003.01805-2016.

[194] T. Pera, R. Gosens, A. H. Lesterhuis, R. Sami, M. van der Toorn, J. Zaagsma, and H. Meurs. Cigarette smoke and lipopolysaccharide induce a proliferative airway smooth muscle phenotype. *Respir Res* 11 (2010):48. DOI: 10.1186/1465-9921-11-48.

[195] P. Guan, W. Cai, H. Yu, Z. Wu, W. Li, J. Wu, J. Chen, and G. Feng. Cigarette smoke extract promotes proliferation of airway smooth muscle cells through suppressing C/EBP-alpha expression. *Exp Ther Med* 13 (2017):1408–1414. DOI: 10.3892/etm.2017.4126.

[196] M. Pavel, M. Renna, S. J. Park, F. M. Menzies, T. Ricketts, J. Fullgrabe, A. Ashkenazi, R. A. Frake, A. C. Lombarte, C. F. Bento, K. Franze, and D. C. Rubinsztein. Contact inhibition controls cell survival and proliferation via YAP/TAZ-autophagy axis. *Nat Commun* 9 (2018):2961. DOI: 10.1038/s41467-018-05388-x.

[197] J. Fu, M. Zheng, X. Zhang, Y. Zhang, Y. Chen, H. Li, X. Wang, and J. Zhang. Fibulin-5 promotes airway smooth muscle cell proliferation and migration via modulating Hippo-YAP/TAZ pathway. *Biochem Biophys Res Commun* 493 (2017):985–991. DOI: 10.1016/j.bbrc.2017.09.105.

[198] P. K. Davis, A. Ho, and S. F. Dowdy. Biological methods for cell-cycle synchronization of mammalian cells. *Biotechniques* 30 (2001):1322–6, 1328, 1330–1. DOI: 10.2144/01306rv01.

[199] A. Churg, S. Zhou, and J. L. Wright. Series "matrix metalloproteinases in lung health and disease": Matrix metalloproteinases in COPD. *Eur Respir J* 39 (2012):197–209. DOI: 10.1183/09031936.00121611.

[200] K. Imai, S. S. Dalal, E. S. Chen, R. Downey, L. L. Schulman, M. Ginsburg, and J. D'Armiento. Human collagenase (matrix metalloproteinase-1) expression in the lungs of patients with emphysema. *Am J Respir Crit Care Med* 163 (2001):786–91. DOI: 10.1164/ajrccm.163.3.2001073.

[201] S. U. Naveed, D. Clements, D. J. Jackson, C. Philp, C. K. Billington, I. Soomro, C. Reynolds, T. W. Harrison, S. L. Johnston, D. E. Shaw, and S. R. Johnson. Matrix Metalloproteinase-1 Activation Contributes to Airway Smooth Muscle Growth and Asthma Severity. *Am J Respir Crit Care Med* 195 (2017):1000–1009. DOI: 10.1164/rccm.201604-0822OC.

[202] N. K. Rogers, D. Clements, A. Dongre, T. W. Harrison, D. Shaw, and S. R. Johnson. Extra-cellular matrix proteins induce matrix metalloproteinase-1 (MMP-1) activity and increase airway smooth muscle contraction in asthma. *PLoS One* 9 (2014):e90565. DOI: 10.1371/journal.pone.0090565.

[203] J. Winkler, A. Abisoye-Ogunniyan, K. J. Metcalf, and Z. Werb. Concepts of extracellular matrix remodelling in tumour progression and metastasis. *Nat Commun* 11 (2020):5120. DOI: 10.1038/s41467-020-18794-x.

[204] J. Merl-Pham, T. Basak, L. Knuppel, D. Ramanujam, M. Athanason, J. Behr, S. Engelhardt, O. Eickelberg, S. M. Hauck, R. Vanacore, and C. A. Staab-Weijnitz. Quantitative proteomic profiling of extracellular matrix and site-specific collagen post-translational modifications in an in vitro model of lung fibrosis. *Matrix Biol Plus* 1 (2019):100005. DOI: 10.1016/j.mbplus.2019.04.002.

[205] A. L. Hellewell, S. Rosini, and J. C. Adams. A Rapid, Scalable Method for the Isolation, Functional Study, and Analysis of Cell-derived Extracellular Matrix. *J Vis Exp* (2017). DOI: 10.3791/55051.

[206] H. S. Nam, E. Izumchenko, S. Dasgupta, and M. O. Hoque. Mitochondria in chronic obstructive pulmonary disease and lung cancer: where are we now? *Biomark Med* 11 (2017):475–489. DOI: 10.2217/bmm-2016-0373.

[207] G. Baffy, Z. Derdak, and S. C. Robson. Mitochondrial recoupling: a novel therapeutic strategy for cancer? *Br J Cancer* 105 (2011):469–74. DOI: 10.1038/bjc.2011.245.

[208] C. H. Yao, R. Wang, Y. Wang, C. P. Kung, J. D. Weber, and G. J. Patti. Mitochondrial fusion supports increased oxidative phosphorylation during cell proliferation. *Elife* 8 (2019). DOI: 10.7554/eLife.41351.

[209] L. Diebold and N. S. Chandel. Mitochondrial ROS regulation of proliferating cells. *Free Radic Biol Med* 100 (2016):86–93. DOI: 10.1016/j.freeradbiomed.2016.04.198.

[210] K. M. Connor, S. Subbaram, K. J. Regan, K. K. Nelson, J. E. Mazurkiewicz, P. J. Bartholomew, A. E. Aplin, Y. T. Tai, J. Aguirre-Ghiso, S. C. Flores, and J. A. Melendez. Mitochondrial H2O2 regulates the angiogenic phenotype via PTEN oxidation. *J Biol Chem* 280 (2005):16916–24. DOI: 10.1074/jbc.M410690200.

[211] C. Vaamonde-Garcia, R. R. Riveiro-Naveira, M. N. Valcarcel-Ares, L. Hermida-Carballo, F. J. Blanco, and M. J. Lopez-Armada. Mitochondrial dysfunction increases inflammatory responsiveness to cytokines in normal human chondrocytes. *Arthritis Rheum* 64 (2012):2927–36. DOI: 10.1002/art.34508.

[212] B. Dib, H. J. Lin, D. E. Maidana, B. Tian, J. B. Miller, P. Bouzika, J. W. Miller, and D. G. Vavvas. Mitochondrial DNA has a pro-inflammatory role in AMD. *Biochimica Et Biophysica Acta-Molecular Cell Research* 1853 (2015):2897–2906. DOI: 10.1016/j.bbamcr.2015.08.012.

[213] J. Dutra Silva, Y. Su, C. S. Calfee, K. L. Delucchi, D. Weiss, D. F. McAuley, C. O'Kane, and A. D. Krasnodembskaya. Mesenchymal stromal cell extracellular vesicles rescue mitochondrial dysfunction and improve barrier integrity in clinically relevant models of ARDS. *Eur Respir J* 58 (2021). DOI: 10.1183/13993003.02978-2020.

[214] Y. Yao, X. L. Fan, D. Jiang, Y. Zhang, X. Li, Z. B. Xu, S. B. Fang, S. Chiu, H. F. Tse, Q. Lian, and Q. L. Fu. Connexin 43-Mediated Mitochondrial Transfer of iPSC-MSCs Alleviates Asthma Inflammation. *Stem Cell Reports* 11 (2018):1120–1135. DOI: 10.1016/j.stemcr.2018.09.012.

[215] L. A. Kane, M. Lazarou, A. I. Fogel, Y. Li, K. Yamano, S. A. Sarraf, S. Banerjee, and R. J. Youle. PINK1 phosphorylates ubiquitin to activate Parkin E3 ubiquitin ligase activity. *J Cell Biol* 205 (2014):143–53. DOI: 10.1083/jcb.201402104.

[216] D. W. Summers, A. DiAntonio, and J. Milbrandt. Mitochondrial dysfunction induces Sarm1-dependent cell death in sensory neurons. *J Neurosci* 34 (2014):9338–50. DOI: 10.1523/JNEUROSCI.0877-14.2014.

[217] K. Golan, A. K. Singh, O. Kollet, M. Bertagna, M. J. Althoff, E. Khatib-Massalha, E. Petrovich-Kopitman, A. M. Wellendorf, H. Massalha, S. Levin-Zaidman, T. Dadosh, B. Bohan, V. G. M, B. Dasgupta, T. Lapidot, and J. A. Cancelas. Bone marrow regeneration requires mitochondrial transfer from donor Cx43-expressing hematopoietic progenitors to stroma. *Blood* 136 (2020):2607–2619. DOI: 10.1182/blood.2020005399.

[218] K. A. Sinclair, S. T. Yerkovich, P. M. Hopkins, and D. C. Chambers. Characterization of intercellular communication and mitochondrial donation by mesenchymal stromal cells derived from the human lung. *Stem Cell Res Ther* 7 (2016):91. DOI: 10.1186/s13287-016-0354-8.

[219] M. Mahrouf-Yorgov, L. Augeul, C. C. Da Silva, M. Jourdan, M. Rigolet, S. Manin, R. Ferrera, M. Ovize, A. Henry, A. Guguin, J. P. Meningaud, J. L. Dubois-Rande, R. Motterlini, R. Foresti, and A. M. Rodriguez. Mesenchymal stem cells sense mitochondria released from damaged cells as danger signals to activate their rescue properties. *Cell Death and Differentiation* 24 (2017):1224–1238. DOI: 10.1038/cdd.2017.51.

[220] P. M. McClatchey, A. C. Keller, R. Bouchard, L. A. Knaub, and J. E. Reusch. Fully automated software for quantitative measurements of mitochondrial morphology. *Mitochondrion* 26 (2016):58–71. DOI: 10.1016/j.mito.2015.12.003.

[221] C. C. Polo, M. H. Fonseca-Alaniz, J. H. Chen, A. Ekman, G. McDermott, F. Meneau, J. E. Krieger, and A. A. Miyakawa. Three-dimensional imaging of mitochondrial cristae complexity using cryo-soft X-ray tomography. *Sci Rep* 10 (2020):21045. DOI: 10.1038/s41598-020-78150-3.

[222] E. Macia, M. Ehrlich, R. Massol, E. Boucrot, C. Brunner, and T. Kirchhausen. Dynasore, a cell-permeable inhibitor of dynamin. *Dev Cell* 10 (2006):839–50. DOI: 10.1016/j.devcel.2006.04.002.

[223] C. Thery et al. Minimal information for studies of extracellular vesicles 2018 (MISEV2018): a position statement of the International Society for Extracellular Vesicles and update of the MISEV2014 guidelines. *J Extracell Vesicles* 7 (2018):1535750. DOI: 10.1080/20013078.2018.1535750.

[224] S. Gurke, J. F. V. Barroso, E. Hodneland, N. V. Bukoreshtliev, O. Schlicker, and H. H. Gerdes. Tunneling nanotube (TNT)-like structures facilitate a constitutive, actomyosin-dependent exchange of endocytic organelles between normal rat kidney cells. *Experimental Cell Research* 314 (2008):3669–3683. DOI: 10.1016/j.yexcr.2008.08.022.

[225] N. V. Bukoreshtliev, X. Wang, E. Hodneland, S. Gurke, J. F. V. Barroso, and H. H. Gerdes. Selective block of tunneling nanotube (TNT) formation inhibits

intercellular organelle transfer between PC12 cells. *Febs Letters* 583 (2009):1481–1488. DOI: 10.1016/j.febslet.2009.03.065.

[226] H. R. Chinnery, E. Pearlman, and P. G. McMenamin. Cutting edge: Membrane nanotubes in vivo: a feature of MHC class II+ cells in the mouse cornea. *J Immunol* 180 (2008):5779–83. DOI: 10.4049/jimmunol.180.9.5779.

[227] H. Lee, D. Zhang, Z. Zhu, C. S. Dela Cruz, and Y. Jin. Epithelial cell-derived microvesicles activate macrophages and promote inflammation via microvesicle-containing microRNAs. *Sci Rep* 6 (2016):35250. DOI: 10.1038/srep35250.

[228] K. R. Genschmer, D. W. Russell, C. Lal, T. Szul, P. E. Bratcher, B. D. Noerager, M. Abdul Roda, X. Xu, G. Rezonzew, L. Viera, B. S. Dobosh, C. Margaroli, T. H. Abdalla, R. W. King, C. M. McNicholas, J. M. Wells, M. T. Dransfield, R. Tirouvanziam, A. Gaggar, and J. E. Blalock. Activated PMN Exosomes: Pathogenic Entities Causing Matrix Destruction and Disease in the Lung. *Cell* 176 (2019):113–126 e15. DOI: 10.1016/j.cell.2018.12.002.

[229] S. Y. Kim, J. H. Lee, H. J. Kim, M. K. Park, J. W. Huh, J. Y. Ro, Y. M. Oh, S. D. Lee, and Y. S. Lee. Mesenchymal stem cell-conditioned media recovers lung fibroblasts from cigarette smoke-induced damage. *Am J Physiol Lung Cell Mol Physiol* 302 (2012):L891–908. DOI: 10.1152/ajplung.00288.2011.

[230] T. R. Doeppner, J. Herz, A. Gorgens, J. Schlechter, A. K. Ludwig, S. Radtke, K. de Miroschedji, P. A. Horn, B. Giebel, and D. M. Hermann. Extracellular Vesicles Improve Post-Stroke Neuroregeneration and Prevent Postischemic Immunosuppression. *Stem Cells Transl Med* 4 (2015):1131–43. DOI: 10.5966/sctm.2015-0078.

[231] H. Ni, S. Yang, F. Siaw-Debrah, J. Hu, K. Wu, Z. He, J. Yang, S. Pan, X. Lin, H. Ye, Z. Xu, F. Wang, K. Jin, Q. Zhuge, and L. Huang. Exosomes Derived From Bone Mesenchymal Stem Cells Ameliorate Early Inflammatory Responses Following Traumatic Brain Injury. *Front Neurosci* 13 (2019):14. DOI: 10.3389/fnins.2019.00014.

[232] L. B. Shao, Y. Zhang, B. B. Lan, J. J. Wang, Z. W. Zhang, L. L. Zhang, P. L. Xiao, Q. Y. Meng, Y. J. Geng, X. Y. Yu, and Y. X. Li. MiRNA-Sequence Indicates That Mesenchymal Stem Cells and Exosomes Have Similar Mechanism to Enhance Cardiac Repair. *Biomed Research International* 2017 (2017). DOI: Artn415070510.1155/2017/4150705.

[233] D. Feller, J. Kun, I. Ruzsics, J. Rapp, V. Sarosi, K. Kvell, Z. Helyes, and J. E. Pongracz. Cigarette Smoke-Induced Pulmonary Inflammation Becomes Systemic by Circulating Extracellular Vesicles Containing Wnt5a and Inflammatory Cytokines. *Front Immunol* 9 (2018):1724. DOI: 10.3389/fimmu.2018.01724.

[234] S. Gandham, X. Su, J. Wood, A. L. Nocera, S. C. Alli, L. Milane, A. Zimmerman, M. Amiji, and A. R. Ivanov. Technologies and Standardization in Research on Extracellular Vesicles. *Trends Biotechnol* 38 (2020):1066–1098. DOI: 10.1016/j.tibtech.2020.05.012.

[235] R. Sahu, S. Kaushik, C. C. Clement, E. S. Cannizzo, B. Scharf, A. Follenzi, I. Potolicchio, E. Nieves, A. M. Cuervo, and L. Santambrogio. Microautophagy of

cytosolic proteins by late endosomes. *Dev Cell* 20 (2011):131–9. DOI: 10.1016/j.devcel.2010.12.003.

[236] A. I. May, M. Prescott, and Y. Ohsumi. Autophagy facilitates adaptation of budding yeast to respiratory growth by recycling serine for one-carbon metabolism. *Nat Commun* 11 (2020):5052. DOI: 10.1038/s41467-020-18805-x.

[237] A. Kuma and N. Mizushima. Physiological role of autophagy as an intracellular recycling system: with an emphasis on nutrient metabolism. *Semin Cell Dev Biol* 21 (2010):683–90. DOI: 10.1016/j.semcdb.2010.03.002.

[238] L. H. Boudreau, A. C. Duchez, N. Cloutier, D. Soulet, N. Martin, J. Bollinger, A. Pare, M. Rousseau, G. S. Naika, T. Levesque, C. Laflamme, G. Marcoux, G. Lambeau, R. W. Farndale, M. Pouliot, H. Hamzeh-Cognasse, F. Cognasse, O. Garraud, P. A. Nigrovic, H. Guderley, S. Lacroix, L. Thibault, J. W. Semple, M. H. Gelb, and E. Boilard. Platelets release mitochondria serving as substrate for bactericidal group IIA-secreted phospholipase A2 to promote inflammation. *Blood* 124 (2014):2173–83. DOI: 10.1182/blood-2014-05-573543.

[239] K. Fukumitsu, T. Hatsukano, A. Yoshimura, J. Heuser, K. Fujishima, and M. Kengaku. Mitochondrial fission protein Drp1 regulates mitochondrial transport and dendritic arborization in cerebellar Purkinje cells. *Mol Cell Neurosci* 71 (2016):56–65. DOI: 10.1016/j.mcn.2015.12.006.

[240] M. Giovarelli, S. Zecchini, E. Martini, M. Garre, S. Barozzi, M. Ripolone, L. Napoli, M. Coazzoli, C. Vantaggiato, P. Roux-Biejat, D. Cervia, C. Moscheni, C. Perrotta, D. Parazzoli, E. Clementi, and C. De Palma. Drp1 overexpression induces desmin disassembling and drives kinesin-1 activation promoting mitochondrial trafficking in skeletal muscle. *Cell Death Differ* 27 (2020):2383–2401. DOI: 10.1038/s41418-020-0510-7.

[241] P. H. Willems, R. Rossignol, C. E. Dieteren, M. P. Murphy, and W. J. Koopman. Redox Homeostasis and Mitochondrial Dynamics. *Cell Metab* 22 (2015):207–18. DOI: 10.1016/j.cmet.2015.06.006.

[242] D. C. Chambers, W. S. Tunnicliffe, and J. G. Ayres. Acute inhalation of cigarette smoke increases lower respiratory tract nitric oxide concentrations. *Thorax* 53 (1998):677–9. DOI: 10.1136/thx.53.8.677.

[243] D. H. Cho, T. Nakamura, J. Fang, P. Cieplak, A. Godzik, Z. Gu, and S. A. Lipton. S-nitrosylation of Drp1 mediates beta-amyloid-related mitochondrial fission and neuronal injury. *Science* 324 (2009):102–5. DOI: 10.1126/science.1171091.

[244] H. G. Moon, S. H. Kim, J. Gao, T. Quan, Z. Qin, J. C. Osorio, I. O. Rosas, M. Wu, Y. Tesfaigzi, and Y. Jin. CCN1 secretion and cleavage regulate the lung epithelial cell functions after cigarette smoke. *Am J Physiol Lung Cell Mol Physiol* 307 (2014):L326–37. DOI: 10.1152/ajplung.00102.2014.

[245] A. Saxena, M. S. Walters, J. H. Shieh, L. B. Shen, K. Gomi, R. J. Downey, R. G. Crystal, and M. A. S. Moore. Extracellular vesicles from human airway basal cells respond to cigarette smoke extract and affect vascular endothelial cells. *Sci Rep* 11 (2021):6104. DOI: 10.1038/s41598-021-85534-6.

[246] S. W. Ballinger, T. G. Bouder, G. S. Davis, S. A. Judice, J. A. Nicklas, and R. J. Albertini. Mitochondrial genome damage associated with cigarette smoking. *Cancer Res* 56 (1996):5692–7.

[247] L. Doyle and M. Wang. Overview of Extracellular Vesicles, Their Origin, Composition, Purpose, and Methods for Exosome Isolation and Analysis. *Cells* 8 (2019). DOI: 10.3390/cells8070727.

[248] A. Trappe, S. C. Donnelly, P. McNally, and J. A. Coppinger. Role of extracellular vesicles in chronic lung disease. *Thorax* 76 (2021):1047–1056. DOI: 10.1136/thoraxjnl-2020-216370.

[249] K. T. Chang, R. F. Niescier, and K. T. Min. Mitochondrial matrix Ca2+ as an intrinsic signal regulating mitochondrial motility in axons. *Proceedings of the National Academy of Sciences of the United States of America* 108 (2011):15456–15461. DOI: 10.1073/pnas.1106862108.

[250] P. J. Barnes. Cellular and molecular mechanisms of chronic obstructive pulmonary disease. *Clin Chest Med* 35 (2014):71–86. DOI: 10.1016/j.ccm.2013.10.004.

[251] J. M. Hughes, C. A. Arthur, S. Baracho, S. M. Carlin, K. M. Hawker, P. R. Johnson, and C. L. Armour. Human eosinophil-airway smooth muscle cell interactions. *Mediators Inflamm* 9 (2000):93–9. DOI: 10.1080/096293500411550.

[252] C. W. Lee, C. C. Lin, S. F. Luo, H. C. Lee, I. T. Lee, W. C. Aird, T. L. Hwang, and C. M. Yang. Tumor necrosis factor-alpha enhances neutrophil adhesiveness: induction of vascular cell adhesion molecule-1 via activation of Akt and CaM kinase II and modifications of histone acetyltransferase and histone deacetylase 4 in human tracheal smooth muscle cells. *Mol Pharmacol* 73 (2008):1454–64. DOI: 10.1124/mol.107.038091.

[253] N. K. Malavia, C. B. Raub, S. B. Mahon, M. Brenner, J. Panettieri R. A., and S. C. George. Airway epithelium stimulates smooth muscle proliferation. *Am J Respir Cell Mol Biol* 41 (2009):297–304. DOI: 10.1165/rcmb.2008-0358OC.

[254] A. K. Majors, R. Chakravarti, L. M. Ruple, R. Leahy, D. J. Stuehr, M. Lauer, S. C. Erzurum, A. Janocha, and M. A. Aronica. Nitric oxide alters hyaluronan deposition by airway smooth muscle cells. *PLoS One* 13 (2018):e0200074. DOI: 10.1371/journal.pone.0200074.

[255] B. Lan, J. A. Mitchel, M. J. O'Sullivan, C. Y. Park, J. H. Kim, W. C. Cole, J. P. Butler, and J. A. Park. Airway epithelial compression promotes airway smooth muscle proliferation and contraction. *Am J Physiol Lung Cell Mol Physiol* 315 (2018):L645–L652. DOI: 10.1152/ajplung.00261.2018.

[256] E. Bourdonnay, Z. Zaslona, L. R. Penke, J. M. Speth, D. J. Schneider, S. Przybranowski, J. A. Swanson, P. Mancuso, C. M. Freeman, J. L. Curtis, and M. Peters-Golden. Transcellular delivery of vesicular SOCS proteins from macrophages to epithelial cells blunts inflammatory signaling. *J Exp Med* 212 (2015):729–42. DOI: 10.1084/jem.20141675.

[257] X. Wang, D. Qiao, L. Chen, M. Xu, S. Chen, L. Huang, F. Wang, Z. Chen, J. Cai, and L. Fu. Chemotherapeutic drugs stimulate the release and recycling of

extracellular vesicles to assist cancer cells in developing an urgent chemoresistance. *Mol Cancer* 18 (2019):182. DOI: 10.1186/s12943-019-1114-z.

[258] M. P. Murphy and R. C. Hartley. Mitochondria as a therapeutic target for common pathologies. *Nature Reviews Drug Discovery* 17 (2018):865–886. DOI: 10.1038/nrd.2018.174.

[259] M. J. Kang, C. M. Yoon, B. H. Kim, C. M. Lee, Y. Zhou, M. Sauler, R. Homer, A. Dhamija, D. Boffa, A. P. West, G. S. Shadel, J. P. Ting, J. R. Tedrow, N. Kaminski, W. J. Kim, C. G. Lee, Y. M. Oh, and J. A. Elias. Suppression of NLRX1 in chronic obstructive pulmonary disease. *J Clin Invest* 125 (2015):2458–62. DOI: 10.1172/JCI71747.

[260] S. M. Cloonan and A. M. Choi. Mitochondria in lung disease. *J Clin Invest* 126 (2016):809–20. DOI: 10.1172/JCI81113.

[261] B. Camoretti-Mercado and R. F. Lockey. Airway smooth muscle pathophysiology in asthma. *J Allergy Clin Immunol* 147 (2021):1983–1995. DOI: 10.1016/j.jaci.2021.03.035.

[262] B. R. Dye, D. R. Hill, M. A. Ferguson, Y. H. Tsai, M. S. Nagy, R. Dyal, J. M. Wells, C. N. Mayhew, R. Nattiv, O. D. Klein, E. S. White, G. H. Deutsch, and J. R. Spence. In vitro generation of human pluripotent stem cell derived lung organoids. *Elife* 4 (2015). DOI: 10.7554/eLife.05098.

[263] T. G. Guney, A. M. Herranz, S. Mumby, I. E. Dunlop, and I. M. Adcock. Epithelial-stromal cell interactions and extracellular matrix mechanics drive the formation of airway-mimetic tubular morphology in lung organoids. *iScience* 24 (2021):103061. DOI: 10.1016/j.isci.2021.103061.

[264] M. van der Vlist, R. Raoof, H. Willemen, J. Prado, S. Versteeg, C. Martin Gil, M. Vos, R. E. Lokhorst, R. J. Pasterkamp, T. Kojima, H. Karasuyama, W. Khoury-Hanold, L. Meyaard, and N. Eijkelkamp. Macrophages transfer mitochondria to sensory neurons to resolve inflammatory pain. *Neuron* (2021). DOI: 10.1016/j.neuron.2021.11.020.

[265] J. W. Hwang, S. Rajendrasozhan, H. Yao, S. Chung, I. K. Sundar, H. L. Huyck, G. S. Pryhuber, V. L. Kinnula, and I. Rahman. FOXO3 deficiency leads to increased susceptibility to cigarette smoke-induced inflammation, airspace enlargement, and chronic obstructive pulmonary disease. *J Immunol* 187 (2011):987–98. DOI: 10.4049/jimmunol.1001861.

[266] B. Leclercq, J. Kluza, S. Antherieu, J. Sotty, L. Y. Alleman, E. Perdrix, A. Loyens, P. Coddeville, J. M. Lo Guidice, P. Marchetti, and G. Garcon. Air pollution-derived PM2.5 impairs mitochondrial function in healthy and chronic obstructive pulmonary diseased human bronchial epithelial cells. *Environ Pollut* 243 (2018):1434–1449. DOI: 10.1016/j.envpol.2018.09.062.

[267] V. Ghorani, M. H. Boskabady, M. R. Khazdair, and M. Kianmeher. Experimental animal models for COPD: a methodological review. *Tob Induc Dis* 15 (2017):25. DOI: 10.1186/s12971-017-0130-2.

[268] L. Tanner and A. B. Single. Animal Models Reflecting Chronic Obstructive Pulmonary Disease and Related Respiratory Disorders: Translating Pre-Clinical Data into Clinical Relevance. *J Innate Immun* 12 (2020):203–225. DOI: 10.1159/000502489.